

Design and implementation of environment chamber for
interfacial phenomenon processes

Gurdeep Singh Saini

A THESIS SUBMITTED TO THE FACULTY OF GRADUATE
STUDIES IN PARTIAL FULFILLMENT OF THE REQUIREMENTS
FOR THE DEGREE OF MASTERS OF APPLIED SCIENCE

GRADUATE PROGRAM IN MECHANICAL ENGINEERING
YORK UNIVERSITY
TORONTO, ONTARIO

January 2022

© Gurdeep Saini, 2022

Abstract

With the goal of simulating the environmental conditions necessary for various droplet related phenomenon, a portable environment chamber was built and tested in this thesis. The “House of Quality” design methodology was used as a roadmap for the iterative design process. The chamber comprises a temperature control system, an anti-condensation system, and a humidity control system. The performance of the chamber was tested afterwards at different temperature and humidity setpoints, to quantitate the chambers working capabilities. The chamber can generate an environment inside it with a temperature range of 10 °C to 70 °C, and a relative humidity range of ambient to 80%. The chamber was benchmarked against experiments done in the literature; involving surface tension and contact angle. The experiments that were done for both contact angles measurements corroborated what was in the literature, however we discovered potential problem for literature values of surface tension at lower temperatures.

Acknowledgements

Alidad Amirfazli for taking me as his student

Huanchen Chen for his guidance and support

Manmohan and Varinder Saini for supporting me

Satbir Saini and Savreet Brar for their encouragement

Samuel Wu and Ali Mozafari for always taking my mind away from work

Gurbinder Nagra for listening to me vent

My lab mates for all the good times

Table of Contents

Abstract.....	ii
Acknowledgements.....	iii
Table of Contents.....	iv
List of tables.....	vi
List of Figures.....	vii
Abbreviations.....	xi
Preface.....	xii
Scope of work (pre-covid).....	xii
Chapter 1 - Introduction.....	1
1.1 - Objectives and outline.....	2
Chapter 2 - Background and Literature review.....	3
2.1 - Contact angle.....	4
2.2 - Evaporation.....	6
2.3 - Measurement Techniques.....	7
2.4 - Design methodologies.....	9
2.5 - Control systems.....	10
2.5.1 - PID.....	11
2.5.2 - Bang-bang.....	13
2.6 - Review of other chambers.....	13
Chapter 3 - Mechanical Design.....	17
3.1 - Design plan.....	17
3.1.1 - Outline of design.....	17
3.1.2 - Scope of work.....	18
3.1.3 - Fundamental building blocks.....	19
3.2 - QFD approach - House of Quality.....	20
3.2.1 - Pair wise comparison.....	21
3.3 - Level 1 QFD-Design requirements.....	24
3.4 - Level 2 QFD-System level.....	27
3.5 - Level 2 QFD-temperature sub system.....	31
3.6 - Level 2 QFD-humidity sub system.....	36
3.7 - Final Design.....	39
3.7.1 - Overall design.....	39

3.7.2 - Breakdown of important components	39
3.7.3 - Alternative version due to pandemic conditions.....	47
Chapter 4 - Instrumentation Design	48
4.1 - Breakdown of important components and systems	49
4.1.1 - Control systems components	49
4.1.2 - Electronic control components.....	49
4.1.3 - Sensors.....	50
4.1.4 - Mass and energy transfer components.....	50
4.2 - Design Evolution	51
4.2.1 - First iteration	51
4.2.2 - Second iteration.....	51
4.2.3 - Third iteration	53
4.2.4 - Forth iteration.....	55
4.3 - Code logic.....	57
Chapter 5 - Capability and Performance Tests	63
Chapter 6 – Benchmarking and performance tests	75
6.1 - Surface tension	75
6.2 - Receding contact angle.....	76
6.3 - Advancing contact angle	79
Chapter 7 – Summary and future studies	81
7.1 - Summary and conclusion.....	81
7.2 - Future works	82
References	84
Appendices.....	91
Appendix A - Analysis and Calculation Data for QFD method.....	91
Appendix B - Drawings for physical components used in design.....	92
Appendix C - Control system code	126
Appendix D - Benchmark and literature tests raw data	152

List of tables

Table 2-A - Effects of increasing tuning parameters on the PID control output	13
Table 2-B - Review of chambers found commercially or in the literature (continuous on the next page)	14
Table 3-A - Results of pairwise comparison of features necessary for a functioning environment chamber	23
Table 3-B - QFD relationship weighting scale used in a QFD matrix to correlate the input parameters with known weighting and output parameters with unknown weighting	26
Table 3-C – Bill of materials for Figure 3-14.....	40
Table 5-A - Limit test setpoints. Tests were done in order to determine the high and low temperature, and high humidity environments that the chamber can generate.	64
Table 5-B - Summary of spec tests for chamber temperature and humidity control performance	74
Table 6-A - Initial conditions for receding contact angle experiments.....	77

List of Figures

Figure 0-1 - Destructive temperature and humidity test.....	xiii
Figure 1-1 - Schematic of the imaging system used for contact angle and surface tension measurements in an environment chamber. A camera is used for image capture, with a light source illuminating the droplet. The Pendent droplet configuration is used for surface tension measurements and the sessile droplet configuration for contact angle.....	2
Figure 2-1 – Schematic to show molecular origins of the surface tension	3
Figure 2-2 – Schematic of a sessile droplet on a solid surface showing contact angle	5
Figure 2-3 - Schematic of experimentally extracted and theoretical drop profile; frame of reference perpendicular to the contact plane of droplet and surface	7
Figure 2-4 - Young-Laplace fitting; the dots representing the detected profile of the droplet; a needle/capillary cannot be present without it interfering with the fitting	8
Figure 2-5- Polynomial fitting; The dots representing the detected profile; a needle/capillary can be present inside the droplet provided it is not in detectable range of the fitting algorithm	8
Figure 2-6 – ADSA-D method, the diameter (represented by the dashed line) is extracted from the profile of the droplets top view (represented by the solid circle) using edge detection, represented by the dots	9
Figure 2-7 - House of quality template; is a matrix that uses two inputs. The first input set with known numerical values that define the weight/importance of each input parameter; and a second set of inputs with unknown weights. The two inputs sets are compared, with the parameters of the second set given a relationship ranking with the first set. The output of this matrix is the weighting of each parameter for the second input set.	10
Figure 2-8 - PID Visualization; illustrates the components and flow of the closed loop system. The input for the PID is the numeric difference between the setpoint and the current state of the system. The input is then used to calculate the proportion, integral, and derivative terms, which the summation of is the output of the system. This output then changes the current state of the system; thus, completing the loop. This process is repeated until the current state of the system is equal to the set point.....	12
Figure 3-1- Summery of the design history of the chamber. The first column shows the chronological history of the design stages from the basic design to the third iteration. The rows show the chronological history of the steps taken at each stage.	17
Figure 3-2 - Schematic showing the region of interest for the chamber. The goal of the chamber is to have homogeneous temperature and humidity conditions in the volume marked the region of interest, where the droplet will be located.....	19
Figure 3-3 - QFD roadmap illustrates the flow of the QFD design process. Each step is a matrix comparing two sets of parameters. The output of one step becomes the input for the next step.....	21
Figure 3-4 - Level 1 QFD matrix; comparing the desired features to the functional requirements, to generate a weighting for the functional requirements [65].....	26
Figure 3-5 - Level 2 QFD matrix; comparing the functional requirements to the system components required for the chamber, to generate a weighting for the system component	28
Figure 3-6- Initial prototypes; the first iteration on the left and the second on the right. Tests run with the two prototypes were critical in aiding the design process, as they gave insight on the relationship between the different components in the system. The dimensions shown apply to both iterations, not show is the depth which is 4 in.	31

Figure 3-7 - Level 2 QFD matrix, the features related to temperature control inside the chamber are further analyzed by breaking them down into their baser components 32

Figure 3-8 - Temperature control system cross section and bill of materials 33

Figure 3-9 - Isometric render of temperature control system, see Figure 3-8 for details..... 34

Figure 3-10 - Sample preliminary simulations to gauge the effects of modifying the chamber on the temperature distribution inside the chamber. The top view is on the left and the side view on the right. The boundary conditions are as follows: boundary type is outer wall, external air temperature was 22°C, and adjacent wall heat transfer coefficient is 0.025 N/s/mm/°C. the governing equation is the Navier-Stokes equation 35

Figure 3-11 - Resulting design of "inner heat sink" after multiple simulations, the scale is in inches 36

Figure 3-12 - Level 2 QFD matrix, the features related to humidity control inside the chamber are further analyzed by breaking them down into their baser components..... 37

Figure 3-13 - Humidity control system and bill of materials..... 38

Figure 3-14 - Exploded view of chamber; for label description see Table 3-C. 39

Figure 3-15 – Top and isometric view of wall Assembly of chamber; the three darkened frames encompass the components for the three chamber walls. The overlapping parts of the frame have components that are shared between assemblies..... 42

Figure 3-16 - External components. A) corresponds to the side view and B) corresponds to the top view. The LED light and phone were used in the image capture and processing during experimentation. The syringe holder was used to steady and manipulate the position of the syringe. The chamber platform is used to position the environment chamber. The mounting plate is used to fix each component in the system. 43

Figure 3-17 - Syringe holder. The syringe holders main components are a jack for movement in the z-axis with a 2.5" translation range, a precision translation stage for y-axis movement with a 10mm translation range, and a translation rail for x-axis movement with 100mm translation range. All axes are 90° angle from the other. Magnetic switches in 3D printed housings can lock the stage anywhere on the baseplate. Not labeled are the mounting plates. 44

Figure 3-18- LED backlight. This component has a jack for vertical movement with a 2.5" translation range, and a housing for the LED backlight screen and electronic components. Not labeled is the mounting plate..... 45

Figure 3-19 - Phone holder. This component has a jack for vertical movement with a 2.5" translation range and a housing for the smart phone. Not labeled is the mounting plate. 46

Figure 3-20 - Chamber platform. This component has a translation stage for vertical movement with a 20mm translation range. 47

Figure 3-21 - Alternative design. On the left is the CAD model and on the right is the physical prototype.. 47

Figure 4-1 - History of instrumentation aspect of design. The first column represents the iteration, while the rows represent the components within that iteration. The vertical arrows going from one component to the next represent modifications in the design..... 48

Figure 4-2 - First iteration of chamber's electronic data acquisition and control system..... 51

Figure 4-3 - Second iteration of chamber's electronic data acquisition and control system 52

Figure 4-4 - PID tests for second iteration of design. A slow with a sample time of 2 minutes was required for the system to settle on the set point 11°C above ambient (setpoint 35 °C) after 70 minutes. 53

Figure 4-5 - Third iteration of chamber's electronic data acquisition and control system 54

Figure 4-6 - Forth iteration of chamber’s electronic data acquisition and control system 55

Figure 4-7 - Wiring diagram for Driver and Relay. The driver controls the Peltier and ITO glass with pulse width modulation, varying the voltage applied to both components individually. The relays switches from either having the circuit open, to completing the circuit. 56

Figure 4-8 – Cross section of chamber showing the location of sensors inside chamber, cross section taken at the center of the chamber 57

Figure 4-9 - Stage 1 and 2 PID heating implementation. The two flow charts on the left are a visualization of the control loop for the Peltier and the ITO glass; they are separated since they work independently from one another with different sensors. The two blocks on the right show the conditions and parameters of each stage. 58

Figure 4-10 - Stage 3 PID heating implementation. The flow chart on the left is a visualization of the control loop for the Peltier and the ITO glass; they are combined in this stage as they share the same sensor and work together to have that sensor reach the setpoint. The block on the right shows the conditions and parameters for the third stage of the PID. 59

Figure 4-11 - PID Response for setpoint 70°C, system over and undershoot and steady system error less than 1°C. Both graphs illustrate the response of the system at different stages of the PID. The first graph A) shows the voltage given to the Peltier and ITO glass of the system where PWN 0 represents 0V and PWN 255 representing 15V. The second graph B) shows the sensor readings at different stages of the PID; where temp al is the Peltier temperature, tempITO is the ITO glass temperature, and tempC2 is the air temperature..... 60

Figure 4-12 - Stage 1 and 2 PID cooling implementation. The flow chart on the left is a visualization of the control loop for the Peltier; they are separated since they work independently from one another with different sensors. The two blocks on the right show the conditions and parameters of each stage. 61

Figure 4-13 - PID response for set point 9 °C with a fan on inside the chamber. Both graphs illustrate the response of the system at different stages of the PID. The first graph A) shows the voltage given to the Peltier where PWN 0 represents 0V and PWN 255 representing 15V. The second graph B) shows the sensor readings at different stages of the PID; where temp al is the Peltier temperature, tempITO is the ITO glass temperature, and tempC2 is the air temperature..... 61

Figure 4-14 - Bang-bang humidity implementation. The two flow charts on the left illustrate the two active states of the humidity system. On the right, are the conditions for the active states. 62

Figure 5-1 - History of spec and benchmark tests. The first column represents the test type; and the rows represent the chronological order of experimentation..... 63

Figure 5-2 – a) Average of cooling test at 15°C, No fan; the error bars denote the standard deviation of the tests b) sample data of cooling test for Peltier (temp al), air (tempC2), and ITO glass (tempITO) temperature..... 65

Figure 5-3 – a) Average of cooling test at setpoint 9°C, with a fan circulating air inside the chamber; the error bars denote the standard deviation of the tests b) sample data of cooling test for Peltier (temp al), air (tempC2), and ITO glass (tempITO) temperature 67

Figure 5-4 – a) Average of heating test at setpoint 70°C; the error bars denote the standard deviation of the tests b) sample data of heating test for Peltier (temp al), air (tempC2), and ITO glass (tempITO) temperature..... 68

Figure 5-5 – Average of base case test of setpoint 100%RH at room temperature (22 °C) ; the error bars denote the standard deviation of the tests 69

Figure 5-6 – Average of humidity test at setpoint 15°C and 70%RH; the error bars denote the standard deviation of the tests 70

Figure 5-7 – Average of humidity test at setpoint 40°C and 80%RH; the error bars denote the standard deviation of the tests 70

Figure 5-8 - Three humidity tests at setpoint 40°C and, 80%RH; where hum 1, hum 2, and hum 3 are the three separate humidity test results, and Average Temp the average temperature of the air inside the chamber for all three tests 72

Figure 5-9 - Three humidity tests at setpoint 15°C and, 70%RH; where hum 1, hum 2, and hum 3 are the three separate humidity test results, and Average Temp the average temperature of the air inside the chamber for all three tests 73

Figure 6-1 - Location of droplet for pendent drop experiment, the needle is located at the center of the chamber, the volume of the droplet is 39 μL 75

Figure 6-2 - Surface tension of DI water at constant temperature and varied humidity 76

Figure 6-3 - Location of droplet for sessile drop experiment, the needle is located at the center of the chamber, the volume of the droplet is 18.6 μL 77

Figure 6-4 - Evaporation of DI water at 27.5°C and 61%RH on a glass substrate 78

Figure 6-5 - The effects of temperature and humidity on the advancing contact angle of DI water on a Teflon substrate 80

Abbreviations

γ Surface tension

θ Contact angle

ITO Tin indium oxide

QFD Quality function development

PID Proportion integral derivative

Preface

Concessions due to Covid-19

Instrumentation was originally one part of the project, the other part was meant to investigate the effects of an auxiliary sessile droplet on a pair of sessile droplets for binary liquids (Water and Propylene Glycol) on a high energy surface. The chamber was meant specifically to conduct these experiments, as other chambers in the literature did not meet all the requirements. However, due to lockdown restrictions resulting in loss of lab access; the plasma cleaner critical to the experiments could not be used; making further experiments impossible. Thus, part way through the thesis, the focus of the chamber was changed toward general droplet experiments; rather than a specialized chamber for the auxiliary droplet experiments.

Scope of work (pre-covid)

The following is a list of requirements for the minimum viable product

- Temperature range from 0 °C to 100 °C
- Reach temperature setpoint within $\pm 1^\circ\text{C}$ in less than 1 hour
- Humidity range from 0 to 100 %
- Reach humidity set point within ± 5 within less than 1 hour
- Chamber suited to image acquisition (Transmittance > 80%)
- Chamber large enough for standard substrate (3x1 in)
- Overall Portable chamber

Before the start of the pandemic caused massive delays in manufacturing and supply chain issues, the original scope was meant to be the minimum specifications of the chamber's capabilities, and much of the design process revolved around achieving these parameters. This unfortunately had to be revised later on, as achieving these levels were not viable with the compromised design. The temperature range was reduced to between 15°C to 70°C; and the maximum relative humidity decreased to 80%RH.

The consequences to the current prototype is that the capabilities and range of the chamber must be reduced, since it cannot be run to its maximum settings without failure. As previously stated, due to COVID-19 related manufacturing delays; a makeshift design was used for the current iteration. As a consequence, the electronic systems that are specified to the original design; are too powerful for the current iteration. An example of this is Figure 0-1; where at a test for 90°C and 100% relative humidity;

the silicon holding the chamber together began to fail at the 1200 second mark; a flaw not present in the original design which uses mechanical fasteners and gaskets. Thus, for this iteration, certain parameters and test conditions were capped.

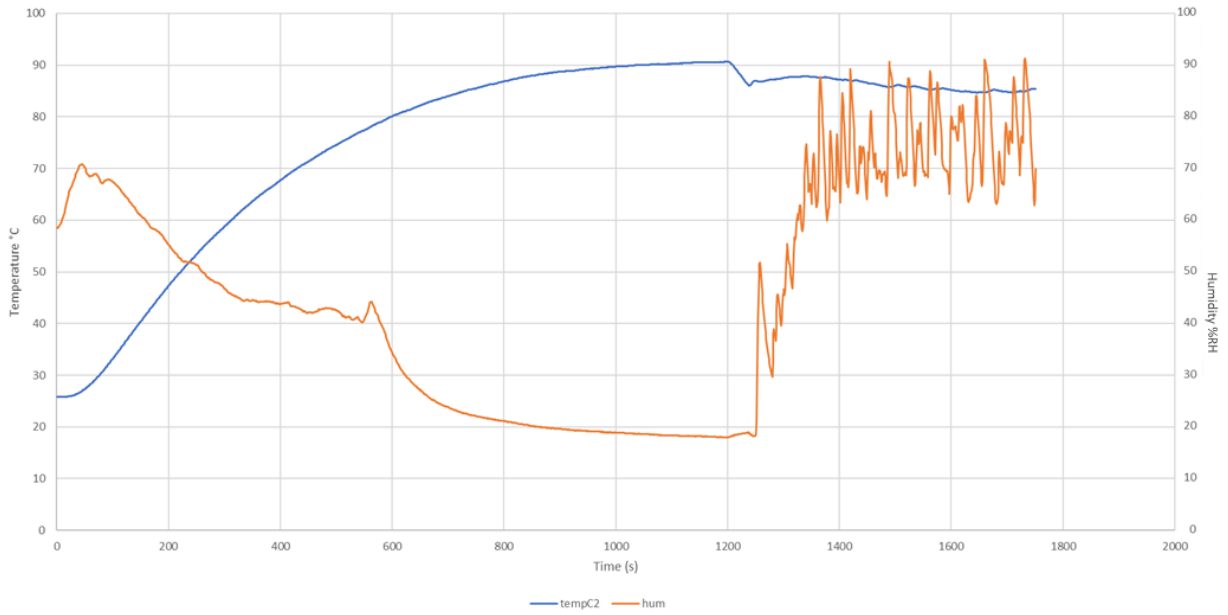


Figure 0-1 - Destructive temperature and humidity test

Chapter 1 - Introduction

Analyzing the shape of a droplet can give both the contact angle (θ) and its surface tension (γ); As such, the measurement of θ and γ can be used to explain interfacial phenomenon in a wide variety of applications; such as spray coatings [1] [2], surfactants [3] [4] [5], and friction of cartilage in joints [6].

The interaction between water drops and surfaces can be affected by many parameters. Two of the more prominent parameters that effect water droplets in particular, are temperature and relative humidity [7]. For cases involving interfacial phenomenon; the effects of temperature and humidity have been studied with respect to applications such as condensation based heat transfer [8], anti fog systems [9], and steam power generation [10].

Temperature and relative humidity have an effect on both the droplet itself and the composition of the vapor cloud surrounding and generated by the evaporation of droplet [11]. Many experiments have been done with temperature and humidity effects on single droplet systems, such as investigating the evaporating contact angle and surface tension of liquids; however further experiments can be done when investigating systems with more than one droplet [12] [11] [13] [14], where the composition of the vapor field dictates the motion of sessile droplets on top of a surface; these experiments can be extended by varying both temperature and humidity as both parameters influence the vapor cloud.

Since surface tension and contact angle have such a wide variety of applications in the industry, an easily implemented system that allows for different tests would be a useful tool. Thus, a chamber with the ability to control its internal temperature and humidity would be a useful tool in investigating interfacial phenomenon through drop shape analysis that is a widely used method for surface tension and contact angle measurement (see Figure 1-1). The main goal of this thesis is to create a portable environment chamber, that can be used in a wide variety of locations, as well as a module that could be easily integrated into a variety of different systems. The system itself can also be used beyond drop shape analysis, and can cover tests for experiments such as the effects of temperature and humidity on resin bonding [15], fungal growth of different species [16]. The portability focus of the chamber forces the design into a certain path; the chamber is meant to be a self-contained system, requiring the basics of water and electricity to function. Portability also as focused the design towards miniaturization, as a smaller chamber can be more easily integrated into another system/experimental setup; and can be easily swapped out when needed for another system. Portability of the control system was another factor in the development of the chamber, the chamber was built to be controlled by a smart phone

instead of a PC, and the components chosen for the instrumentation of the system were selected based on compatibility with smart phone control as a factor. This thesis will cover the design and fabrication of a portable temperature and humidity control chamber, and will demonstrate its capabilities for surface tension studies by benchmarking it against similar studies within the literature.

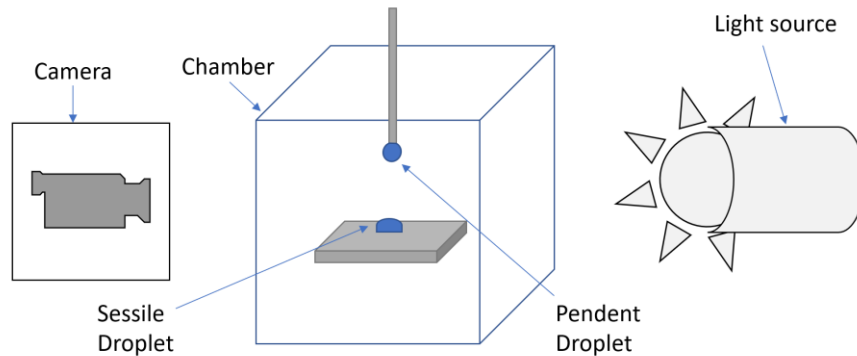


Figure 1-1 - Schematic of the imaging system used for contact angle and surface tension measurements in an environment chamber. A camera is used for image capture, with a light source illuminating the droplet. The Pendent droplet configuration is used for surface tension measurements and the sessile droplet configuration for contact angle.

1.1 - Objectives and outline

The objective of this thesis is to develop a portable environment chamber that allows the user to specify the environmental conditions, and have the system automatically create the desired environment. The focus of this thesis is divided into 3 main parts. First is the mechanical design of the environment chamber; where the thesis will chronicle the design method used and how the chamber was created using a structured design methodology. Preliminary research for the chamber is summarized in Chapter 2, where other chambers and systems are investigated, to aid in the design process. Chapter 3 covers the iterative design of the mechanical components of the system. The second part; covers the instrumentation aspect of the design; from its original prototype to its final iteration; chronicling the various changes and refinements; all covered in Chapter 4. Lastly, the thesis will demonstrate the capability of the system, by investigating the effects of environmental variables of temperature and humidity on surface tension, contact angle, and by extension evaporation. This part of the thesis will cover first the upper and lower temperature and humidity set point limits of the chamber in Chapter 5; and the applications of the chamber by benchmarking the results from the chamber with experiments found in the literature in Chapter 6.

Chapter 2 - Background and Literature review

The concept of surface tension was first introduced by Johann Andreas von Segner in 1704 [17] [18], and later expanded by Thomas Young's pioneering work for surface tension at the liquid interface; by defining it with his three assertions [18]; and at the same time tying surface tension to contact angle.

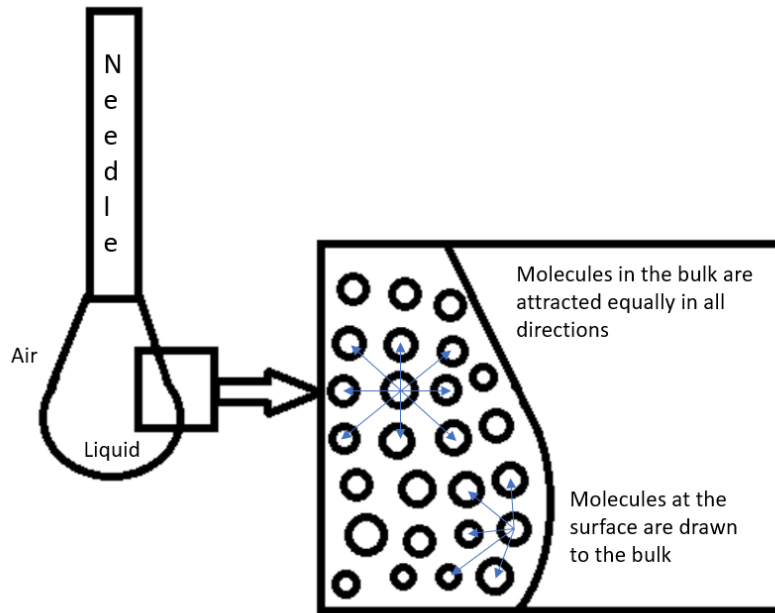


Figure 2-1 – Schematic to show molecular origins of the surface tension

Surface tension arise from the difference in attractive forces between the liquid-liquid bonds and liquid-air bonds. Due to the liquid-liquid molecular interaction being magnitudes stronger than that of the liquid-air, the molecules in the surface of the liquid experience a stronger intermolecular attraction towards the molecules in the bulk of the liquid. Surface tension of a droplet in air manifests from the tendency of to settle towards the most energetically favorable state, which tends towards a shape with the lowest surface area possible [19].

The link between surface tension and temperature has been well established for deionized (DI) water (water purified by a chemical process removing ions [20]), with increasing temperatures lowering the surface tension of water [21]. The increase in temperature causes molecules to be ejected out of the liquid [7], since the molecules on the meniscus of the liquid have a weaker interactions than the molecules in the bulk. This is due to the increase in temperature exciting the molecules in the liquid; the

excitation gives the molecules enough energy to break their liquid-liquid bonds. This results in a lower surface tension, as the molecules in the meniscus have a weakened interactions with the molecules in the bulk [22]. An instrument that can be used to cover a range of temperatures to test new formulations of a liquid would be a useful tool to help create characteristic curves for surface tension at different temperatures. This has applications in the 3D printing world with the advent of photocuring resin printing [23].

Humidity has an effect of slowing the evaporation rate of water [24], as well as decreases the surface tension [7] [22]. Humidity is measure of water vapor in the air. A high concentration of water vapor results in a lower evaporation rate, as the reverse; with water vapor from the air condensing on the surface of the droplet [25]. The resulting overpressure has an effect of reducing the liquid-air surface tension [7] [22]. Extensive research within the literature exploring the effects of temperature and humidity on pure water, however there are gaps with respect to other binary and non-binary liquids; such as photocuring resins used in 3D printers, as the technology is new and the data sheet is limited to health and safety rather than material properties [26]. The chamber being designed is meant to be an apparatus that can facilitate further research in the area.

2.1 - Contact angle

Contact angle was first defined by Thomas Young in 1805 as a measurement to understand the interaction of the surface in three phase systems; where they intersect at the contact line; particularly for solid, liquid, and gas systems [27]. Young defined the contact angle at equilibrium with the energy balanced approach by describing in words the following equation:

$$\cos\theta = \frac{\gamma_{SG}-\gamma_{SL}}{\gamma_{LG}} \quad (2.1)$$

where θ is the contact angle; and γ_{SG} , γ_{SL} , γ_{LG} are the solid-gas, solid-liquid, and liquid-gas interfacial tensions respectively [28]. For non-ideal cases, the contact angle of a system can have a range of values meaning that the static contact angle is not indicative of the nature of the system; thus the dynamic contact angle gives a better representation of the system [29]. This is split into the advancing (upper limit of range) and receding contact angle (lower limit of range); which are formed as the droplet slowly expands and contracts on the surface respectively. The difference between these two values is defined as the contact angle hysteresis [30].

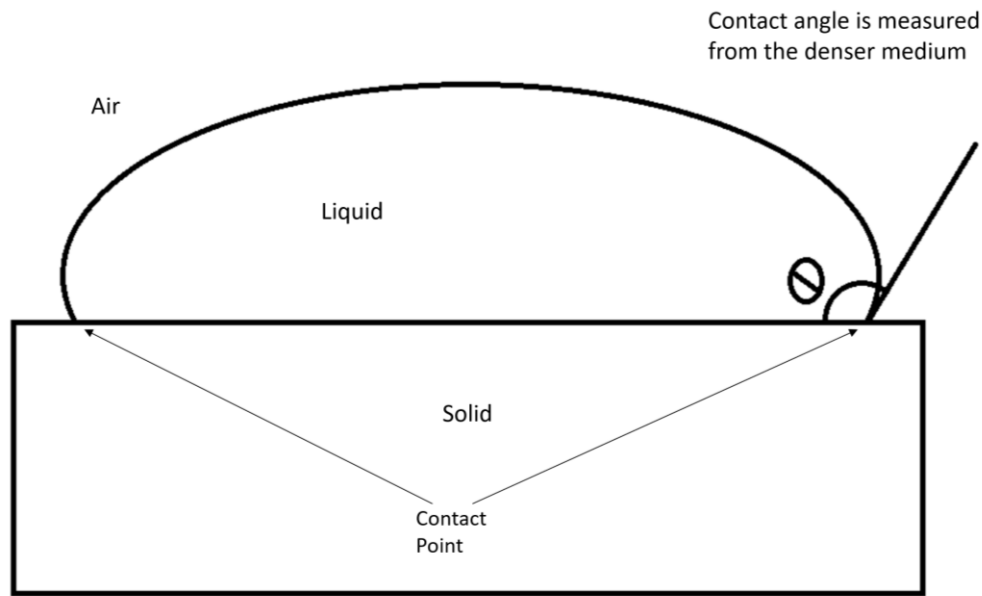


Figure 2-2 – Schematic of a sessile droplet on a solid surface showing contact angle

Contact angle is an important property that indicates the wettability of water on a surface; and a way to characterize the surface [31]. It is typically measured from the denser medium up to the meniscus as shown in Figure 2-2. It is a localized phenomenon that depends on the point where the liquid-air, liquid-solid, and solid-air boundaries meet [28]. A small contact angle indicates a high degree of wettability, while a large contact angle indicates a low degree of wettability [32].

Besides the material of the substrate, its surface roughness/smoothness also has an effect on the contact angle. Literature shows that for hydrophilic surface, increase of the roughness can typically causing an increase of contact angle hysteresis. However, for hydrophobic surface, depending on if it is in Wenzel or Cassie state, the contact angle hysteresis may increase (Wenzel) or decrease (Cassie). For rough surfaces in general, the contact angle can vary dramatically; depending on whether the droplet can penetrate the crevices of the surface (Wenzel state [33]) or whether the droplet sits on the tips of the peaks of the rough surface above pockets of air (Cassie-Baxter state [34]).

It is important to note that contact angle is not a constant value, most surfaces have a contact angle hysteresis; meaning a droplet has a range of possible contact angle values on a given surface which is a value between the advancing and receding contact angle. This is mainly caused by surface heterogeneity, and the causes can range from surface roughness [35] to uneven coatings [36].

Temperature has an effect on the evaporation rate of a droplet, this effect is compounded at the edges of a droplet (location of the contact points) since the volume to surface area ratio is much smaller [14]; the evaporation rate is higher at the edges than at the bulk near the center of the droplet [14]. As the droplet evaporates, the contact angle will decrease until it reaches the critical point which is its receding contact angle value [37]. Elevated temperatures increase the evaporation rate, with the evaporated water creating a vapor cloud around the droplet, thereby increasing the localized relative humidity around the droplet since the air around it is saturated with water vapor [38]. Humidity has the effect of lowering evaporation, thus countering the effect of elevated temperature. This is due the water molecules in humid air depositing onto the droplet, thus replenishing the evaporated liquid [39].

Temperature itself may change the advancing and receding contact angle; however, this is dependent on the surface used. There are cases where temperature has no effect at all [40]. For the purpose of investigating different surfaces and to eliminate any sources of error; a finely temperature controlled isolated environment is needed. This would allow for multiple controlled experiments, at different temperatures, to observe and characterize various liquid surface combination interactions. Thus, the chamber was designed to control and hold the temperature of the air inside the chamber.

Humidity is also a temperature dependent, with the amount of water vapor air can hold decreasing with increasing temperature. At higher temperature, air is able to absorb a greater amount of moisture; thus, the saturation amount for water increases as temperature raises; requiring more moisture to maintain the same relative humidity [41].

2.2 - Evaporation

Evaporation is the phenomenon where molecules at the surface of the liquid constituting the liquid air interface break their liquid-liquid bonds and move to the gas phase [42].

Evaporation is heavily influenced by the interplay of temperature and humidity; for water specifically, they heavily influence the evaporation rate of a droplet. Both temperature and humidity affect the rate at which water changes state from liquid to gas [43], as well as influence the shape of the droplet [44]; which in turn changes the contact angle of the droplet [45].

Evaporation itself also changes the nature of the vapor cloud surrounding a droplet; by creating localized areas of saturated vapor, influencing its contact angle for liquid surfaces systems [11].

An evaporating droplet has also been observed to create surface tension gradient induced flows within the droplet [46], which could also affect the drop contact angle.

A system that can maintain a desired value for relative humidity at certain temperature setpoints would be a useful in investigating the effects of a constant vapor fields at various temperatures. Thus, the chamber was designed to hold the desired humidity setpoint.

2.3 - Measurement Techniques

Contact angle and surface tension are typically measured using optical image analysis [47]. One of the most prominent optical methods of measuring surface tension and contact angle is through axisymmetric drop shape analysis (ADSA) method (see Figure 2-3).

The profile of an axisymmetric drop can be obtained by solving Young-Laplace equation [48]. The ASDA-P (-P stands for profile) method uses the profile of a droplet (see Figure 2-4), the value of the density difference across the interface, the magnitude of the local gravitational constant, and the distance between the base of the drop and the horizontal coordinate axis; to yield the following variables: interfacial tension, contact angle, volume, surface area, radius of curvature, and contact radius of the drop [49]. The ASDA-P method assume that the droplet is perfectly axisymmetric, thus it will assume that the left and right contact angle are equal, and averages out errors [47].

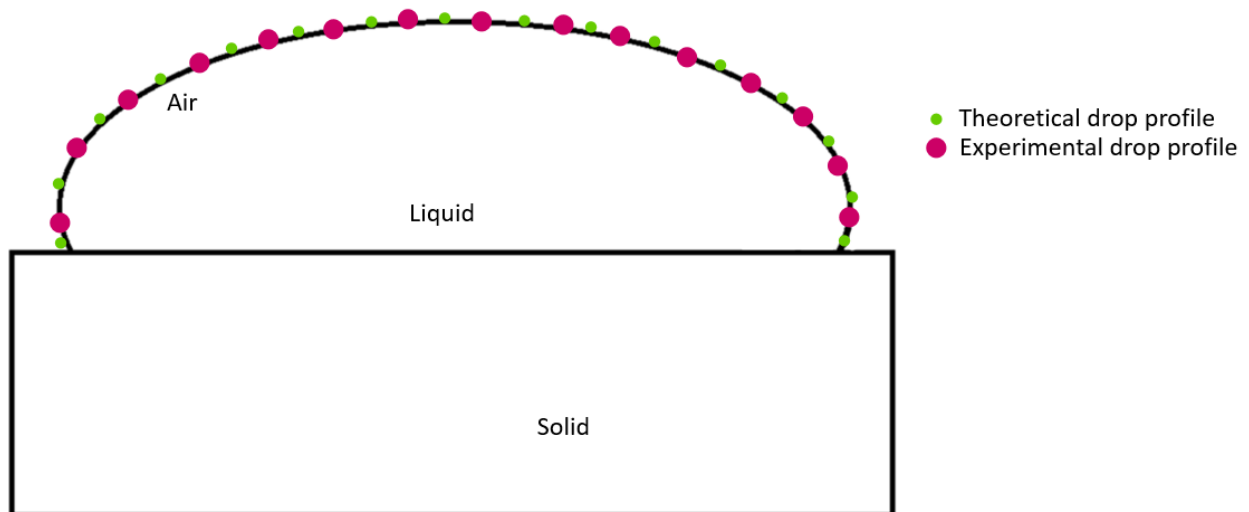


Figure 2-3 - Schematic of experimentally extracted and theoretical drop profile; frame of reference perpendicular to the contact plane of droplet and surface

The polynomial method for drop shape analysis fits a high order polynomial to the curve of a droplet on the left and right sides independently (see Figure 2-5). It does not use the entire profile of the droplet, but just measures in the vicinity of the contact points. This method only allows for the contact angle to be measured, not the surface tension; but unlike the ADSA-P algorithm, the polynomial algorithm can complete the measurement with the capillary still inside the droplet. [47]. This algorithm is very useful for contact angle and sliding contact angle measurements.

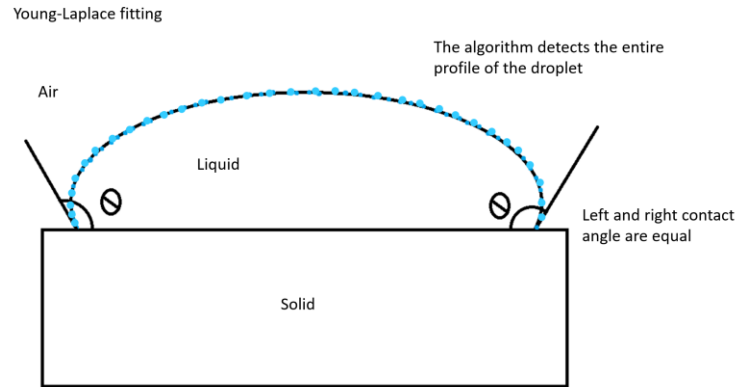


Figure 2-4 - Young-Laplace fitting; the dots representing the detected profile of the droplet; a needle/capillary cannot be present without it interfering with the fitting

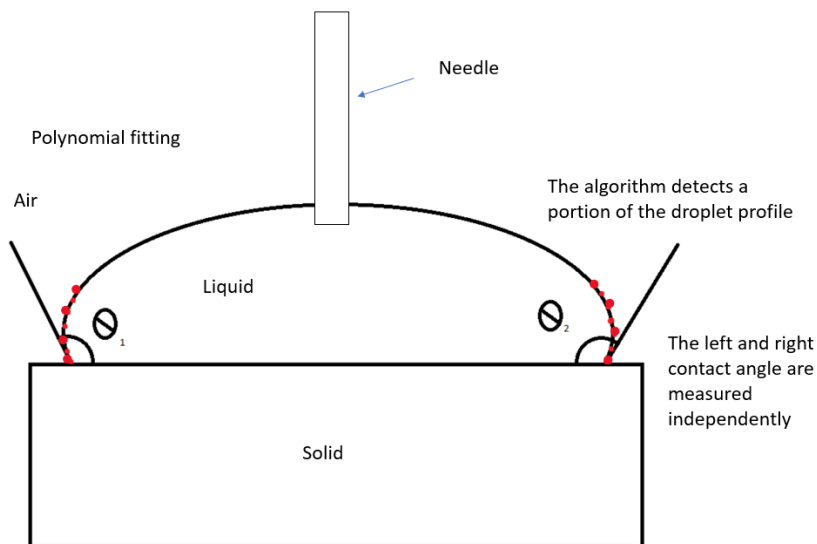


Figure 2-5- Polynomial fitting; The dots representing the detected profile; a needle/capillary can be present inside the droplet provided it is not in detectable range of the fitting algorithm

ADSA-D (-D stands for diameter) method uses the droplet diameter (contact or equatorial), its volume, and its surface tension to yield the contact angle of a droplet. This analysis is usually done using the perspective taken above the droplet, rather than the side view to the droplet as with ADSA-P [49]; seen in Figure 2-6. ADSA-D is reliant on the accuracy and precision of all its individual variables in order to estimate the shape of the droplet. This is due to the fact that the top view of the droplet only confers the apex diameter of the droplet, and considering that a sessile droplet's shape is influenced by a variety of factors such as gravity (becomes critical when the droplet is sufficiently large) and the presence of an electric field, there is a large margin of error when attempting to model the shape of a droplet since it fundamentally relies on its variables to take into account the potential shape of the droplet in order to yield its contact angle [49].

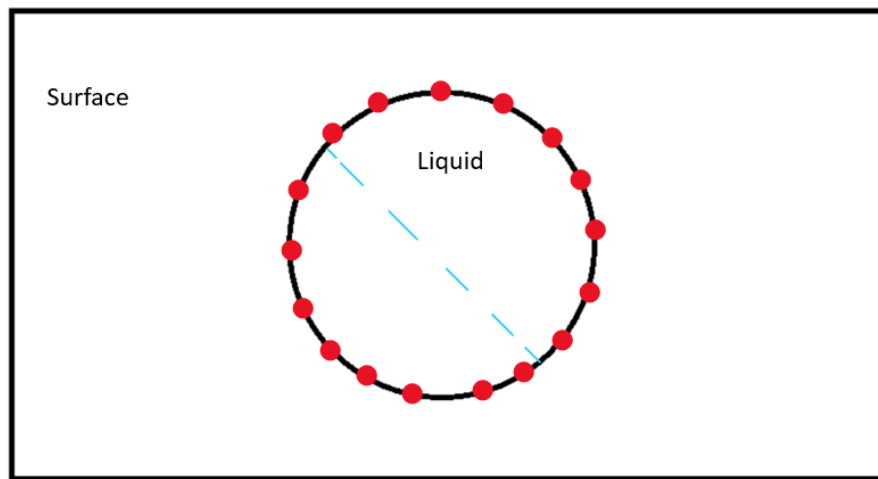


Figure 2-6 – ADSA-D method, the diameter (represented by the dashed line) is extracted from the profile of the droplet's top view (represented by the solid circle) using edge detection, represented by the dots

This thesis will mainly use ADSA-P for surface tension; and both ADSA-P and polynomial for contact angle measurements.

2.4 - Design methodologies

Design methodologies are useful engineering tools that aid in the design process, by providing both a framework for the design at various phases; as well as designing towards certain desired characteristics/metric. Examples of design methodologies include the Boothroyd-Dewhurst method, the Hitachi method, the Lucas method, and the quality function development (QFD) method.

The Boothroyd-Dewhurst, Hitachi, and Lucas methods are both mainly design for assembly focused design methodologies, for production [50] [51]. Thus, the QFD was chosen as the design path, since it is more oriented towards component and product design.

The QFD approach is a design methodology used as a road map for the engineering process. It uses a system of matrices, with the output of one matrix feeding into another. This is done by the matrix taking in two inputs; a set of inputs with known weighting with respect to each other for the first column, and another set of inputs with no weighting for the first row of the matrix. The first row and column are compared to rank, if there is any relationship between them. The output of this matrix is a set of weights for the first-row input (Figure 2-7).

This design methodology takes the instinct out of the design process and reveals the relationships each design parameter has on the effect on each other parameter, as well as the system as a whole. This methodology was originally developed in Japan, in order to translate the voice of the customer into actual engineering parameters. For this thesis, the product planning, parts development, and sub system matrices were used.

		Second inputs
First inputs	Weights for first inputs	Relationship: Strong, Moderate, Weak, None
		Weights for second input

Figure 2-7 - House of quality template; is a matrix that uses two inputs. The first input set with known numerical values that define the weight/importance of each input parameter; and a second set of inputs with unknown weights. The two inputs sets are compared, with the parameters of the second set given a relationship ranking with the first set. The output of this matrix is the weighting of each parameter for the second input set.

2.5 - Control systems

A control system is necessary to automatically to reach and maintain a certain set point; these can include temperature [52] and RPM [53]. Two of the most commonly implemented control systems are Proportional-Integral-Derivative (PID) and Bang-bang.

2.5.1 - PID

The Proportional-Integral-Derivative in PID are the three parameters the govern the system. The basic concept of a PID is to define a set point for the system to reach, and the PID implementation resulting in adjustments in the inputs to drive the output to reach the set point. A reading of the system is done after a predefined sample time has passed, and the error term (difference between the current value and the setpoint value of the system) calculated. This error is then fed into the PID algorithm, and the PID adjusts its output depending on how far the reading is to the set point. This is repeated until the error term becomes close to zero [53]. The output of the PID is defined by the following equation:

$$y(t) = K_p e(t) + K_I \int_0^t e(t) dt + K_d \frac{de(t)}{dt} \quad 2.2$$

where $y(t)$ is the PID output, $e(t)$ is the error, and the tuning constants; K_p , K_i , and K_d for the Proportional Integral and Derivative systems respectively [54]. PID was used as a closed loop control algorithm to control the temperature inside the chamber. This allows for automatic control to settle at the desired setpoint. The advantage for this algorithm is that it can compensate for changes in the initial conditions. Chaos theory dictates that small changes in the initial conditions results in large variances in later states [55] [56]; thus a lookup table style system would be ineffectual for controlling the temperature inside the chamber, since the chamber is meant to be a portable device used in different environments. The PID is able to take into account the initial conditions and control the temperature systems inside the chamber to reach steady state in a reasonable amount of time.

For a PID system to be implemented, the following parameters must also be defined.

- Set point: the desired final numeric state of the system (e.g., temperature, RPM, pressure, brightness)
- Output: A controllable numeric parameter that the PID can manipulate (e.g., voltage, luminosity)
- Reading: a numeric reading of the current state of the system
- Error: the difference between the current reading and the setpoint
- Sample time: the time between every iteration of the PID

The Proportion term handles the magnitude of error at that specific point in time, and is the main driving force in the initial stages of the PID loop. The larger the error, the larger the proportion response in increasing the output value. The main weakness of a proportion controller is that it cannot eliminate

the steady state error for some systems [53]. An example of this is electrical heating using voltage control for the heater; as the error between the reading and set point reaches zero, so does the voltage output for the heater. At this point, the temperature will start to drop and the proportion controller will once again calculate a non-zero value for the output. Thus, there will always be a steady state error.

Integral controls the steady state error, by taking into account the past error values with each iteration of the PID; the integral value will continuously increase until the steady state error is zero [53].

Derivative takes into account the rate of change of the error, and is the driving force to stabilize the system. This term is mainly in charge of blunting the overshoot of the system, by either adding to or subtracting from output value, depending on the speed of the approach to the setpoint [53].

The magnitude of the effects of each parameter are based on three the tuning constants; K_p , K_i , and K_d ; as well as the sample time s [57]. Changing these parameters has an effect on the rise time, overshoot, settling time, and steady state error of the system. Table 2-A shows the effect on increasing each contestant has on the systems response [58] [59].

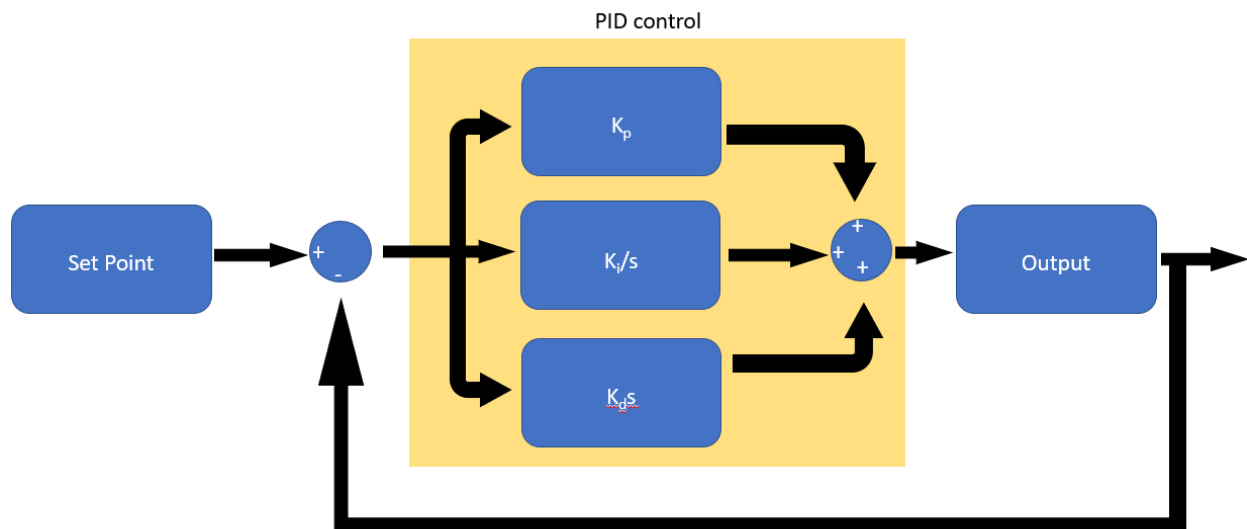


Figure 2-8 - PID Visualization; illustrates the components and flow of the closed loop system. The input for the PID is the numeric difference between the setpoint and the current state of the system. The input is then used to calculate the proportion, integral, and derivative terms, which the summation of is the output of the system. This output then changes the current state of the system; thus, completing the loop. This process is repeated until the current state of the system is equal to the set point.

Table 2-A - Effects of increasing tuning parameters on the PID control output

	Rise time	Overshoot	Settling time	Steady state error
K_p	Decrease	Increase	Small change	Decrease
K_i	Decrease	Increase	Increase	Eliminate
K_d	Increase	Decrease	Decrease	No Change

2.5.2 - Bang-bang

Bang-bang control is one of the simplest and cost-effective control systems to implement [60]. The control system will swap between two states, in order to reach a desired outcome. A common implementation for this system is the On-Off approach; where the bang-bang controller has predetermined on and off conditions, switching between the two when the conditions are met. These can be implemented in temperature control, flow control, and speed control.

2.6 - Review of other chambers

A review was done of environment chambers that are either commercially available or found in literature. This was done to both gain an understanding about the fundamental components necessary for a system, as well as find what can be improved. The results of the review of chambers was that a system with Peltier and ultrasonic atomizer were the most optimal components.

Peltier cells are the quickest and most cost-effective method of temperature control for such applications, as they can both inject and extract temperature depending on the direction of current flow. Note, it requires a secondary heat dissipation system (either heat sink and fan or water-cooled system) or there is a risk of heat buildup in Peltier cell leading to its failure.

Ultrasonic humidifier: using a piezoelectric transducer to create mist. Essentially using vibrations to break the liquid into very tiny droplets, very easy to implement, since it effectively turns a liquid into an aerosol.

Table 2-B - Review of chambers found commercially or in the literature (continuous on the next page)

Chamber	Observations	What can be improved
<p>Kruss:</p> <p>Peltier Temperature chamber TC40 with humidity chamber add-on</p> <ul style="list-style-type: none"> • 132 × 132 × 27 mm (W × D × H) • -30°C to 160°C • Relative humidity (without insulating hood): 15 to 85% at 22 °C, up to 89% at 10 to 15 °C, up to 5% at 70 to 90 °C • Inert gas used to prevent condensation 	<ul style="list-style-type: none"> • The temperature is controlled by the Peltier for the temperature control chamber only. 	<ul style="list-style-type: none"> • it requires an external chamber connected in series to generate the humidity, and the Peltier disabled; instead, an external thermostat chamber is used to control the temperatures in both chambers. • Requires insert gas line
<p>Data physics</p> <p>TFC 100Pro</p> <ul style="list-style-type: none"> • Liquid temperature control • Maximal sample dimensions (L x W x H): 93 mm x 93 mm x 24 mm • -10°C to 100°C (depending on working fluid) 	<ul style="list-style-type: none"> • Requires external humidity generator addon • 3 windows 	<ul style="list-style-type: none"> • requires dry gas line for anti-condensation on windows • Requires large external source for liquid temperature control
<p>Data physics</p> <p>TPC 160</p> <ul style="list-style-type: none"> • Peltier temperature control with liquid cooling • 94 mm x 94 mm x 24 mm • -30°C to 160°C • Relative humidity: 5% to 90% at 25°C, 10% to 85% at 85°C 	<ul style="list-style-type: none"> • Water cooled peltier • 3 windows 	<ul style="list-style-type: none"> • Requires external water source to keep cool • Requires external humidity generator

<p>Rame hart Peltier Environmental Chamber</p> <ul style="list-style-type: none"> • Peltier temperature control • 81 x 55 x 44 mm • -50°C to 150°C 	<ul style="list-style-type: none"> • Peltier is water cooled instead of convective cooling 	<ul style="list-style-type: none"> • Does not feature humidity control • Requires external source for water cooling
<p>Rame hart Advanced Chamber with Temperature and Humidity Control</p> <ul style="list-style-type: none"> • Maximum specimen size diameter 6 in 	<ul style="list-style-type: none"> • Thermal resistors for heating • ambient to 85°C, or 230°C with humidity • Relative humidity, 0 to 100% • Ultrasonic humidity control 	<ul style="list-style-type: none"> • Incredibly large • Requires water or refrigerant line for temperatures below ambient
<p>Literature [61] Vacuum chamber for experiments in water vapor environment</p> <ul style="list-style-type: none"> • Chamber dimensions unknown, can support droplet volumes of at least 10 μL 	<ul style="list-style-type: none"> • Heating coil that's partially submerged in a pool of water • Range between 36°C to 100°C • No humidity control mechanism, but humidity never below 76 %RH 	<ul style="list-style-type: none"> • Small sample size • No humidity control system
<p>Literature [62] Development of a low-cost mini environment chamber for precision instruments</p> <ul style="list-style-type: none"> • 1000x1000x1000 mm • Range unknown, can hold temperature at 20°C \pm0.02 	<ul style="list-style-type: none"> • 9 Peltiers in a matrix above the chamber; natural convection is used to cool the chamber • Silica gel used to dehumidify chamber • Mini dehumidifiers used inside chamber to lower humidity 	<ul style="list-style-type: none"> • Mainly cooling and low humidity focused design

Although the systems in Table 2-B are similar in either sample size and temperature/humidity ranges to the desired design, they lack portability; and are meant to be integrated into proprietary systems. These chambers also cannot be customized for specific experiments, such as having a customizable lid to allow multiple droplets generated at once. The review was done for both inspiration and to find areas of improvement in available designs, to build a unique portable chamber.

The main focus on portability manifested in creating a standalone system that can function without the need of external intake sources and control systems. The commercially available chambers require either or a combination of inert gas for anti-condensation, a continuous source of liquid coolant for either the peltier or to cool the chamber below ambient, and an external control system such as a PC to control and function.

Tradeoffs and concessions had to be considered when designing the chamber to create a portable system; and can be separated into the following categories: anti-condensation, temperature control, humidity generation, and electronic control system/interface.

For anti-condensation, the goal was to circumvent the need for an inert gas intake; and instead use a solid-state anti-condensation system.

Rather than having temperature control being separated into heating and cooling components, a combined system is the more optimum solution, particularly for cooling. The goal is to create a cooling system without the need of having a coolant intake. This is not a focus for heating since all of the commercially available systems utilize solid state heating.

Humidity generation requires an external water source regardless of the system used, however the volume required is minimal for the desired range. Unlike for a cooling system, only a finite amount of water is required to reach the desired humidity level, rather than continuous amount of water for cooling. Therefore, a portable humidity system needs to be designed.

One of the main weaknesses of the available systems is that they require a PC to control the chambers, and a camera setup for image acquisition. Considerations have to be made about the control system, such that it can be integrated into other imaging systems, as well as its own custom system.

Chapter 3 - Mechanical Design

A design methodology was utilized in order to remove human instinct from the design process. This gave a defined framework and path to a functional final product. This process is described in detail in this chapter.

3.1 - Design plan

With the Peltier and the ultrasonic atomizer chosen as the fundamental components, the rest of the design process revolved around creating a design to utilize them to meet the desired outcome and feature for the environment chamber.

3.1.1 - Outline of design

An iterative process was followed for both the conceptual and physical design of the chamber.

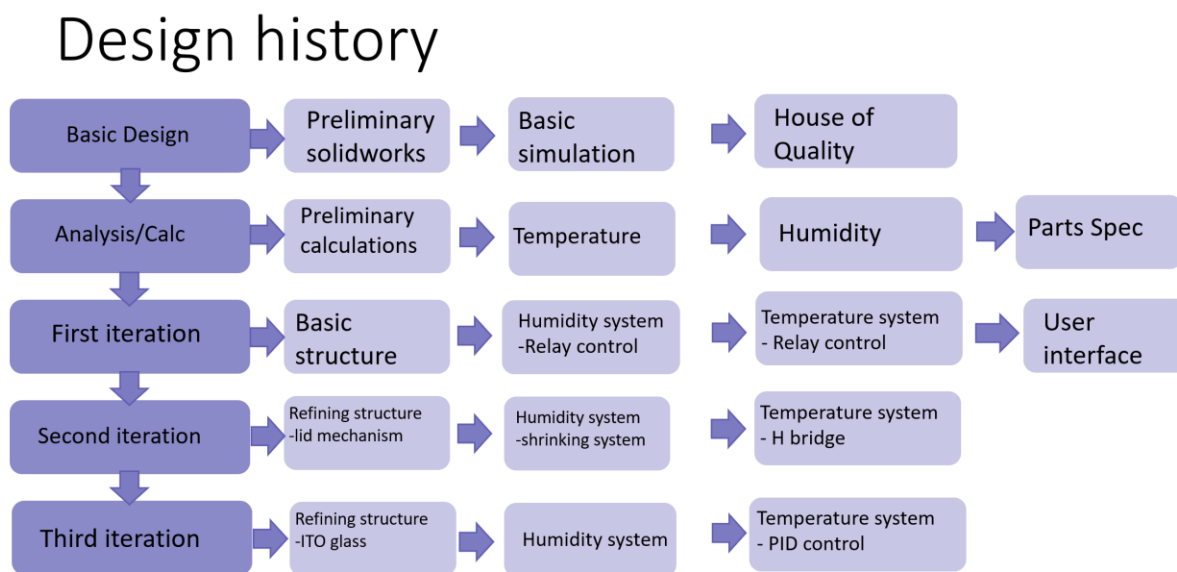


Figure 3-1- Summary of the design history of the chamber. The first column shows the chronological history of the design stages from the basic design to the third iteration. The rows show the chronological history of the steps taken at each stage.

Figure 3-1 gives a generalized map of the design history in this work. It illustrates the iterative nature of designing an instrument; with every iteration refining the design and adding more layers of control and complexity. The literature review gave insight into possible components for the system, which helped with the initial design; and choosing the fundamental components. The fundamental components were

those meant to be the core of the design, as they are fundamental to the function of the end product. The literature review also helped in identifying what could be improved in the available or previously made systems.

3.1.2 - Scope of work

The following is a list required features and limits that had to be achieved with the design

- Temperature range from 10 °C to 70 °C
- Reach temperature setpoint within $\pm 1^\circ$ C in less than 1 hour
- Humidity range from ambient to 80 %
- Reach humidity set point within ± 5 within less than 1 hour
- Chamber suited to image acquisition (Transmittance > 80%)
- Chamber large enough for standard substrate (3x1 in)
- Overall Portable chamber

For normal liquids, water has one of the highest surface tension values making it the preferred probing liquid in science and technology [63]. This was one of the main deciding factors for the temperature range; the instrument should envelope as much of the temperature range for water as possible. If the range or water can be covered, then most normal liquids can also be covered.

Although the volume of the chamber is mainly to accommodate the size of a standard substrate , the main area of focus is the center of the chamber. thus, the temperature and humidity limits only correspond to near the center of volume of the controlled environment inside the chamber, not the inner corners or edges inside the chamber.

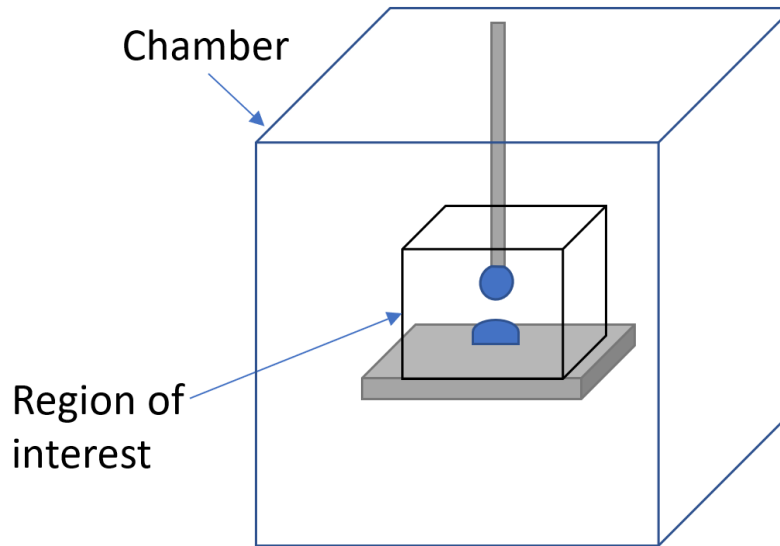


Figure 3-2 - Schematic showing the region of interest for the chamber. The goal of the chamber is to have homogeneous temperature and humidity conditions in the volume marked the region of interest, where the droplet will be located.

3.1.3 - Fundamental building blocks

The desirable features in a product are found through customer surveys in a usual QFD study, however, in this case they were gathered by researching similar systems and gathering a list of product requirements. Also, our own in house brainstorming and collective experience with requirements in scientific studies discussed earlier. Simultaneously, this also allowed into research into what features do not exist in the market.

One of the main characteristics of this design is its portability. The common anti condensation system used in available chambers uses inert air constantly sprayed on the glass walls inside the chamber. This requires either a gas line or portable canisters, while also having the potential drawback of contaminating the environment inside the chamber. The proposed system was instead built around Indium Tin Oxide (ITO) glass as one of the fundamental components, as a means of solid-state anti condensation as well as a secondary heating source for the system. ITO glass can work as a heating element when voltage is applied; considering dew point, at 100 %RH, the temperature of the surface must be greater or equal to the temperature of the air to prevent condensation. Thus, the ITO glass can be used as both an anti-condensation system as well as a booster system for the heating system of the chamber when needed. The use of ITO glass, a novel aspect that is implemented in this work.

Another fundamental component chosen was a thermal electric cooler, also known as a Peltier. Peltier is the quickest and most cost-effective method of temperature control, as it can both inject and extract heat depending on the direction of current flow; but requires a secondary heat dissipation system (either heat sink and fan or water-cooled system) or there is a risk of heat buildup in Peltier leading to failure. The secondary heat dissipation system was chosen to be a heat sink and fan assembly, rather than a liquid cooling system. This would allow for simplification of the design, since it eliminates the need for an external liquid cooling sources, allowing for a portable design.

An ultrasonic atomizer was chosen for the fundamental component of the humidity system, for its cost effectiveness and ease of implementation, when compared to the water boiling method for humidity generation. As such, a portable humidity system with a portable reservoir is a viable solution.

Lastly, rather than having a chamber that only usable near a computer; a smart phone-controlled system would be a portable design. As such, the electronic components chosen must be able to eventually integrate with smartphone control.

3.2 - QFD approach - House of Quality

The fundamentals of the chamber have already been defined in Scope of work; thus, the main goal of the QFD process was to remove the gut instinct of the designers inherit bias; and to reveal the critical aspects for a successful design. As shown in Figure 3-3, this thesis will follow a four-step process in the QFD methodology. Step one is the pairwise comparison matrix, which will address the desirable features that are prominent in a standard environment chamber, by ranking them based on their importance to the end design. Step 2 is the level 1 QFD design requirements matrix, which addresses the desirable features from the first matrix, with controllable engineering parameters. Step 3 is the level 2 QFD system design matrix, which correlates the engineering parameters with the systems and components that will comprise the chamber. Step 4 is the level 2 QFD sub-system design matrix, which is used to address particularly complex systems in the design, by breaking them into a sub-system and analyzing it at a component level.

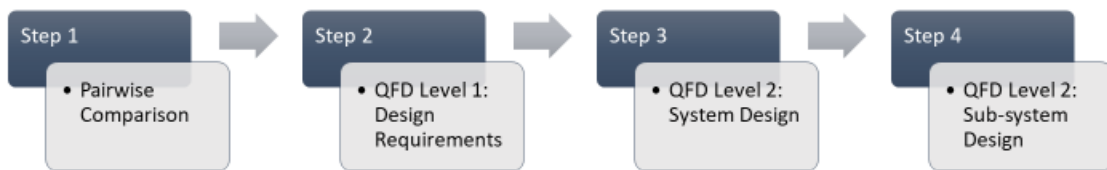


Figure 3-3 - QFD roadmap illustrates the flow of the QFD design process. Each step is a matrix comparing two sets of parameters. The output of one step becomes the input for the next step.

3.2.1 - Pair wise comparison

With the fundamental components set, the rest of the design was built around them. After researching and compiling the list of features, the next step in the design process was ranking the desirable features. A pairwise comparison was done in order to assign a weight to each feature by comparing them all to decide whether one component was more, less, or equally as important by assigning each condition with a numeric value (for details see: Appendix A - 1). The output of the pairwise comparison reveals the most important features that should be addressed as provided in Table 3-A - Results of pairwise comparison; and an explanation of each parameter is described below.

3.2.1.1 - Pairwise comparison parameters

The following is an explanation of each pair wise parameter; it should be noted that these parameters are more conceptual rather than quantitative metrics.

Temperature control auto (electronics/sensor based)

The system's ability to electronically reach a certain inputted temperature by automatically adjusting the heating system.

Temperature stability

The system's ability to maintain a set temperature (i.e., when lid is partially open for drop generation, the system must have an adequate response).

Humidity control auto (electronics/sensor based)

System's ability to reach a certain inputted relative humidity value.

Humidity stability

The system's ability to maintain a set relative humidity (i.e., when lid is partially open for drop generation, the system must have an adequate response).

Clear view of inside of chamber

A unobstructed view of the experiments inside for image capture and observation.

Easy to open and close lid

A mechanism for easily opening and closing of chamber lid, without compromising the stability of the environment inside the chamber.

Chamber size

Working space for experimentation; dictating the sample size hat the chamber can support.

Temperature control manual

User ability to manually adjust temperature by directly controlling the power source output.

Humidity control manual

User ability to manually adjust humidity by directly controlling the power source output.

Temperature setpoint speed

The ability for the system to reach a certain temperature in a reasonable time (thermal conductivity and insulation based).

Humidity setpoint speed

The ability for the system to create a homogenous vapor field in a reasonable time (orifice design based).

Stylish

Aesthetics of the design e.g. surface finish, corner and edge call outs, protruding fasteners, etc.

Needle entry

Generating droplets without compromising internal chamber environment.

Temperature range

Range of temperature capable for the system to reach and hold.

Humidity range

Range of relative humidity possible at a given temperature.

With the weighted sum of the pairwise comparison calculated, QFD uses the “house of quality” [64] matrix to establish relationships between the vague important features versus discernible engineering functional requirements/metrics of the environment chamber [64]. The functional requirements are parameters and features that can be controlled; and are as follows: power (wattage), sealing (of chamber), insulation, shape, size, thermal conductivity, temperature control system, humidity control system, weight, material, control system, and anti-condensation system. These general/broad metrics will be refined in subsequent matrices, for now they are chosen to capture the essence of the design.

Table 3-A - Results of pairwise comparison of features necessary for a functioning environment chamber

temperature control auto	8
temperature stability	11.5
humidity control auto	8
humidity stability	11.5
clear view of inside of chamber	10
easy to open and close lid	1
chamber size	8
temperature control manual	2
humidity control manual	2
temp setpoint speed	6
humidity setpoint speed	6
stylish	2
needle entry	5
temp range	10.5
humidity range	10.5

The results of the pairwise comparison immediately makes the most important parameters apparent.

The most significant parameters (highest weight): temperature stability, humidity stability, temperature

range, humidity range, clear view inside the chamber. The least significant parameters (lowest weight): ease of opening and closing the chamber, temperature/humidity manual controls, and style. Although these least significant parameters would be desirable, the main focus is on the minimum viable product for the system that can functionally be used for experimentation.

3.3 - Level 1 QFD-Design requirements

Using the resulting importance ranking of the pairwise comparison, the house of quality matrix was used to relate and establish the relationships between all the features and functional requirements (see Appendix A-1). The relationships have a weight rating of either strong, moderate, weak, or no relation with each other. This house of quality system allows for the ranking of the functional requirements based on how important each function is to the design features.

3.3.1.1 - Level 1 QFD – Functional requirements

The following are the functional requirements/engineering metrics used to address the desired features that were in input of the of the pair wise comparison. The functional requirements are controllable parameters that can be modified to address the desired features.

Power

The size of the power supply to power all the electronics (has a significant effect on the possible temperature range, as the necessary wattage is required to run the Peltier and ITO glass to their full potential).

Sealing

Sealing of the atmosphere of the environment chamber (greatly affects both temperature and humidity stability inside chamber).

Insulation

Thermal insulation used for the environmental chamber, to keep internal temperature constant.

Shape

Overall shape of chamber, e.g. cylindrical chamber, cubic chamber, window sizes, heat sink location, etc.

Size

Overall size of the chamber, what sample size and experimental volume can be supported.

Thermal conductivity

The thermal conductivity of the materials that make up the components of the chamber.

Heating system

Chosen heating system used to control the temperatures above ambient inside the chamber.

Cooling system (made redundant, combined with heating system in level 2 QFD)

Chosen cooling system used to control the temperatures below ambient inside the chamber.

Humidity system

Chosen humidity system used to control the humidity inside the chamber.

Weight

Overall weight of chamber.

Material

Materials chosen for chamber components of the chamber, e.g. For gaskets, bolts, spacers, adhesives, thermal paste, etc.

Control system

Microcontroller and sensors used.

Anti-condensation system

To allow for a clear view of inside of chamber from windows.

For the first matrix, the functional requirements in the matrix are then applied to each of the initial product characteristics, to find if they have either a strong, weak, or no relationship to each other. The output of this matrix is the ranking/weighting of each functional requirement.

As shown in Figure 3-4; the desired features from the pairwise comparison and the functional requirements are correlated in the matrix, using the relationship scale shown in Table 3-B. The output of this matrix is a technical importance rating or a weighing, for each functional requirement. Thus, the functional requirements are now ranked based on how important each one is in the entire design.

Table 3-B - QFD relationship weighting scale used in a QFD matrix to correlate the input parameters with known weighting and output parameters with unknown weighting

Relationships	
Strong	●
Moderate	○
Weak	▽

Relative Weight	Customer Importance	Maximum Relation	Customer Requirements (Explicit and Implicit)	power	sealing	insulation	shape	size	thermal conductivity	temp system		humidity system	weight	material	control system	anti condensation system
8%	8	9	temperature control auto	●					●	●					●	
11%	11.5	9	temperature stability		●	●		▽	○	○		▽		○	○	▽
8%	8	9	humidity control auto	▽				●				●			●	
11%	11.5	9	humidity stability		●	▽		▽	▽			●			○	▽
10%	10	9	clear view of inside	▽		▽	○	▽	▽					▽		●
1%	1	9	easy to open and close		●	▽	▽	▽								
8%	8	9	chamber size			▽	●	●	▽			▽	▽	▽		
2%	2	9	temperature control manual												●	
2%	2	9	humidity control manual												●	
6%	6	9	temp speed	●			▽	○	●	●					●	
6%	6	9	humidity speed	●			▽	○				●			●	
2%	2	9	stylish			▽	●	▽						●		
5%	5	3	needle entry		○	○	▽	▽								
10%	10.5	9	temp range	●	▽	●			▽	●				○		
10%	10.5	9	humidity range	▽	●			▽		●		●		▽		●
			Max Relationship	9	9	9	9	9	9	9	9	9	1	9	9	9
			Technical Importance Rating	297.06	329.41	240.69	135.29	226.96	196.57	342.65	0	336.76	7.8431	110.29	350	203.43
			Relative Weight	11%	12%	9%	5%	8%	7%	12%	0%	12%	0%	4%	13%	7%
			Weight Chart													

Figure 3-4 - Level 1 QFD matrix; comparing the desired features to the functional requirements, to generate a weighting for the functional requirements [65]

The results of the matrix indicated that firstly, the temperature and humidity generation systems should be one of the main focuses, as they are the two critical design requirements; hence, for the system level design, both these systems should be fragmented into their separate components. Secondly, the control system is critical to the design, and should be further split into separate systems for temperature and humidity since it is strongly related to both. This is due to the fact that the mechanism to control temperature and humidity both differ greatly from one another, thus it is more logical to create their control systems separately the control system encompasses both the software and electronic components. Thirdly, the power source is another major component that effects the range and speed of the response of the temperature and humidity systems, as well as the control systems for each; thus electronics used must be able to handle the required wattage. This is especially critical for the Peltier, as they require 60W for one Peltier.

Lastly, both the sealing and insulation is critical to the internal environmental stability of the system. They however are not systems in of themselves, as they are their own material or material property of the components. Thus, they are not given their own function in the level 2 QFD, but will be included in the subsystem design level.

3.4 - Level 2 QFD-System level

The weighted engineering functional requirements/metrics output of the level 1 QFD becomes the input of the level two QFD. The level two QFD compares the engineering functional requirements to chosen parts characteristics/system components chosen to address them. The system components are grouped into four distinct sub systems: humidity system, temperature system, mechanical system, and structure; and the components themselves are becoming less broad and more specific as the design slowly begins to take form.

The humidity and temperature systems have components that govern the source, delivery, dispersion, and control of their respective parameters. These two systems will be given their own sub system matrices to further refine them due to their complexity.

The mechanical systems govern any moving components or mechanical systems necessary for operation or experimentation, which simplifies to the lid and drop generation.

Structure encompasses the skeletal structure of the chamber itself; it is important to note that the ITO glass system is considered to be part of the chamber wall parameters.

3.4.1.1 - Level 2 QFD – System components

The following are the system components used to address the functional requirements from the level 1 QFD. The system components are physical components, systems, or features that will comprise the chamber.

Humidity source

Design of the refillable water tank and humidity generator.

Humidity delivery

Mode of humid air movement and piping.

Humidity dispenser

Method of dispersing humid air inside chamber.

Humidity control

Method of controlling the humidity inside chamber.

Heat source/sink

Design of heat generation/removal system.

Heat delivery

Method of heat conduction into chamber.

Surface area for heating chamber

Heatsink design for controlling temperature of chamber.

Temperature control

Sensors and control system .

Lid

Design of chamber opening mechanism.

Drop generation

Syringe entry system.

Chamber structure base

Base of chamber, where all components are mounted to.

Chamber walls

Walls of the chamber.

Chamber supports (skeletal)

Support structure of chamber.

Chamber volume

Working volume for experiments .

The output from the level 2 QFD reveals the following for each system.

The main focus of the humidity system is the method to homogeneously disperse humidity inside the chamber. Humidity distribution is critical for the ease of control and stability of the humidity system.

The main focus of the temperature system is the heat source/sink, which is essentially the heat generation system, with the is main component being the high powered Peltier. The electronics driving it must be able to withstand the required wattage, for both the Peltier and the secondary cooling system to dissipate the access heat generated to prevent damage to the Peltier.

The main focus of the mechanical system is the drop generation mechanism. This system must be able to generate a droplet inside the chamber, without compromising the steady state conditions of the environment generated inside the chamber.

The main focus of the structure is the chamber walls. The chamber walls include the chambers skeletal support structure as well as transparent windows for w view inside the chamber. The walls dictate the quality of the images that can be acquired from a sample inside of the chamber, from outside the chamber. The chamber walls also account for a significant percentage of the surface area of the chamber, thus must be insulated to prevent heat transfer with the environment.

Two iterations of a prototype (see Figure 3-6) was created at this point in order to gauge the effects and relationships of each component; before starting the level 2 subsystem design matrix, as well as creating the preliminary code for the PID system and gauging the number and placement of the sensors.

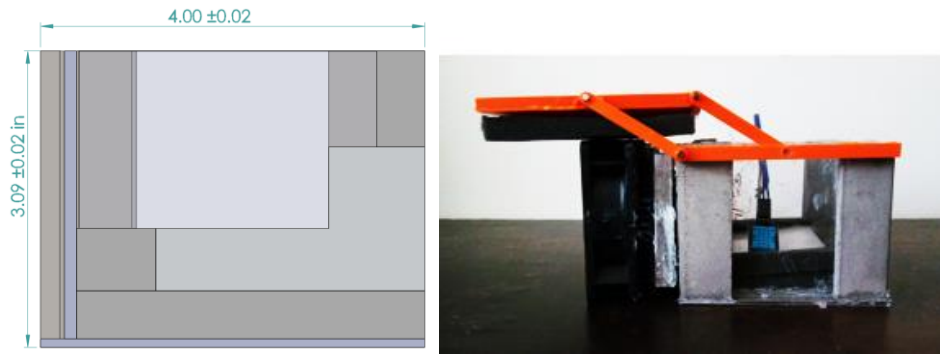


Figure 3-6- Initial prototypes; the first iteration on the left and the second on the right. Tests run with the two prototypes were critical in aiding the design process, as they gave insight on the relationship between the different components in the system. The dimensions shown apply to both iterations, not show is the depth which is 4 in.

With the knowledge gained from the prototypes, the sub system QFD matrix was created to quantify the significance of each sub-system component.

3.5 - Level 2 QFD-temperature sub system

The results of the two prototypes indicated that the temperature control system should be isolated further broken down into a sub system analysis; allowing for the correlation of specific components, to find the main area of focus for a successful design. The analysis consists of components only directly related to the heating and cooling of the chamber.

The sub system component parameters are as follows:

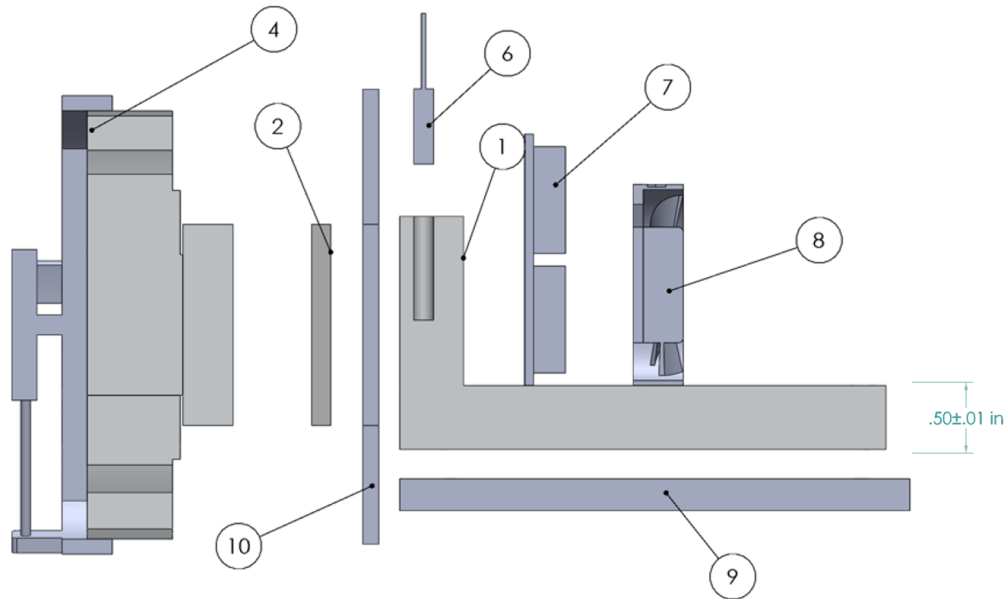
- Heating/cooling system: The Peltier and its supporting heat sink to remove excess heat
- Insulation: the insulating material in direct contact with the heating system
- Material of heat sink inside chamber and shape of heat sink: the part that conducts and disperses the heat into the inside of the chamber. This is mainly referred to as the L heat sink in the documentation
- Temperature sensor: the range and accuracy of the sensors
- Micro controller: the capabilities of the controller
- Joining: the method and material used to fasten all the components

Row #	Weight Chart	Relative Weight	Customer Importance	Maximum Relationship	Customer Requirements (Explicit and Implicit)	Functional Requirements	oHeating/cooling system	oIsolation	oMaterial of heat sink inside chamber	oShape of heat sink	oChamber shape	oTemp sensor	oMicrocontroller	oPID	oJoining	
1		39%	611	9	• Heat source/sink		●	▽	▽							▽
2		21%	332	9	• Heat delivery		▽	●	●	○	▽	▽				
3		17%	267	9	• Surface area (for heating chamber)		▽		○	●	▽					
4		23%	368	9	• Temperature control		●	●	▽	○	○	●	○	●		▽
					Max Relationship		9	9	9	9	3	9	3	9		1
					Technical Importance Rating		596.5	437.79	301.92	285.39	107.94	231	69.997	209.99		62.062
					Relative Weight		26%	19%	13%	12%	5%	10%	3%	9%		3%
					Weight Chart											

Figure 3-7 - Level 2 QFD matrix, the features related to temperature control inside the chamber are further analyzed by breaking them down into their baser components

The results of the thermal subsystem design (Figure 3-7) indicates that the thermal generator is the most important component in the system. Practically, the thermal generator encompasses the Peltier, its heat sink, and its heat dissipation system. This is particularly important for reaching temperatures below ambient; as the cold side temperature of the Peltier is dependent on how low the hot side temperature of the Peltier can be maintained. Figure 3-8 and Figure 3-9 show the resulting design created from the subsystem analysis. The critical thermal generator parameter was addressed with a high power/high temperature Peltier. The insulation is addressed in Figure 3-8; where the part labeled “inner heat sink” (item 1 in Figure 3-8 and Appendix B, drawing 8) is critical to controlling the temperature inside the chamber. This component acts as the heat exchanger between the inside of the chamber and the Peltier, and must be isolated from the ambient environment to prevent heat loss and promote effective heat transfer. This is done with a combination of insulating material and air gaps. Heat sink in has two faces in direct contact with other components; the bottom face that is bolted though insulating PTFE (item 9 in Figure 3-8 and Appendix B, drawing 3) with PEEK bolts, and the other face that is in direct contact with the Peltier (item 2 in Figure 3-8, Note: thermal paste is used to improve the conductive heat transfer with the Peltier) that is surrounded by closed cell insulation (not shown).

The rest of the faces are either meant to heat the chamber through natural convection or are separated from other features with an air gap.



Item No.	Part name	Manufacturer/supplier	Manufacturer code	QTY.
1	Inner heat sink	Custom	-	1
2	Peltier	Larid	ETX6-12-F1-4040-TA-RT-W6	1
4	Heat sink and fan	Delta	FHS-A9025S19	1
6	RTD Peltier	Adafruit	PT100	1
7	Adhesive-mount heat sink for surfaces	McMaster Carr	8822T13	1
8	Low-voltage equipment cooling fan	McMaster Carr	1939K17	1
9	PTFE base	Custom	-	1
10	PTFE back plate	Custom	-	1

Figure 3-8 - Temperature control system cross section and bill of materials

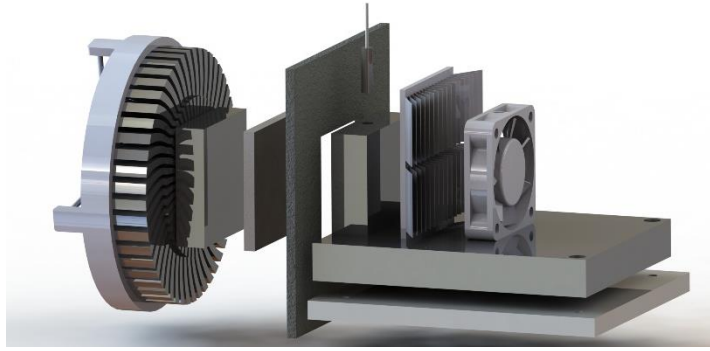


Figure 3-9 - Isometric render of temperature control system, see Figure 3-8 for details

The parameters “material heat sink into chamber” and “shape of heat sink” in Figure 3-7 refer to the material and shape of the part “inner heat sink” (item 1 in Figure 3-8). A material that has high thermo conductivity was needed for “inner heat sink”, as well as corrosion resistance as the inside of the chamber would go through multiple moisture and thermal cycles. Thus, aluminum was chosen as it meets both criteria [66]. The shape of “heat sink in” was chosen for a variety of reasons. Firstly, it was decided early in the design that Peltier would be located on one of the vertical walls, and not on the bottom of the chamber; as to allow better integration with existing contact angle goniometer systems (since systems from Kruss and Ramehart have limited range for their vertical platforms; see Table 2-B), as well as allow for easier integration of the thermal management “heat sink and fan” part (item 4 in Figure 3-8) for the Peltier. Particularly for “heat and sink fan”; as it accounts for nearly a third of the chambers overall size; having it protruding from one of the walls was convenient as increasing or decreasing the size of this part would not affect the usability or functionality of the overall chamber. Thus, the optimal shape for “inner heat sink” would be an L shaped aluminum extrusion, as it allows for both heating the chamber from base and cooling from a vertical wall with natural convection. “Inner heat sink” would be made from an off the shelf L-extrusion machined to meet the tolerances and surface specifications. Before “inner heat sink” was manufactured, preliminary simulations were done in order to gauge the effects of varying the thicknesses and size of some features; and how it affects the way heat is distributed inside the chamber. Very basic simulations were done for gathering preliminary data to manage the expectation of the system and help with the intuition of what to expect from the preliminary ideation. Thus simple simulations were done to compare the results with each other, to gauge whether more material or more machining could be justified for the part. A sample of these simulations is shown in Figure 3-10.

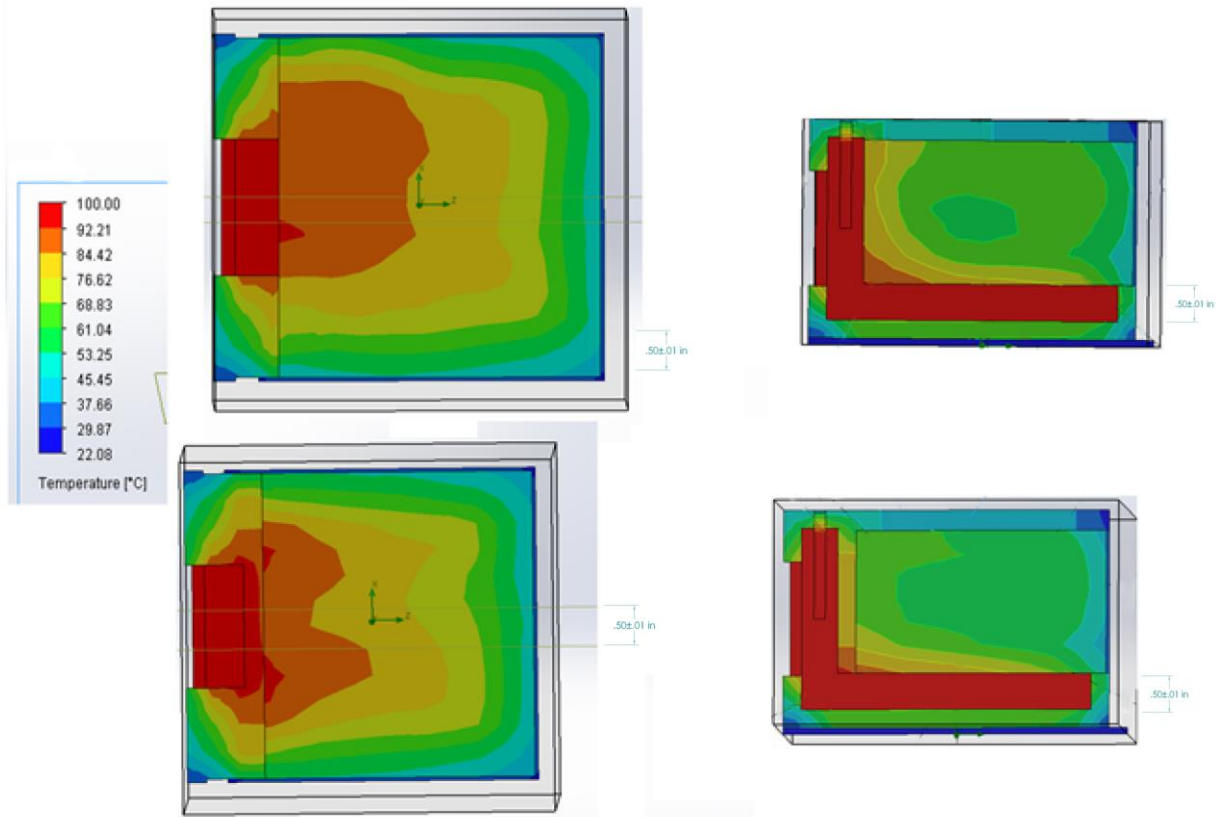


Figure 3-10 - Sample preliminary simulations to gauge the effects of modifying the chamber on the temperature distribution inside the chamber. The top view is on the left and the side view on the right. The boundary conditions are as follows: boundary type is outer wall, external air temperature was 22°C, and adjacent wall heat transfer coefficient is 0.025 N/s/mm/°C. the governing equation is the Navier-Stokes equation

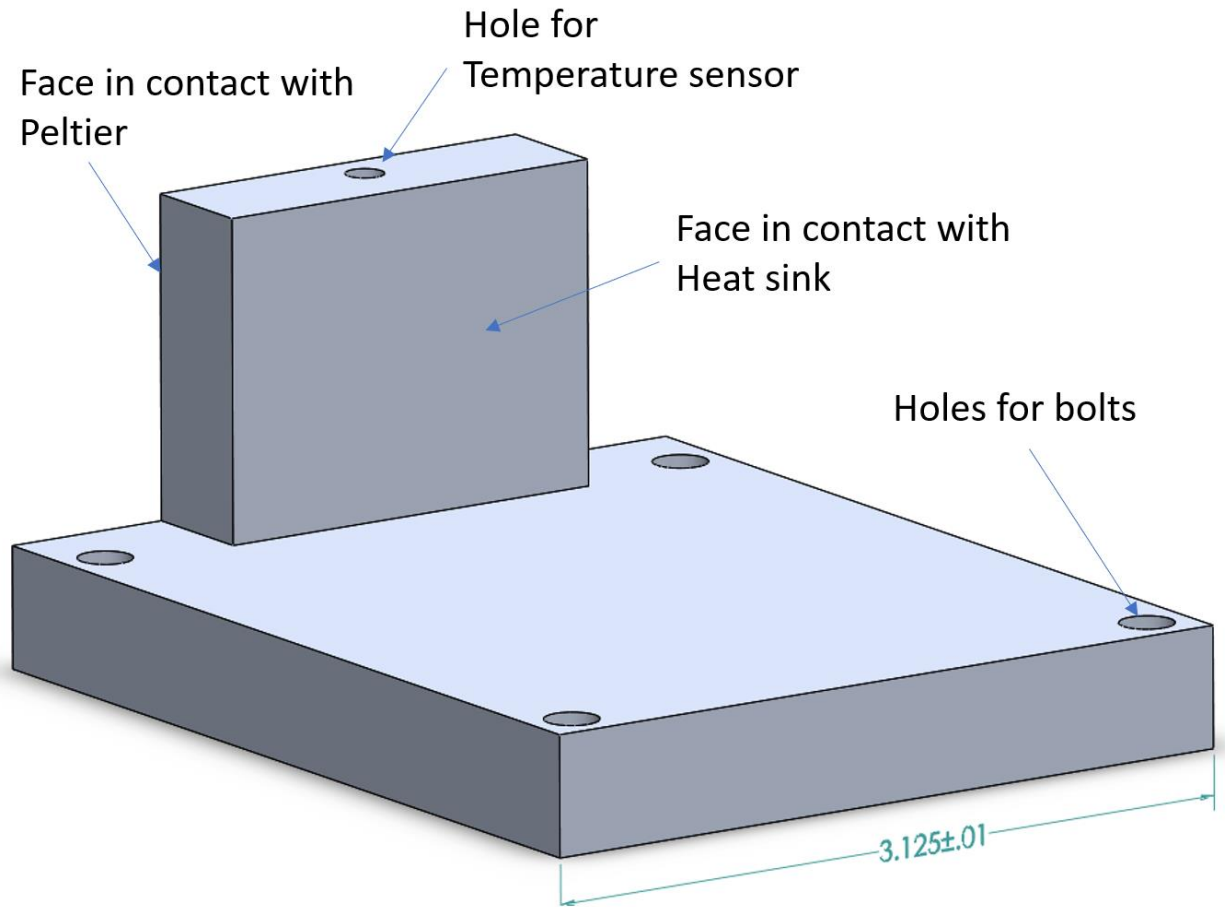


Figure 3-11 - Resulting design of "inner heat sink" after multiple simulations, the scale is in inches

Figure 3-11 shows the resulting design of "inner heat sink" after multiple simulations. This design is optimized for transferring the heat from the vertical wall to the floor of the chamber to allow the chamber to be even heating of the chamber with natural convection. This shape has the added bonus of being an off the shelf standard extrusion, thus greatly reducing the cost of material and machining when compared to an equivalent aluminum block.

3.6 - Level 2 QFD-humidity sub system

The results of the humidity subsystem design in Figure 3-12 indicates that the humidity sensor, control system, and piping system are critical to a successful design. Figure 3-13 shows the resulting design created from the subsystem analysis. All parts are off the shelf components, which are the atomizer, the pipes, the water reservoir, and the air pump. Humidity control does not require much complexity, as the system relies on pumping small bursts of humid air into the chamber. The natural diffusion of humid air evenly distributes the moist air inside the chamber. Thus, only an ultrasonic atomizer and pump are the

main components governing the system; as they control the volume and flow rate of moist air into the chamber. The atomizer and pump were chosen not just for their capabilities, but also their size. A 24W ultrasonic atomizer was chosen, for both its power and for size considerations. Higher wattage variants were larger than the chamber itself, negating the portability aspect of the design. The smaller lower wattage atomizers proved unreliable due to the limited water depth to allow it to function.

Row #	Weight Chart	Relative Weight	Customer Importance	Maximum Relationship	Customer Requirements (Explicit and Implicit)	oWater chamber	oHumidity generator	oPipe system	oHumid air mover	oorifice design	oHumidity sensor	oMicrocontroller (resolution)	oControl system	Joining
1		27%	311	9	• Humidity source	○	●							
2		17%	196	9	• Humidity delivery	▽	○	●	●	▽	●	▽	●	▽
3		33%	373	9	Humidity dispenser (homogenous distributi			●	○	●	●	▽	●	○
4		22%	252	9	• Humidity control		▽	●	●	●	●	▽	●	○
Max Relationship						3	9	9	9	9	9	1	9	3
Technical Importance Rating						99.646	321.22	653.03	455.31	514.44	653.03	72.559	653.03	183.03
Relative Weight						3%	9%	18%	13%	14%	18%	2%	18%	5%
Weight Chart														

Figure 3-12 - Level 2 QFD matrix, the features related to humidity control inside the chamber are further analyzed by breaking them down into their baser components

In the first iteration, a 96mW DC fan was used to move the moist air though the pipes and into the chamber, however this proved not powerful enough to fully utilize the capability of the atomizer. The fan could not be scaled up without increasing the size of multiple components; thus a vacuum pump was chosen to replace it, as it was not significantly bigger than the fan, but was more powerful. This allowed for a greater volume of humid air to be pumped into the chamber, improving the response rate of the humidity system.

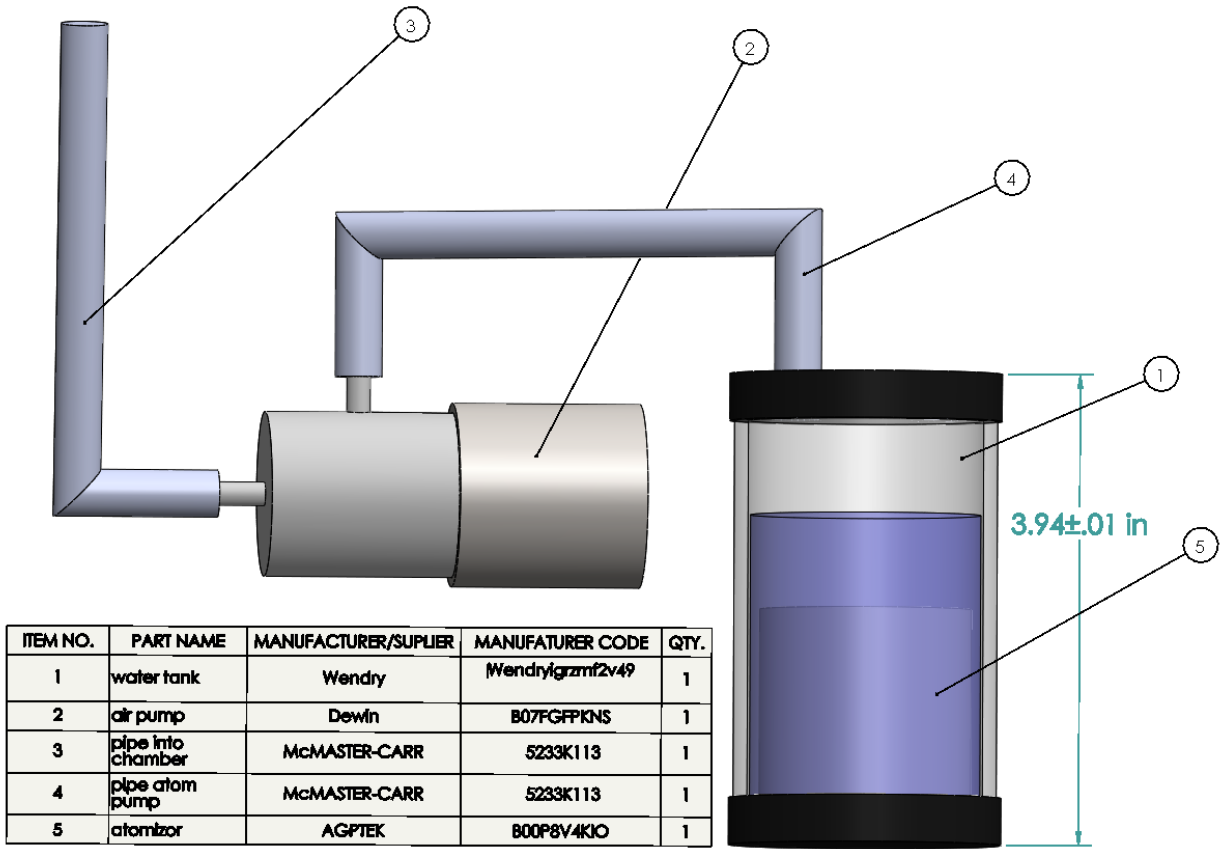


Figure 3-13 - Humidity control system and bill of materials

3.7 - Final Design

3.7.1 - Overall design

The overall design shown in Figure 3-14 has both the temperature and humidity systems integrated into the main chamber (see external CAD files package labeled “original chamber”).

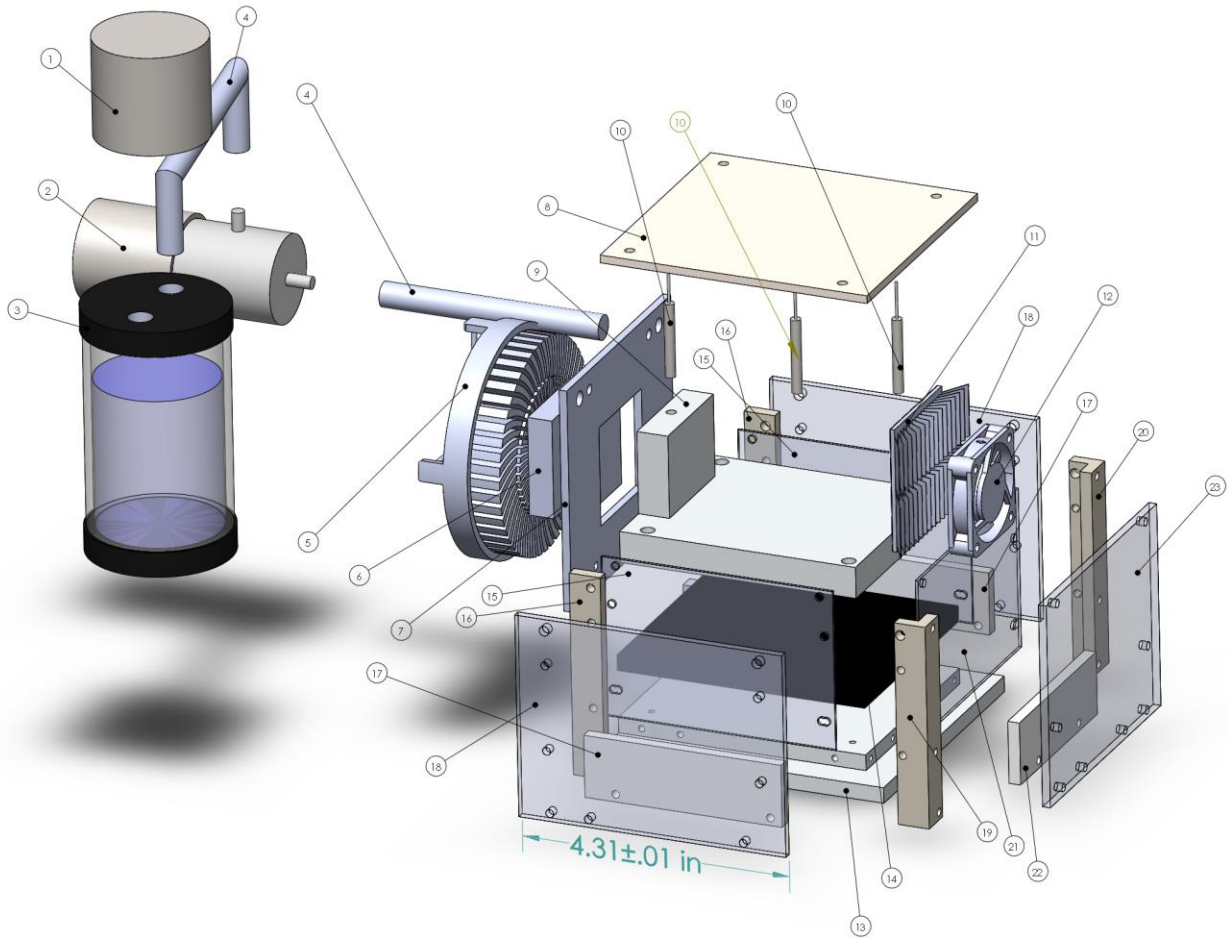


Figure 3-14 - Exploded view of chamber; for label description see Table 3-C.

3.7.2 - Breakdown of important components

The following is a detailed breakdown of the various components used in the design; including the parts making up each component, the logic behind the material selection, the roles of each part in the functionality of the design, and how the parts are fastened.

Table 3-C – Bill of materials for Figure 3-14

Item No.	Part name	Manufacturer/supplier	Manufacturer code	QTY.
1	Atomizer	AGPTEK	B00P8V4KIO	1
2	Air pump	Dewin	B07FGFPKNS	1
3	Water tank	Wendy	Wendryigrzmf2v49	1
4	Pipe	McMaster-Carr	5233K113	2
5	Heat sink and fan	Delta	FHS-A9025S19	1
6	Aluminum block	Marhynchus	Marhynchusevkgho0rma-01	1
7	PTFE back plate	Custom	Appendix B. Drawing 6	1
8	Lid	Custom	Appendix B. Drawing 7	1
9	Inner heat sink	Custom	Appendix B. Drawing 8	1
10	RTD	Adafruit	PT100/PT1000	3
11	Adhesive-mount heat sink for surfaces	McMaster-Carr	8822T13	1
12	Low-voltage equipment cooling fan	McMaster-Carr	1939K17	1
13	Base	Custom	Appendix B. Drawing 1	1
14	PTFE base	Custom	Appendix B. Drawing 3	1
15	ITO glass side	Custom	Appendix B. Drawing 12	2
16	Back Peek col	Custom	Appendix B. Drawing 2	2
17	PTFE booth sides	Custom	Appendix B. Drawing 9	2
18	Side acrylic	Custom	Appendix B. Drawing 14	2
19	Peek right front col	Custom	Appendix B. Drawing 5	1
20	Peek left front col	Custom	Appendix B. Drawing 4	1
21	ITO glass front	Custom	Appendix B. Drawing 11	
22	PTFE front side	Custom	Appendix B. Drawing 10	
23	Front acrylic	Custom	Appendix B. Drawing 13	

3.7.2.1 - Structure

The final design for the chamber uses a combination of insulating material, airgaps, and custom gaskets to create a thermally and vapor sealed chamber. PEEK (polyetheretherketone) parts for structure (parts requiring rigidity) and insulation (see Appendix B, drawings No. 2,4, and 5). PTFE (Polytetrafluoroethylene) was used for spacing and insulation that does not require rigidity. The main reason PTFE was used was to lower the cost of the chamber (see Appendix B, drawings No. 3, 6, 9, and 10). PEEK was the superior material because of its rigidity, while having equal insulating properties to PTFE; however the cost of PEEK was much higher than PTFE. Instead of PEEK walls, PEEK columns were used as part of the skeletal structure. These columns are directly bolted into the aluminum base plate (see Appendix B, drawings No. 1).

3.7.2.2 - Glass walls

The ITO glass (Appendix B, drawings No. 11 and 12) and acrylic windows (Appendix B, drawings No. 13 and 14) are permanently mounted to the PEEK columns (Appendix B, drawings No. 2, 4, and 5) with PEEK nuts and bolts, with rings sealing the holes. The columns also feature threaded holes for the lid to be bolted with set screws, to allow the lid (Appendix B, drawing No. 7) to be removable. Rigidity was necessary for the columns for the structural integrity of the chamber, and to prevent any stress on the ITO glass (glass thickness is 1.1mm); since any deformation in the columns would directly transfer to the bolted ITO glass. PTFE parts (Appendix B, drawings No. 9 and 10) are used to fill in the gap between the PEEK columns and to act as a spacer making contact with the ITO glass and acrylic wall. This was done in order to apply pressure to gaskets that surround both the ITO glass and acrylic wall, to seal the chamber. Off the shelf ITO glass is used with sheet resistance less than 10 Ω /square and an optical transmittance of greater than 80%.

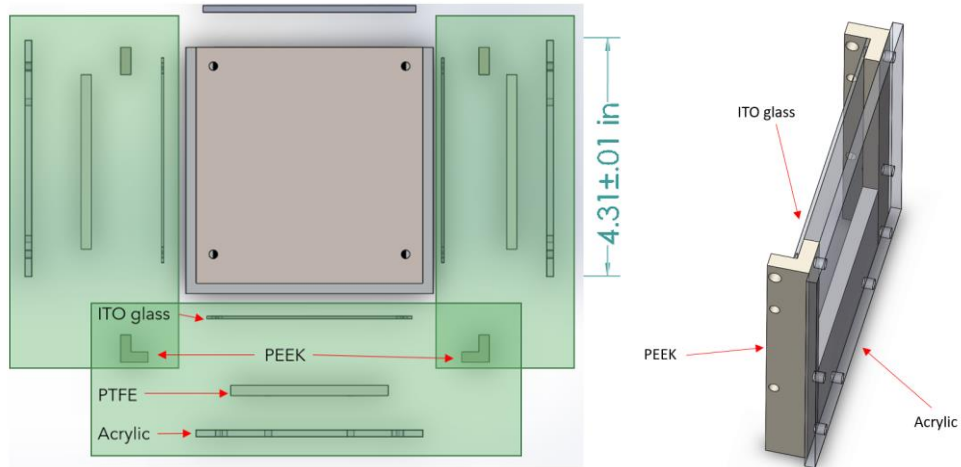


Figure 3-15 – Top and isometric view of wall Assembly of chamber; the three darkened frames encompass the components for the three chamber walls. The overlapping parts of the frame have components that are shared between assemblies.

3.7.2.3 - Lid

The current method of injecting a droplet into the system is a needle penetrating a self-healing syringe port that is emended into the lid of the chamber. These ports are disposable and are easily press fit once they are worn.

3.7.2.4 - External parts

An external mounting system was designed to aid in the image acquisition process. The system is made of a base plate, phone holder, chamber platform, syringe holder, and LED back light (see external CAD files package labeled “external parts”).

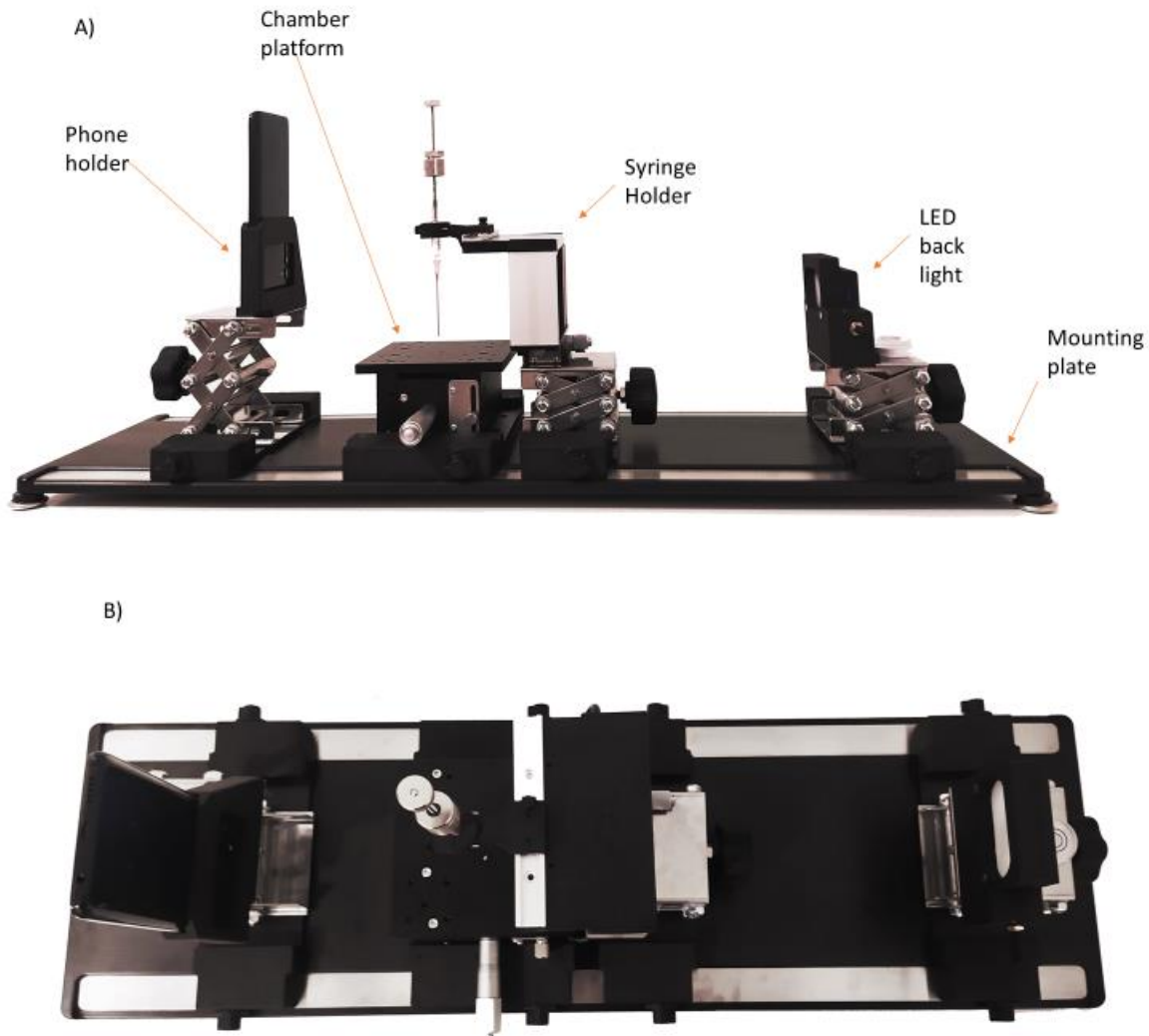


Figure 3-16 - External components. A) corresponds to the side view and B) corresponds to the top view. The LED light and phone were used in the image capture and processing during experimentation. The syringe holder was used to steady and manipulate the position of the syringe. The chamber platform is used to position the environment chamber. The mounting plate is used to fix each component in the system.

3.7.2.5 - Base plate

The base plate (Appendix B, drawings No. 15) is made from 6061 aluminum; this design has been adopted from the commercial product from Droplet SmartTech company in Toronto. The critical features of this part are the two 410 stainless steel insets (Appendix B, drawings No. 16) and the four off the self-leveling mounts on the bottom of the plate. The insets allow for the components in Figure 3-16 such as the phone holder (design adapted from the commercial product from Droplet SmartTech

company in Toronto) to be aligned and locked with the base plate with magnetic switches with embedded neodymium magnets (Appendix B, drawings No. 17, 18, and 19).

3.7.2.6 - Syringe holder

A syringe holder was used to hold a 1750 μL syringe, with a screw plunger that injects 5 μL per rotation. The syringe holder (design adapted from the commercial product from Droplet SmartTech company in Toronto) was necessary to keep the syringe stable for pendent droplet experiments, where simply holding the syringe by hand produced too much vibration, shaking the droplet. The syringe holding stage translates the syringe in all 3 axis (see Figure 3-17). The parts drawings for this component correspond to Appendix B, drawings 17, 18, 19, 20, 21, 30, 31, 32, and 33.

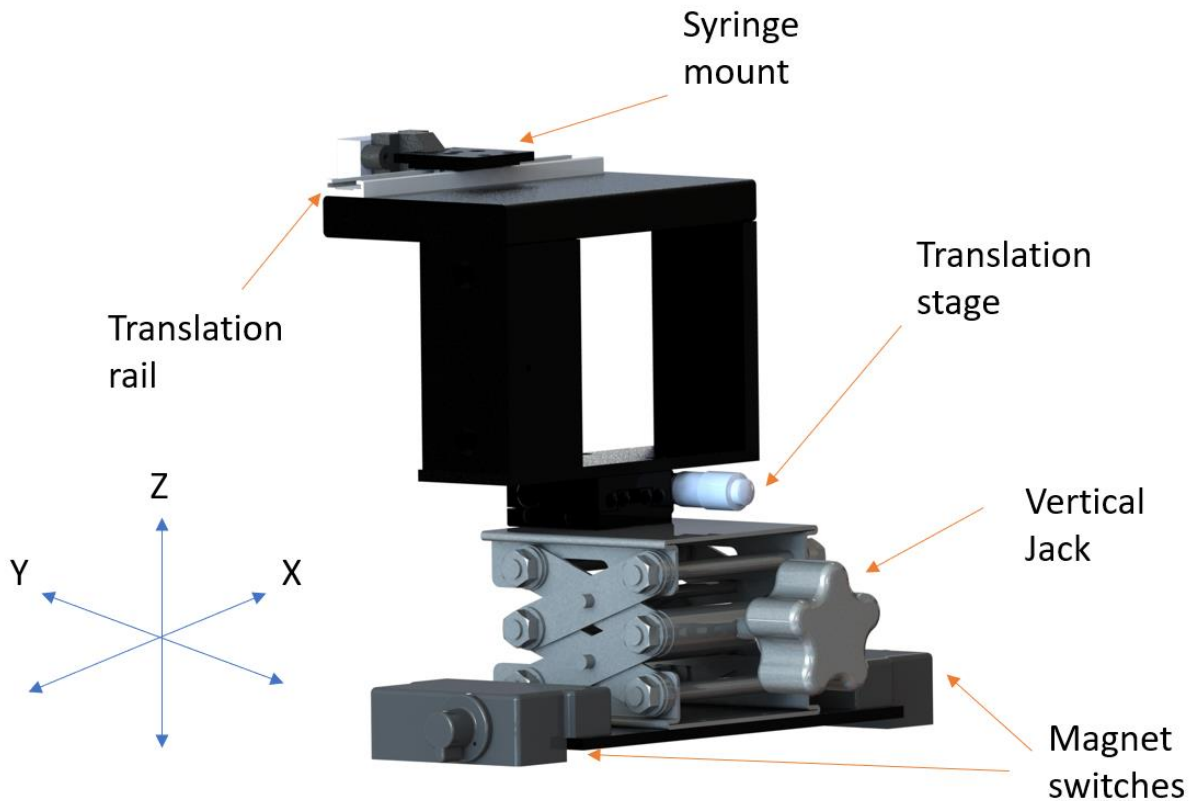


Figure 3-17 - Syringe holder. The syringe holders main components are a jack for movement in the z-axis with a 2.5" translation range, a precision translation stage for y-axis movement with a 10mm translation range, and a translation rail for x-axis movement with 100mm translation range. All axes are 90° angle from the other. Magnetic switches in 3D printed housings can lock the stage anywhere on the baseplate. Not labeled are the mounting plates.

3.7.2.7 - LED back light

An LED back light (Figure 3-18) was used to increase the contrast between a droplet and its surroundings (design adapted from the commercial product from Droplet SmartTech company in Toronto); leading to better image quality, and intern quality of measurement. This improved contrast allows the imaging software to accurately extract the outline of the droplet from the image, which is necessary for both contact angle and surface tension measurements. The parts drawings for this component correspond to Appendix B, drawings 17, 18, 19, 26, and 27.

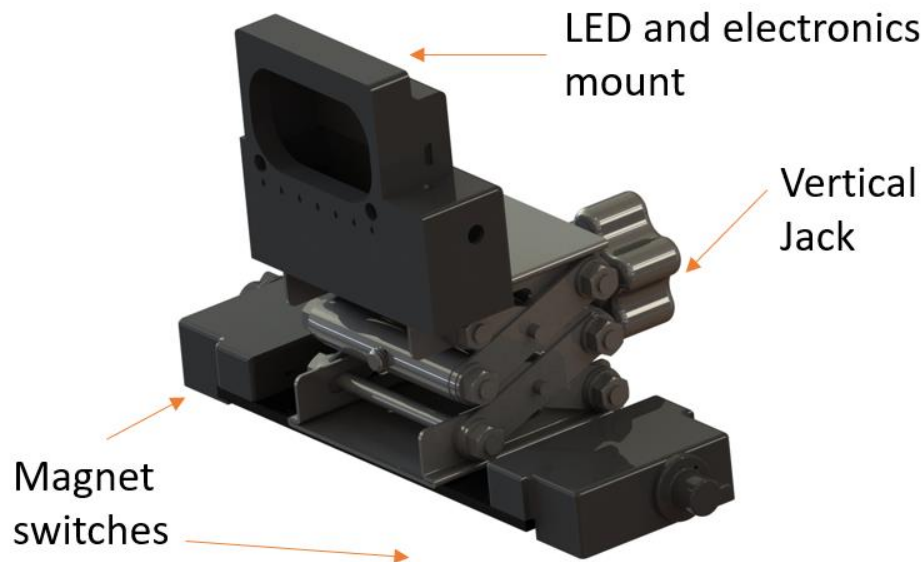


Figure 3-18- LED backlight. This component has a jack for vertical movement with a 2.5" translation range, and a housing for the LED backlight screen and electronic components. Not labeled is the mounting plate.

3.7.2.8 - Phone apps

A phone was used for image acquisition and image processing, using the DropletLab© sessile and pendent apps [47]. By aligning the phone with a window in the chamber, images and measurements could easily be taken with the smart phone. The smart phone is held in the phone holder (Figure 3-19). The parts drawings for this component correspond to Appendix B, drawings 17, 18, 19, and 22.

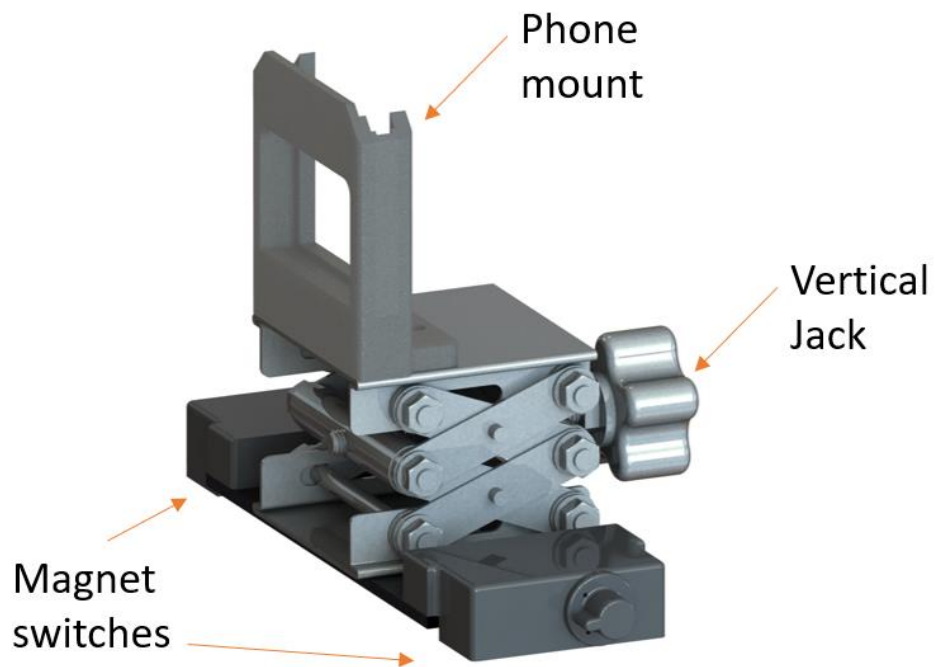


Figure 3-19 - Phone holder. This component has a jack for vertical movement with a 2.5" translation range and a housing for the smart phone. Not labeled is the mounting plate.

3.7.2.9 - Chamber platform

The chamber platform as a base for the environment chamber. It has a precision translation stage to adjust the height of the chamber. The parts drawings for this component correspond to Appendix B, drawings 24, 25, and 29.

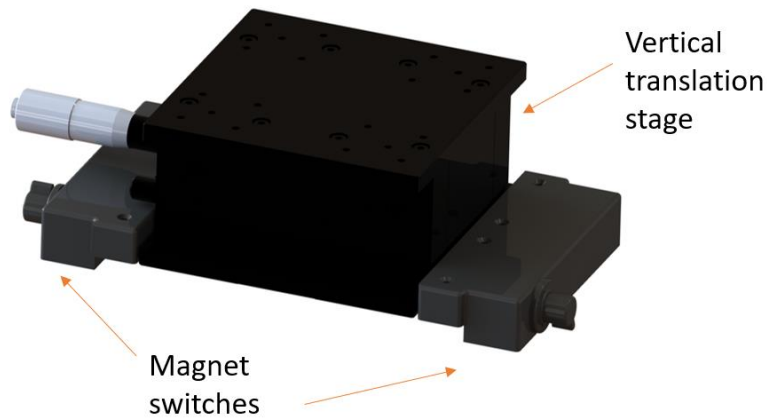


Figure 3-20 - Chamber platform. This component has a translation stage for vertical movement with a 20mm translation range.

3.7.3 - Alternative version due to pandemic conditions

Due to Covid-19 slowing down manufacturing early in the year; concessions had to be made in the current iteration. The intended chamber could not be made, instead a prototype was created as a proof of concept. Instead of the original mechanical fasteners made of peek, high temperature gaskets, and O-rings; silicon was used to glue/seal chamber, insulation was used for spacing Ito glass and acrylic windows, and the lid was made from acrylic (glued with silicon to the top of the ITO glass walls), insulation, and PTFE (see external CAD files package labeled "Alt chamber").

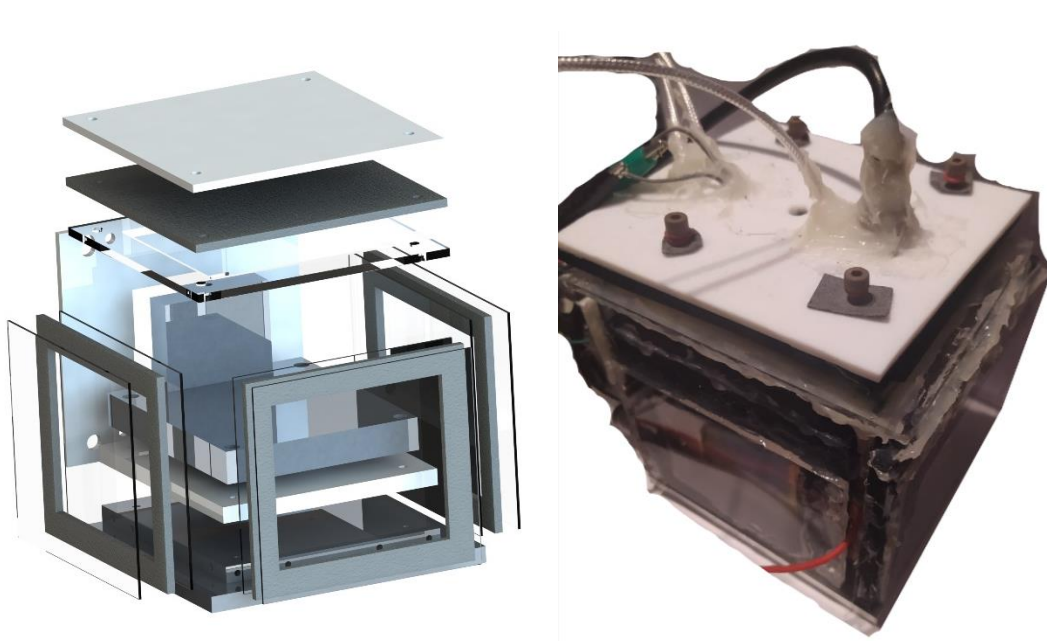


Figure 3-21 - Alternative design. On the left is the CAD model and on the right is the physical prototype.

Chapter 4 - Instrumentation Design

The control system for the chamber was developed in multiple stages, with each iteration adding more improvements to both the electronics and code for controlling the chamber.

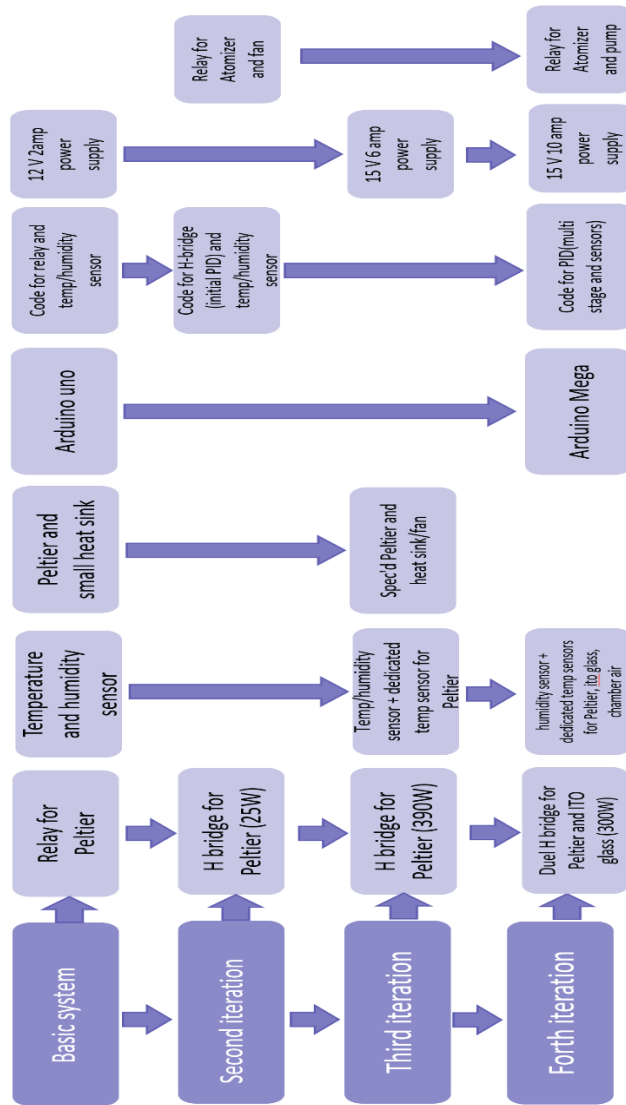


Figure 4-1 - History of instrumentation aspect of design. The first column represents the iteration, while the rows represent the components within that iteration. The vertical arrows going from one component to the next represent modifications in the design

4.1 - Breakdown of important components and systems

The following is a brief description of the components and systems used in the instrumentation of the chamber.

4.1.1 - Control systems components

The following are the control system types that were programmed and implemented to control aspects of the chamber's functionality.

PID

A PID control system was used for the temperature control system; implemented with the voltage driver.

Bang-bang

Bang-bang was used to control the humidity system, implemented with a relay.

4.1.2 - Electronic control components

The following are the electronic control and modulation components used in the electronic system of the chamber.

Micro controller

An Arduino Mega 2560 was used for the micro controller and data acquisition device, controlling the electronics and reading from the sensors.

Relays

Dual channel relay was used as a control component for both the pump and ultrasonic atomizer, as part of the humidity system.

Drivers

A dual channel high voltage driver was used as part of the control systems for both the Peltier and ITO glass.

4.1.3 - Sensors

The following are the sensors used to provide information to the micro controller and the user.

Temperature

Three RTD's; one for the Peltier, ITO glass, and air temperature inside the chamber respectively.

Humidity

One humidity sensor for the measurement of relative humidity inside the chamber.

4.1.4 - Mass and energy transfer components

The following are the components related to mass and energy transfer in the system.

Pump

A 4.8W air pump was used to pump humid air into the chamber.

Fan

A 9W CPU fan/heat sink was used to regulate the Peltier to prevent over heating; and a 0.72W fan to circulate air inside the chamber.

Peltier

A high Voltage Peltier was used to raise or lower the temperature inside the chamber.

ITO glass

Iridium tin oxide coated glass used to heat the inside of the chamber and as an anti-condensation system for the chamber walls.

4.2 - Design Evolution

4.2.1 - First iteration

The initial prototype consisted of a Peltier controlled via a relay module [67]. A relay module was used to implement Bang-bang temperature control. A temperature/humidity sensor [68] was used with an Arduino micro controller [69] to switch the relay on and off, which would either power up or turn off the peltier. The Arduino itself would control the relay by sending a binary signal to the relay, whenever the temperature was not equal to the set point. It became readily apparent that it was impossible for the system to stabilize at a consistent temperature, without almost near perfect insulation. Thus, it was determined that a bang-bang control system was not viable for temperature control. It should be noted that an Arduino was also chosen for the future prospect of smart phone integration, via low powered Bluetooth.

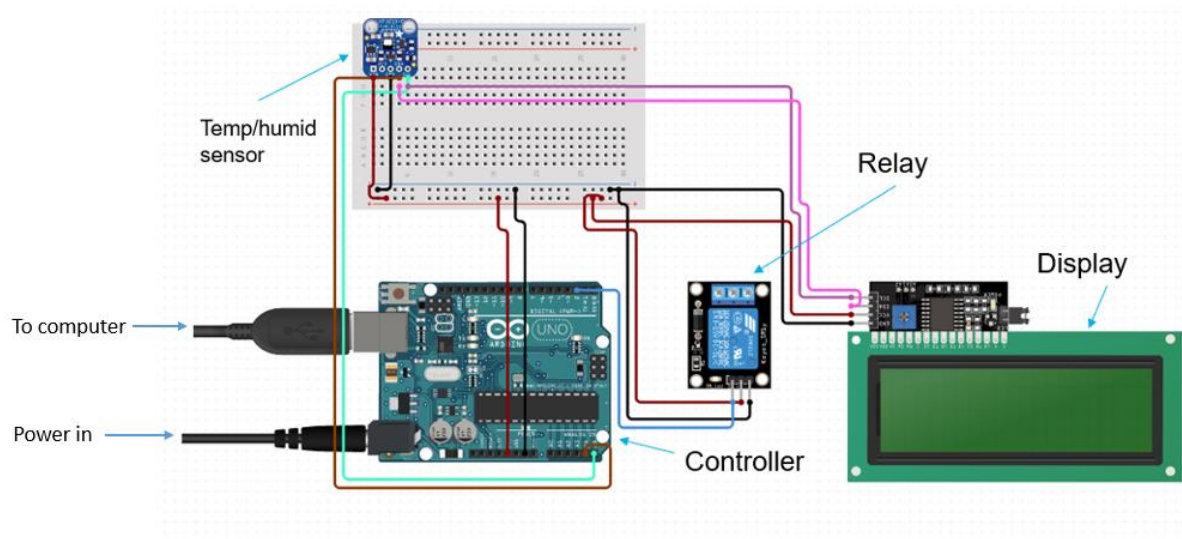


Figure 4-2 - First iteration of chamber's electronic data acquisition and control system

4.2.2 - Second iteration

The second iteration had two goals: (1) to upgrade the control system for the Peltier, and (2) to introduce humidity control. This iteration replaced the relay with an H-bridge [70] that was controlled with the Arduino using 8-bit pulse width modulation (PWM). An 8-bit PWM signal is an integer value between 0-255; which corresponds to 0-100% of the voltage of the power supply (power supply outputted 12V in this iteration). This upgraded the system, as instead of constantly switching from a high and low state for the Peltier (effectively zero to maximum voltage), it could instead be kept to a

constant value; meaning the Peltier could be supplied with constant voltage, and thus be kept at a constant temperature. A preliminary PID was programmed and used to control the voltage of the Peltier. Practical testing revealed that for the PID to settle on a value, a significantly large sample time was required (as seen in Figure 4-4). This is due to the time lag between the Peltier reaching the set point in under a minute; and the air in the chamber itself heating up in a matter of at least several minutes. This causes the PWM signal to continually fluctuate from 0-255 instead of settling on a value; unless a long enough sample time was used or significantly small values for the PID tuning parameters were used.

The initial humidity system was comprised of the following components; water chamber [71], ultrasonic atomizer [72], DC fan [73], plastic tubing, and a dual channel relay [67]. The ultrasonic atomizer sits submerged in water inside the partially filled water chamber, where it produces humid air that gathers at the top of the chamber. A DC fan at the top of the chamber forces the humid air into the piping and into the chamber. Both the atomizer and fan are controlled with a relay.

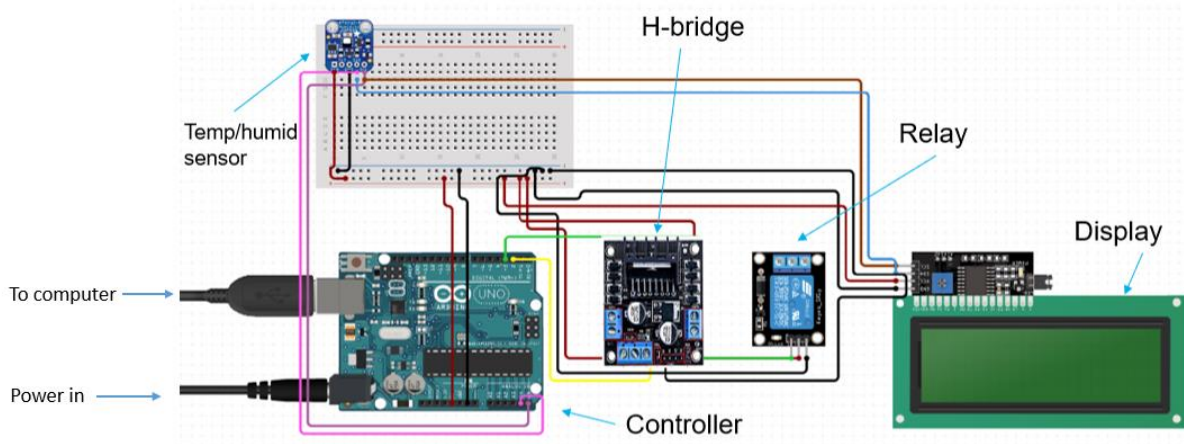


Figure 4-3 - Second iteration of chamber's electronic data acquisition and control system

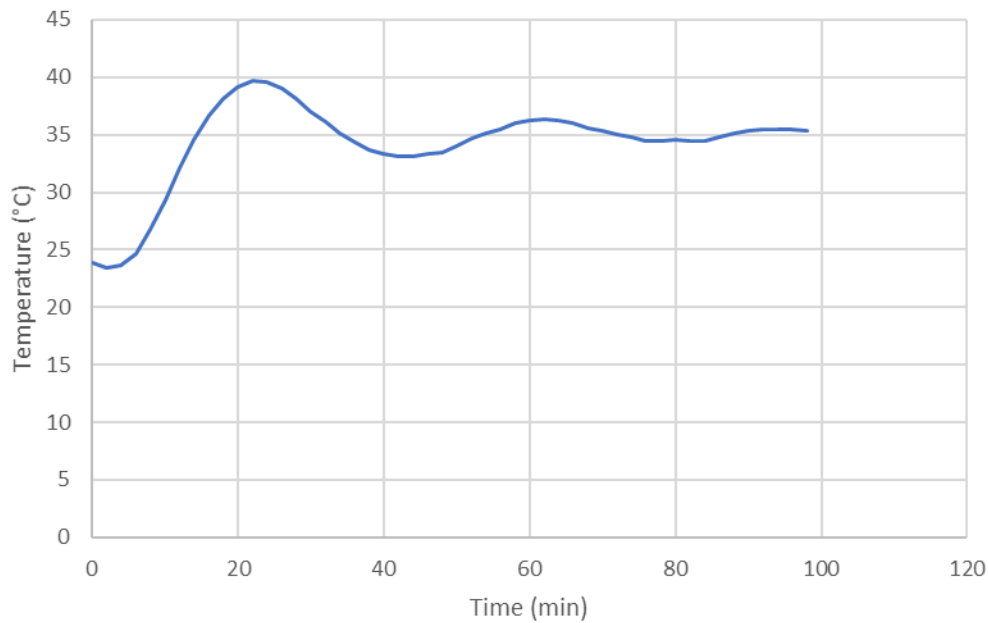


Figure 4-4 - PID tests for second iteration of design. A slow with a sample time of 2 minutes was required for the system to settle on the set point 11°C above ambient (setpoint 35 °C) after 70 minutes.

4.2.3 - Third iteration

The third iteration had two goals: (1) to reduce the settling time for the temperature inside the chamber and (2) to increase the power of the system from 24W to 60W. This increase in power would allow for the full utilization of the Peltier; so that the maximum wattage could be applied, giving it a higher temperature range.

This iteration included a temperature sensor embedded into the L heat sink; where the L heat sink makes contact with the Peltier (see Figure 3-8). This was done in order to split the PID into two parts; an initial PID for the Peltier and the secondary PID for the chamber. This allowed the Peltier to settle and hold a temperature, and allow the chamber to heat up. Once the chamber temperature is in a specified range, the PID system enters its second stage. Here the PID uses the chamber temperature sensor instead of the L heat sink; where the PID is set to get the air inside the chamber to settle on the setpoint.

The increase in wattage allows for the Peltier to run at its full operating range; but this requires scaling up the electronics and heat dissipation for the Peltier. The H bridge was replaced by a more powerful

one [74], and a heat sink spec calculation was done to select the appropriate heat sink for the Peltier (see section 4.2.3.1 -).

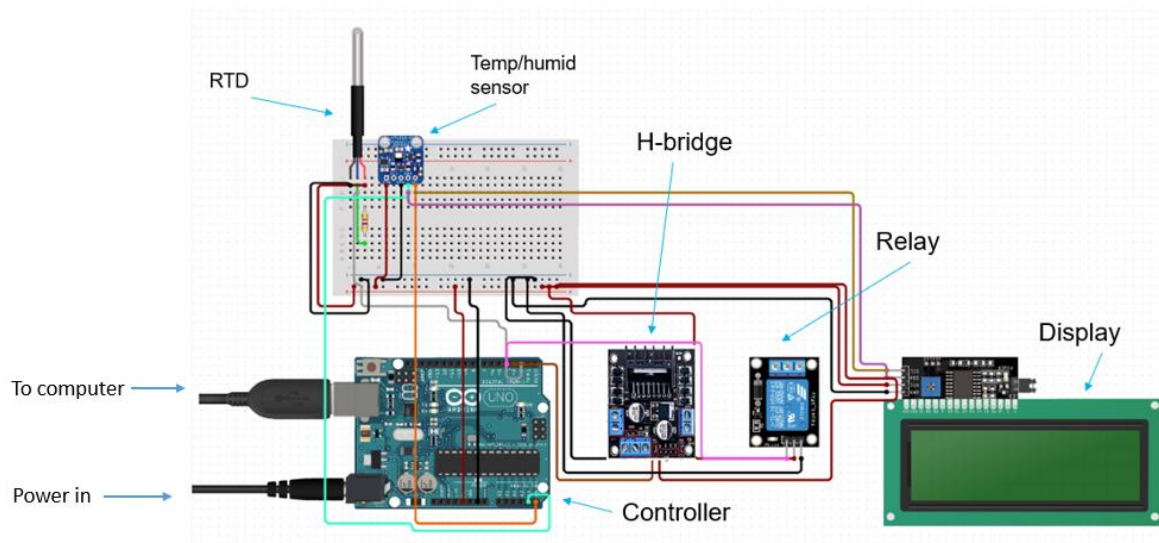


Figure 4-5 - Third iteration of chamber's electronic data acquisition and control system

4.2.3.1 - Peltier and heat sink spec

A high temperature/performance Peltier was used. Based on the manufacturer's recommendation at maximum voltage and current, the hot side temperature should hold at 50°C, with the maximum temperature of the Peltier not exceeding 150 °C [75]. Using 50°C as the temperature not to be exceeded, the following heatsink calculation was done:

Heat sink spec

P = power

I = current

V = voltage

Q̇ = Heat transfer

T₁ = Temperature ambient

T₂ = Temperature not to be exceeded

R = resistance

$$P = I \times V \quad 4.1$$

$$P = 4 \times 12 = 48 \text{ W}$$

$$R = \frac{T_2 - T_1}{Q} \quad 4.2$$

$$R = \frac{50 - 23}{48} = 0.56 \text{ } ^\circ\text{C} / \text{W}$$

Thus, a heatsink with a resistance below 0.56 °C/W is required. The chosen heat sink was the Delta electronics inc. FHS-A9025S19 (0.36 °C/W) [76].

4.2.4 - Forth iteration

The final system uses 3 RTD temperature sensors for the Peltier, ITO glass, and chamber air temperature; and 1 humidity sensor for the relative humidity inside the chamber. The RTD's are connected to the Arduino analog pins (10 bit resolution) with an amplifier in between to boost the signal. The humidity sensor is connected to the Arduino with I2C interface. The humidity sensor is connected to the Arduino with I2C interface.

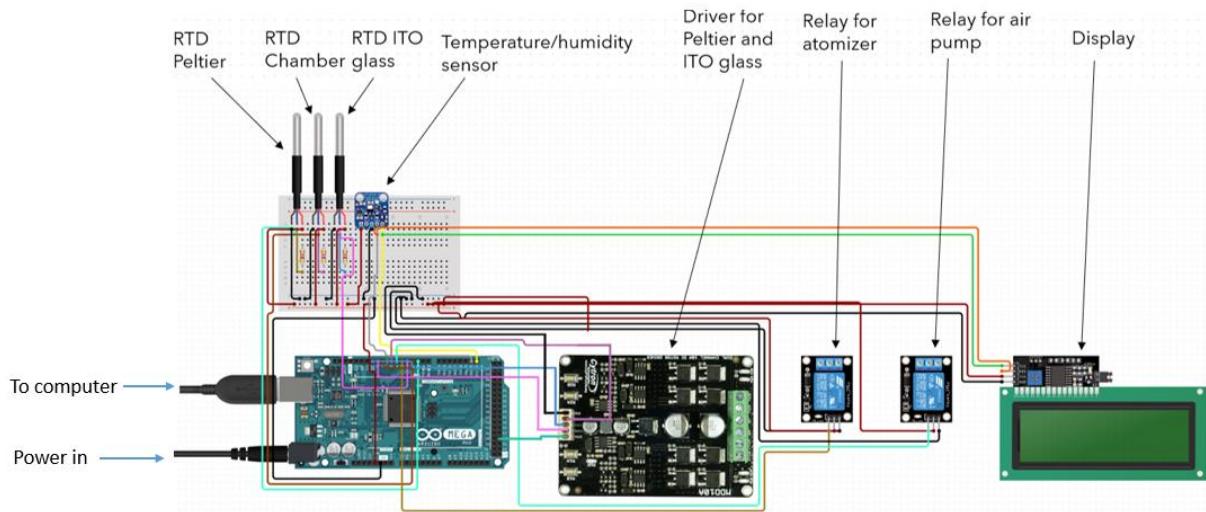


Figure 4-6 - Forth iteration of chamber's electronic data acquisition and control system

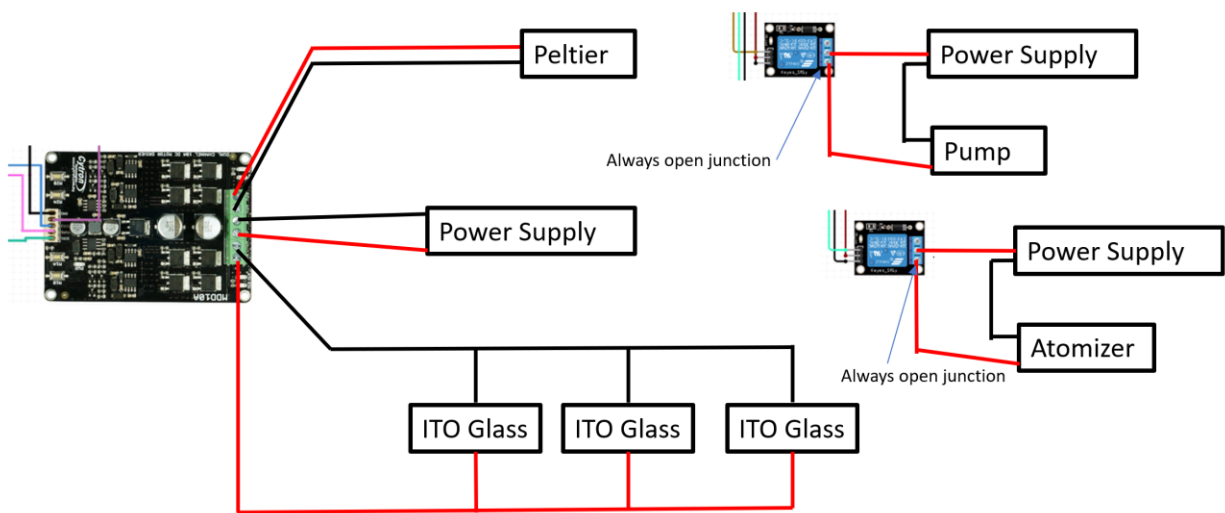


Figure 4-7 - Wiring diagram for Driver and Relay. The driver controls the Peltier and ITO glass with pulse width modulation, varying the voltage applied to both components individually. The relays switches from either having the circuit open, to completing the circuit.

4.2.4.1 - Electronic specifications

The following is the sources for the electronics used in the 4th iteration of the electronic design

Table 4-A - Electronics in 4th iteration of design

Part name	Manufacturer/Supplier	Manufacturer code	Quantity
RTD Peltier (PT100)	Adafruit	3290	1
RTD ITO glass (PT100)	Adafruit	3290	1
PT100 amplifier	Adafruit	3328	2
RTD Chamber (PT1000)	Adafruit	3984	1
PT1000 amplifier	Adafruit	3648	1
SHT-30 Temperature/Humidity sensor	Adafruit	4099	1
Microcontroller MEGA 2560 R3 Board ATmega2560 ATMEGA16U2	Elegoo	EL-CB-003	1
10Amp 5V-30V DC Motor Driver for Peltier and ITO glass	Cytron	MDD10A	1
2-Channel Relay Module for atomizer and pump	SainSmart	B0057OC6D8	1
Display	DFRobot	DFR0009	1

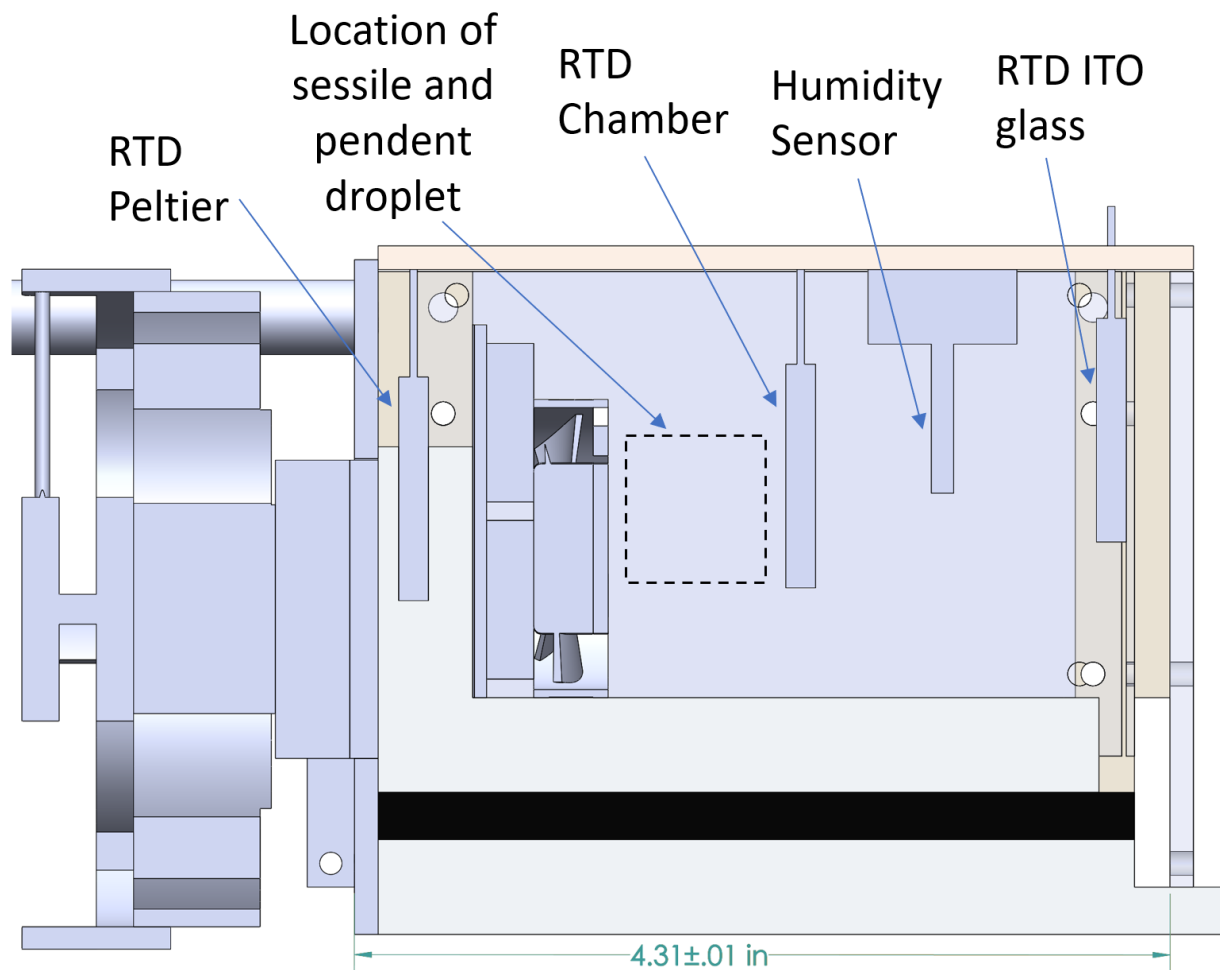


Figure 4-8 – Cross section of chamber showing the location of sensors inside chamber, cross section taken at the center of the chamber

4.3 - Code logic

The code for the instrument is divided into three distinct parts: heating, cooling, and humidity control. An important parameter in this system is the error term, which is defined by the absolute difference between the desired setpoint, and the reading given by the sensor.

For the heating system where the set point temperature is above ambient, the system heats the chamber such that the reading of the air sensor inside the chamber is equal to the desired setpoint. The heating system is split into three stages. This allows the system to rapidly reach the set point while still blunting the system from overshooting the set point. See Appendix C for full code.

The Initial stage for the heating system is defined as the error being greater than 20 °C. Since the difference between the set point and current air temperature is so large, a fast-acting PID is used to

rapidly raise the temperature, making this stage a booster stage. To prevent overshoot, two separate PID's are used for the Peltier and the ITO glass. Both PID's are set to converge to the set point temperature, using data acquired from their own sensors, respectively, rather than the air temperature sensor inside the chamber. This is to take into account the temperature of the Peltier and ITO glass will reach the setpoint faster than the air inside the chamber. Thus, the Peltier and ITO reach and hold the setpoint temperature to allow the air inside the chamber to heat up, until the conditions for the second stage are met (as show in Figure 4-11, labeled stage 1 in both graphs).

The second stage for the heating system is defined as the error being greater than 7 °C, but less than 20 °C. At this stage, the Peltier setpoint is of set to 15 °C higher than the setpoint; this value was found after multiple trails as around the temperature the Peltier settles when the chamber reaches steady state. The Peltier temperature is higher than the set point, to take into account heat loss from the system. The tuning parameters for the PID are also changed, with a decrease to the proportion and increase to the integral and derivative terms. This has the effect of blunting the overshoot of the first stage; as seen in Figure 4-11, where the air temperature inside the chamber (labeled tempC2 in Figure 4-11 B) in the second stage is still increasing, but at a slower rate when compared to stage 1.

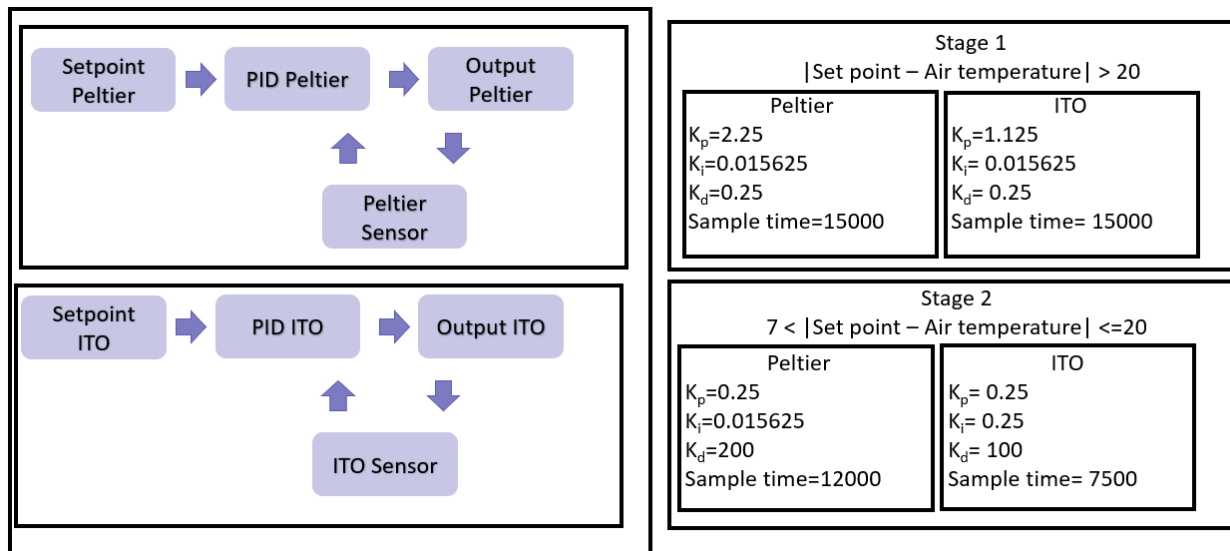


Figure 4-9 - Stage 1 and 2 PID heating implementation. The two flow charts on the left are a visualization of the control loop for the Peltier and the ITO glass; they are separated since they work independently from one another with different sensors. The two blocks on the right show the conditions and parameters of each stage.

The third stage for the heating system is defined as the error being less than 7 °C. At this stage, the ITO glass and Peltier are both changed from their own sensors, to the sensor measuring the temperature of the air inside the chamber. The PID tuning parameters here are set to account for subtle changes, to take into account the time lag with the response from the Peltier and ITO glass to the sensors reading. The third stage is also when the humidity system activates. As shown in Figure 4-11, at the third stage, the temperature of the air inside the chamber slowly plateaus.

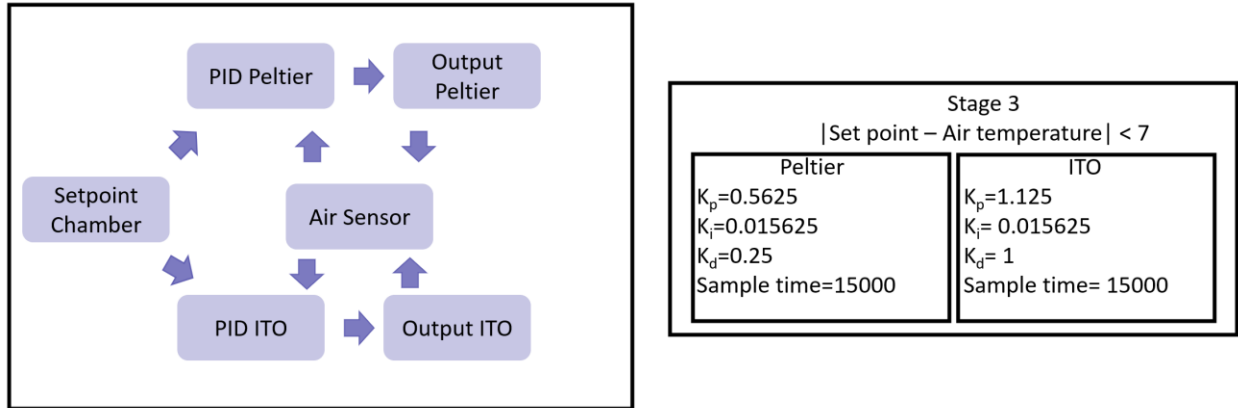


Figure 4-10 - Stage 3 PID heating implementation. The flow chart on the left is a visualization of the control loop for the Peltier and the ITO glass; they are combined in this stage as they share the same sensor and work together to have that sensor reach the setpoint. The block on the right shows the conditions and parameters for the third stage of the PID.

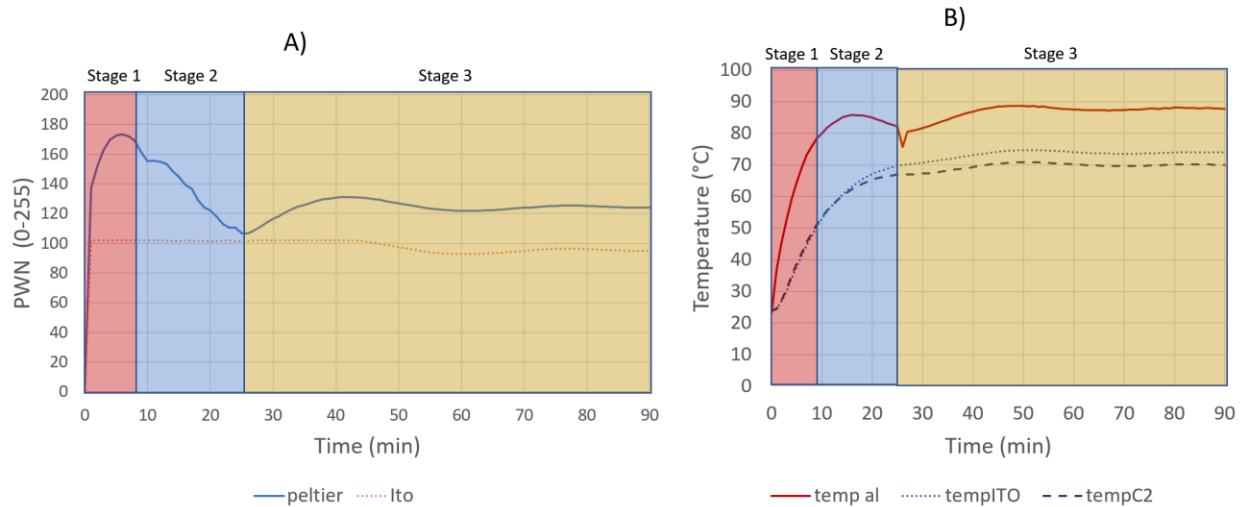


Figure 4-11 - PID Response for setpoint 70°C, system over and undershoot and steady system error less than 1°C. Both graphs illustrate the response of the system at different stages of the PID. The first graph A) shows the voltage given to the Peltier and ITO glass of the system where PWN 0 represents 0V and PWN 255 representing 15V. The second graph B) shows the sensor readings at different stages of the PID; where temp al is the Peltier temperature, tempITO is the ITO glass temperature, and tempC2 is the air temperature.

The cooling system has two stages, as seen in Figure 4-13. The initial stage is defined as the absolute difference between the temperature inside the chamber and the setpoint being greater than 1 °C. The PID system uses fast acting tuning parameters to rapidly lower the temperature to necessary range. Once the absolute difference is less than 1 °C the second stage activates. This stage uses more refined tuning parameters to make subtle changes to the response of the system, as well as the humidity system activating in this stage.

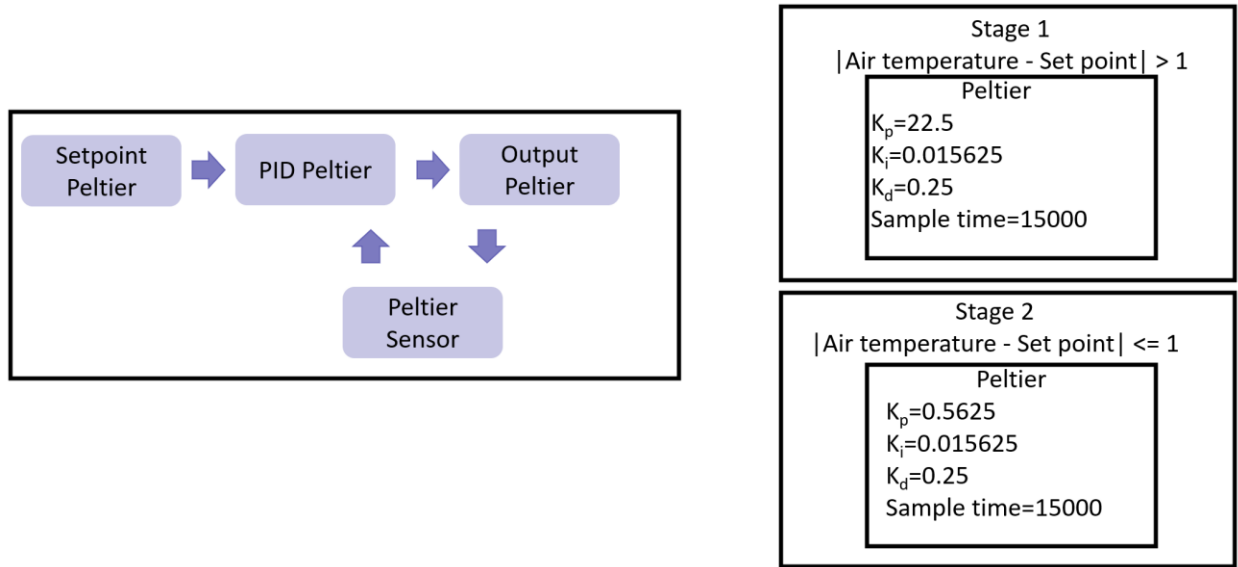


Figure 4-12 - Stage 1 and 2 PID cooling implementation. The flow chart on the left is a visualization of the control loop for the Peltier; they are separated since they work independently from one another with different sensors. The two blocks on the right show the conditions and parameters of each stage.

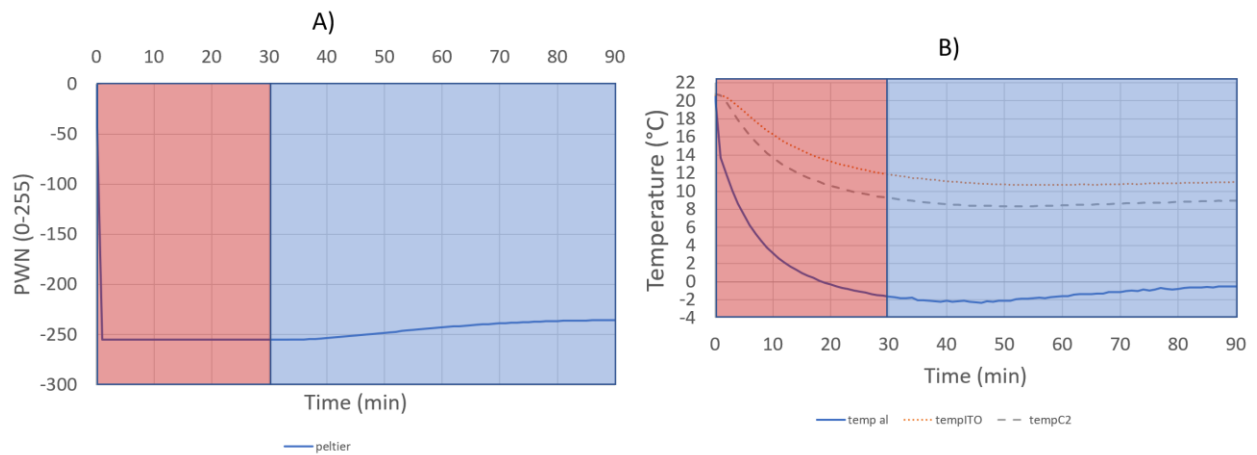


Figure 4-13 - PID response for set point 9 °C with a fan on inside the chamber. Both graphs illustrate the response of the system at different stages of the PID. The first graph A) shows the voltage given to the Peltier where PWN 0 represents 0V and PWN 255 representing 15V. The second graph B) shows the sensor readings at different stages of the PID; where temp al is the Peltier temperature, tempITO is the ITO glass temperature, and tempC2 is the air temperature.

The humidity system works on bang-bang relay logic. The humidity system is only active while the sensor reading is below the humidity set point and the temperature system is in stage 3. The humidity system has two stages.

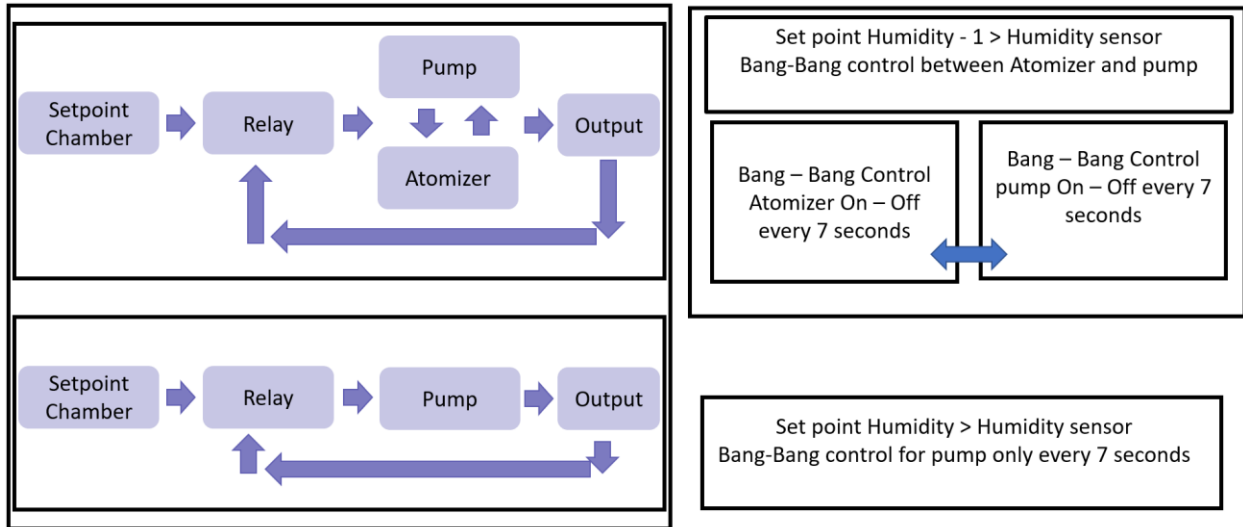


Figure 4-14 - Bang-bang humidity implementation. The two flow charts on the left illustrate the two active states of the humidity system. On the right, are the conditions for the active states.

The first stage is when the humidity in the chamber is one minus the set point. In this stage, both the atomizer and pump are both active. First the atomizer generates humidity for seven seconds and then powers off, followed by the pump sucking the humid air into the chamber for 7 seconds. This switching between both states approach was used to prevent the atomizer from overheating, since it cannot be run for more than 1 hour continuously without significant thermal build-up. The time of 7 seconds was also chosen since this was the time it took for the vacuum pump to completely extract the humidity that was generated. Once the humidity is greater than one minus the set point, but still smaller than the set point, only the pump was active. The pump still continues switching between on and off states to account for the time lags between the humidity pumped into the chamber, the humid air dispersing inside the chamber, and the sensor stabilizing around a value. If the humidity is at or above the set point, the system is in the off state for both the pump and atomizer.

Chapter 5 - Capability and Performance Tests

The capability tests were split in two categories: (1) specification sheet tests, and (2) benchmarking tests. The specification tests were done to obtain the upper and lower capabilities of the system. The benchmarking tests were done by replicating experiments done in the literature, to verify the accuracy of the system and to investigate any discrepancies within the literature.

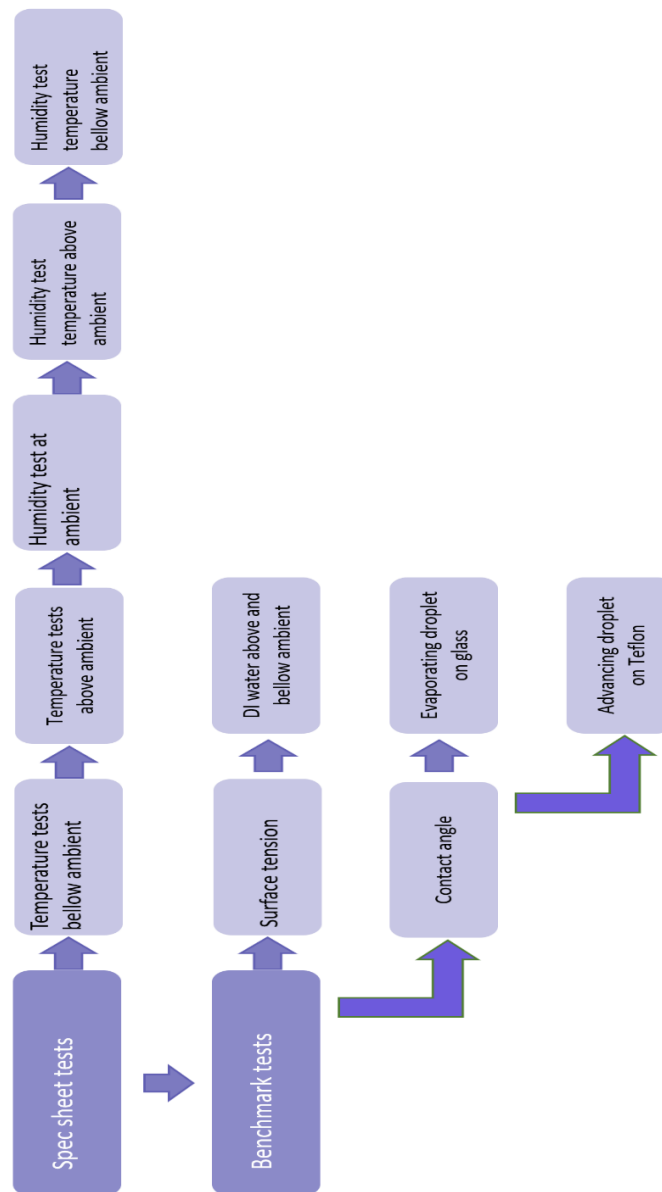


Figure 5-1 - History of spec and benchmark tests. The first column represents the test type; and the rows represent the chronological order of experimentation

Table 5-A - Limit test setpoints. Tests were done in order to determine the high and low temperature, and high humidity environments that the chamber can generate.

Upper limit tests setpoints	Lower limit tests setpoints
<ul style="list-style-type: none">• 70 °C• 40 °C at 80 %RH	<ul style="list-style-type: none">• 15 °C no fan• 9 °C with fan• 15 °C 70 %RH

Each test was done a minimum of three times, with the average results plotted along with the error bars denoting the standard deviation of the tests. The starting conditions for each test was 22°C±1 and 60%RH±5.

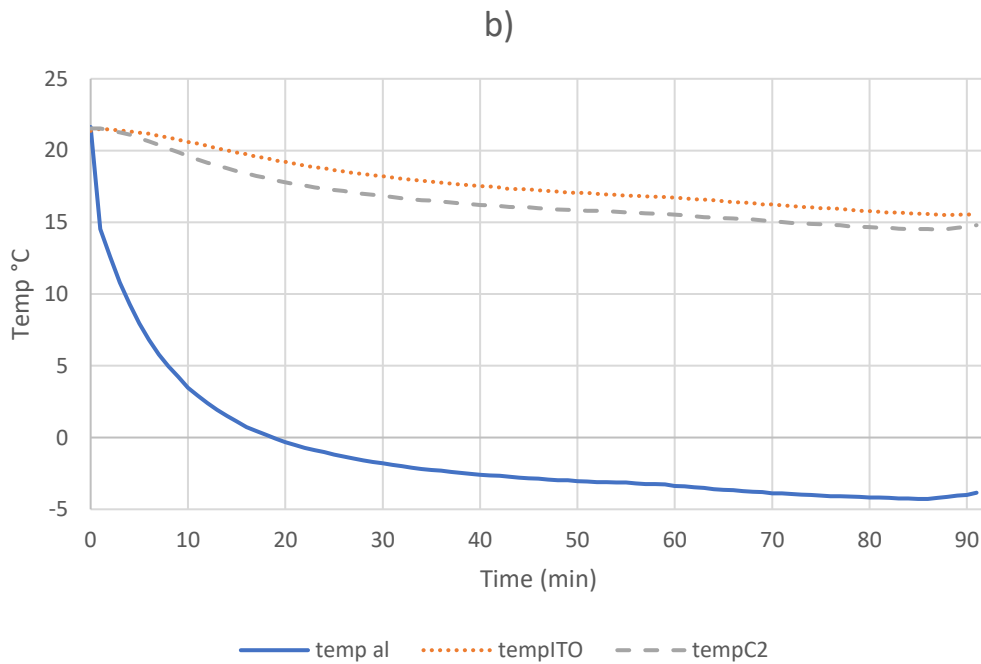
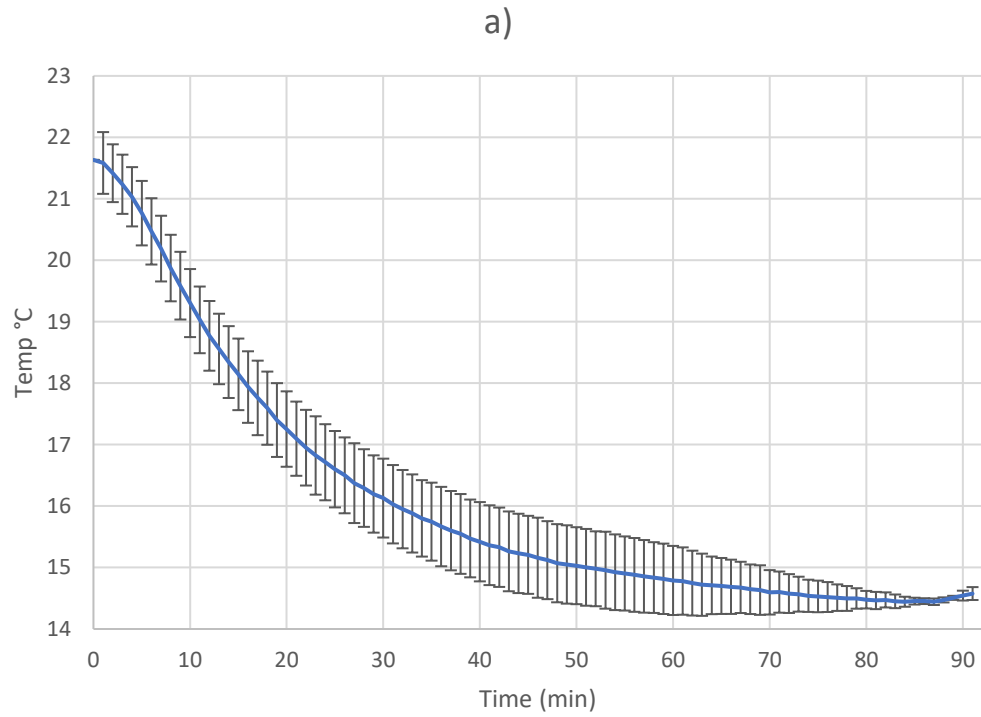


Figure 5-2 – a) Average of cooling test at 15°C, No fan; the error bars denote the standard deviation of the tests b) sample data of cooling test for Peltier (temp al), air (tempC2), and ITO glass (tempITO) temperature

One of the major complexities of the physical design of the chamber is with regards to the cooling system. Due to the nature of the natural convection, cooling the system is not effective without the aid of gravity. This is because the system utilizes the L shaped heat sink which cools the chamber from the base and a side wall. Although this is perfect for the heating, due to natural convection causing the hot air to rise; for cooling it results in the cool air stagnating at the bottom of the chamber. The lowest temperature that could be stability achieved at room temperature conditions was 15°C as shown in Figure 5-2-a. This was without the aid of a fan to circulate the air inside the chamber. Figure 5-2-b shows the readings of all 3 temperature sensors (Peltier, ITO glass, and air temperature inside chamber). Although the temperature of the Peltier rapidly drops to below 0°C in 20 minutes (temp a1); cooling the chamber from the bottom results in a significant delay for the cooling of the air (tempC2), since the chamber is working against natural convection by not cooling from the top of the chamber. Thus, it takes 70 minutes for the air temperature to reach its set point.

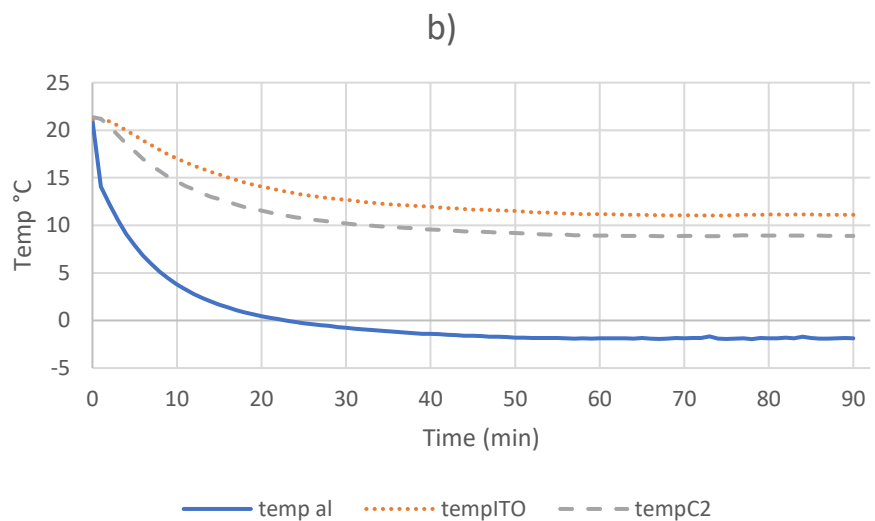
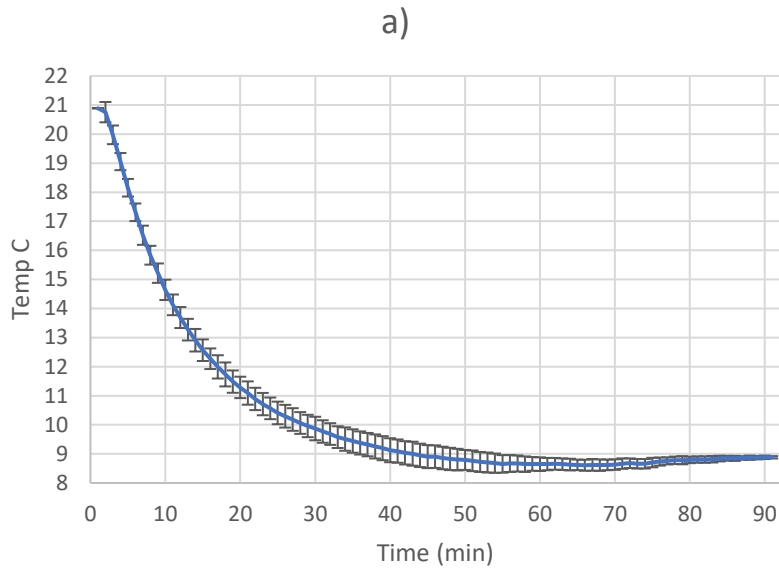


Figure 5-3 – a) Average of cooling test at setpoint 9°C, with a fan circulating air inside the chamber; the error bars denote the standard deviation of the tests b) sample data of cooling test for Peltier (temp al), air (tempC2), and ITO glass (tempITO) temperature

The lowest temperature that could be stability achieved at room temperature conditions with a fan was 9°C as shown in Figure 5-3-a. Figure 5-3-b shows that the curve for the air and ITO glass temperature experiences a similar slope as the Peltier temperature, as the fan helps circulate the stagnant air and allows the air cooled by the Peltier to disperse inside the chamber. Thus, it takes 53 minutes for the air temperature to reach its set point; since the fan significantly increased the speed of cooling inside the chamber.

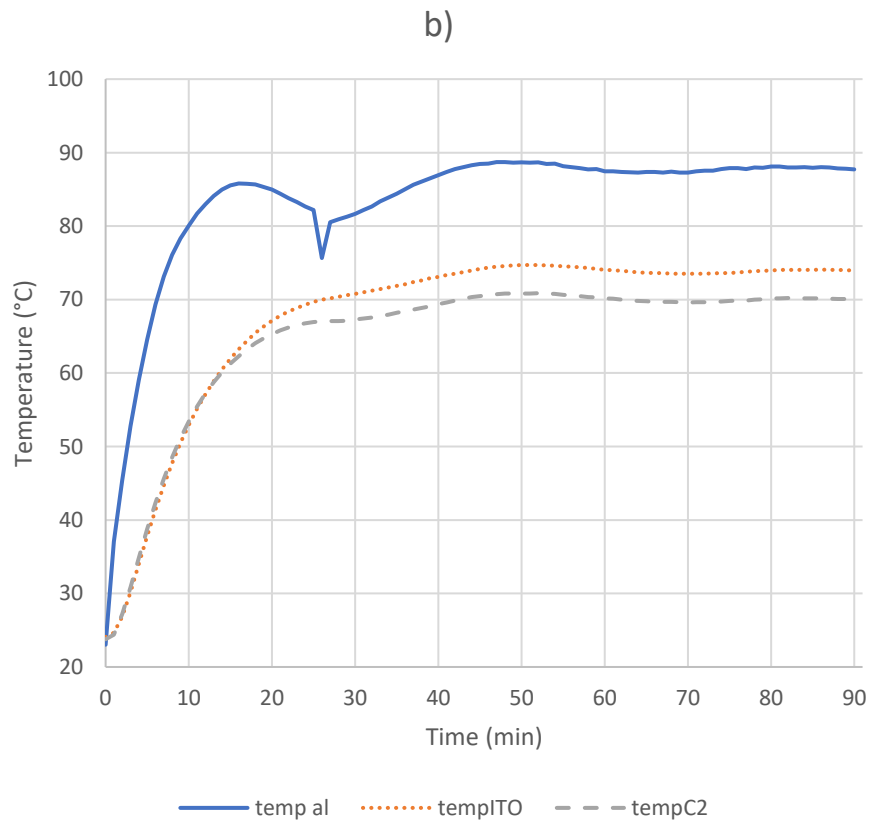
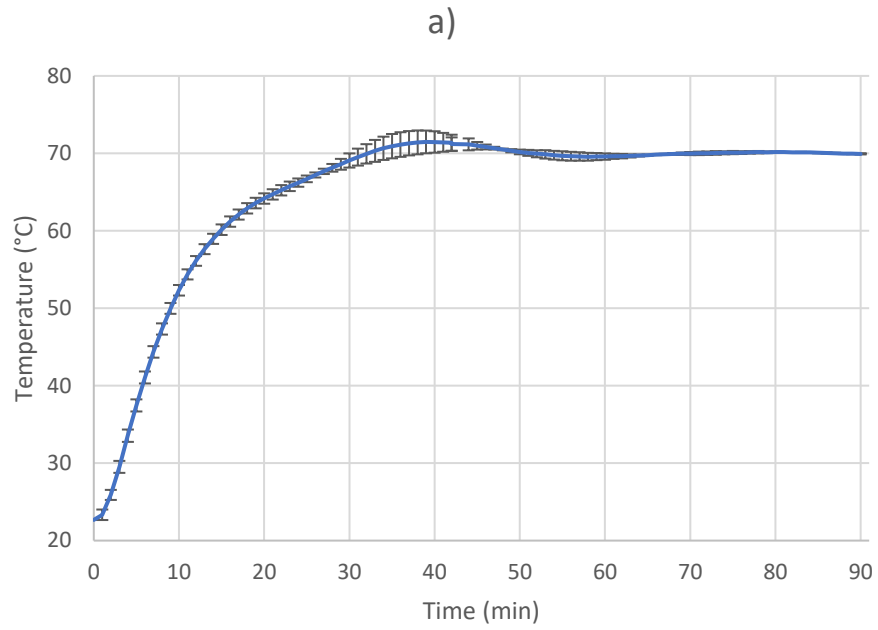


Figure 5-4 – a) Average of heating test at setpoint 70°C; the error bars denote the standard deviation of the tests

b) sample data of heating test for Peltier (temp al), air (tempC2), and ITO glass (tempITO) temperature

In the case of heating, the highest temperature tested was 70 °C as shown in Figure 5-4. the system experiences an overshoot of 1.2 °C \pm 0.45 (see Figure 5-4-a); but does not deviate more than this. Further tuning of the PID algorithm, particularly the derivative term can be used to address this in the future; however, the overshoot was deemed acceptable for the experiments necessary in this thesis.

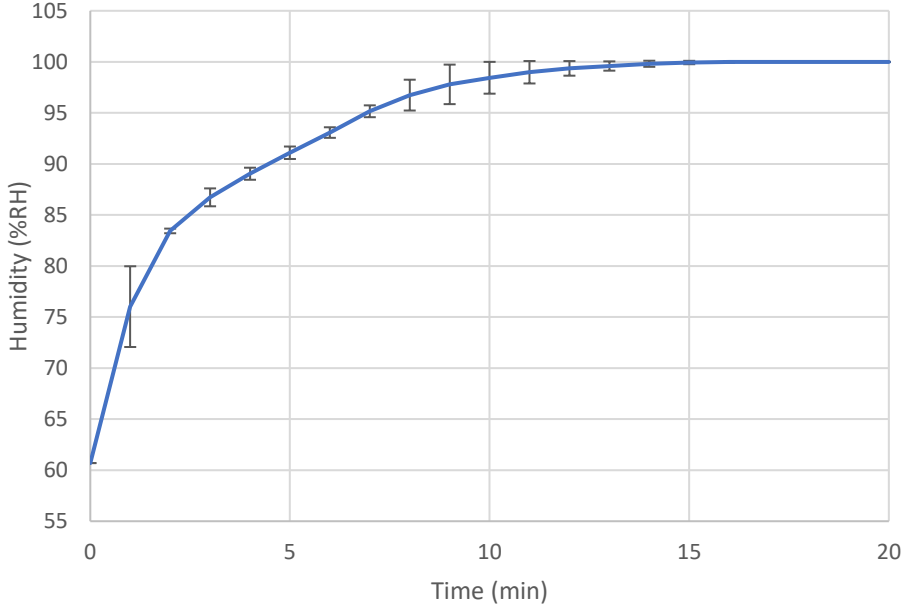


Figure 5-5 – Average of base case test of setpoint 100%RH at room temperature (22 °C) ; the error bars denote the standard deviation of the tests

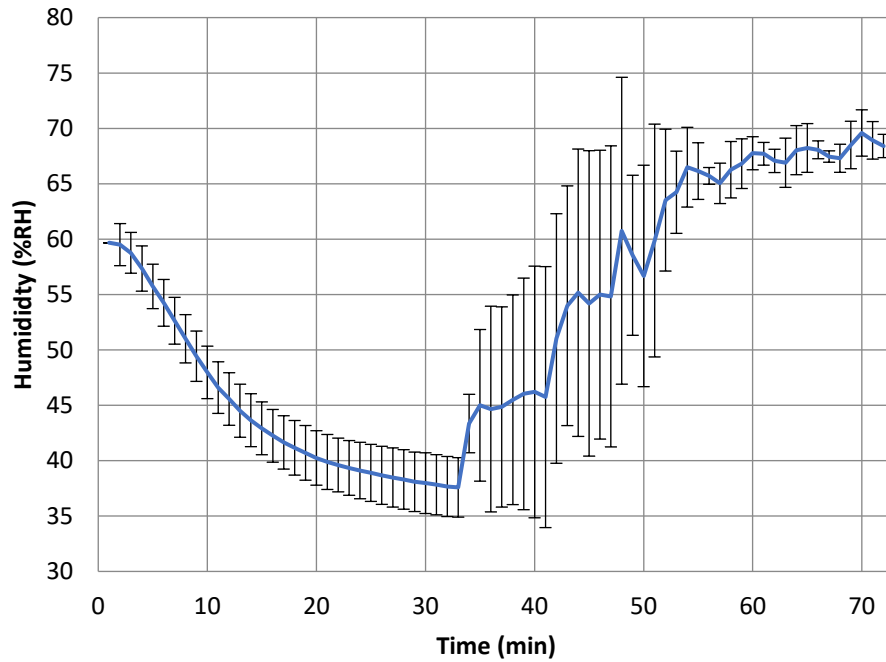


Figure 5-6 – Average of humidity test at setpoint 15°C and 70%RH; the error bars denote the standard deviation of the tests

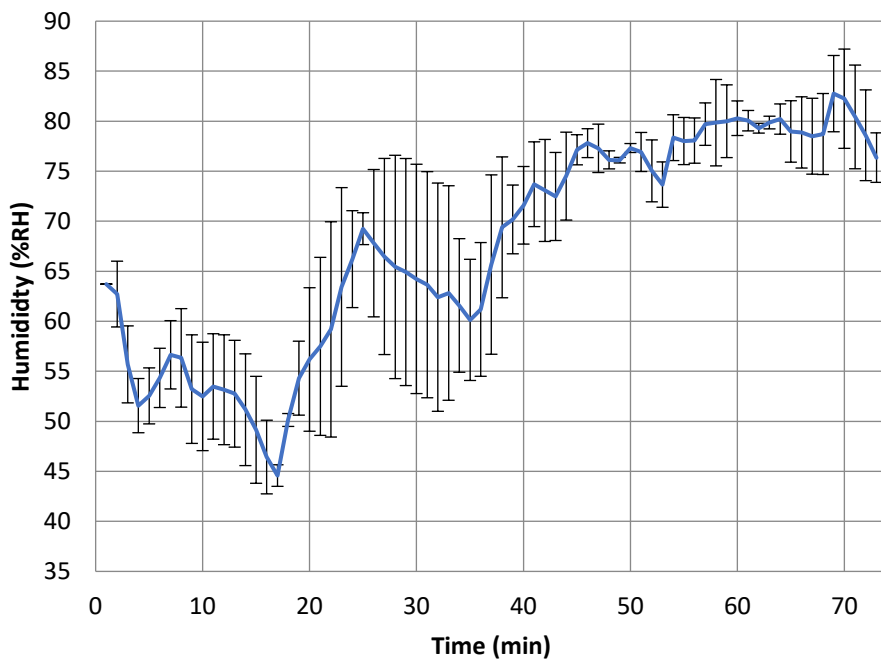


Figure 5-7 – Average of humidity test at setpoint 40°C and 80%RH; the error bars denote the standard deviation of the tests

For humidity, Figure 5-5 shows the test done at ambient temperature; while Figure 5-6 and Figure 5-7 shows the results of below and above ambient, respectively. It should be noted that there is significant fluctuations for the error bars in both tests done above and below ambient temperature. This is mainly due to the time lag between a burst of humid air injected into the chamber and the time it takes the humid air to dissipate. This is further amplified by the constantly changing temperature in the chamber before the temperatures stabilizes at its setpoint. For the case of ambient room temperature (22 °C), the temperature of the air was constant, meaning the amount of water vapor needed to reach saturation was a constant value; thus, there was little fluctuation in the humidity levels between tests. However, for the tests above and below ambient, the amount of water vapor required for a certain relative humidity setpoint will contently fluctuate until the temperature stabilizes.

In the case of heating, as the temperature of the air increases, so does its capacity to hold humid air; thus, the amount of water vapor needed is always increasing. This can be seen in both Figure 5-7 and Figure 5-8; where before the humidity system activates, the humidity inside the chamber decreases as the temperature of the air inside the chamber increases. Once the temperature of the chamber stabilizes, the relative humidity also stabilizes at its set point soon after (as seen when the average temperature reaches it setpoint in Figure 5-8, the relative humidity for three different tests stabilizes 5 minutes after). The humidity system activates around the 15 to 20 minute mark, which is about the time the temperature system is within stage 3 (when the difference between the setpoint and the temperature of the air inside the chamber is less than 7 °C). Note that the variation between the activation time of the humidity system is the main cause of the wide error bars between 20 and 40 minutes in Figure 5-7; the cause of which can be seen in Figure 5-8 where one of the tests (hum 3) the humidity system activates at around the 20 minute mark (see the spike in the humidity level).

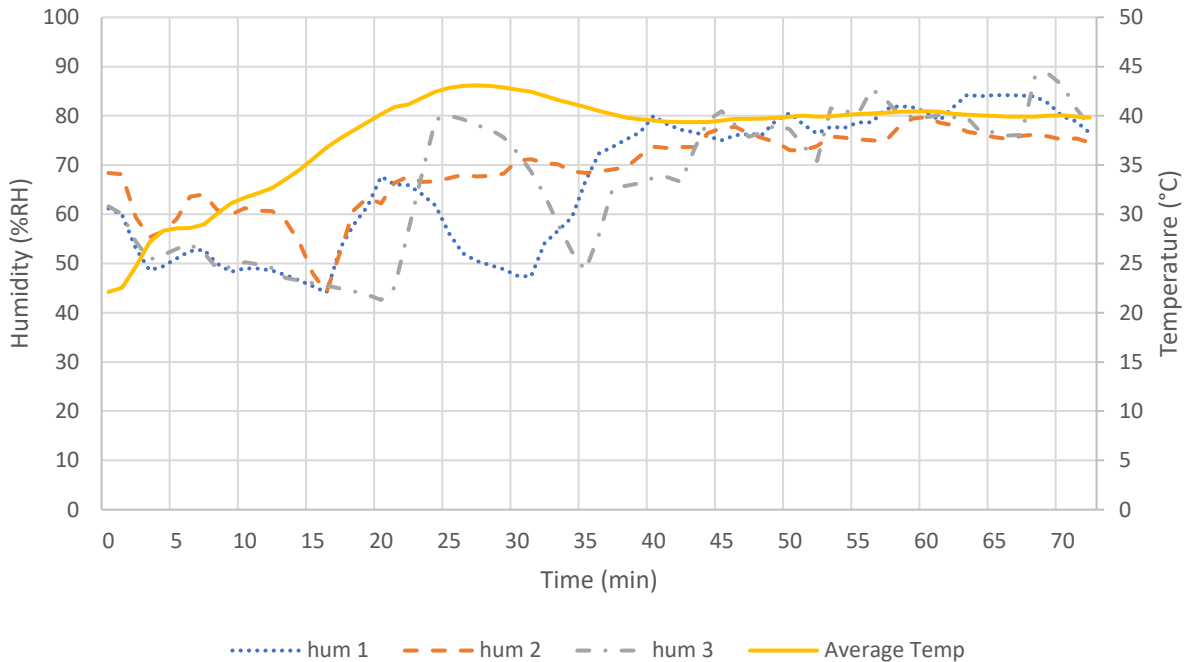


Figure 5-8 - Three humidity tests at setpoint 40°C and, 80%RH; where hum 1, hum 2, and hum 3 are the three separate humidity test results, and Average Temp the average temperature of the air inside the chamber for all three tests

In the case of cooling, it is similar to the heating system where the humidity system only activates when the temperature of the air inside the chamber is within 1 °C of the setpoint. This causes a delay in the activation of the humidity system between tests, which results in the wide error bars seen in Figure 5-6 between the 32 and 55 minute marks. This difference in the activation of the humidity system between tests can be seen in Figure 5-9 where the three separate humidity tests (hum 1, hum 2, and hum 3 respectively) all activate at different times (which can be seen with the spikes of humidity). Once the temperature of the air inside the chamber stabilizes at its setpoint, so does the humidity reading inside the chamber. The cooling block inside the chamber is at a much lower temperature than the air inside the chamber causing constant condensation from the humid air to form on the aluminum surface inside the chamber, which must be constantly replenished. This results in the humidity reading constantly fluctuating.

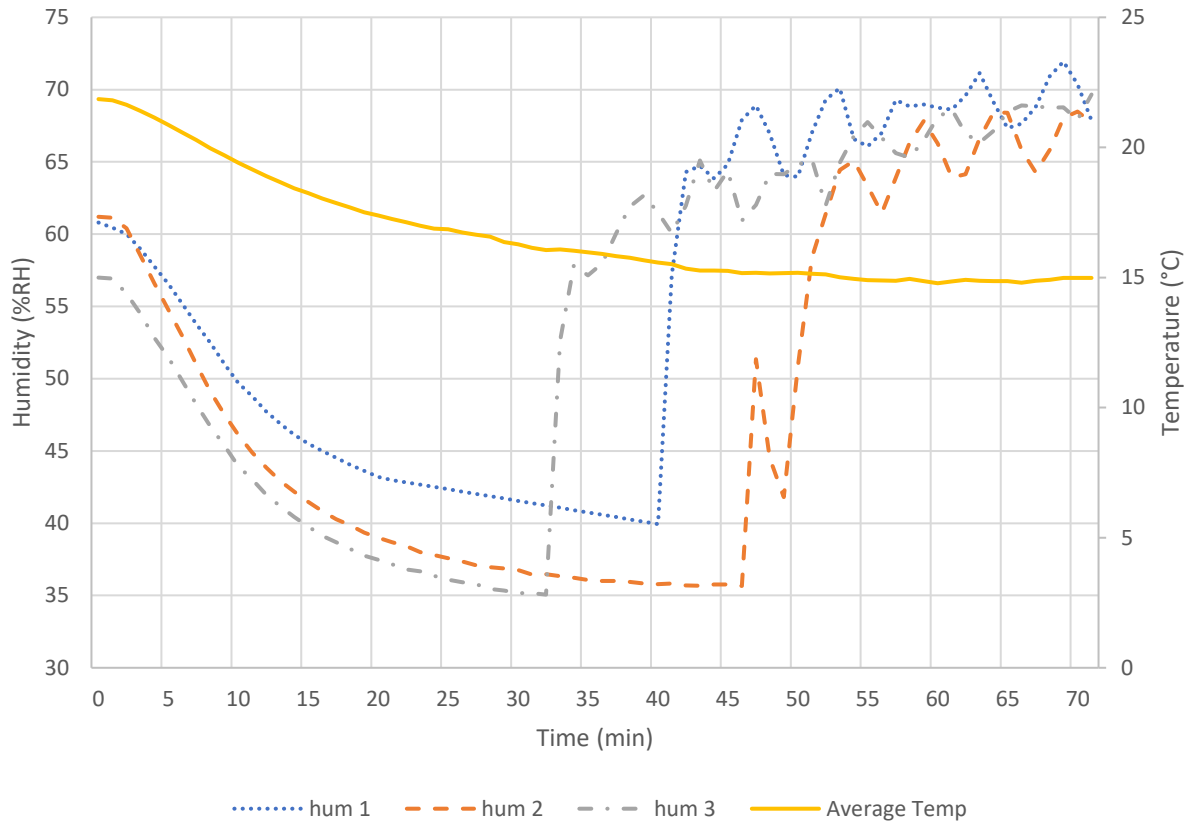


Figure 5-9 - Three humidity tests at setpoint 15°C and, 70%RH; where hum 1, hum 2, and hum 3 are the three separate humidity test results, and Average Temp the average temperature of the air inside the chamber for all three tests

The results of the tests have been shown in Table 5-B and summarized as follows, with the rise time defined as the time to reach 90% of the set point, and settling time 98% of the set point. It should be noted that some of the settling times were taken after the overshoot; if the overshoot value as greater than +2% of the setpoint value. In these cases, once the temperature of the air inside the chamber reaches within $\pm 2\%$ of the setpoint and there was no significant over or undershoot, it was considered settled.

Table 5-B - Summary of spec tests for chamber temperature and humidity control performance

Test-Set point	Rise time (min)	Settling time (min)
70 °C	18	38
80 %RH (at 40 °C)	40	57
15 °C no fan	35	40
9 °C with fan	26	38
70 %RH (at 15 °C)	52	65

Overall, the heating and cooling the chamber without humidity control had about the same results with respect to reaching there settling time. Although the rise time was quicker with heating the chamber, due to the boost from the ITO glass; the PID system is able to have the settling time for both temperatures above and below ambient was about 40 minutes.

Chapter 6 – Benchmarking and performance tests

6.1 - Surface tension

The surface tension test was done using the pendent drop method. An image of a droplet sufficiently deformed by gravity was taken, and the ADSA-P method was applied. The goal was to replicate the results of Portuguez et al. [22], where the surface tension of DI water was taken as the temperature was kept constant, but the humidity was varied. Two sets of experiments were done: one above and one below ambient temperature, specifically repeating Portuguez's experiments at 40°C and 15°C, respectively.

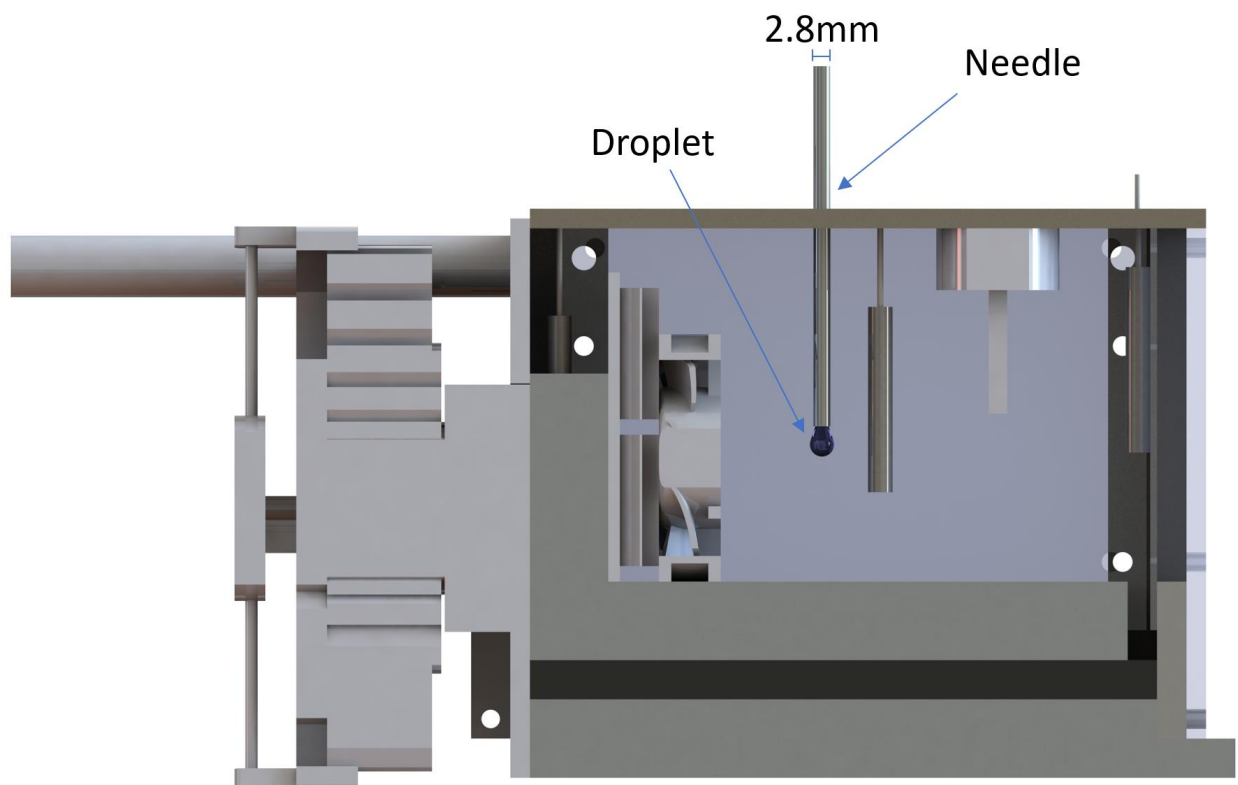


Figure 6-1 - Location of droplet for pendent drop experiment, the needle is located at the center of the chamber, the volume of the droplet is 39 μL

Plotting the experimentally obtained values in the literature, a similar trend can be observed for 40°C where the surface tension decreases with increasing humidity (see Figure 6-2). This is in line with established theory, as higher humidity results in less dissimilarity between the droplet interface and the surrounding gas. Although this dissimilarity property is anisotropic, and applies to the axis normal to the meniscus [77] [78].

The results were not the same for 15°C where the trend reported by literature could not be replicated with the chamber. Through multiple experiments at both 45 and 80 %RH; the largest surface tension recorded was between 73 mN/m and 71 mN/m. The literature claims values between 73.5 mN/m and 78mN/m for humidity 99 and 20 %RH, respectively [7]. It should be noted that the accepted value for surface tension at 15°C is 73.5 mN/m \pm 0.4 (The International Association for the Properties of Water and Steam) [79]. The value of 78mN/m is reachable for water, when it has been super cooled to -16.5°C [80]. These two facts indicate that the values given in [7] should be further investigated to find the source of the discrepancy between [7] and our experimentally obtained values that are in line with the accepted values from the literature [80]. All experimental data is recorded in Appendix D-1.

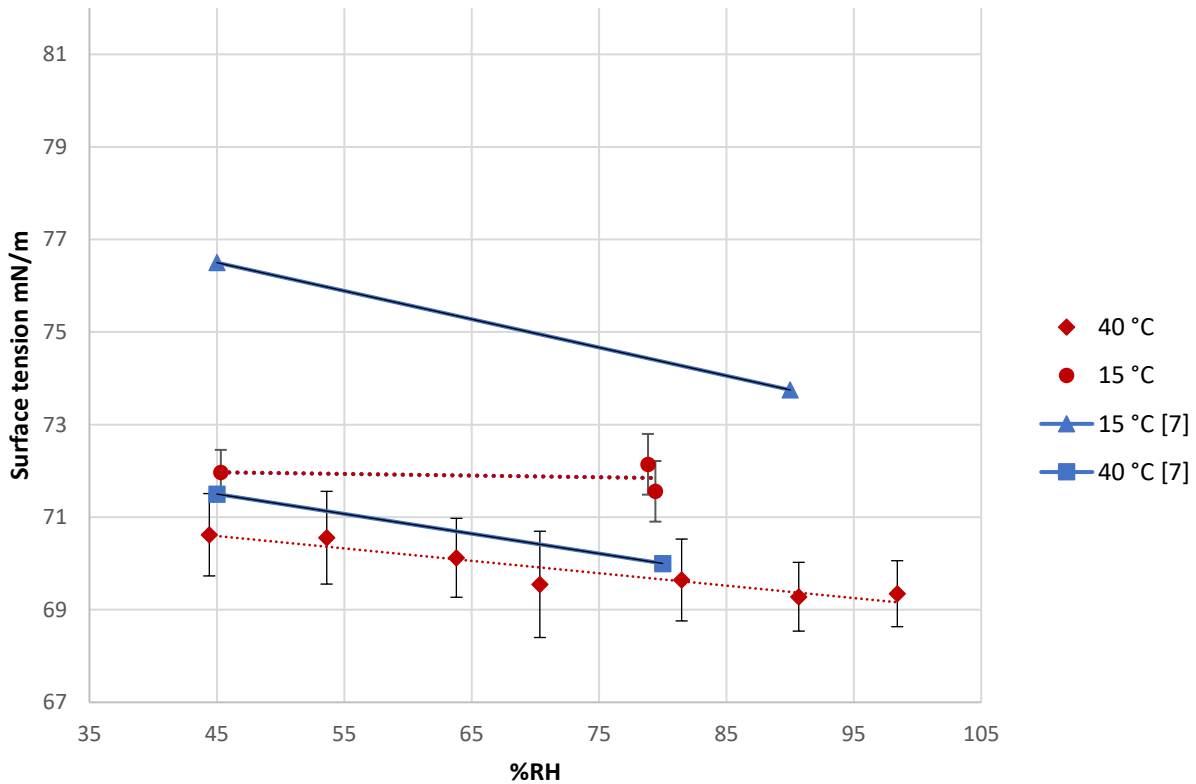


Figure 6-2 - Surface tension of DI water at constant temperature and varied humidity

6.2 - Receding contact angle

Receding contact angle was investigated by replicating the experiments of Panwar et al [37]. Experiments on the effect of evaporation on the contact angle of sessile drop on solid surfaces; mainly the experiments conducted on glass substrates with DI water droplets [37]. The main goal was to verify that the contact angle will decrease almost linearly with time; while the contact angle radius remains

constant. Four parameters made up the initial conditions for the experiment; temperature and humidity of the environment, contact radius of the droplet, and initial contact angle of the droplet.

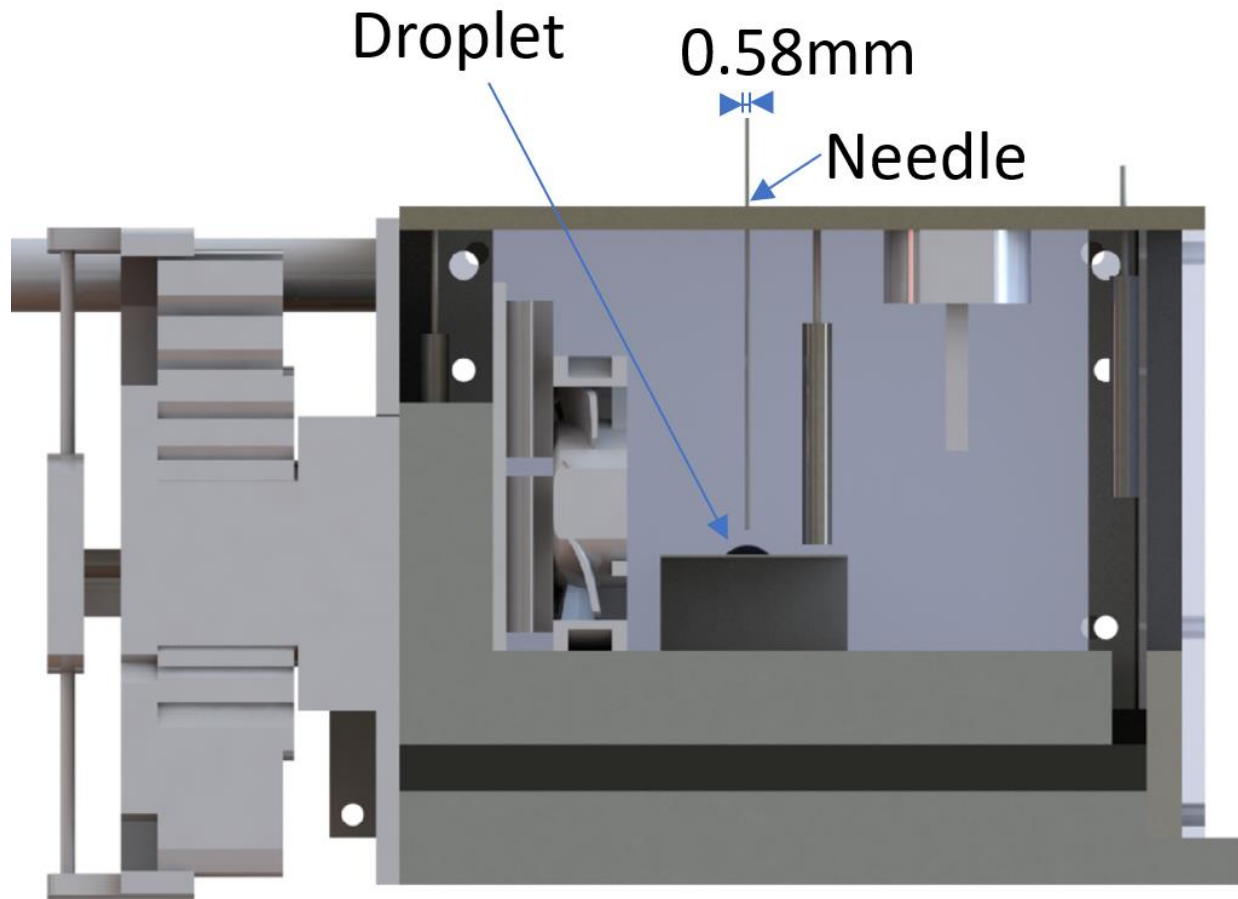


Figure 6-3 - Location of droplet for sessile drop experiment, the needle is located at the center of the chamber, the volume of the droplet is 18.6 μL

Table 6-A - Initial conditions for receding contact angle experiments

	Literature	Experiment (average)
Temperature	27-28°C	27.5°C
Initial Contact angle	42	45
Contact angle radius	0.27 cm	0.3cm
Initial Volume	15.4 mg	14.28 mg
Humidity	61-63 %RH	61 %RH

The results of the experiments were in line with the literature (see Figure 6-4). The droplet contact angle linearly decreased during evaporation; never changing states from constant contact angle radius to constant contact angle. This indicates that the surface energy of the substrate is significantly high, keeping the left and right ends of the droplet composing the point where the 3 phase boundaries meet [81]. All experimental data is recorded in Appendix D-2.

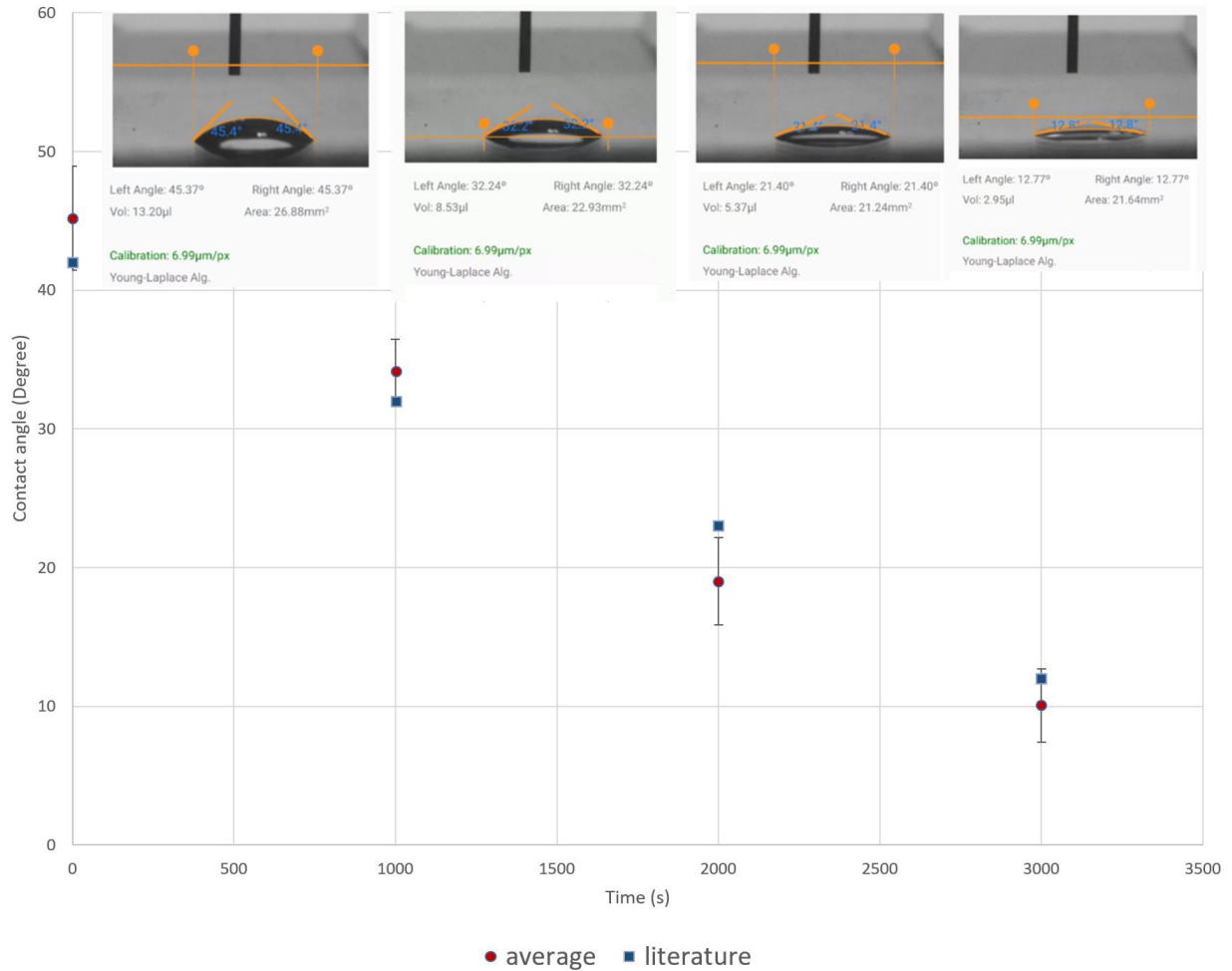


Figure 6-4 - Evaporation of DI water at 27.5°C and 61%RH on a glass substrate

6.3 - Advancing contact angle

For the advancing contact angle test, the advancing contact angle of DI water was recorded for Teflon in a high temperature and humidity environment. The goal of these experiments was to investigate the effects of temperature on the advancing contact angle for flat hydrophobic Teflon surfaces [61]. Flat in this case is defined as a continuous coating without any geometric features of note. For the set of experiments, spin coated Teflon on aluminum substrates was used to get an even coating. The contact angle of a spin coat surface under dry conditions can be affected by many parameters, e.g., spin rate, rotational acceleration, environmental humidity, temperature, substrate topography, and so on [82] [40]. Therefore, it is difficult to fabricate a surface with identical contact angles as in [61]. However, the focus of the comparison (as shown in Figure 6-5) is on the evolving trend of the contact angle value at different temperatures and range of relative humidity. The difference in the contact angle value between our surfaces and the ones used in literature under ambient room conditions (22 °C and around 60% relative humidity) will not affect our conclusion; the contact angle values will just be shifted by a constant. All experimental data is recorded in Appendix D-3.

The results of the experiments were in line with the literature, although offset due to the nature of a prepared Teflon surface having high contact angle hysteresis. The advancing contact angle was measured to be around a value of 127° for temperatures between 50-70 °C at humidity levels between 53-65 %RH. Although increasing the temperature results in a lower value for the surface tension of water; it has been observed in the literature that for low energy surfaces; the work of adhesion for the droplet to the solid is negligible [83]. Thus, although the surface tension of the water is one of the main components defining the contact angle of the system [28] and the surface tension is drastically affected by temperature [79]; the change in surface tension at this level is not enough to significantly change the contact angle of the water droplet on a Teflon surface.

According to the literature, at humidity levels close to saturation, the contact angle values for the same temperature range decreased by around 9° [61]. A similar trend was observed as seen in Figure 6-5 with an average contact angle difference between the ranges of 53%-65% and 94%-100% relative humidity being 5.1°, regardless of temperature. According to the literature [61], this trend is unique to a flat coating, and does not manifest for surfaces with nano or microstructures. The change in contact angle on a flat coating at almost saturated levels of water vapor; is in line with the literature, that proposes the effective surface energy of the low energy solid is increased with vapor deposition on the surface of the coating [84]. The increased surface energy is enough to decrease the contact angle of the droplet.

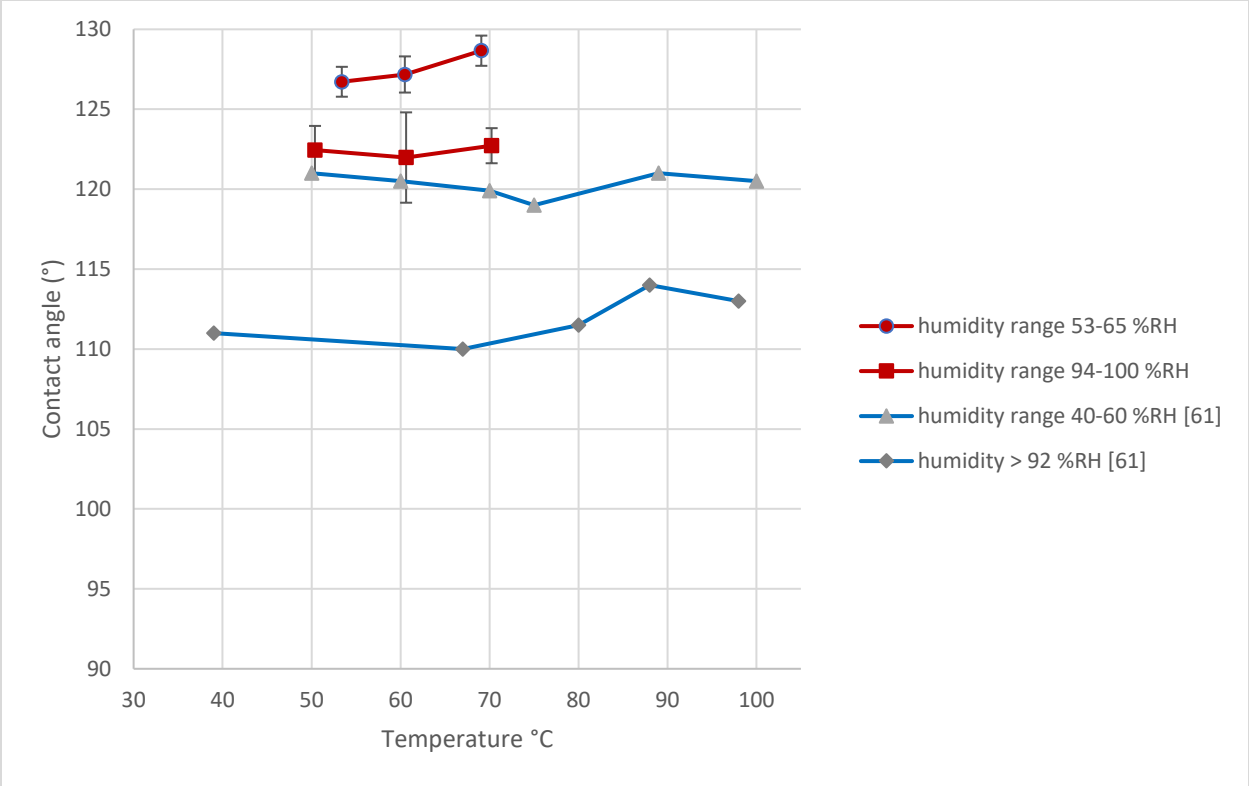


Figure 6-5 - The effects of temperature and humidity on the advancing contact angle of DI water on a Teflon substrate

Chapter 7 – Summary and future studies

The study of interfacial phenomenon involving temperature and humidity was the motivation behind the development of the environment chamber. Below conclusions from this work and areas of future work is discussed in detail.

7.1 - Summary and conclusion

The portable environment chamber was designed and prototyped with the help of the QFD methodology. The house of quality matrix tool was used to remove the instinct from designer, and create a logical framework to achieve a functional product. The electronic instrumentation of the design was an iterative process, with each iteration adding a greater degree of refinement and complexity to the system. The data obtained from the literature was then analysis and replicated, to show the capability of the system.

The chamber successfully implements a novel solid state ITO glass anti condensation system, not seen in commercial chambers or chambers made in the literature. This allowed for a more consistent internal environment of the inside of the chamber without the need for an inert gas line as most environment chambers require. The main heating/cooling system of the chamber only requires electricity to function; and does not require coolant like most commercially available chambers. The chamber was designed with portability and ease of integration into commercial and custom droplet imaging systems.

The final device had the capability of temperature and humidity control; it was able to reach and maintain a given setpoint within its temperature and humidity range limits.

Surface tension and contact angle were the main measurements tested with the device, with DI water as the probing liquid. Surface tension measurements at 40°C with varying relative humidity yielded similar results with the literature; however, measurements taken at 15°C showed significant deviation from the literature. Evaporative contact angle measurements at 27.5°C and 61%RH on a glass substrate yielded the same trend as the literature with the contact angle reducing as the droplet stays pinned to the surface. There were similar results with the literature for advancing contact angle measurements on a Teflon surface where at the temperature range of 50 °C to 70°C the contact angle did not change significantly, however the change in humidity resulted in a decreased contact angle.

In conclusion, the chamber was able to replicate the different test conditions in the literature. The chamber is able to automatically generate and hold different isolated temperature and humidity

conditions internally, allowing for precise and accurate measurements of contact angle and surface tension. The tests performed for contact angle within the chamber yielded measurement values within the respected range of what was reported in the literature. This was also true for surface tension, with the exception of surface tension at lower temperatures which requires further investigation.

7.2 - Future works

Future work for the thesis revolves around refining and improving the capabilities, functionality, and manufacturability of the chamber.

Instead of adhesives like silicon used in the manufacturing and assembly of the chamber; mechanical fasteners and gaskets would allow for a more repairable and easier to assemble chamber. Switching to mechanical fasteners would also allow for a larger temperature and humidity ranges the chamber is capable of generating inside of it; especially at a high temperatures and high humidity environment where silicon glues adhesive strength is too weak to handle the pressure in such an environment.

A more complex lid and droplet generation mechanism is another aspect that can be improved. The current lid mechanism uses four set screws to attach the lid and seal the chamber. Instead, for usability a mechanical mechanism such as a four-bar linkage system could be implemented.

Another aspect of the lid that can be improved is with respect to the location of the drop generation port. The current chamber has a hole in the lid that can be embedded with a self-healing injection port; for the needle to enter and while still keeping the chamber sealed. The location of this port is in the center of the lid, to allow the droplet to be generated in the center of the chamber. This configuration does not allow for the generation of a droplet anywhere else inside the chamber unless the lid is modified with another though hole. A more adapted system would allow for more complex multiple droplet experiments to be tested.

The lid can also be modified for transparency; this would allow for image acquisition for ADSA-D measurements, which require the top view of the droplet.

Increasing the number of sensors inside the chamber would result in a more accurate representation of the temperature and humidity conditions inside the chamber. In the future, the temperature and humidity readings of the air inside the chamber should be an average of multiple sensors distributed inside the chamber.

The amount of wiring and chips used can also be reduced with a complete redesign of the electronics. Rather than having modules like an h-bridge wired to the micro controller; a layered board with all the electronics built in would drastically simplify the design.

Another area of improvement is the control system and user interface. The current system requires the setpoint to be hard coded into the micro controller. For future work, the goal would be to have a smart phone control the setpoint for the chamber. This would be done with a Bluetooth master/slave protocol, where the smartphone is the master device and the microcontroller the slave device.

With a benchmarked and proven chamber, conducting experiments with different liquids will become the main purpose of the chamber. These liquids can include 3D printing resins or multi component droplets (e.g., DI water and propylene glycol). Experiments would revolve around observing the contact angle and surface tension of the liquids at various elevated temperatures and to observe the evaporative behavior of the droplet in humid conditions.

References

- [1] S. Pan, R. Guo, M. Björnmalm, J. J. Richardson, L. Li, C. Peng, N. Bertleff-Zieschang, W. Xu, J. Jiang and F. Caruso, "Coatings super-repellent to ultralow surface tension liquids," *Nature Materials*, *17*(11), pp. 1040-1047, 2018.
- [2] X. Zhanga and O. A. Basaran, "Dynamic Surface Tension Effects in Impact of a Drop," *Journal of Colloid and Interface Science*, vol. 187, no. 1, pp. 166-178, 1997.
- [3] W. Schoel, S. Schürch and J. Goerke, "The captive bubble method for the evaluation of pulmonary surfactant: surface tension, area, and volume calculations," *Biochimica et Biophysica Acta (BBA) - General Subjects*, vol. 1200, no. 3, p. 281–290, 1994.
- [4] A. Bonfillon, F. Sicoli and D. Langevin, "Dynamic Surface Tension of Ionic Surfactant Solutions," *Journal of Colloid and Interface Science*, vol. 168, no. 2, p. 497–504, 1994.
- [5] J. Eastoe and J. Dalton, "Dynamic surface tension and adsorption," *Advances in Colloid and Interface Science* *85*(2-3), 103-144., 2000.
- [6] J. Chappuis, I. A. Sherman and A. W. Neumann, "Surface tension of animal cartilage as it relates to friction in joints," *Annals of Biomedical Engineering*, vol. 11, p. 435–449, 1983.
- [7] J. L. Pérez-Díaz, M. A. Álvarez-Valenzuela and J. C. García-Prada, "The effect of the partial pressure of water vapor on the surface tension of the liquid water–air interface," *Journal of Colloid and Interface Science*, vol. 381, no. 1, pp. 180-182, 2012.
- [8] M. ABU-ORABI, "Modeling of heat transfer in dropwise condensation," *International Journal of Heat and Mass Transfer*, vol. 41, no. 1, pp. 81-87, 1998.
- [9] L. I. Davis, G. A. Dage and J. D. Hoeschele, "Conditions for Incipient Windshield Fogging and Anti-Fog Strategy for Automatic Climate Control.," *SAE Transactions*, vol. 110, pp. 537-545, 2001.
- [10] O. Jonas, "Steam turbine corrosion," *Corrosion: Environments and Industries*, vol. 13C, pp. 469-476, 2006.
- [11] H. Sadafi, S. Dehaeck, A. Rednikov and P. Colinet, "Vapor-Mediated versus Substrate-Mediated Interactions between Volatile Droplets," *Langmuir*, vol. 35, no. 21, pp. 7060-7065, 2019.
- [12] A. W. Wray, B. R. Duffy and S. K. Wilson, "Competitive evaporation of multiple," *Journal of Fluid Mechanics*, vol. 884, no. A45, pp. 1-19, 2019.
- [13] N. Cira, A. Benusiglio and M. Prakash, "Vapour-mediated sensing and motility in two-component droplets," *Nature*, vol. 519, p. 446–450, 2015.

- [14] X. Man and M. Doi, "Vapor-Induced Motion of Liquid Droplets on an Inert Substrate," *Phys Rev Lett.*, vol. 119, no. 4, p. 044502, 2017.
- [15] X.-M. Wang, B. Riedl, A. Christiansen and R. Geimer, "The effects of temperature and humidity on phenol-formaldehyde resin bonding," *Wood Science and Technology*, vol. 29, no. 4, pp. 253-266, 1995.
- [16] A.-L. Pasanen, P. Kalliokoski, P. Pasanen, M. J. Jantunen and A. Nevalainen, "Laboratory studies on the relationship between fungal growth and atmospheric temperature and humidity.," *Environment International*, vol. 17, no. 4, pp. 225-228, 1991.
- [17] The Editors of Encyclopaedia Britannica, "Johann Andreas von Segner," *Encyclopedia Britannica*, 5 October 2021. [Online]. Available: <https://www.britannica.com/biography/Johann-Andreas-von-Segner>. [Accessed 10 December 2021].
- [18] R. Finn, J. McCuan and H. C. Wentz, "Thomas Young's Surface Tension Diagram: Its History, Legacy, and Irreconcilabilities," *Journal of Mathematical Fluid Mechanics*, vol. 14, no. 3, p. 445-453, 2011.
- [19] J. W. M. Bush, "New Trends in the Physics and Mechanics of Biological Systems: Lecture Notes of the Les Houches Summer School," *Oxford University Press*, vol. 29, no. 92, pp. 27-63, 2009.
- [20] P. J. Louis and H. F. J. Kenneth, "Deionized Water — An Evaluation," *American Journal of Hospital Pharmacy*, vol. 21, no. 11, p. 497-500, 1964.
- [21] N. B. Vargaftik, B. N. Volkov and L. D. Voljak, "International Tables of the Surface Tension of Water," *Journal of Physical and Chemical Reference Data*, vol. 12, no. 3, pp. 817-820, 1983.
- [22] E. Portuguez, A. Alzina, P. Michaud, M. Oudjedi and A. Smith, "Evolution of a Water Pendant Droplet: Effect of Temperature and Relative Humidity," *Natural Science*, vol. 9, no. 1, pp. 1-20, 2017.
- [23] K. W. Gyak, N. K. Vishwakarma, Y.-H. Hwang, J. H. Kim, H. Yun and D.-P. Kim, "3D-printed Monolithic SiCN Ceramic Microreactors from a Photocurable Pre-ceramic Resin for High Temperature Ammonia Cracking Process," *Reaction Chemistry & Engineering*, vol. 4, no. 8, pp. 1393-1399, 2019.
- [24] T. Yoshida and T. Hyōdō, "Evaporation of Water in Air, Humid Air, and Superheated Steam," *Industrial & Engineering Chemistry Process Design and Development*, vol. 9, no. 2, p. 207-214, 1970.
- [25] J. E. R. Coney, C. G. W. Sheppard and E. A. M. El-Shafei, "Fin performance with condensation from humid air: a numerical investigation," *International Journal of Heat and Fluid Flow*, vol. 10, no. 3, p. 224-231, 1989.
- [26] Elegoo, *Photopolymer resin from elegoo, material safety data sheet*, 2019.

- [27] T. Young, "An essay on the cohesion of fluids.," *Philosophical Transactions of the Royal Society of London*, vol. 95, no. 1805, pp. 65-87, 1805.
- [28] R. S. Hebbar, A. M. Isloor and A. F. Ismail, "Contact Angle Measurements.," in *Membrane Characterization*, Elsevier Inc., 2017, p. chapter 12.
- [29] H. Eral, D. 't Mannetje and J. M. Oh, "Contact angle hysteresis: a review of fundamentals and applications," *Colloid and Polymer Science volume*, vol. 291, no. 2, pp. 247-260, 2013.
- [30] E. J. De Souza, L. Gao, T. J. McCarthy, E. Arzt and A. J. Crosby, "Effect of contact angle hysteresis on the measurement of capillary forces," *Langmuir*, vol. 24, no. 4, pp. 1391-1396, 2008.
- [31] D. P. Subedi, "Contact Angle Measurement for The Surface Characterization of Solids," *Himalayan Physics*, vol. 2, no. 2, pp. 1-4, 2011.
- [32] K. Mittal, *Contact angle, wettability and adhesion*, CRC Press, 2003.
- [33] R. J. Good, "Contact angle, wetting, and adhesion: a critical review," *Journal of Adhesion Science and Technology*, vol. 6, no. 12, p. 1269–1302, 1992.
- [34] A. J. B. Milne and A. Amirfazli, "The Cassie equation: How it is meant to be used," *Advances in Colloid and Interface Science*, vol. 170, no. 1-2, pp. 48-55, 2012.
- [35] J. Wang, Y. Wu, Y. Cao, G. Li and Y. Liao, "Influence of surface roughness on contact angle hysteresis," *Colloid and Polymer Science*, vol. 298, no. 8, p. 1107–1112, 2020.
- [36] R. H. Dettre and R. E. Johnson, "Contact Angle Hysteresis. IV. Contact Angle Measurements on Heterogeneous Surfaces," *The Journal of Physical Chemistry*, vol. 69, no. 5, p. 1507–1515, 1965.
- [37] A. K. Panwar, S. K. Barthwal and S. Ray, "Effect of evaporation on the contact angle of a sessile drop on solid substrates," *Journal of Adhesion Science and Technology*, vol. 17, no. 10, pp. 1321-1329, 2003.
- [38] H. Y. Erbil, "Evaporation of pure liquid sessile and spherical suspended drops: A review," *Advances in Colloid and Interface Science*, vol. 170, no. 1-2, pp. 67-86, 2012.
- [39] J. E. Castillo, J. A. Weibel and S. V. Garimella, "The Effect of Relative Humidity on Dropwise Condensation Dynamics," *International Journal of Heat and Mass Transfer*, Vol. 80, pp. 759-766, vol. 80, no. 1, pp. 759-766, 2015.
- [40] M. Nilsson, R. Daniello and J. Rothstein, "A novel and inexpensive technique for creating superhydrophobic surfaces using Teflon and sandpaper.," *Journal of Physics D: Applied Physics*, vol. 43, no. 4, p. 045301, 2010.
- [41] M. G. Lawrence, "The Relationship between Relative Humidity and the Dewpoint Temperature in Moist Air: A Simple Conversion and Applications," *Bulletin of the American Meteorological Society*, vol. 86, no. 2, p. 225–234, 2005.

- [42] Y. Nagata, K. Usui and M. Bonn, "Molecular Mechanism of Water Evaporation," *Physical Review Letters*, vol. 115, no. 23, p. 134707, 2015.
- [43] Y. Wu, X. Zhang, X. Zhang and M. Munyalo, "Modeling and experimental study of vapor phase-diffusion driven sessile drop evaporation.," *Applied Thermal Engineering*, vol. 70, no. 1, p. 560–564, 2014.
- [44] D. E. Walton, "The Evaporation of Water Droplets. A Single Droplet Drying Experiment," *Drying Technology: An International Journal*, vol. 22, no. 3, pp. :431-456, 2004.
- [45] F. Giorgiutti-Dauphiné and L. Pauchard, "Drying drops containing solutes: From hydrodynamical to mechanical instabilities," *The European Physical Journal E*, 41(3)., vol. 41, no. 3, p. 32, 2018.
- [46] X. Xu and J. Luo, "Marangoni flow in an evaporating water droplet.," *Applied Physics Letters*, vol. 91, no. 12, p. 124102, 2007.
- [47] H. Chen, J. L. Muros-Cobos and A. Amirfazli, "Contact angle measurement with a smartphone," *REVIEW OF SCIENTIFIC INSTRUMENTS*, vol. 89, no. 3, p. 035117, 2018.
- [48] S. M. I. Saad, Z. Policova and A. W. Neumann, "Design and accuracy of pendant drop methods for surface tension measurement.," *Colloids and Surfaces A: Physicochemical and Engineering Aspects*, vol. 384, no. 1-3, pp. 442-452, 2011.
- [49] P. Chen, D. Y. Kwok, R. M. Prokop, O. I. del Rio, S. S. Susnar and A. W. Neumann, "Axisymmetric Drop Shape Analysis (ADSA) and its Applications," *Studies in Interface Science*, vol. 6, pp. 61-138, 1998.
- [50] S. V. S. Dochibhatla, M. Bhattacharya and B. Morkos, "Evaluating Assembly Design Efficiency: A Comparison Between Lucas and Boothroyd-Dewhurst Methods," in *ASME 2017 International Design Engineering Technical Conferences and Computers and Information in Engineering Conference*, 2017.
- [51] P. G. Leaney and G. Wittenberg, "Design For Assembling: The Evaluation Methods Of Hitachi, Boothroyd And Lucas," *Assembly Automation*, vol. 12, no. 2, pp. 8-17, 1992.
- [52] Z. Gao, T. A. Trautzsch and J. G. Dawson, "A Stable Self-Tuning Fuzzy Logic Control System," *IEEE Transactions on Industry Applications*, vol. 38, no. 2, p. 414–424, 2002.
- [53] G. Ellis, *Control System Design Guide. Using Your Computer to Understand and Diagnose Feedback Controllers* [4 ed.], Elsevier, 2012.
- [54] F. Naz, Z. Wajid, A. A. Amin, O. Saleem, M. H. Shahbaz, M. G. Khan and M. Adnan, "PID Tuning with reference tracking and plant uncertainty along with disturbance rejection," *Systems Science & Control Engineering*, vol. 9, no. 1, pp. 160-166, 2021.

- [55] M. Misaghi and M. Yaghoobi, "Improved invasive weed optimization algorithm (IWO) based on chaos theory for optimal design of PID controller," *Journal of Computational Design and Engineering*, vol. 6, no. 3, p. 284–295, 2019.
- [56] X.-M. Ma and L. Guo, "Optimization of PID Parameters for Mine Hoisting DTC System Based on Chaos Theory," *International Conference on Artificial Intelligence and Computational Intelligence.*, vol. 2, no. 2, pp. 128-131, 2009.
- [57] K. K. Ahn and D. Q. Truong, "Online tuning fuzzy PID controller using robust extended Kalman filter," *Journal of Process Control*, vol. 19, no. 6, pp. 1011-1023, 2009.
- [58] L. Dos Santos Coelho, "Tuning of PID controller for an automatic regulator voltage system using chaotic optimization approach.," *Chaos, Solitons & Fractals*, vol. 39, no. 4, p. 1504–1514, 2009.
- [59] T. 6624, "Tuning a PID Controller," compendium, [Online]. Available: <https://compendium.readthedocs.io/en/latest/robotcode/components/pid/pidcontroller2.html>. [Accessed 10 12 2021].
- [60] G. K. H. Pang and S. A. Mesbah, "Design of bang-bang controller based on a fuzzy-neuro approach," in *Joint Conference on Control Applications Intelligent Control and Computer Aided Control System Design*, 1996.
- [61] P. B. Weisensee, N. K. Neelakantan, K. Suslick, A. M. Jacobi and W. P. King, "Impact of air and water vapor environments on the hydrophobicity of surfaces," *Journal of Colloid and Interface Science*, vol. 453, p. 177–185, 2015.
- [62] J. Feng, R.-J. Li, Y.-X. He and K.-C. Fan, "Development of a low-cost mini environment chamber for precision instruments.," *Sensors and Materials*, vol. 27, no. 4, pp. 329-340, 2015.
- [63] T. Huhtamäki, X. Tian, J. T. Korhonen and R. H. A. Ras, "Surface-wetting characterization using contact-angle measurements," *Nature Protocols*, vol. 13, no. 7, p. 1521–1538, 2018.
- [64] J. B. ReVelle, J. W. Moran and C. A. Cox, *The QFD Handbook*, John Wiley & Sons Inc., 1998.
- [65] C. Battles, "QFD template," 21 4 2010. [Online]. Available: https://www.uw-s.com/media/Full_HOQ_0.9.xlsx.
- [66] H. Peacock, R. Sindelar and P. Lam, "Temperature and humidity effects on the corrosion of aluminum-base reactor fuel cladding materials during dry storage," in *International meeting on reduced enrichment for research and test reactors*, 1995.
- [67] MICROBOT, "Dual-Channel-Relay-Module-Datasheet.pdf," [Online]. Available: https://components101.com/sites/default/files/component_datasheet/Dual-Channel-Relay-Module-Datasheet.pdf. [Accessed 2021].
- [68] adafruit, "DHT11, DHT22 and AM2302 Sensors," [Online]. Available: <https://learn.adafruit.com/dht>. [Accessed 2021].

- [69] Arduino , "Arduino Uno Rev3 SMD," [Online]. Available: <https://store.arduino.cc/products/arduino-uno-rev3-smd>. [Accessed 2021].
- [70] STMicroelectronics, "Dual full-bridge driver," [Online]. Available: https://www.sparkfun.com/datasheets/Robotics/L298_H_Bridge.pdf. [Accessed 2021].
- [71] Richer-R, "Richer-R Water Cooling Reservoir," [Online]. Available: <https://www.newegg.com/p/1B4-079T-0KCS0>. [Accessed 2021].
- [72] Fitnate, "Machine Atomizer Air Humidifier," [Online]. Available: <http://www.fitnate.com/product/Mist-Maker.html>. [Accessed 2021].
- [73] adafruit , "Miniature 5V Cooling Fan," [Online]. Available: <https://www.adafruit.com/product/4468>. [Accessed 2021].
- [74] Cytron, "Cytron 10A Motor Driver Shield," [Online]. Available: <https://www.robotshop.com/media/files/PDF/manual-shield-md10.pdf>. [Accessed 2021].
- [75] Laird, "ETX6-12-F1-4040-TA-RT-W6," [Online]. Available: <https://lairdthermal.com/products/thermoelectric-cooler-modules/peltier-hitemp-etx-series/ETX6-12-F1-4040-TA-RT-W6>. [Accessed 2021].
- [76] Delta electronics inc, "FHS-A9025S19," [Online]. Available: <https://www.delta-fan.com/Download/Spec/FHS-A9025S19.pdf>. [Accessed 2021].
- [77] L.-D. Chen, "Effects of Ambient Temperature and Humidity on Droplet Lifetime – A Perspective of Exhalation Sneeze Droplets with COVID-19 Virus Transmission.," *International Journal of Hygiene and Environmental Health*, vol. 229, p. 113568, 2020.
- [78] F. Girard, M. Antoni, S. Faure and A. Steinchen, "Influence of heating temperature and relative humidity in the evaporation of pinned droplets.," *Colloids and Surfaces A: Physicochemical and Engineering Aspects*, vol. 323, no. 1-3, p. 36–49, 2008.
- [79] T. Petrova, "Revised Release on Surface Tension of Ordinary Water Substance," in *The International Association for the Properties of Water and Steam* , Moscow, 2014.
- [80] J. Hrubý, V. Vinš, R. Mareš, J. Hykl and J. Kalová, "Surface Tension of Supercooled Water: No Inflection Point down to -25 °C.," *J Phys Chem Lett.*, vol. 5, no. 3, p. 425–428, 2014.
- [81] E. M. A. Bormashenko and M. Zinigrad, "Evaporation of droplets on strong and low-pinning surfaces and dynamics of the triple line," *Eur Phys J E Soft Matter*, vol. 385, no. 1, pp. 235-240, 2011.
- [82] M. D. Tyona, "“A theoretical study on spin coating technique.”," *Advances in materials research*, vol. 2, no. 4, pp. 195-208, 2013.

- [83] A. B. PONTER and A. P. BOYES, "Temperature Dependence of Contact Angles of Water on a Low Energy Surface under Conditions of Condensation and at Reduced Pressures," *Nature Physical Science*, vol. 231, no. 24, p. 152–153, 1971.
- [84] B. Jańczuk and T. Białopiotrowicz, "Surface free-energy components of liquids and low energy solids and contact angles," *Journal of Colloid and Interface Science*, vol. 127, no. 1, pp. 189-204, 1989.

Appendices

Appendix A - Analysis and Calculation Data for QFD method

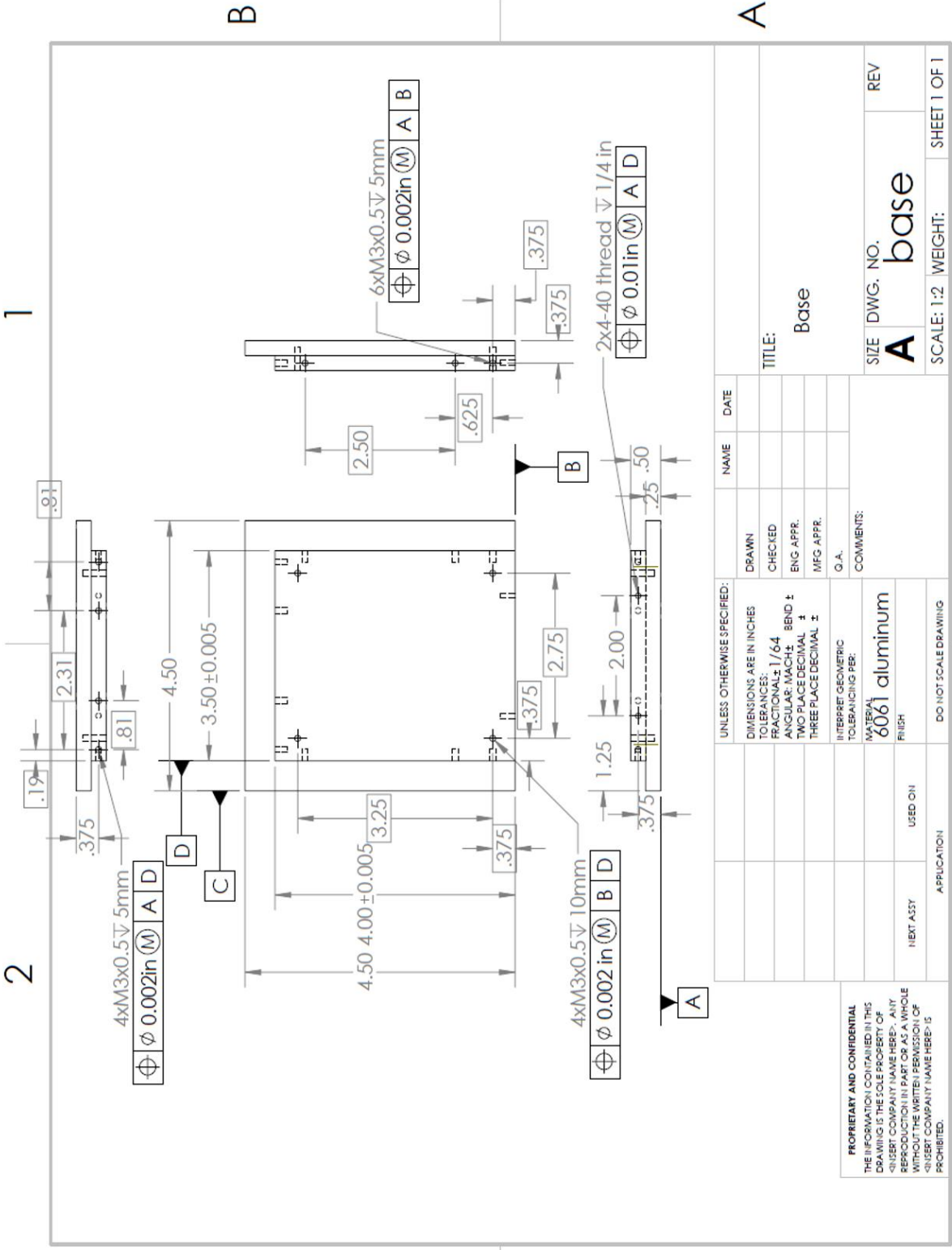
Appendix A - 1, Pairwise Comparison for QFD

	temperature control auto	temperature stability	humidity control auto	humidity stability	clear view of inside	easy to open and close	chamber size	temperature control manuel	humidity control manuel	temperature speed	humidity speed	stylish	needle entry	temperature range	humidity range	sum
temperature control auto	1	0	0	0.5	0.5	1	1	1	1	0.5	0.5	1	0.5	0	0	8
temperature stability	0	1	0	0.5	0	1	1	1	1	1	1	1	1	0.5	0.5	11.5
humidity control auto	0	0	1	0	0.5	1	1	1	1	0.5	0.5	1	0.5	0	0	8
humidity stability	0.5	0.5	0	1	0	1	1	1	1	1	1	1	1	0.5	0.5	11.5
clear view of inside	0.5	0.5	0.5	0	1	1	1	0.5	0.5	1	1	1	1	0.5	0.5	10
easy to open and close	0	0	0	0	1	1	0	0	0	0	0	0	1	0	0	1
chamber size	0	0	0	0	0	1	0	1	1	1	1	1	1	0.5	0.5	8
temperature control manuel	0	0	0	0	0.5	1	0	1	0.5	0	0	0	0	0	0	2
humidity control manuel	0	0	0	0	0	0	0	0	0	0	0	0	0	0	0	2
temp speed	0.5	0	0.5	0	0	1	0	1	1	0	0.5	1	0.5	0	0	6
humidity speed	0	0	0	0	0	0	0	0	0	0.5	1	0.5	0	0	0	6
stylish	0	0	0	0	0	0	0	1	1	0	0	1	0	0	0	2
needle entry	0.5	0	0.5	0	0	1	0	0	0	0.5	0.5	1	0	0	0	5
temp range	1	0.5	1	0.5	0.5	1	0.5	0	1	1	1	1	1	0	0.5	10.5
humidity range	1	0.5	1	0.5	0.5	1	0.5	0	1	1	1	1	1	0.5	0	10.5

Row vs Collom	
row win	1
netrual	0.5
row lose	0

Appendix B - Drawings for physical components used in design

No.	Name	Quantity
1	Base	1
2	Back Peek col	2
3	PTFE base	1
4	Peek left front col	1
5	Peek right front col	1
6	PTFE back plate	1
7	Lid	1
8	Inner Heat sink	1
9	PTFE booth sides	2
10	PTFE front side	1
11	ITO glass front	1
12	ITO glass side	2
13	Front acrylic	1
14	Side acrylic	2
15	Base plate	1
16	Inset	2
17	Magnet body	8
18	Magnet switch	8
19	Magnet switch nob	8
20	Magnet housing side 1	3
21	Magnet housing side 2	3
22	Phone mount	1
23	Syringe holder parts	1
24	Magnet housing chamber side 1	1
25	Magnet housing chamber side 2	1
26	Light body	1
27	Light lid	1
28	Base plate for jacks	3
29	Base plate for chamber stage	1
30	Al plate mid	1
31	Square column	1
32	Support pillar	1
33	Al top plate	1

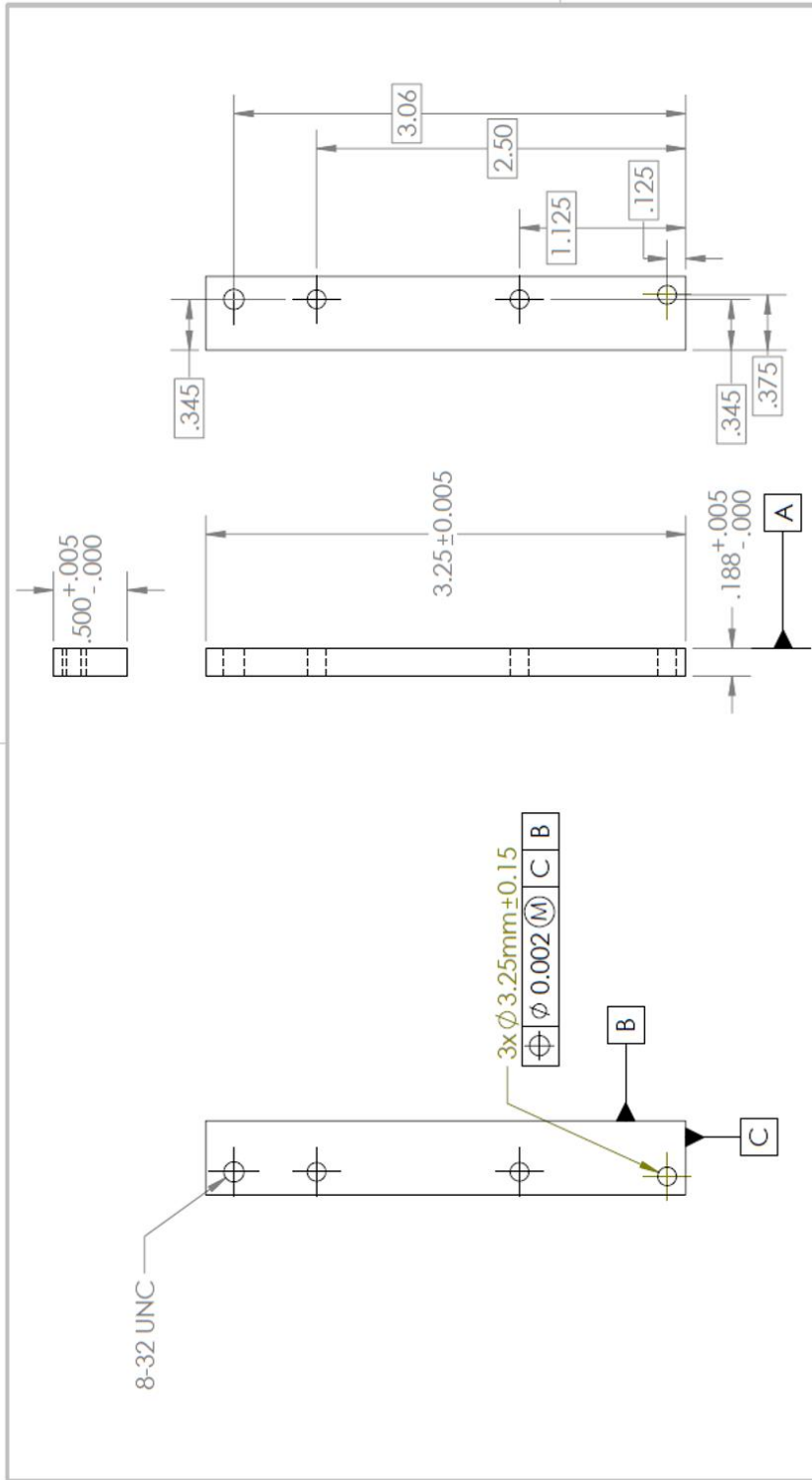


UNLESS OTHERWISE SPECIFIED:		NAME	DATE
DIMENSIONS ARE IN INCHES		DRAWN	
TOLERANCES:		CHECKED	
FRACTIONAL: 1/64		ENG. APPR.	
ANGULAR: MACH ±		MFG APPR.	
BEND ±		G.I.A.	
TWO PLACE DECIMAL ±		COMMENTS:	
THREE PLACE DECIMAL ±			
INTERPRET GEOMETRIC TOLERANCING PER:			
MATERIAL		SIZE	DWG. NO.
6061 aluminum		A	base
FINISH		SCALE: 1:2	WEIGHT:
NEXT ASSY		USED ON:	SHEET 1 OF 1
APPLICATION			

PROPRIETARY AND CONFIDENTIAL
 THE INFORMATION CONTAINED IN THIS DRAWING IS THE SOLE PROPERTY OF <INSERT COMPANY NAME HERE>. ANY REPRODUCTION IN PART OR AS A WHOLE WITHOUT THE WRITTEN PERMISSION OF <INSERT COMPANY NAME HERE> IS PROHIBITED.

2

1



8-32 UNC

3x Ø 3.25mm ± 0.15

A

A

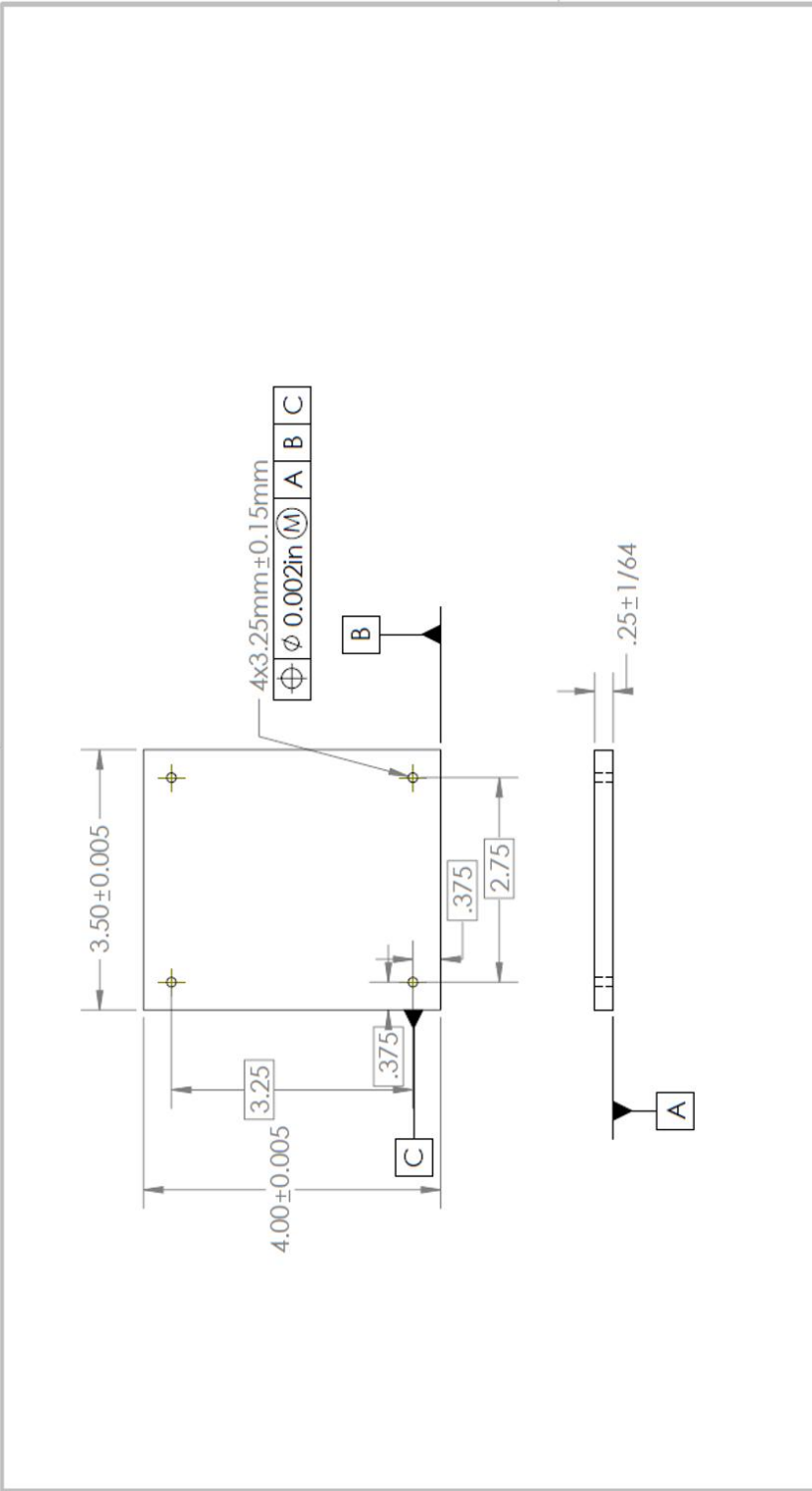
UNLESS OTHERWISE SPECIFIED:		NAME	DATE
DIMENSIONS ARE IN INCHES		DRAWN	
TOLERANCES:		CHECKED	
FRACTIONAL ± 1/64		ENG APPR.	
ANGULAR: MACH ±		IMFG APPR.	
TWO PLACE DECIMAL ±		G.A.	
THREE PLACE DECIMAL ±		COMMENTS:	
INTERPRET GEOMETRIC TOLERANCING PER:		MATERIAL	PEEK
		FINISH	
		NEXT ASSY	USED ON
		APPLICATION	
<p>PROPRIETARY AND CONFIDENTIAL THE INFORMATION CONTAINED IN THIS DRAWING IS THE SOLE PROPERTY OF <INSERT COMPANY NAME HERE>. ANY REPRODUCTION IN PART OR AS A WHOLE WITHOUT THE WRITTEN PERMISSION OF <INSERT COMPANY NAME HERE> IS PROHIBITED.</p>		<p>DO NOT SCALE DRAWING</p>	
TITLE:		Back peek col	
SIZE	DWG. NO.	REV	
Back peek col			
SCALE: 1:1	WEIGHT:	SHEET 1 OF 1	

2

1

1

2



B

B

A

A

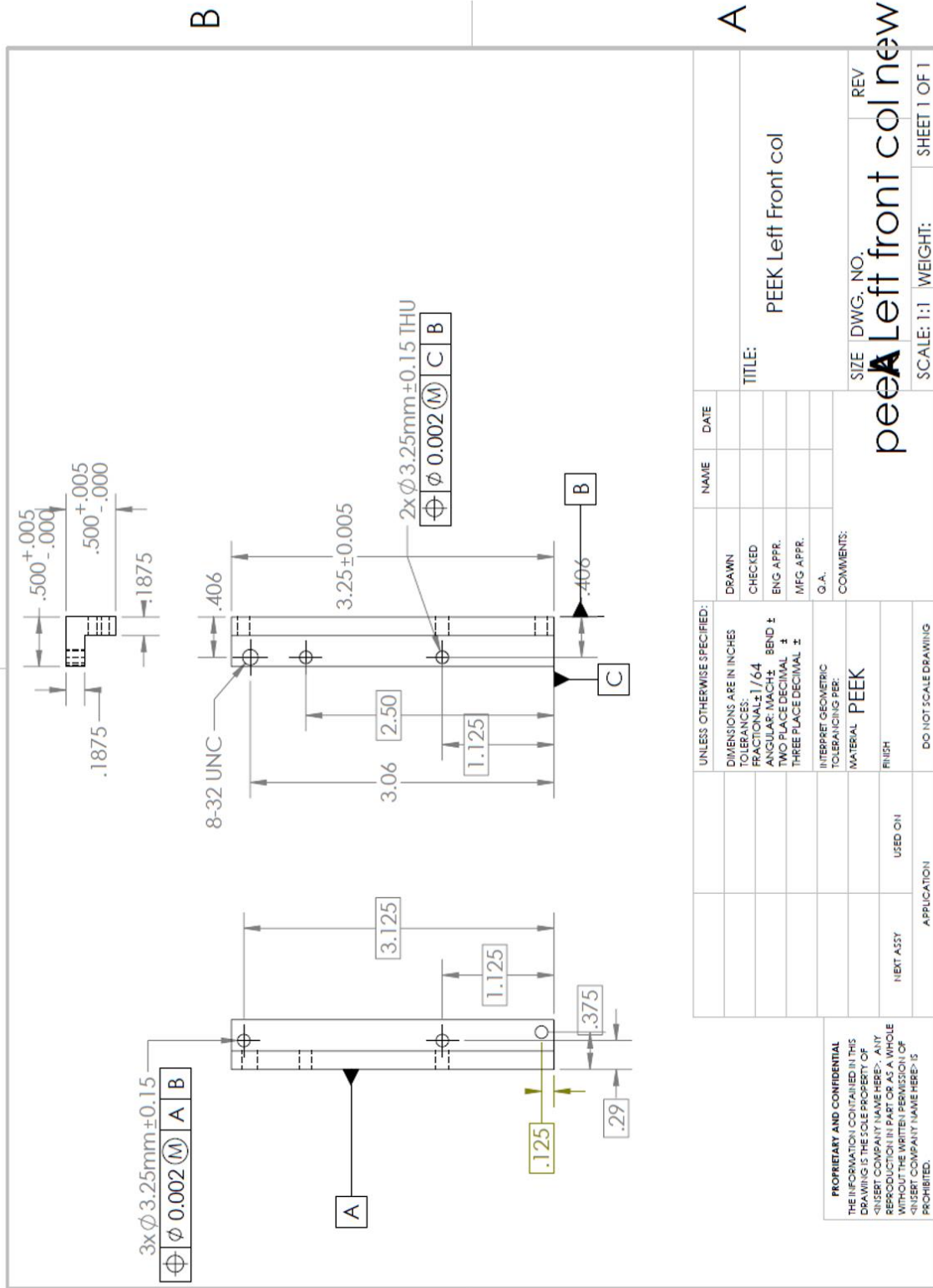
UNLESS OTHERWISE SPECIFIED: DIMENSIONS ARE IN INCHES TOLERANCES: FRACTIONAL: ± ANGULAR: MACH ± BEND ± TWO PLACE DECIMAL ± THREE PLACE DECIMAL ±		DRAWN	NAME	DATE	TITLE: PTFE base
INTERPRET GEOMETRIC TOLERANCING PER: MATERIAL: PTFE FINISH		CHECKED			
NEXT ASSY		ENG APPR.			SIZE DWG. NO. A
APPLICATION		MFG APPR.			REV
DO NOT SCALE DRAWING		Q. A.			SCALE: 1:2
		COMMENTS:			WEIGHT:
					SHEET 1 OF 1

1

2

1

2



A

A

UNLESS OTHERWISE SPECIFIED:	NAME	DATE
DIMENSIONS ARE IN INCHES		
TOLERANCES:	DRAWN	
FRACTIONAL: 1/64	CHECKED	
ANGULAR: MACH ± BEND ±	ENG APPR.	
TWO PLACE DECIMAL ±	MFG APPR.	
THREE PLACE DECIMAL ±	G.A.	
INTERPRET GEOMETRIC TOLERANCING PER:	COMMENTS:	
	MATERIAL: PEEK	
	FINISH:	
	USED ON:	
	APPLICATION:	
	DO NOT SCALE DRAWING	

PROPRIETARY AND CONFIDENTIAL
 THE INFORMATION CONTAINED IN THIS DRAWING IS THE SOLE PROPERTY OF <INSERT COMPANY NAME HERE>. ANY REPRODUCTION IN PART OR AS A WHOLE WITHOUT THE WRITTEN PERMISSION OF <INSERT COMPANY NAME HERE> IS PROHIBITED.

SIZE: DWG. NO. **REV**
peeA Left front col new

TITLE: PEEK Left front col

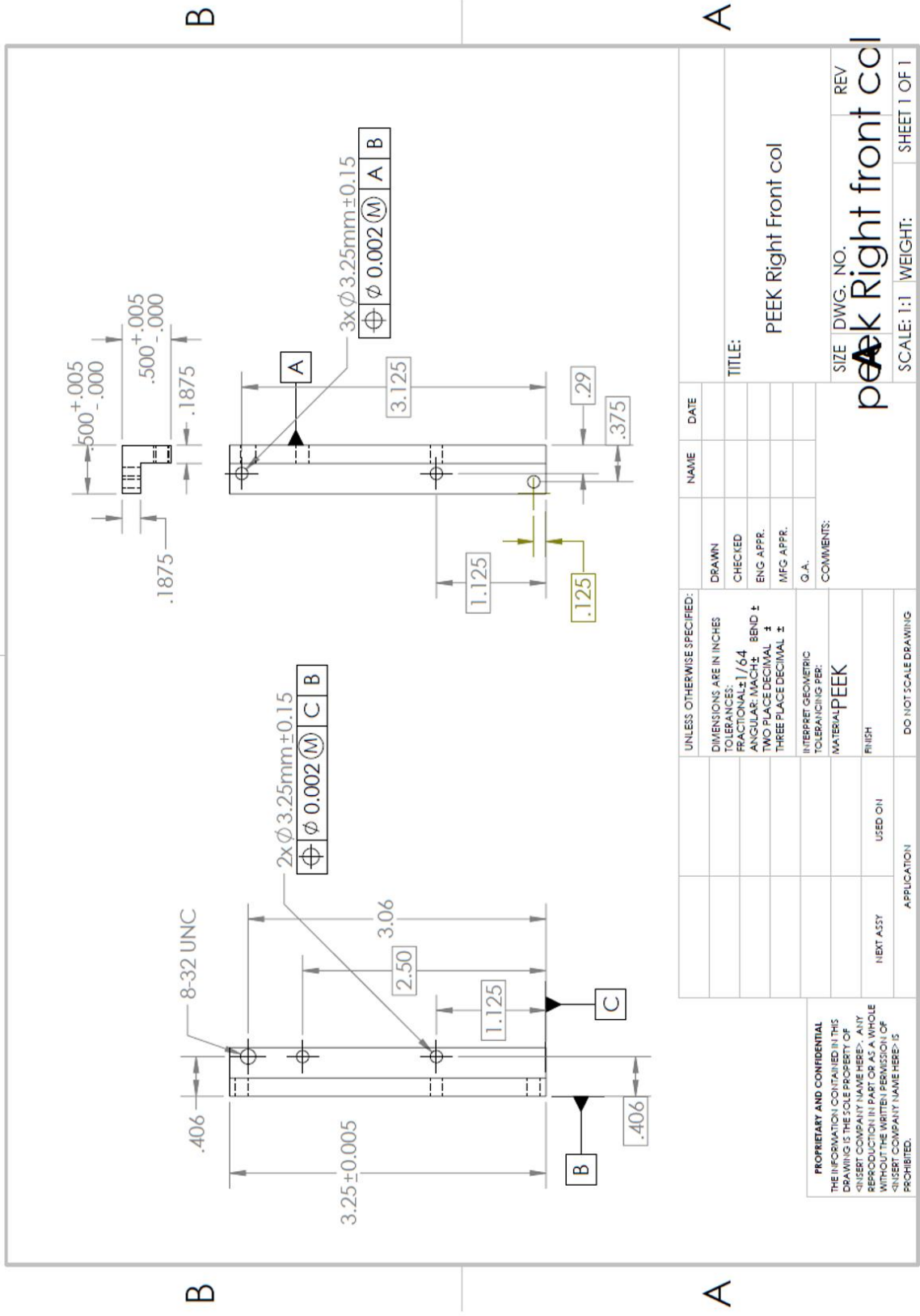
SCALE: 1:1 **WEIGHT:** **1** **SHEET 1 OF 1**

1

2

2

1



B

B

A

A

PROPRIETARY AND CONFIDENTIAL
 THE INFORMATION CONTAINED IN THIS
 DRAWING IS THE SOLE PROPERTY OF
 <INSERT COMPANY NAME HERE>. ANY
 REPRODUCTION IN PART OR AS A WHOLE
 WITHOUT THE WRITTEN PERMISSION OF
 <INSERT COMPANY NAME HERE> IS
 PROHIBITED.

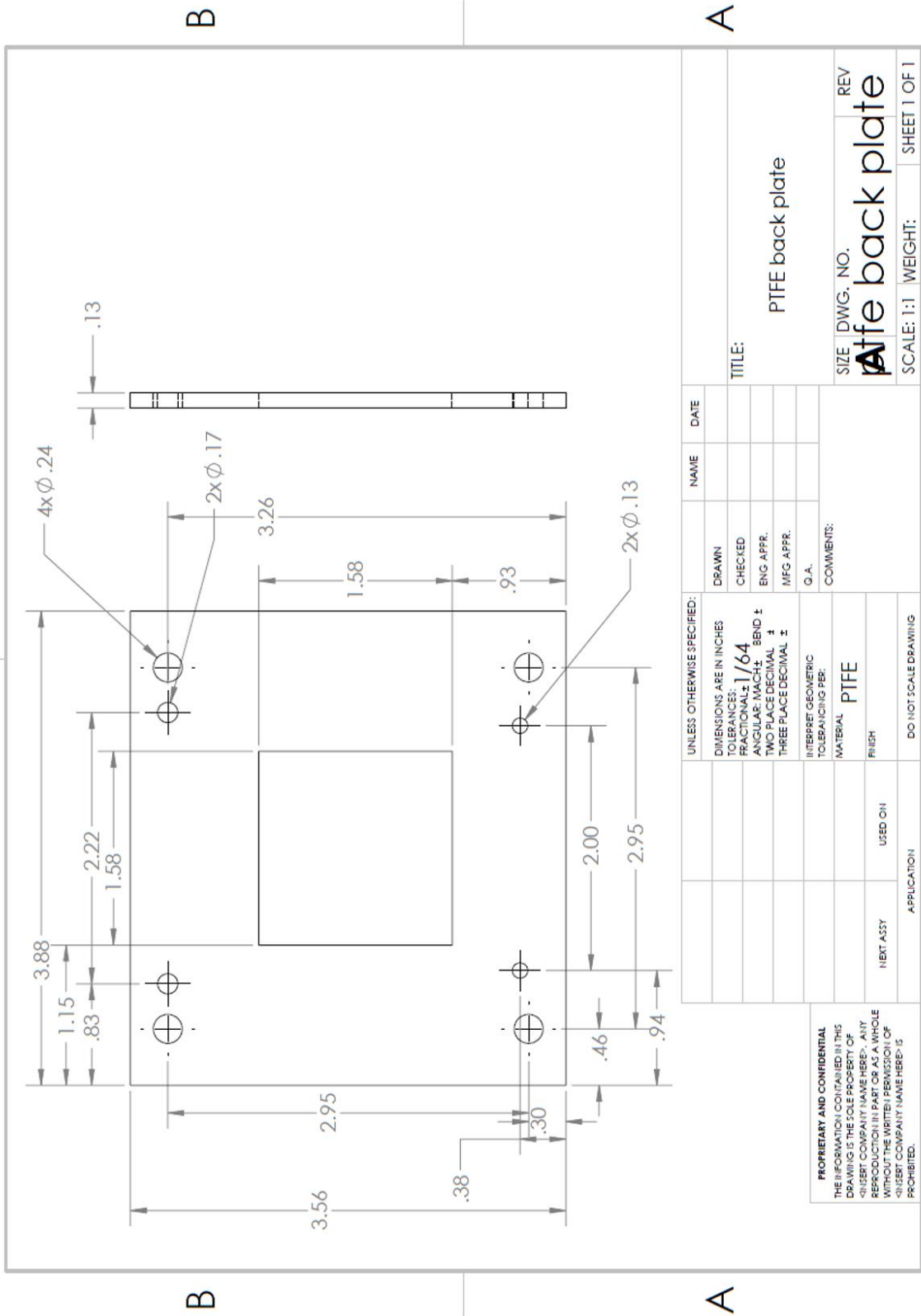
UNLESS OTHERWISE SPECIFIED:		DRAWN		NAME		DATE	
DIMENSIONS ARE IN INCHES		CHECKED					
TOLERANCES:		ENG. APPR.					
FRACTIONAL: 1/64		MFG APPR.					
ANGULAR: MACH: BEND: ±		Q.A.					
TWO PLACE DECIMAL: ±		COMMENTS:					
THREE PLACE DECIMAL: ±		MATERIAL: PEEK					
INTERPRET GEOMETRIC TOLERANCING PER:		FINISH					
		USED ON:					
		NEXT ASSY:					
		APPLICATION:					
		DO NOT SCALE DRAWING					
TITLE: PEEK Right Front col				SIZE: DWG. NO. REV		SHEET 1 OF 1	
SCALE: 1:1				WEIGHT:			

2

1

1

2



A

A

UNLESS OTHERWISE SPECIFIED:		NAME	DATE
DIMENSIONS ARE IN INCHES		DRAWN	
TOLERANCES:		CHECKED	
FRACTIONAL: 1/64 BEND ±		ENG APPR.	
ANGULAR: MACH ±		MFG APPR.	
TWO PLACE DECIMAL ±		G.A.	
THREE PLACE DECIMAL ±		COMMENTS:	
INTERPRET GEOMETRIC TOLERANCING PER:			
MATERIAL PTFE			
FINISH			
IN EXT ASSY	USED ON		
APPLICATION			
DO NOT SCALE DRAWING			
PROPRIETARY AND CONFIDENTIAL THE INFORMATION CONTAINED IN THIS DRAWING IS THE SOLE PROPERTY OF AIRBENT COMPANY NAME HERE. ANY REPRODUCTION IN PART OR AS A WHOLE WITHOUT THE WRITTEN PERMISSION OF AIRBENT COMPANY NAME HERE IS PROHIBITED.		TITLE: PTFE back plate	
SIZE DWG. NO. Airbent PTFE back plate		REV	
SCALE: 1:1		WEIGHT: SHEET 1 OF 1	

1

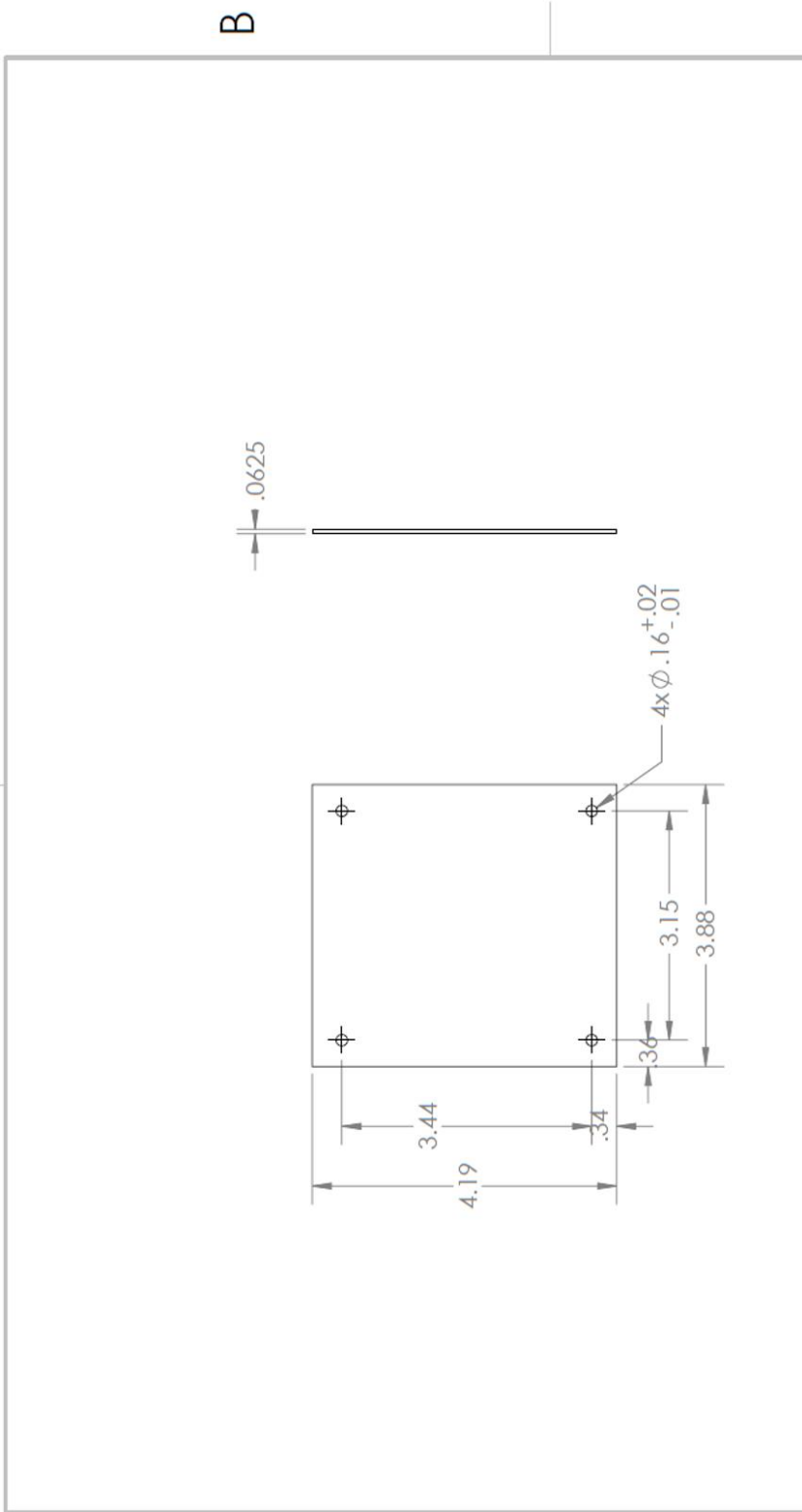
2

1

2

B

B



A

A

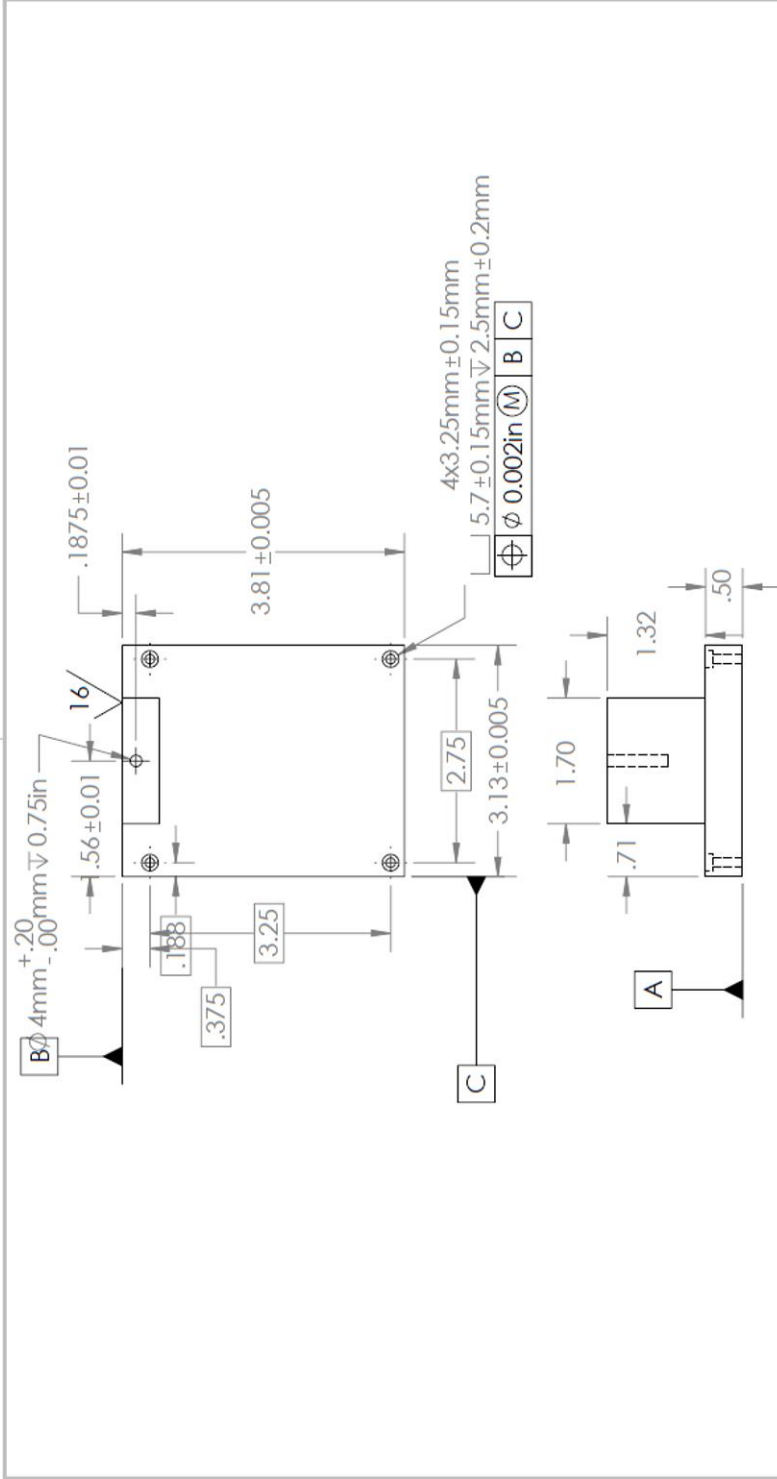
UNLESS OTHERWISE SPECIFIED:		NAME	DATE
DIMENSIONS ARE IN INCHES		DRAWN	
TOLERANCES:		CHECKED	
FRACTIONAL: 1/64		ENG APPR.	
ANGULAR: MACH ± BEND ±		MFG APPR.	
TWO PLACE DECIMAL ±		Q.A.	
THREE PLACE DECIMAL ±		COMMENTS:	
INTERPRET GEOMETRIC TOLERANCING PER:		SIZE DWG. NO. lid 2	
MATERIAL 6060 aluminum		REV	
FINISH		SCALE: 1:2 WEIGHT: SHEET 1 OF 1	
NEXT ASSY		APPLICATION	
USED ON		DO NOT SCALE DRAWING	

PROPRIETARY AND CONFIDENTIAL
 THE INFORMATION CONTAINED IN THIS
 DRAWING IS THE SOLE PROPERTY OF
 <INSERT COMPANY NAME HERE>. ANY
 REPRODUCTION IN PART OR AS A WHOLE
 WITHOUT THE WRITTEN PERMISSION OF
 <INSERT COMPANY NAME HERE> IS
 PROHIBITED.

1

2

2 1



B

B

A

A

UNLESS OTHERWISE SPECIFIED:		NAME		DATE	
DIMENSIONS ARE IN INCHES		DRAWN			
TOLERANCES:		CHECKED			
FRACTIONAL: 1/64		ENG. APPR.			
ANGULAR: MACH ±		MFG APPR.			
TWO PLACE DECIMAL ±		G.A.			
THREE PLACE DECIMAL ±		COMMENTS:			
INTERPRET GEOMETRIC TOLERANCING PER:		MATERIAL:		SIZE DWG. NO. REV	
ASME Y14.5		6061 aluminum		Heat sink in v3	
FINISH:		USED ON:		SCALE: 1:2 WEIGHT: SHEET 1 OF 1	
NEXT ASSY:		APPLICATION:			
DO NOT SCALE DRAWING					

PROPRIETARY AND CONFIDENTIAL
 THE INFORMATION CONTAINED IN THIS DRAWING IS THE SOLE PROPERTY OF <INSERT COMPANY NAME HERE>. ANY REPRODUCTION IN PART OR AS A WHOLE WITHOUT THE WRITTEN PERMISSION OF <INSERT COMPANY NAME HERE> IS PROHIBITED.

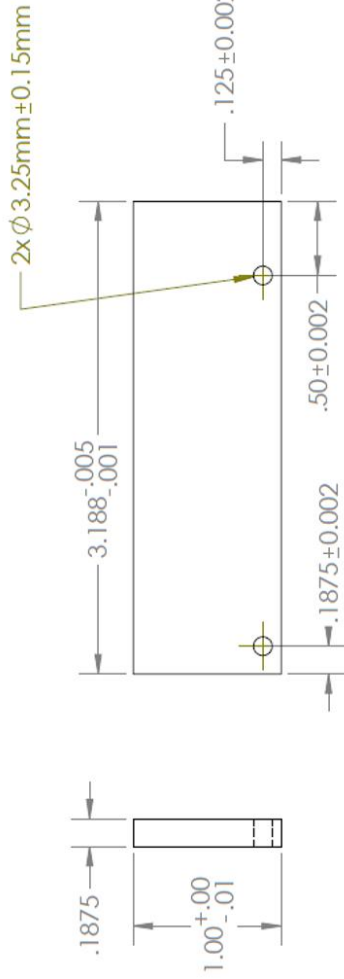
2 1

2

1

B

B



A

A

PROPRIETARY AND CONFIDENTIAL
 THE INFORMATION CONTAINED IN THIS
 DRAWING IS THE SOLE PROPERTY OF
 <INSERT COMPANY NAME HERE>. ANY
 REPRODUCTION IN PART OR AS A WHOLE
 WITHOUT THE WRITTEN PERMISSION OF
 <INSERT COMPANY NAME HERE> IS
 PROHIBITED.

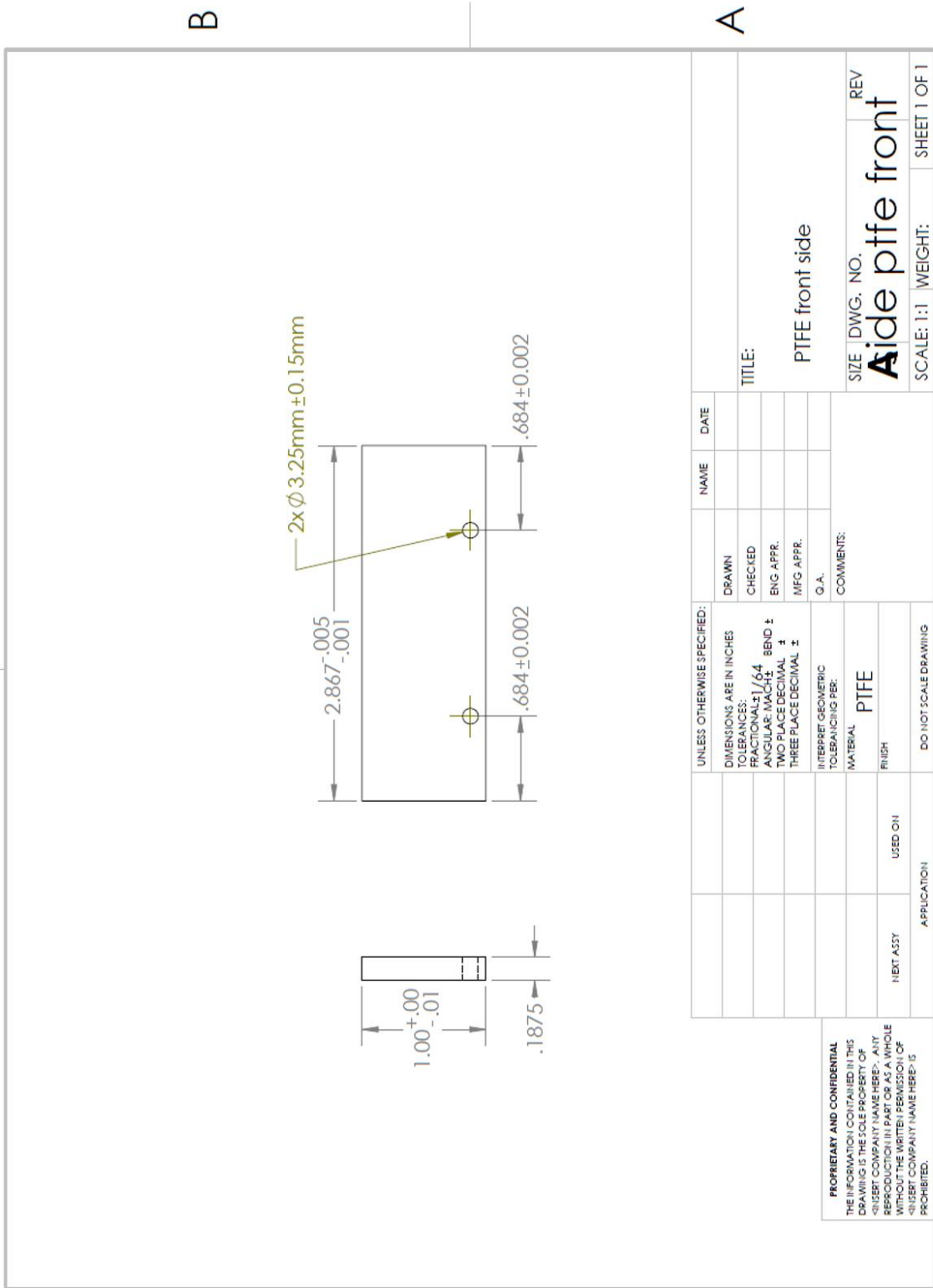
UNLESS OTHERWISE SPECIFIED:		NAME		DATE	
DIMENSIONS ARE IN INCHES		DRAWN			
TOLERANCES:		CHECKED			
FRACTIONAL: ±1/64		ENG APPR.			
ANGULAR: MACH ±		MFG APPR.			
TWO PLACE DECIMAL ±		G.A.			
THREE PLACE DECIMAL ±		COMMENTS:			
INTERPRET GEOMETRIC TOLERANCING PER:		MATERIAL		PTFE	
FINISH		USED ON			
APPLICATION		DO NOT SCALE DRAWING			
NEXT ASSY		TITLE:		PTFE both side	
SIZE		DWG. NO.		REV	
SCALE: 1:1		WEIGHT:		SHEET 1 OF 1	

side ptfе both sides

2

1

1



B

A

2

2

B

A

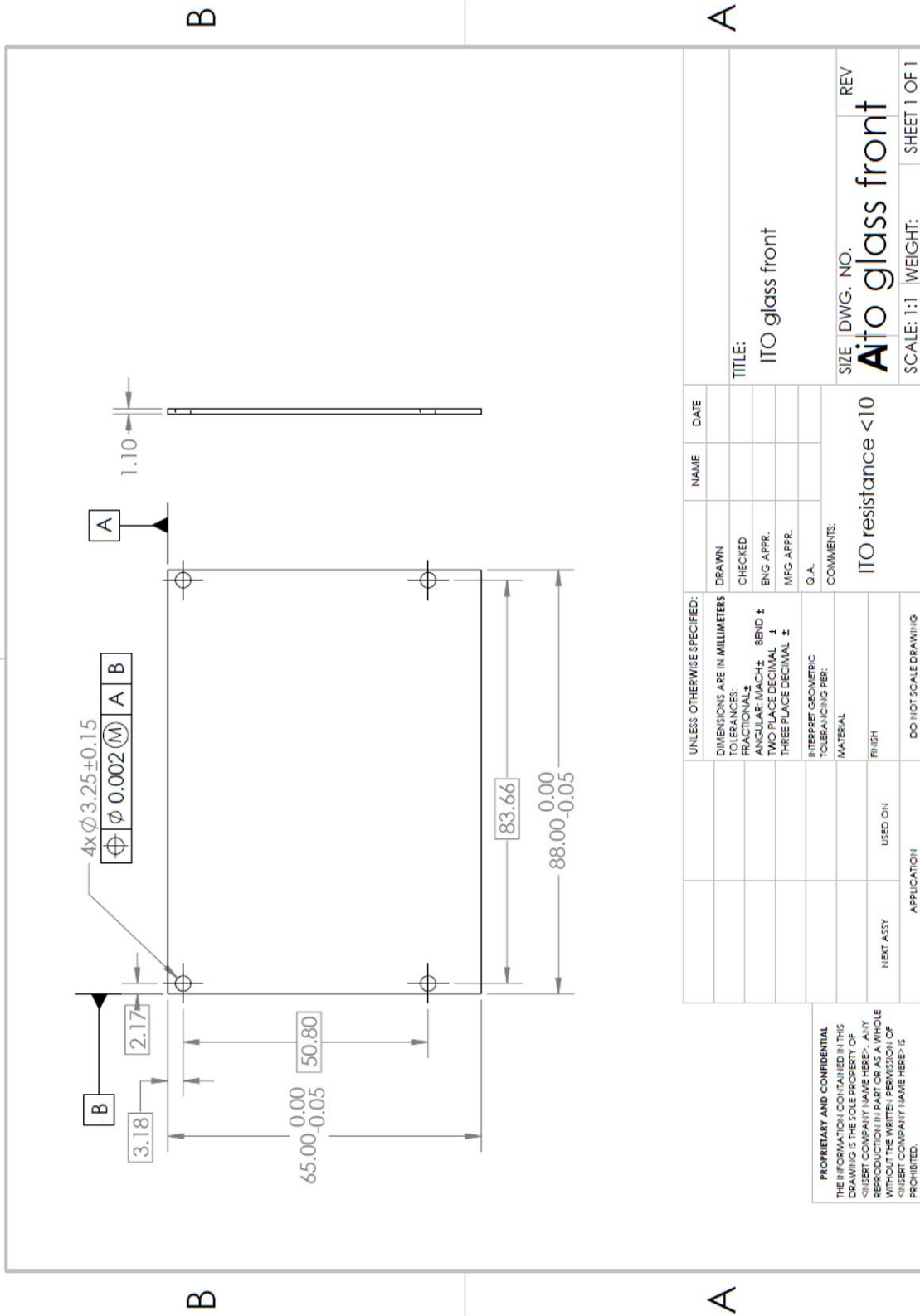
PROPRIETARY AND CONFIDENTIAL
 THE INFORMATION CONTAINED IN THIS DRAWING IS THE SOLE PROPERTY OF <INSERT COMPANY NAME HERE>. ANY REPRODUCTION IN PART OR AS A WHOLE WITHOUT THE WRITTEN PERMISSION OF <INSERT COMPANY NAME HERE> IS PROHIBITED.

UNLESS OTHERWISE SPECIFIED:		DRAWN		NAME		DATE	
DIMENSIONS ARE IN INCHES		CHECKED					
TOLERANCES:		ENG. APPR.					
FRACTIONAL: $\pm 1/64$		MFG APPR.					
ANGULAR: MACH: \pm BEND: \pm		Q.A.					
TWO PLACE DECIMAL \pm		COMMENTS:					
THREE PLACE DECIMAL \pm		PTFE				SIZE: DWG. NO.	
INTERPRET GEOMETRIC TOLERANCING PER:		FINISH				Aide ptfе front	
MATERIAL		USED ON				REV	
HURT ASSY		APPLICATION				SCALE: 1:1	
DO NOT SCALE DRAWING						WEIGHT: SHEET 1 OF 1	

1

1

2



B

A

B

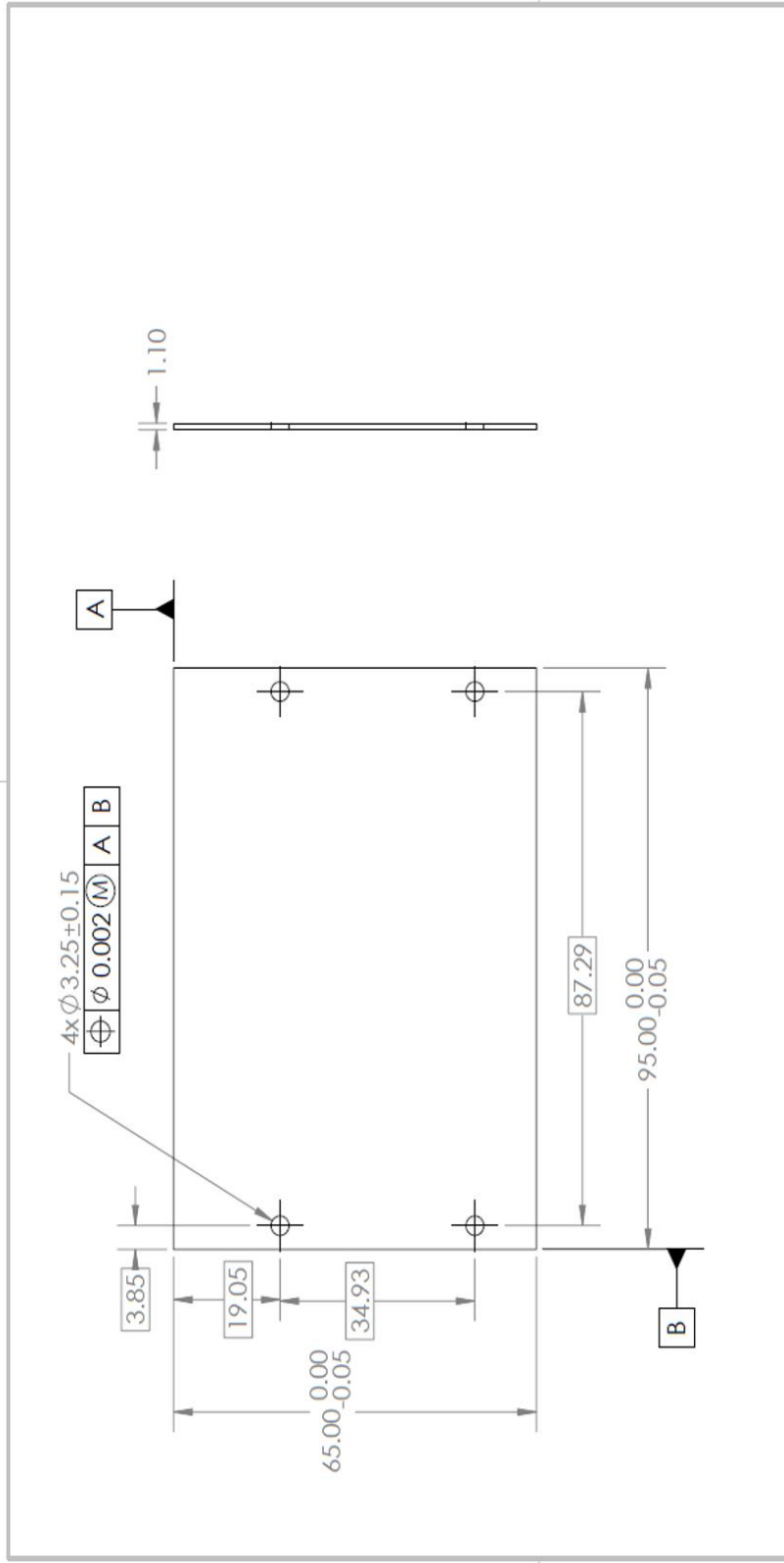
A

1

2

1

2



B

B

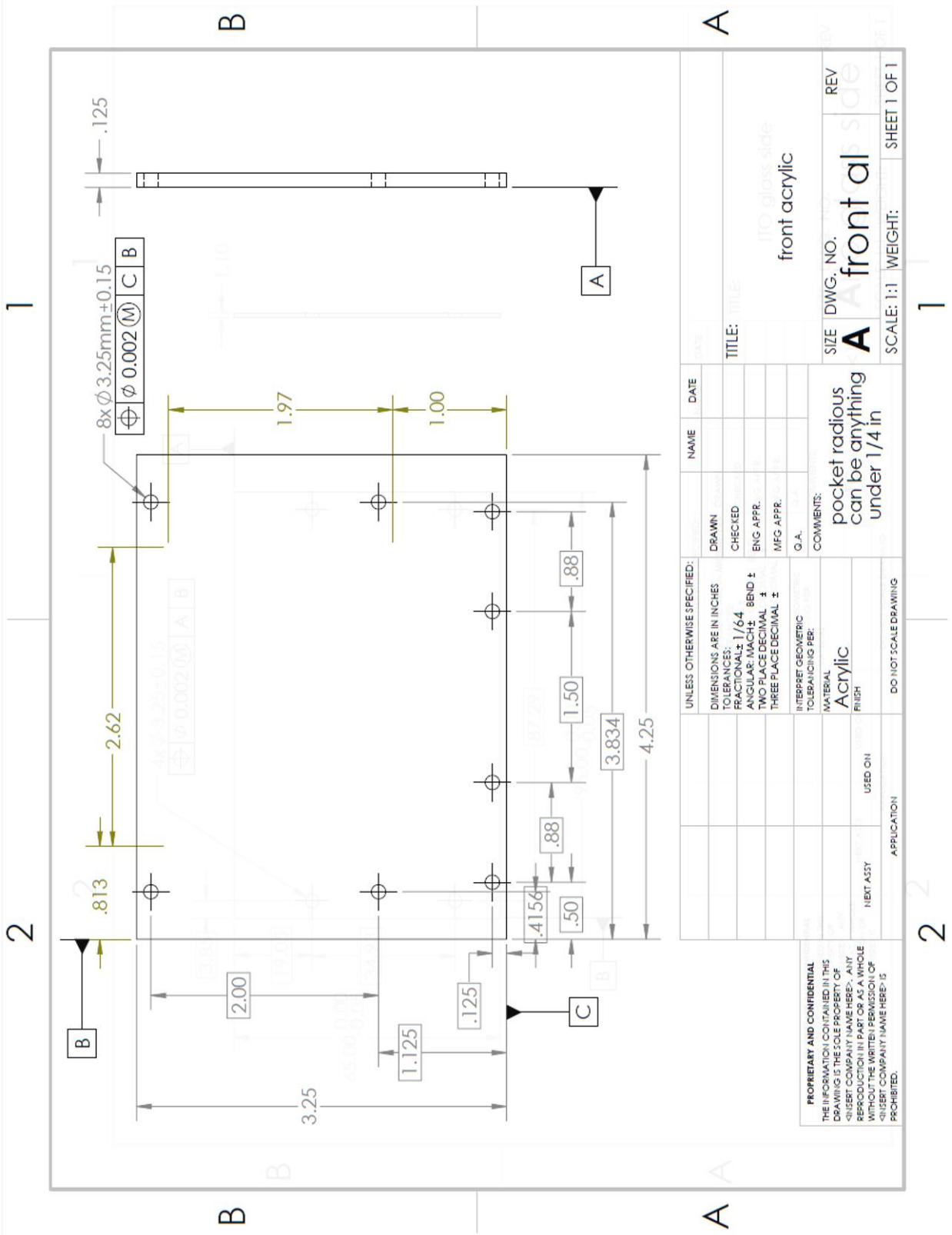
A

A

UNLESS OTHERWISE SPECIFIED: DIMENSIONS ARE IN MILLIMETERS		NAME	DATE
TOLERANCES:	DRAWN		
FRACTIONAL: ±	CHECKED		
ANGULAR: MACH: ± BEND ±	ENG APPR.		
TWO PLACE DECIMAL ±	MFG APPR.		
THREE PLACE DECIMAL ±	G.A.		
INTERPRET GEOMETRIC TOLERANCING PER:	COMMENTS:	TITLE: ITO glass side	
MATERIAL		SIZE	DWG. NO.
FINISH		Aito glass side	
USED ON	ITO resistance <10	SCALE: 1:1	WEIGHT:
APPLICATION	DO NOT SCALE DRAWING	SHEET 1 OF 1	
<p>PROPRIETARY AND CONFIDENTIAL THE INFORMATION CONTAINED IN THIS DRAWING IS THE SOLE PROPERTY OF <INSERT COMPANY NAME HERE>. ANY REPRODUCTION IN PART OR AS A WHOLE WITHOUT THE WRITTEN PERMISSION OF <INSERT COMPANY NAME HERE> IS PROHIBITED.</p>			

1

2

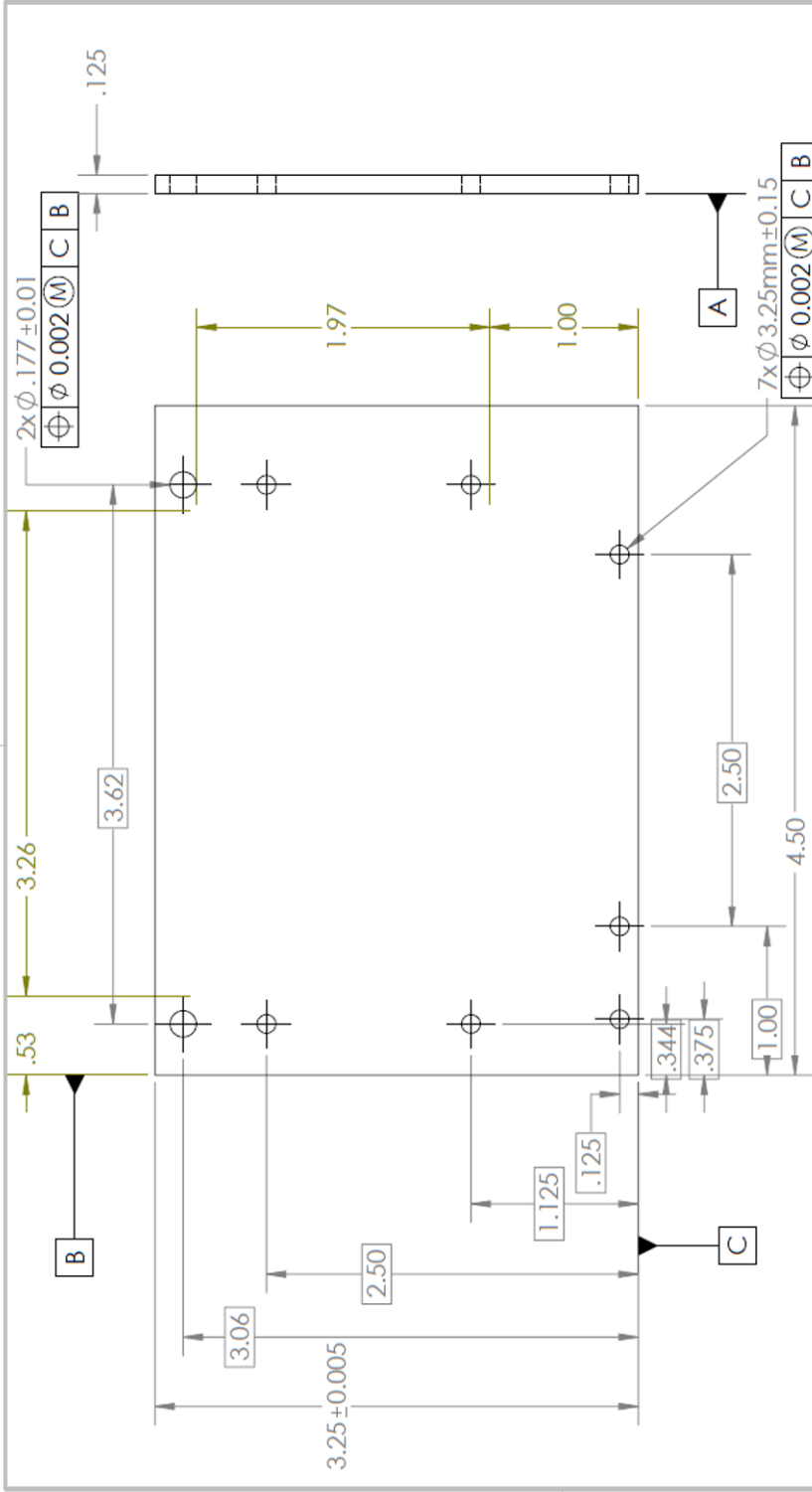


PROPRIETARY AND CONFIDENTIAL
 THE INFORMATION CONTAINED IN THIS DRAWING IS THE SOLE PROPERTY OF
 © INSERT COMPANY NAME HERE. ANY
 REPRODUCTION IN PART OR AS A WHOLE
 WITHOUT THE WRITTEN PERMISSION OF
 © INSERT COMPANY NAME HERE IS
 PROHIBITED.

UNLESS OTHERWISE SPECIFIED:		NAME	DATE
DRAWN			
CHECKED			
ENG. APPR.			
MFG APPR.			
Q. A.			
COMMENTS:		TITLE: 100 glass side front acrylic	
DIMENSIONS ARE IN INCHES		SIZE DWG. NO. A frontal REV	
TOLERANCES: FRACTIONAL ± 1/64 BEND ±		SCALE: 1:1 WEIGHT: SHEET 1 OF 1	
ANGULAR: MACH ±			
TWO PLACE DECIMAL ±			
THREE PLACE DECIMAL ±			
INTERPRET GEOMETRIC TOLERANCING PER: ASME Y14.5-2009			
MATERIAL: Acrylic			
FINISH: 100 glass side front acrylic			
DO NOT SCALE DRAWING			
NICKET ASSY	USED ON		
APPLICATION			

2

1



UNLESS OTHERWISE SPECIFIED:		NAME	DATE
DIMENSIONS ARE IN INCHES		DRAWN	
TOLERANCES:		CHECKED	
FRACTIONAL: 1/64		ENG. APPR.	
ANGULAR: MACH ± BEND ±		MFG APPR.	
TWO PLACE DECIMAL ±		G.A.	
THREE PLACE DECIMAL ±		COMMENTS:	
INTERPRET GEOMETRIC TOLERANCING PER:		pocket radius can be anything under 1/4 in	
MATERIAL:		acrylic	
FINISH:			
APPLICATION:		USED ON	
NEXT ASSY:			
DO NOT SCALE DRAWING			

PROPRIETARY AND CONFIDENTIAL
 THE INFORMATION CONTAINED IN THIS DRAWING IS THE SOLE PROPERTY OF <INSERT COMPANY NAME HERE>. ANY REPRODUCTION IN PART OR AS A WHOLE WITHOUT THE WRITTEN PERMISSION OF <INSERT COMPANY NAME HERE> IS PROHIBITED.

TITLE: side acrylic

SIZE DWG. NO. A side al

SCALE: 1:1 WEIGHT: SHEET 1 OF 1

B

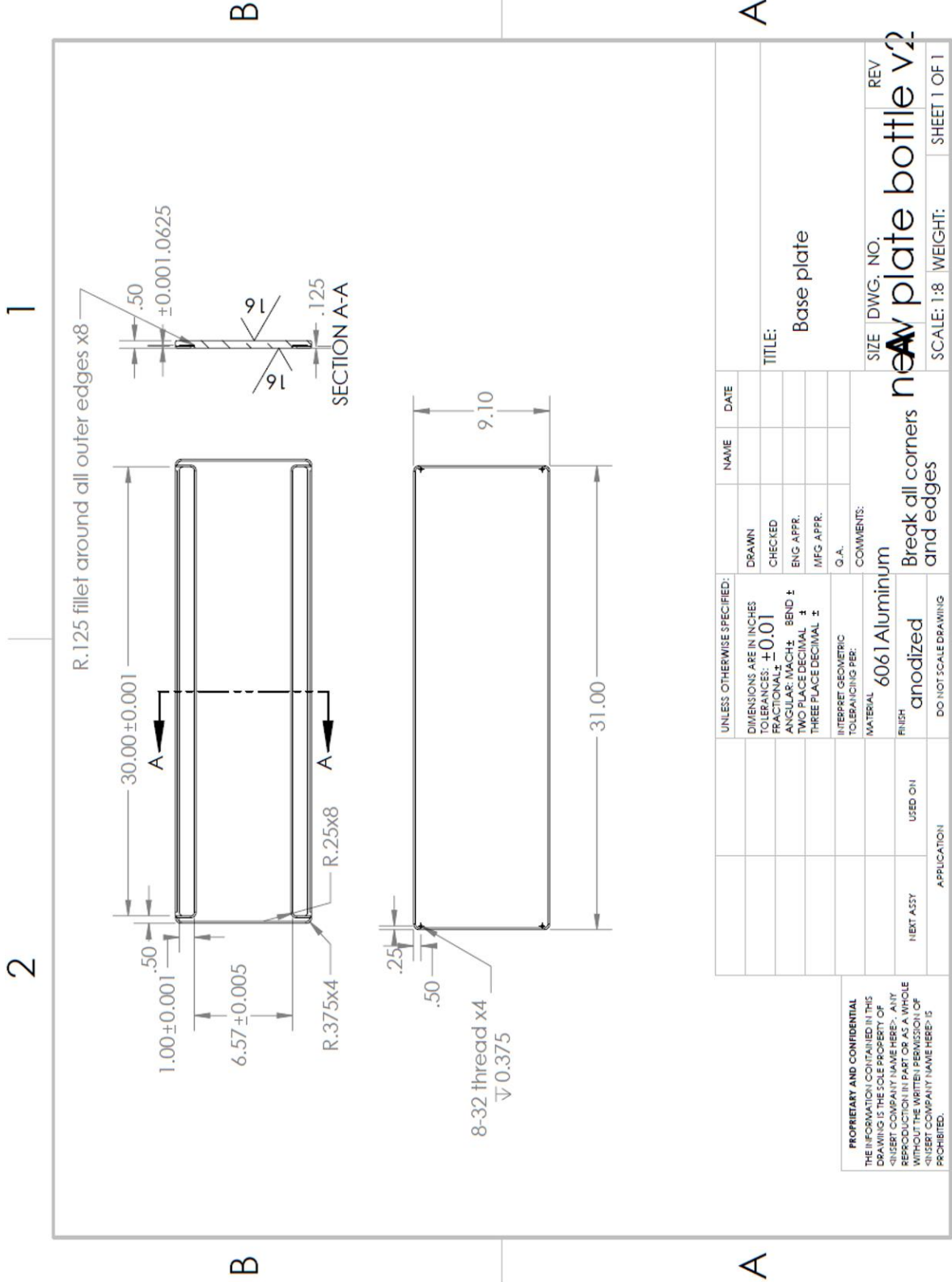
A

B

A

1

2



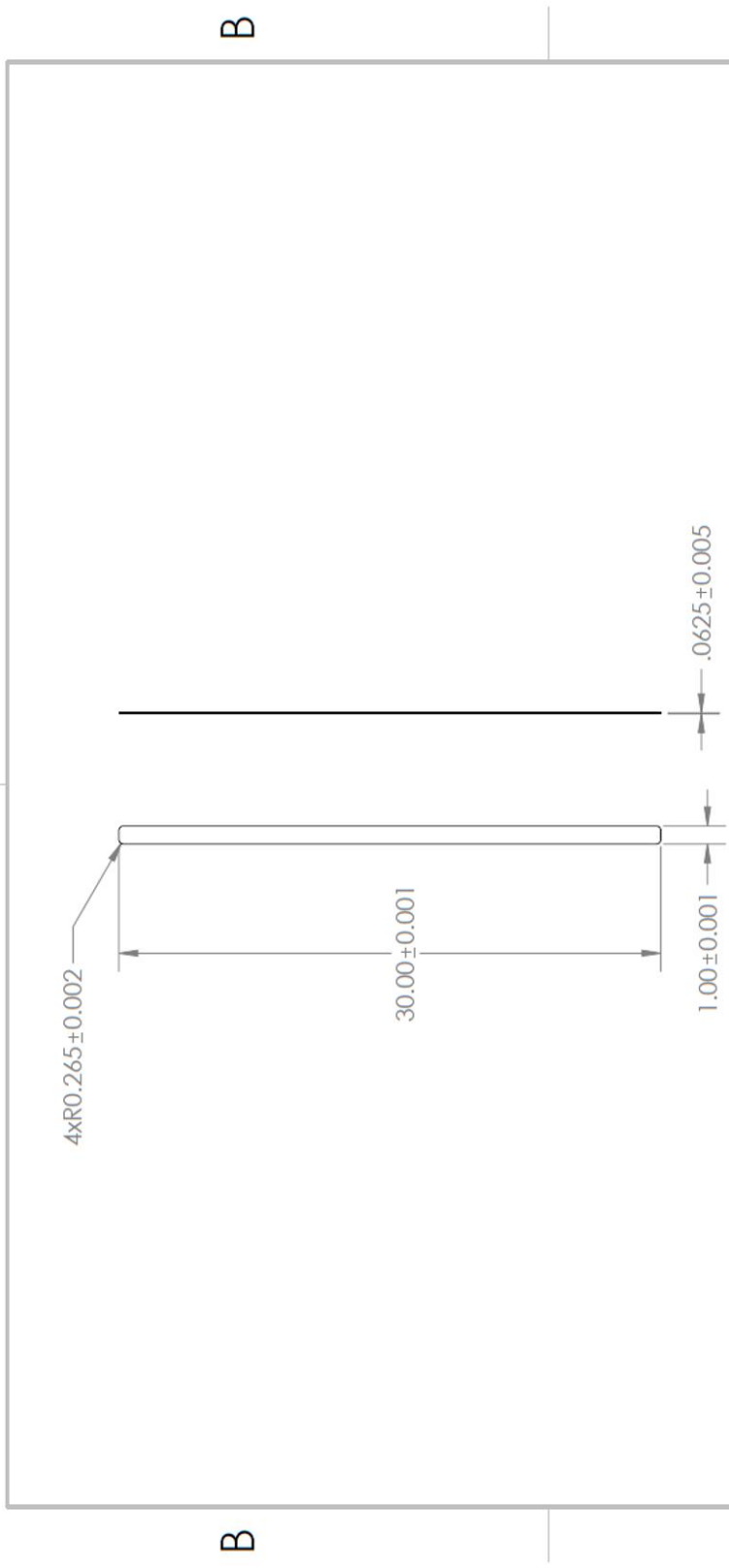
UNLESS OTHERWISE SPECIFIED:		NAME	DATE
DIMENSIONS ARE IN INCHES		DRAWN	
TOLERANCES: ±0.01		CHECKED	
FRACTIONAL: ±0.01		ENG. APPR.	
ANGULAR: MACH: BEND ±		MFG APPR.	
TWO PLACE DECIMAL ±			
THREE PLACE DECIMAL ±			
INTERPRET GEOMETRIC TOLERANCING PER:		G.A.	
MATERIAL:		COMMENTS:	
6061 Aluminum		Break all corners and edges	
FINISH:		anodized	
USED OIL:		DO NOT SCALE DRAWING	
NEXT ASSY:		APPLICATION:	
APPLICATION:		SCALE: 1:8	
APPLICATION:		WEIGHT:	
APPLICATION:		SHEET 1 OF 1	

PROPRIETARY AND CONFIDENTIAL
 THE INFORMATION CONTAINED IN THIS DRAWING IS THE SOLE PROPERTY OF
 <INSERT COMPANY NAME HERE>. ANY REPRODUCTION IN PART OR AS A WHOLE WITHOUT THE WRITTEN PERMISSION OF <INSERT COMPANY NAME HERE> IS PROHIBITED.

SIZE DWG. NO. REV
 new plate bottle v2

1

2



<p>PROPRIETARY AND CONFIDENTIAL THE INFORMATION CONTAINED IN THIS DRAWING IS THE PROPERTY OF THE COMPANY. ANY REPRODUCTION OR TRANSMISSION OF THIS DRAWING IN ANY FORM OR BY ANY MEANS WITHOUT THE WRITTEN PERMISSION OF THE COMPANY IS PROHIBITED.</p>		<p>UNLESS OTHERWISE SPECIFIED: DIMENSIONS ARE IN INCHES TOLERANCES: FRACTIONAL ± ANGULAR: MACH ± .001 TWO PLACE DECIMAL ± THREE PLACE DECIMAL ±</p>		<p>INTERPRET GEOMETRIC TOLERANCING PER: MATERIAL: 410 stainless steel FINISH: USED ON: NEXT ASSY:</p>		<p>DO NOT SCALE DRAWING</p>	
<p>UNLESS OTHERWISE SPECIFIED: DIMENSIONS ARE IN INCHES TOLERANCES: FRACTIONAL ± ANGULAR: MACH ± .001 TWO PLACE DECIMAL ± THREE PLACE DECIMAL ±</p>		<p>DRAWN CHECKED ENG. APPR. MFG. APPR. Q.A.</p>		<p>NAME DATE</p>		<p>SIZE DWG. NO. A insets</p>	
<p>TITLE: insets</p>		<p>COMMENTS:</p>		<p>SCALE: 1:8 WEIGHT:</p>		<p>SHEET 1 OF 1</p>	

A

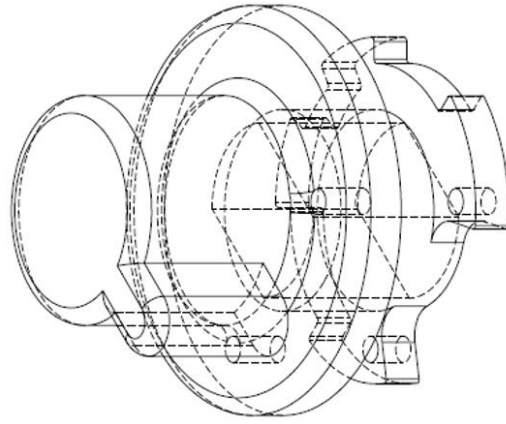
A

1

2

1

2



B

B

A

A

<p>PROPRIETARY AND CONFIDENTIAL THE INFORMATION CONTAINED IN THIS DRAWING IS THE SOLE PROPERTY OF <INSERT COMPANY NAME HERE>. ANY REPRODUCTION IN PART OR AS A WHOLE WITHOUT THE WRITTEN PERMISSION OF <INSERT COMPANY NAME HERE> IS PROHIBITED.</p>		<p>UNLESS OTHERWISE SPECIFIED: DIMENSIONS ARE IN INCHES TOLERANCES: FRACTIONAL ± ANGULAR: MACH ± BEND ± TWO PLACE DECIMAL ± THREE PLACE DECIMAL ±</p>		<p>INTERPRET GEOMETRIC TOLERANCING PER: MATERIAL Glass-filled Nylon FINISH</p>		<p>DO NOT SCALE DRAWING</p>	
<p>APPLICATION</p>		<p>USED ON</p>		<p>NEXT ASSY</p>		<p>REVISIONS</p>	
<p>DATE</p>		<p>NAME</p>		<p>DATE</p>		<p>REV</p>	
<p>TITLE:</p>		<p>Magnet switch nob</p>		<p>SIZE DWG. NO.</p>		<p>Magnet switch nob</p>	
<p>SCALE: 2:1</p>		<p>WEIGHT:</p>		<p>SHEET 1 OF 1</p>		<p>1</p>	

1

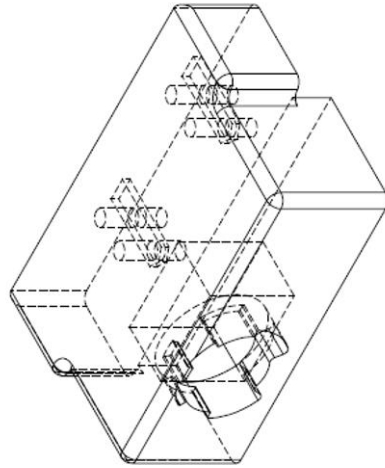
2

1

2

B

B



A

A

UNLESS OTHERWISE SPECIFIED: DIMENSIONS ARE IN INCHES FRACTIONS: ANGULAR: MACH. BEND ± TWO PLACE DECIMAL ± THREE PLACE DECIMAL ±		DRAWN CHECKED ENG. APPR. MFG. APPR. Q. A. COMMENTS:	NAME DATE	TITLE: Magnet housing side 1	SIZE DWG. NO. A magnet housing side 1	REV
INTERPRET GEOMETRIC TOLERANCING PER: MATERIAL: Glass-filled Nylon FINISH		SLS 3D printed		SCALE: 1:1	WEIGHT:	SHEET 1 OF 1
PROPRIETARY AND CONFIDENTIAL THE INFORMATION CONTAINED IN THIS DRAWING IS THE SOLE PROPERTY OF <INSERT COMPANY NAME HERE>. ANY REPRODUCTION IN PART OR AS A WHOLE WITHOUT THE WRITTEN PERMISSION OF <INSERT COMPANY NAME HERE> IS PROHIBITED.		APPLICATION		DO NOT SCALE DRAWING		
NEXT ASSY		USED ON		1		

1

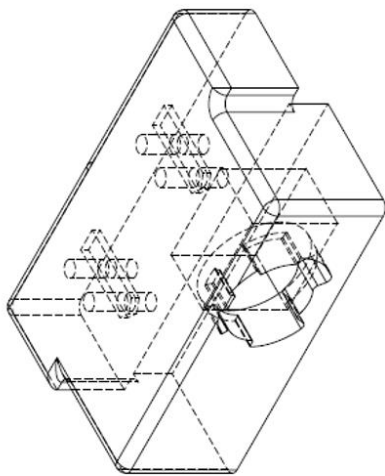
2

1

2

B

B



A

A

<p>PROPRIETARY AND CONFIDENTIAL THE INFORMATION CONTAINED IN THIS DRAWING IS THE SOLE PROPERTY OF [COMPANY NAME]. IT IS TO BE USED ONLY FOR THE PRODUCTION OF THIS PART OR AS A WHOLE WITHOUT THE WRITTEN PERMISSION OF [COMPANY NAME]. REPRODUCTION OR DISSEMINATION OF THIS INFORMATION IS PROHIBITED.</p>		<p>UNLESS OTHERWISE SPECIFIED: DIMENSIONS ARE IN INCHES TOLERANCES: FRACTIONAL: ANGULAR: MACH ± .001 TWO PLACE DECIMAL ± .01 THREE PLACE DECIMAL ± .001</p>		<p>DRAWN CHECKED ENG. APPR. MFG. APPR. O.A. COMMENTS: SLS 3D printed</p>	<p>NAME DATE</p>	<p>TITLE: Magnet housing side 2</p>	<p>SIZE DWG. NO. A Magnet housing side 2 REV</p>
<p>NEXT ASSY</p>	<p>USED ON</p>	<p>DO NOT SCALE DRAWING</p>		<p>SCALE: 1:1 WEIGHT: SHEET 1 OF 1</p>		<p>1</p>	

2

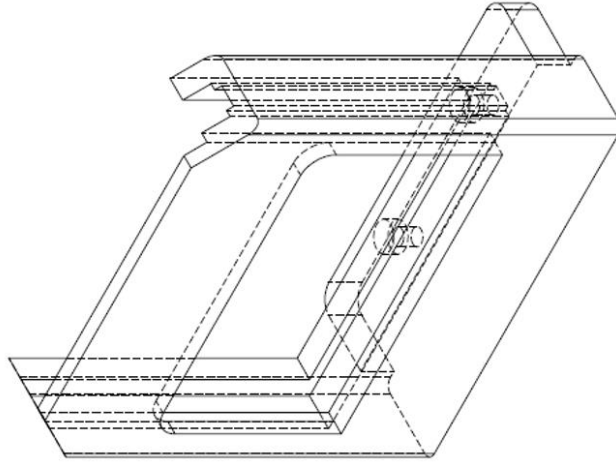
1

2

1

B

B



A

A

PROPRIETARY AND CONFIDENTIAL
 THE INFORMATION CONTAINED IN THIS
 DRAWING IS THE SOLE PROPERTY OF
 <INSERT COMPANY NAME HERE>. ANY
 REPRODUCTION IN PART OR AS A WHOLE
 WITHOUT THE WRITTEN PERMISSION OF
 <INSERT COMPANY NAME HERE> IS
 PROHIBITED.

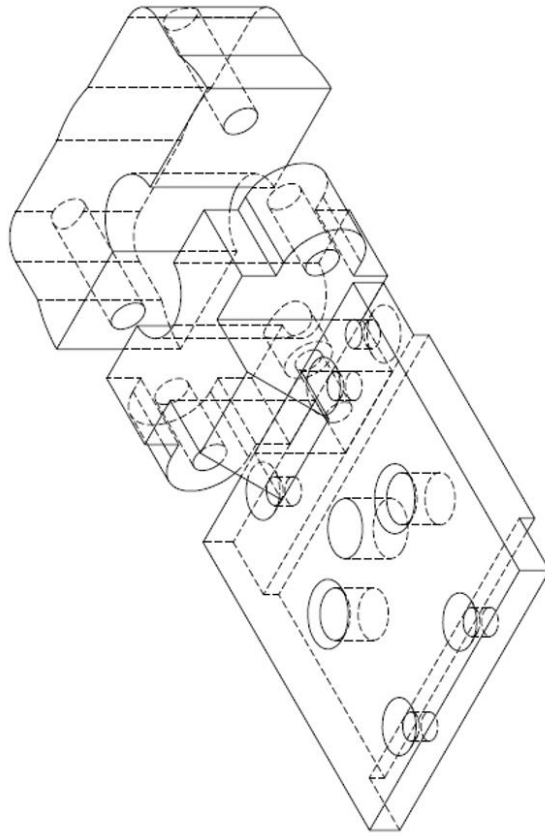
UNLESS OTHERWISE SPECIFIED:		NAME	DATE
DRAWN			
CHECKED			
ENG APPR.			
MFG APPR.			
G.A.			
COMMENTS:			
SLS 3D printed			
MATERIAL:		SIZE DWG. NO. REV	
Glass-filled Nylon		A phone mount 1	
FINISH:		SCALE: 1:2 WEIGHT: SHEET 1 OF 1	
DO NOT SCALE DRAWING			
APPLICATION	USED ON		
NEXT ASSY			

2

1

1

2



B

B

A

A

UNLESS OTHERWISE SPECIFIED: DIMENSIONS ARE IN INCHES TOLERANCES: FRACTIONAL ± ANGULAR: MACH ± BEND ± TWO PLACE DECIMAL ± THREE PLACE DECIMAL ±		DRAWN CHECKED ENG APPR. MFG APPR. Q. A. COMMENTS: SLS 3D printed Nylon	NAME	DATE	TITLE: syringe holder parts	SIZE DWG. NO. REV
PROPRIETARY AND CONFIDENTIAL THE INFORMATION CONTAINED IN THIS DRAWING IS THE SOLE PROPERTY OF <INSERT COMPANY NAME HERE>. ANY REPRODUCTION IN PART OR AS A WHOLE WITHOUT THE WRITTEN PERMISSION OF <INSERT COMPANY NAME HERE> IS PROHIBITED.		INTERPRET GEOMETRIC TOLERANCING PER:	SCALE: 1:1		WEIGHT:	SHEET 1 OF 1
MATERIAL Glass-filled Nylon		FINISH		DO NOT SCALE DRAWING		
NEXT ASSY	USED ON	APPLICATION				

1

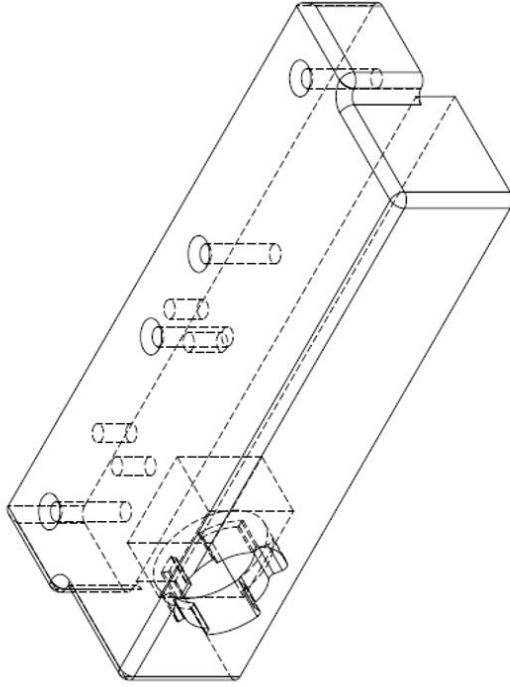
2

1

2

B

B



A

A

<p>PROPRIETARY AND CONFIDENTIAL THE INFORMATION CONTAINED IN THIS DRAWING IS THE SOLE PROPERTY OF <INSERT COMPANY NAME HERE>. ANY REPRODUCTION IN PART OR AS A WHOLE WITHOUT THE WRITTEN PERMISSION OF <INSERT COMPANY NAME HERE> IS PROHIBITED.</p>		<p>UNLESS OTHERWISE SPECIFIED: DIMENSIONS ARE IN INCHES TOLERANCES: FRACTIONAL: ± ANGULAR: MACH: ± BEND ± TWO PLACE DECIMAL ± THREE PLACE DECIMAL ±</p>		<p>DRAWN</p>	<p>NAME</p>	<p>DATE</p>
<p>INTERPRET GEOMETRIC TOLERANCING PER:</p>	<p>Q.A.</p>	<p>COMMENTS:</p>	<p>ENG. APPR.</p>	<p>ENG. APPR.</p>	<p>TITLE:</p>	
<p>MATERIAL</p>	<p>Next Glass-filled Nylon</p>	<p>SLS 3D printed</p>	<p>SIZE DWG. NO.</p>	<p>REV</p>	<p>Magnet housing chamber side 1</p>	
<p>APPLICATION</p>	<p>USED ON</p>	<p>DO NOT SCALE DRAWING</p>	<p>SCALE: 1:2</p>	<p>WEIGHT:</p>	<p>SHEET 1 OF 1</p>	

1

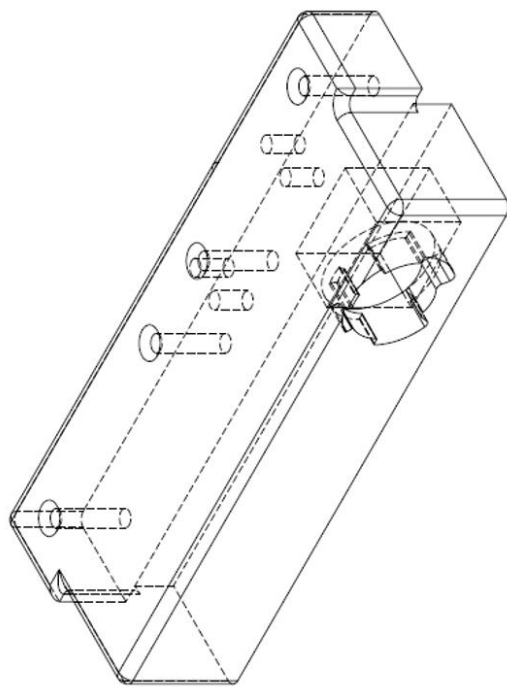
2

1

2

B

B



A

A

PROPRIETARY AND CONFIDENTIAL
 THE INFORMATION CONTAINED IN THIS
 DRAWING IS THE SOLE PROPERTY OF
 <INSERT COMPANY NAME HERE>. ANY
 REPRODUCTION IN PART OR AS A WHOLE
 WITHOUT THE WRITTEN PERMISSION OF
 <INSERT COMPANY NAME HERE> IS
 PROHIBITED.

UNLESS OTHERWISE SPECIFIED:		NAME	DATE
DIMENSIONS ARE IN INCHES		DRAWN	
TOLERANCES:		CHECKED	
FRACTIONAL: ±		ENG. APPR.	
ANGULAR: MACH ± BEND ±		MFG APPR.	
TWO PLACE DECIMAL ±		Q.A.	
THREE PLACE DECIMAL ±		COMMENTS:	
INTERPRET GEOMETRIC TOLERANCING PER:		SLs 3D printed	
MATERIAL: Glass-filled Nylon		SIZE DWG. NO. A magnet housing chamber side 2	
FINISH: USED ON		REV	
NEXT ASSY		SCALE: 1:2 WEIGHT: SHEET 1 OF 1	
APPLICATION			
DO NOT SCALE DRAWING			

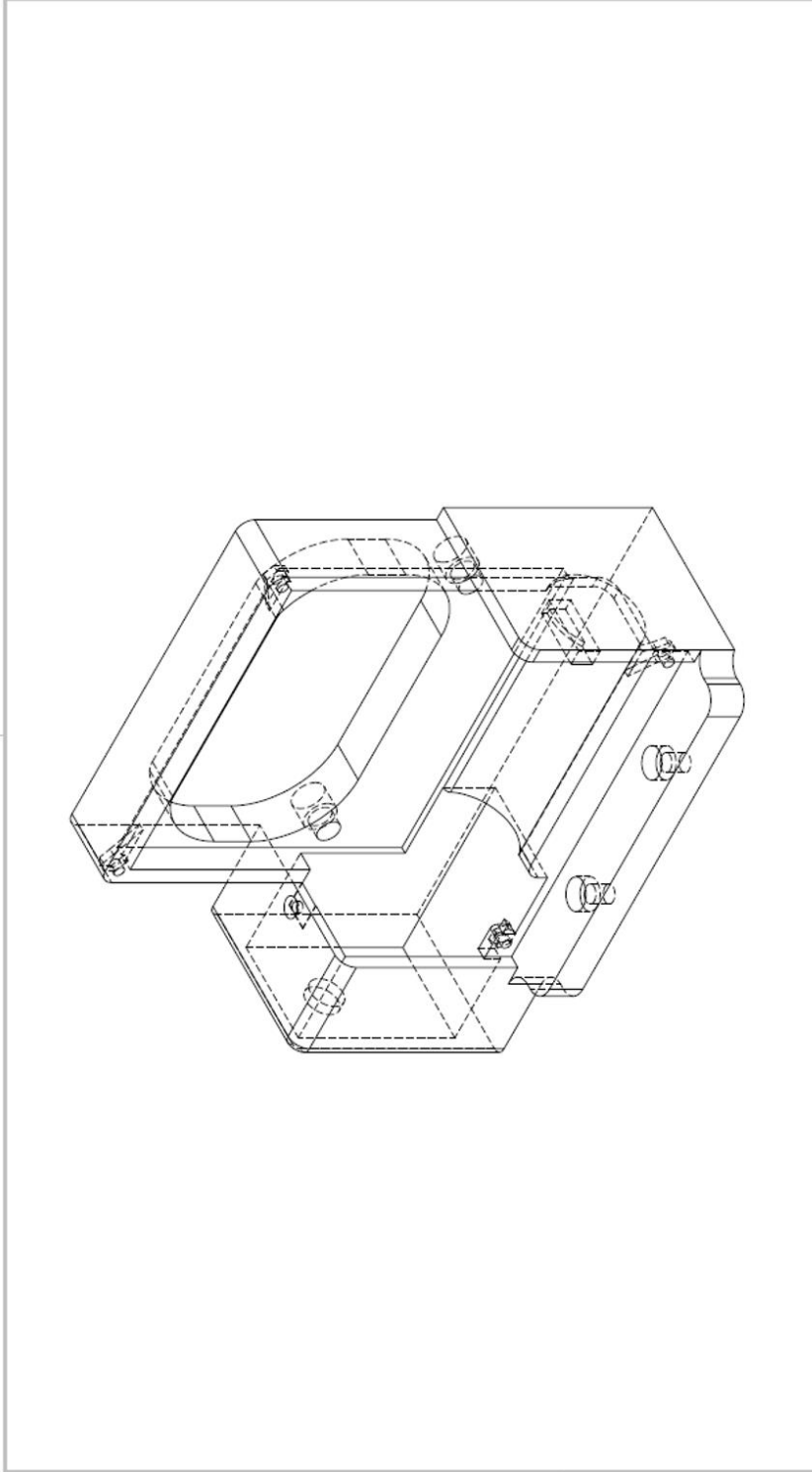
TITLE:
Magnet housing chamber side 2

1

2

1

2



B

B

A

A

<p>PROPRIETARY AND CONFIDENTIAL THE INFORMATION CONTAINED IN THIS DRAWING IS THE SOLE PROPERTY OF [INSERT COMPANY NAME HERE]. ANY REPRODUCTION IN PART OR AS A WHOLE WITHOUT THE WRITTEN PERMISSION OF [INSERT COMPANY NAME HERE] IS PROHIBITED.</p>		<p>UNLESS OTHERWISE SPECIFIED: DIMENSIONS ARE IN INCHES TOLERANCES: FRACTIONAL: ± .005 ANGULAR: ± .01 BEND: ± .01 TWO PLACE DECIMAL: ± .01 THREE PLACE DECIMAL: ± .005</p>		<p>INTERPRET GEOMETRIC TOLERANCING PER: MATERIAL: Glass-filled Nylon FINISH: USED ON</p>		<p>DO NOT SCALE DRAWING</p>		<p>APPLICATION</p>	
<p>DRAWN</p>		<p>CHECKED</p>		<p>ENG. APPR.</p>		<p>MFG. APPR.</p>		<p>Q. A.</p>	
<p>NAME</p>		<p>DATE</p>		<p>COMMENTS: SLS 3D printed</p>		<p>SIZE: DWG. NO. A</p>		<p>REV</p>	
<p>TITLE: Light body</p>		<p>SCALE: 1:2</p>		<p>WEIGHT:</p>		<p>SHEET 1 OF 1</p>		<p>1</p>	

1

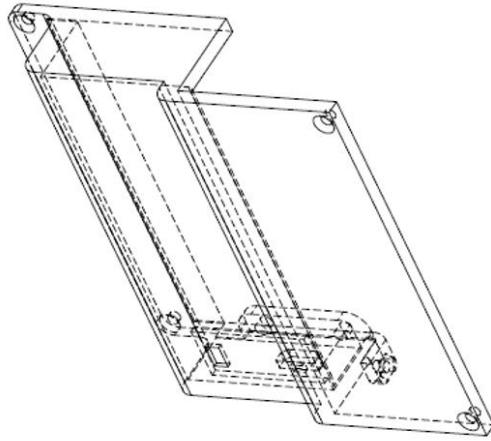
2

1

2

B

B



A

A

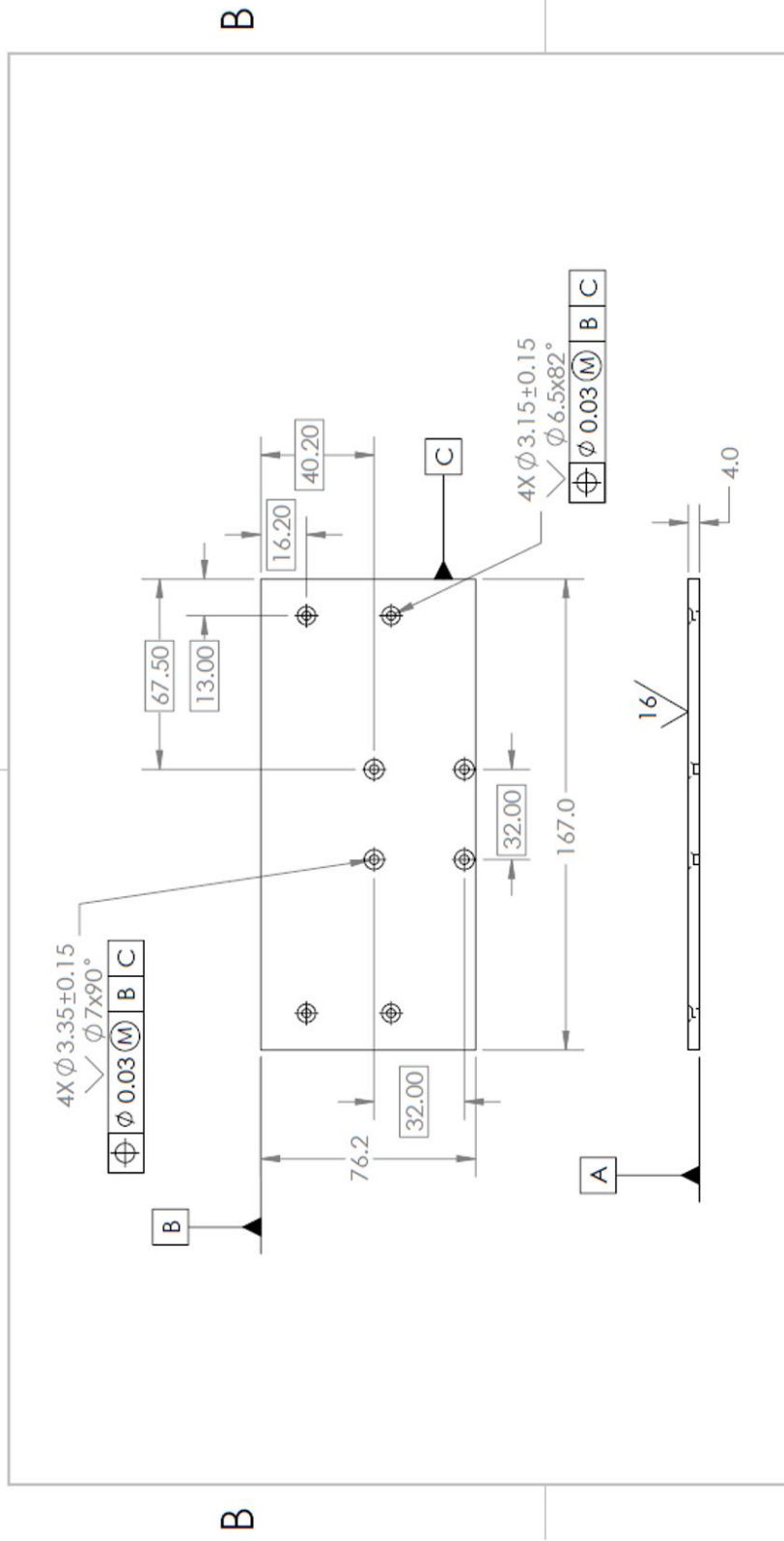
<p>PROPRIETARY AND CONFIDENTIAL THE INFORMATION CONTAINED IN THIS DRAWING IS THE SOLE PROPERTY OF <INSERT COMPANY NAME HERE>. ANY REPRODUCTION IN PART OR AS A WHOLE WITHOUT THE WRITTEN PERMISSION OF <INSERT COMPANY NAME HERE> IS PROHIBITED.</p>		<p>UNLESS OTHERWISE SPECIFIED: DIMENSIONS ARE IN INCHES TOLERANCES: FRACTIONAL: ± ANGULAR: MACH: ± BEND: ± TWO PLACE DECIMAL: ± THREE PLACE DECIMAL: ±</p>		<p>DRAWN CHECKED ENG. APPR. MFG APPR. G.A. COMMENTS: SLS 3D printed</p>		<p>NAME DATE</p>		<p>TITLE: Light lid</p>		<p>SIZE DWG. NO. A light lid</p>		<p>REV</p>	
<p>INTERPRET GEOMETRIC TOLERANCING PER: MATERIAL Glass-filled Nylon FINISH</p>		<p>DO NOT SCALE DRAWING</p>		<p>SCALE: 1:2 WEIGHT:</p>		<p>SHEET 1 OF 1</p>		<p>APPLICATION USED ON</p>		<p>SCALE: 1:2 WEIGHT:</p>		<p>SHEET 1 OF 1</p>	

1

2

2

1



A

A

UNLESS OTHERWISE SPECIFIED:		NAME	DATE
DIMENSIONS ARE IN MILLIMETERS	DRAWN		
TOLERANCES:	CHECKED		
FRACTIONAL: ±	ENG. APPR.		
ANGULAR: MACH ±	MFG APPR.		
TWO PLACE DECIMAL ±	G.A.		
THREE PLACE DECIMAL ±	COMMENTS:		
INTERPRET GEOMETRIC TOLERANCING PER:	Break all corners and edges		
MATERIAL:	6061 Aluminum	SIZE DWG. NO.	REV
FINISH:	Anodized	base plate for jacks	base plate for jacks
USED ON:	DO NOT SCALE DRAWING	SCALE: 1:2	WEIGHT: SHEET 1 OF 1
NEXT ASSY:			
APPLICATION:			

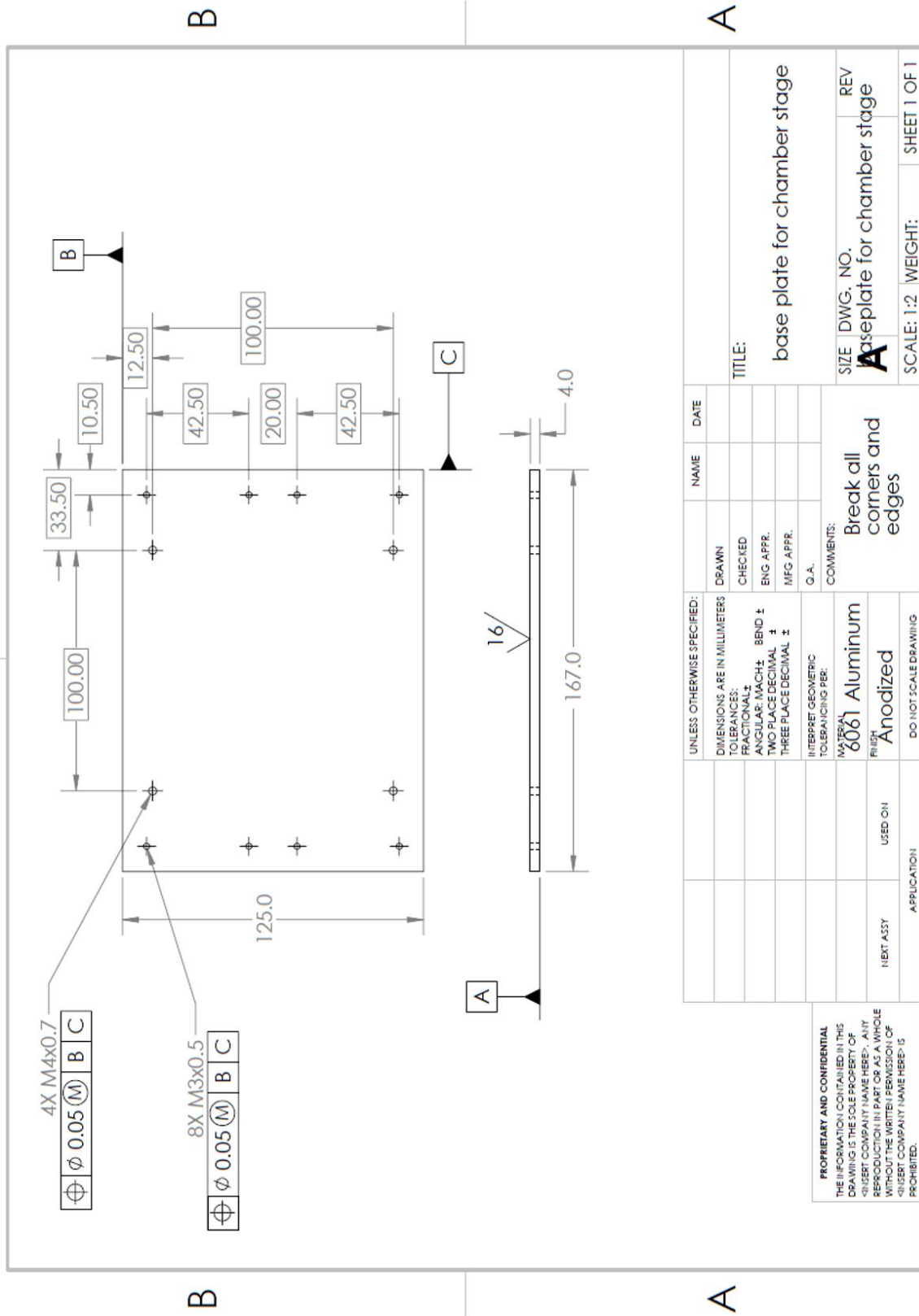
PROPRIETARY AND CONFIDENTIAL
 THE INFORMATION CONTAINED IN THIS DRAWING IS THE SOLE PROPERTY OF <INSERT COMPANY NAME HERE>. ANY REPRODUCTION IN PART OR AS A WHOLE WITHOUT THE WRITTEN PERMISSION OF <INSERT COMPANY NAME HERE> IS PROHIBITED.

2

1

1

2



B

B

A

A

UNLESS OTHERWISE SPECIFIED: DIMENSIONS ARE IN MILLIMETERS TOLERANCES: FRACTIONAL ± ANGULAR: MACH ± BEND ± TWO PLACE DECIMAL ± THREE PLACE DECIMAL ±		DRAWN	NAME	DATE
INTERPRET GEOMETRIC TOLERANCING PER:		CHECKED		
MATERIAL: 6061 Aluminum		ENG. APPR.		
FINISH: Anodized		MFG APPR.		
NEXT ASSY		G.A.		
APPLICATION		COMMENTS:	base plate for chamber stage	
USED ON		Break all corners and edges		
DO NOT SCALE DRAWING		SIZE DWG. NO. A REV		
		Scaleplate for chamber stage		
		SCALE: 1:2 WEIGHT: SHEET 1 OF 1		

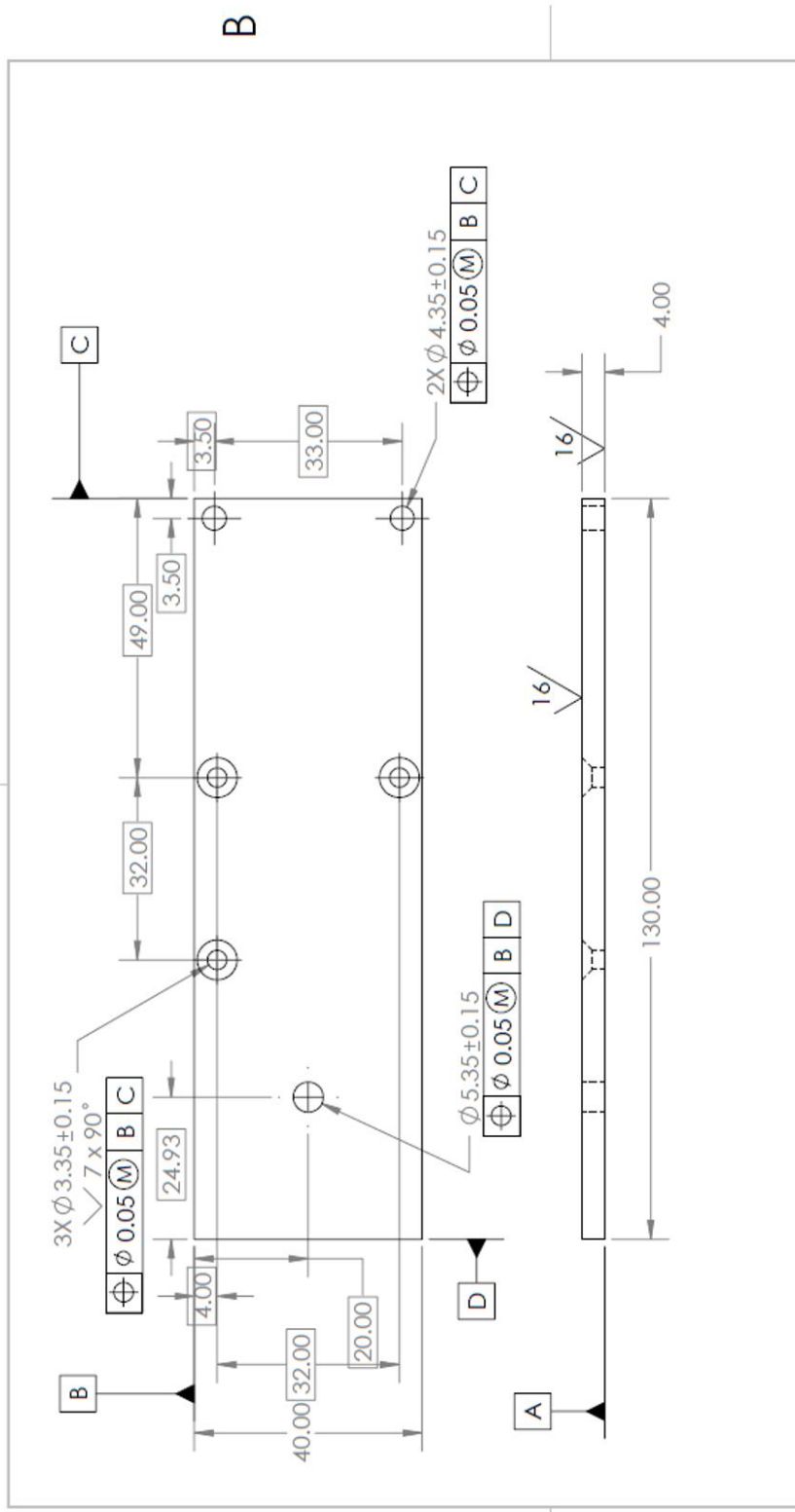
PROPRIETARY AND CONFIDENTIAL
 THE INFORMATION CONTAINED IN THIS DRAWING IS THE SOLE PROPERTY OF [INSERT COMPANY NAME HERE]. ANY REPRODUCTION IN PART OR AS A WHOLE WITHOUT THE WRITTEN PERMISSION OF [INSERT COMPANY NAME HERE] IS PROHIBITED.

1

2

2

1



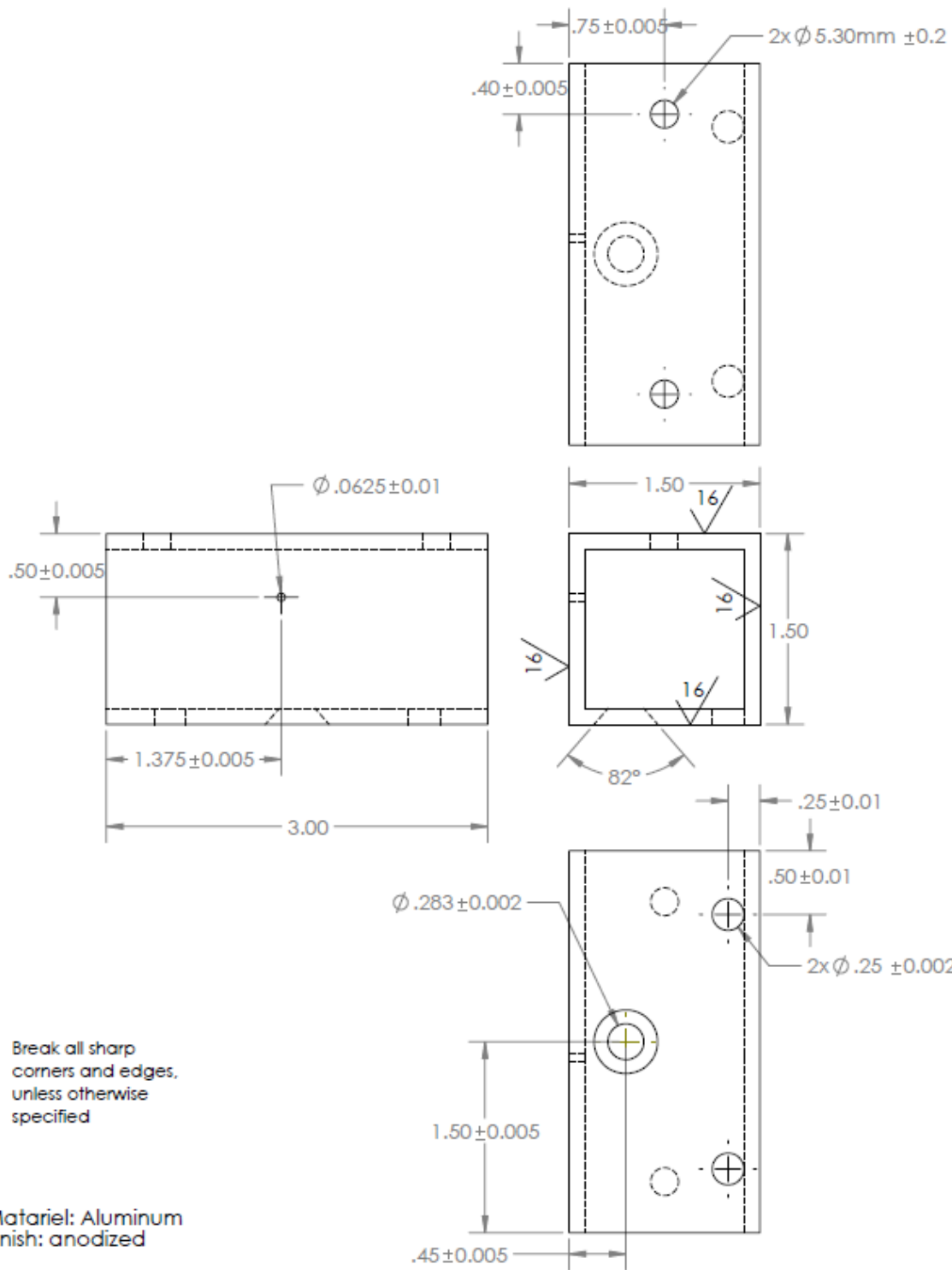
A

A

UNLESS OTHERWISE SPECIFIED: DIMENSIONS ARE IN MILLIMETERS TOLERANCES: FRACTIONS DECIMALS ANGULAR: MACH. BEHOLD TWO PLACE DECIMAL THREE PLACE DECIMAL		DRAWN	NAME	DATE
INTERPRET GEOMETRIC TOLERANCING PER: MATERIAL: FINISH		CHECKED		
NEXT ASSY		ENG APPR.		
USED ON		MFG APPR.		
APPLICATION		G.A.		
DO NOT SCALE DRAWING		COMMENTS: Break all sharp corners and edges, unless otherwise specified		
TITLE:		Al plate mid auto		
PROPRIETARY AND CONFIDENTIAL THE INFORMATION CONTAINED IN THIS DRAWING IS THE PROPERTY OF <INSERT COMPANY NAME HERE>. ANY REPRODUCTION IN PART OR AS A WHOLE WITHOUT THE WRITTEN PERMISSION OF <INSERT COMPANY NAME HERE> IS PROHIBITED.		SIZE	DWG. NO.	REV
		A		
		SCALE: 1:1	WEIGHT:	SHEET 1 OF 1

2

1



Break all sharp corners and edges, unless otherwise specified

Material: Aluminum
Finish: anodized

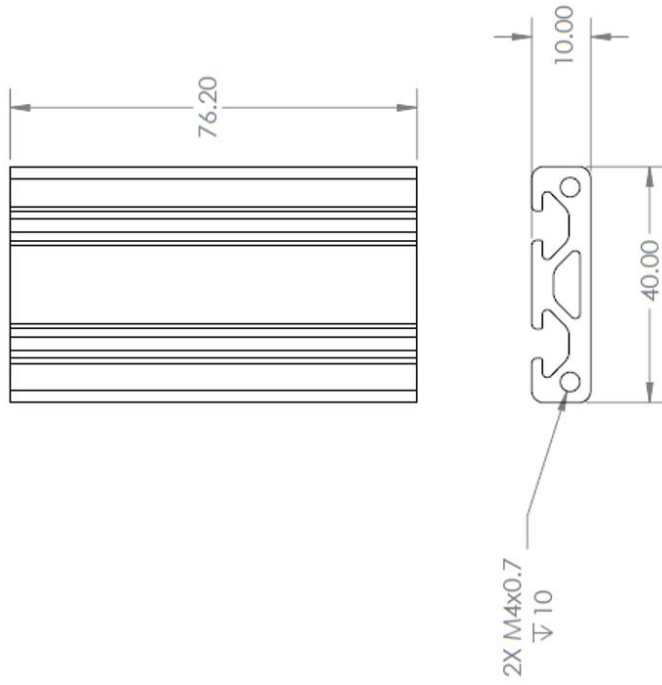
unless otherwise specified
all dimensions are in INCHES

2

1

B

B



A

A

PROPRIETARY AND CONFIDENTIAL
 THE INFORMATION CONTAINED IN THIS DRAWING IS THE SOLE PROPERTY OF <INSERT COMPANY NAME HERE>. ANY REPRODUCTION IN PART OR AS A WHOLE WITHOUT THE WRITTEN PERMISSION OF <INSERT COMPANY NAME HERE> IS PROHIBITED.

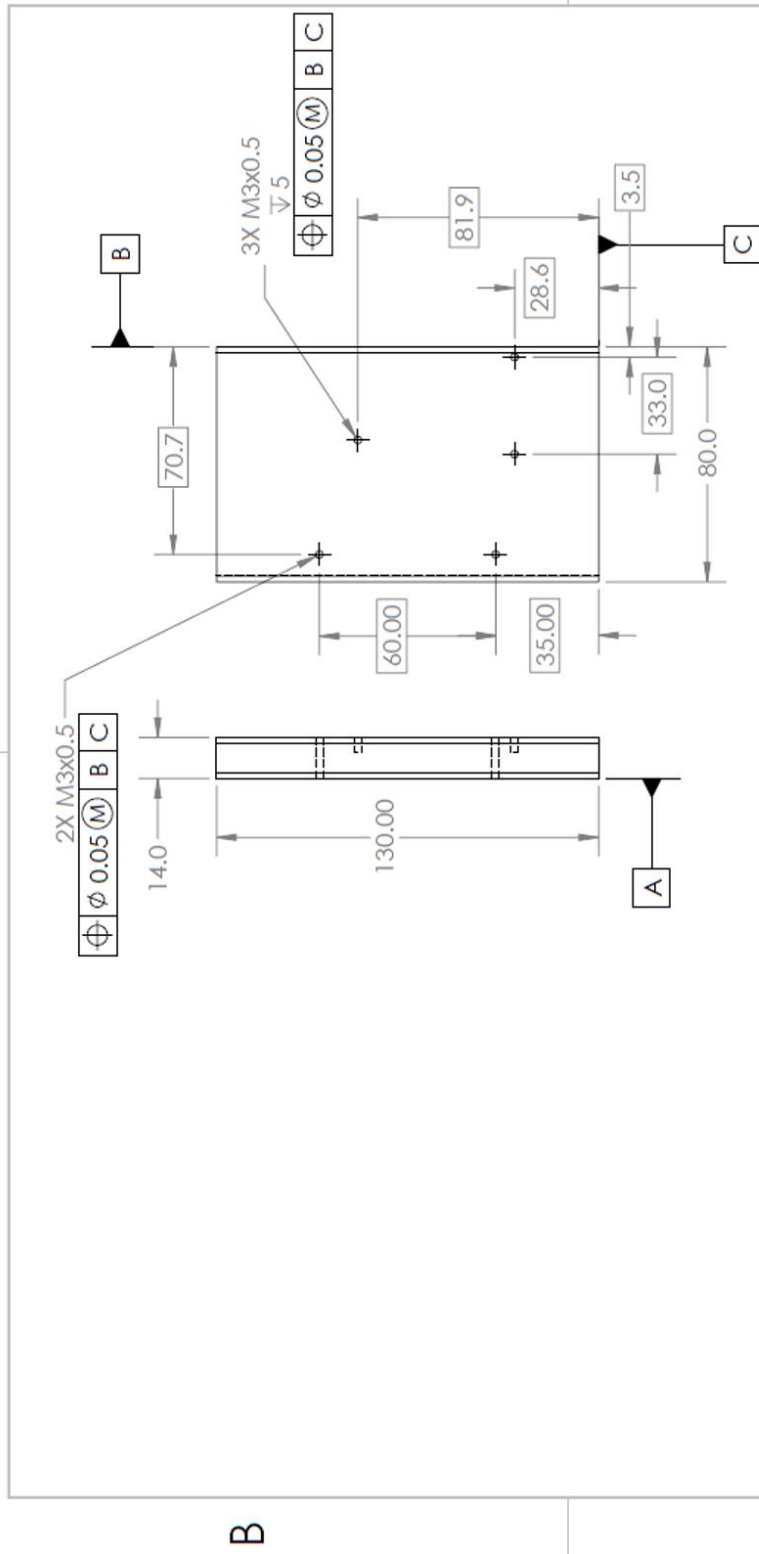
UNLESS OTHERWISE SPECIFIED: DIMENSIONS ARE IN MILLIMETERS TOLERANCES: FRACTIONAL ± ANGULAR: MACH. BEND ± TWO PLACE DECIMAL ± THREE PLACE DECIMAL ±		DRAWN	NAME	DATE
INTERPRET GEOMETRIC TOLERANCING PER:		CHECKED		
MATERIAL: Aluminum		ENG. APPR.		
FINISH: Anodized		MFG. APPR.		
NEXT ASSY		G.A.		
APPLICATION		COMMENTS:	TITLE:	
USED ON		Of the shelf pre cut and anodized aluminum		
DO NOT SCALE DRAWING		Support pillar		
		SIZE	DWG. NO.	REV
		Support pillar auto		
		SCALE: 1:1	WEIGHT:	SHEET 1 OF 1

2

1

2

1



B

B

A

A

PROPRIETARY AND CONFIDENTIAL
 THE INFORMATION CONTAINED IN THIS DRAWING IS THE SOLE PROPERTY OF <INSERT COMPANY NAME HERE>. ANY REPRODUCTION IN PART OR AS A WHOLE WITHOUT THE WRITTEN PERMISSION OF <INSERT COMPANY NAME HERE> IS PROHIBITED.

UNLESS OTHERWISE SPECIFIED:		NAME	DATE
DIMENSIONS ARE IN MILLIMETERS	DRAWN		
TOLERANCES:	CHECKED		
FRACTIONAL: 1	ENG APPR.		
ANGULAR: MACH: 1 BEND: 1	MFG APPR.		
TWO PLACE DECIMAL 1	G.A.		
THREE PLACE DECIMAL 1	COMMENTS:		
INTERPRET GEOMETRIC TOLERANCING PER:	Break all corners and edges		
MATERIAL:	6061 Aluminum		
FLUSH:	Anodized		
DO NOT SCALE DRAWING	APPLICATION		
NEXT ASSY	USED ON	TITLE: Al top plate	
SIZE DWG. NO. A		REV	
SCALE: 1:2	WEIGHT:	SHEET 1 OF 1	

2

1

Appendix C - Control system code

```
#include <PID_v1.h>
#include <LiquidCrystal.h>
#include <DFR_Key.h>
#include "SHT31.h"
uint32_t start;
uint32_t stop;
SHT31 sht;

#define temLowTrigger 35 //Setting the trigger value for the temperture, once the temperture lower
than this trigger value, the heater band will start heating

//#define humLowTrigger 70 //Setting the trigger value for the humidity, once the humidity lower than
this value, start humidification

int RelayPin = 45;
int RelayPin2 = 47;
int stateloop = 0;
int inside_fan = 0;
const int pinPwmfan = 46;//to fan
const int pinDirfan = 16;
const int pinPwmcham = 44;//to chamber
const int pinDircham = 14;
int flagg = 0;
int ii = 1;
double fan;
unsigned long lastMillis;
unsigned long lastTime, lastTime2, lastTime3;
double temp, oldtemp, dtemp = 0, Output, Setpoint = 70;//40 hum 80
double Setpoint_ito, ambient = 25;
double temp_ito, oldtemp_ito, dtemp_ito = 0, Output_ito;
double temp_cham;

double ITerm, lasttemp;
```

```

double kp, ki, kd;
unsigned long SampleTime = 1000; //1 sec
double outMin, outMax;
unsigned long lastTime_ito;
double ITerm_ito, lasttemp_ito;
double kp_ito, ki_ito, kd_ito;
unsigned long SampleTime_ito = 1000; //1 sec
double outMin_ito, outMax_ito;
float t, h, humLowTrigger = 80;
float diff, diffc, diff_ito;
//Pin assignments for DFRobot LCD Keypad Shield
LiquidCrystal lcd(8, 9, 4, 5, 6, 7);
//-----
DFR_Key keypad;
int localKey = 0;
String keyString = "";
int lcd_key = 0;
int adc_key_in = 0;
#define btnRIGHT 0
#define btnUP 1
#define btnDOWN 2
#define btnLEFT 3
#define btnSELECT 4
#define btnNONE 5
int read_LCD_buttons()
{
  adc_key_in = analogRead(0); // read the value from the sensor
  if (adc_key_in > 1500) return btnNONE;
  if (adc_key_in < 50) return btnRIGHT;
  if (adc_key_in < 195) return btnUP;

```

```

if (adc_key_in < 380) return btnDOWN;
if (adc_key_in < 500) return btnLEFT;
if (adc_key_in < 700) return btnSELECT;
return btnNONE; // when all others fail, return this...
}

void ComputeI()
{
    unsigned long now = millis();
    unsigned long timeChange = (now - lastTime);
    double error;
    if (timeChange >= SampleTime)
    {
        /*Compute all the working error variables*/
        // double error = Setpoint - temp;//+10
        if (Setpoint > ambient)
        {
            error = Setpoint - temp + 10;
        }
        if (Setpoint < ambient)
        {
            error = Setpoint - temp - 30;
        }
        ITerm += (ki * error);
        if (ITerm > outMax) ITerm = outMax;
        else if (ITerm < outMin) ITerm = outMin;
        double dtemp = (temp - lasttemp);
        /*Compute PID Output*/
        Output = kp * error + ITerm - kd * dtemp;
        if (Output > outMax) Output = outMax;
        else if (Output < outMin) Output = outMin;
    }
}

```

```

    /*Remember some variables for next time*/
    lasttemp = temp;
    lastTime = now;
}
}
void ComputeC()
{
    unsigned long now = millis();
    // int timeChange = (now - lastTime);
    unsigned long timeChange = (now - lastTime3);
    if (timeChange >= SampleTime)
    {
        /*Compute all the working error variables*/
        double error = Setpoint - temp_cham;
        ITerm += (ki * error);
        if (ITerm > outMax) ITerm = outMax;
        else if (ITerm < outMin) ITerm = outMin;
        double dtemp = (temp_cham - lasttemp);
        /*Compute PID Output*/
        Output = kp * error + ITerm - kd * dtemp;
        if (Output > outMax) Output = outMax;
        else if (Output < outMin) Output = outMin;
        /*Remember some variables for next time*/
        lasttemp = temp_cham;
        lastTime3 = now;
        // Serial.println(t);
    }
}
void Computelto()
{

```

```

unsigned long now = millis();
// int timeChange = (now - lastTime);
unsigned long timeChange = (now - lastTime_ito);

if (timeChange >= SampleTime_ito)
{
  /*Compute all the working error variables*/
  double error = Setpoint_ito - temp_ito;
  ITerm_ito += (ki_ito * error);
  if (ITerm_ito > outMax_ito) ITerm_ito = outMax_ito;
  else if (ITerm_ito < outMin_ito) ITerm_ito = outMin_ito;
  double dtemp_ito = (temp_ito - lasttemp_ito);

  /*Compute PID Output*/
  Output_ito = kp_ito * error + ITerm_ito - kd_ito * dtemp_ito;
  if (Output_ito > outMax_ito) Output_ito = outMax_ito;
  else if (Output_ito < outMin_ito) Output_ito = outMin_ito;

  /*Remember some variables for next time*/
  lasttemp_ito = temp_ito;
  lastTime_ito = now;
  // Serial.println(t);

}
}

void Computelto_c()
{

```

```

unsigned long now = millis();
// int timeChange = (now - lastTime);
unsigned long timeChange = (now - lastTime_ito);

if (timeChange >= SampleTime_ito)
{
    /*Compute all the working error variables*/
    double error = Setpoint - temp_cham;
    ITerm_ito += (ki_ito * error);
    if (ITerm_ito > outMax_ito) ITerm_ito = outMax_ito;
    else if (ITerm_ito < outMin_ito) ITerm_ito = outMin_ito;
    double dtemp_ito = (temp_ito - lasttemp_ito);

    /*Compute PID Output*/
    Output_ito = kp_ito * error + ITerm_ito - kd_ito * dtemp_ito;
    if (Output_ito > outMax_ito) Output_ito = outMax_ito;
    else if (Output_ito < outMin_ito) Output_ito = outMin_ito;
    /*Remember some variables for next time*/
    lasttemp_ito = temp_ito;
    lastTime_ito = now;
}
}

void SetTunings(double Kp, double Ki, double Kd)
{
    double SampleTimeInSec = ((double)SampleTime) / 1000;
    kp = Kp;
    ki = Ki * SampleTimeInSec;
    kd = Kd / SampleTimeInSec;
}

void SetTunings_ito(double Kp, double Ki, double Kd)

```

```

{
    double SampleTimeInSec = ((double)SampleTime) / 1000;
    kp_ito = Kp;
    ki_ito = Ki * SampleTimeInSec;
    kd_ito = Kd / SampleTimeInSec;
}
void SetSampleTime(unsigned long NewSampleTime)
{
    if (NewSampleTime > 0)
    {
        double ratio = (double)NewSampleTime / (double)SampleTime;
        ki *= ratio;
        kd /= ratio;
        SampleTime = (unsigned long)NewSampleTime;
    }
}
void SetSampleTime_ito(unsigned long NewSampleTime)
{
    if (NewSampleTime > 0)
    {
        double ratio = (double)NewSampleTime / (double)SampleTime;
        ki_ito *= ratio;
        kd_ito /= ratio;
        SampleTime_ito = (unsigned long)NewSampleTime;
    }
}
void SetOutputLimits(double Min, double Max)
{
    if (Min > Max) return;
    outMin = Min;

```

```

    outMax = Max;
    if (Output > outMax) Output = outMax;
    else if (Output < outMin) Output = outMin;
    if (ITerm > outMax) ITerm = outMax;
    else if (ITerm < outMin) ITerm = outMin;
}

void SetOutputLimits_ito(double Min, double Max)
{
    if (Min > Max) return;
    outMin_ito = Min;
    outMax_ito = Max;
    if (Output_ito > outMax_ito) Output_ito = outMax_ito;
    else if (Output_ito < outMin_ito) Output_ito = outMin_ito;

    if (ITerm_ito > outMax_ito) ITerm_ito = outMax_ito;
    else if (ITerm_ito < outMin_ito) ITerm_ito = outMin_ito;
}

#include <Adafruit_MAX31865.h>
#include <Arduino.h>
#include <Wire.h>
#include "Adafruit_SHT31.h"
bool enableHeater = false;
bool enablepump = false;
bool enableatom = true;
uint8_t loopCnt = 0;
uint8_t loopCnt2 = 0;
uint8_t loopCnt3 = 0;
Adafruit_SHT31 sht31 = Adafruit_SHT31();
// Use software SPI: CS, DI, DO, CLK
Adafruit_MAX31865 thermo = Adafruit_MAX31865(10, 11, 12, 13);

```

```

Adafruit_MAX31865 thermoITO = Adafruit_MAX31865(3, 11, 12, 13);
Adafruit_MAX31865 thermocham = Adafruit_MAX31865(2, 11, 12, 13);
// use hardware SPI, just pass in the CS pin
// The value of the Rref resistor. Use 430.0 for PT100 and 4300.0 for PT1000
#define RREF 430.0
#define RREF2 4300.0
// The 'nominal' 0-degrees-C resistance of the sensor
// 100.0 for PT100, 1000.0 for PT1000
#define RNOMINAL 100.0
#define RNOMINAL2 1000.0
void oracle()
{
  uint16_t rtd = thermo.readRTD();
  uint16_t rtdito = thermoITO.readRTD();
  uint16_t rtdcham = thermocham.readRTD();
  float ratio = rtd;
  float ratioito = rtdito;
  float ratiocham = rtdcham;
  ratio /= 32768;
  ratioito /= 32768;
  ratiocham /= 32768;
  temp = thermo.temperature(RNOMINAL, RREF);
  temp_ito = thermoITO.temperature(RNOMINAL, RREF);
  temp_cham = thermocham.temperature(RNOMINAL2, RREF2);
  // Check and print any faults
  uint8_t fault = thermo.readFault();
  if (fault) {
    Serial.print("Fault 0x"); Serial.println(fault, HEX);
    if (fault & MAX31865_FAULT_HIGHTHRESH) {
      Serial.println("RTD High Threshold");
    }
  }
}

```

```

}
if (fault & MAX31865_FAULT_LOWTHRESH) {
    Serial.println("RTD Low Threshold");
}
if (fault & MAX31865_FAULT_REFINLOW) {
    Serial.println("REFIN- > 0.85 x Bias");
}
if (fault & MAX31865_FAULT_REFINHIGH) {
    Serial.println("REFIN- < 0.85 x Bias - FORCE- open");
}
if (fault & MAX31865_FAULT_RTDINLOW) {
    Serial.println("RTDIN- < 0.85 x Bias - FORCE- open");
}
if (fault & MAX31865_FAULT_OVUV) {
    Serial.println("Under/Over voltage");
}
thermo.clearFault();
}
// Check and print any faults
uint8_t faultito = thermo.I2C.readFault();
if (faultito) {
    Serial.print("Fault 0x"); Serial.println(faultito, HEX);
    if (faultito & MAX31865_FAULT_HIGHTHRESH) {
        Serial.println("RTD High Threshold");
    }
    if (faultito & MAX31865_FAULT_LOWTHRESH) {
        Serial.println("RTD Low Threshold");
    }
    if (faultito & MAX31865_FAULT_REFINLOW) {
        Serial.println("REFIN- > 0.85 x Bias");
    }
}

```

```

}
if (faultito & MAX31865_FAULT_REFINHIGH) {
    Serial.println("REFIN- < 0.85 x Bias - FORCE- open");
}
if (faultito & MAX31865_FAULT_RTDINLOW) {
    Serial.println("RTDIN- < 0.85 x Bias - FORCE- open");
}
if (faultito & MAX31865_FAULT_OVUV) {
    Serial.println("Under/Over voltage");
}
thermoITO.clearFault();
}
uint8_t faultcham = thermocham.readFault();
if (faultcham) {
    Serial.print("Fault 0x"); Serial.println(faultcham, HEX);
    if (faultcham & MAX31865_FAULT_HIGHTHRESH) {
        Serial.println("RTD High Threshold");
    }
    if (faultcham & MAX31865_FAULT_LOWTHRESH) {
        Serial.println("RTD Low Threshold");
    }
    if (faultcham & MAX31865_FAULT_REFINLOW) {
        Serial.println("REFIN- > 0.85 x Bias");
    }
    if (faultcham & MAX31865_FAULT_REFINHIGH) {
        Serial.println("REFIN- < 0.85 x Bias - FORCE- open");
    }
    if (faultcham & MAX31865_FAULT_RTDINLOW) {
        Serial.println("RTDIN- < 0.85 x Bias - FORCE- open");
    }
}

```

```

if (faultcham & MAX31865_FAULT_OVUV) {
  Serial.println("Under/Over voltage");
}
thermocham.clearFault();
}
unsigned long now = millis();
unsigned long timeChange = (now - lastTime2);
if (timeChange >= 50)
{ sht.read();
  t = sht.getTemperature();
  h = sht.getHumidity();
  lastTime2 = now;
}
while (Wire.available()) {
  Wire.read();
}
lcd.setCursor(0, 0);
lcd.print("Hum: ");
lcd.print(h);
lcd.print("% ");
lcd.print(thermoITO.temperature(RNOMINAL, RREF));
lcd.setCursor(0, 1);
lcd.print("T: ");
lcd.print(temp_cham);//temp
lcd.print(", ");
lcd.print(thermo.temperature(RNOMINAL, RREF));
lcd.print("°C");
}
void setup() {
  SetOutputLimits(-255, 255);
}

```

```

SetOutputLimits_ito(0, 102);//170
pinMode(RelayPin, OUTPUT);
pinMode(RelayPin2, OUTPUT);
pinMode(pinPwmfan, OUTPUT);
pinMode(pinDirfan, OUTPUT);
pinMode(pinPwmcham, OUTPUT);
pinMode(pinDircham, OUTPUT);
digitalWrite(pinDirfan, HIGH);
digitalWrite(pinDircham , HIGH);
digitalWrite(RelayPin, HIGH);
digitalWrite(RelayPin2, HIGH);
Serial.begin(115200);
Serial.println("Meow");
Serial.println("ゝ／ |、");
Serial.println("( ° 、 。 7");
Serial.println(" | ˘ ˘ ");
Serial.println("_U U c )ノ");
Serial.println("It begins, you cannot stop it");
Serial.println("Cat sleeping");
thermo.begin(MAX31865_3WIRE); // set to 2WIRE or 4WIRE as necessary
thermoITO.begin(MAX31865_3WIRE);
thermocham.begin(MAX31865_3WIRE);
while (!Serial)
  delay(10); // will pause Zero, Leonardo, etc until serial console opens
Serial.println("Eyes open, sensors on");
Serial.print("Heater Enabled State: ");
if (sht31.isHeaterEnabled())
  Serial.println("ENABLED");
else
  Serial.println("DISABLED");

```

```

lcd.begin(16, 2);
lcd.clear();
lcd.setCursor(0, 0);
lcd.print("initializing...");
lcd.setCursor(0, 1);
delay(1000);
delay(1000);
lcd.clear();
keypad.setRate(10);
Wire.begin();
sht.begin(0x44); //Sensor I2C Address
Wire.setClock(1000);//100000
uint16_t stat = sht.readStatus();
Serial.print(stat, HEX);
Serial.println();
#if defined(WIRE_HAS_TIMEOUT)
  Wire.setWireTimeout(1000 /* us */, true /* reset_on_timeout */);
#endif
Serial.print("Heater Enabled State: ");
if (sht31.isHeaterEnabled())
  Serial.println("ENABLED");
else
  Serial.println("DISABLED");
h = sht31.readHumidity();
oracle();
Serial.print("Min");
Serial.print("\t");
Serial.print("temp al");
Serial.print("\t");
Serial.print("tempITO");

```

```
Serial.print("\t");
Serial.print("tempC2");
Serial.print("\t");
Serial.print("tempC");
Serial.print("\t");
Serial.print("peltier");
Serial.print("\t");
Serial.print("Ito");
Serial.print("\t");
Serial.print("hum");
Serial.print("\t");
Serial.println("state");
Serial.print("0");
Serial.print("\t");
Serial.print(temp);
Serial.print("\t");
Serial.print(temp_ito);
Serial.print("\t");
Serial.print(temp_cham);
Serial.print("\t");
Serial.print(t);
Serial.print("\t");
Serial.print(Output);
Serial.print("\t");
Serial.print(Output_ito);
Serial.print("\t");
Serial.print(h);
Serial.print("\t");
Serial.println(stateloop);
}
```

```

void loop() {
  #if defined(WIRE_HAS_TIMEOUT)
    Wire.clearWireTimeoutFlag();
  #endif
  #if defined(WIRE_HAS_TIMEOUT)
    if (Wire.getWireTimeoutFlag())
      Serial.println("It was a timeout");
  #endif
  if (millis() - lastMillis >= (60) * 1000UL)
  {
    lastMillis = millis(); //get ready for the next iteration
    Serial.print(ii);
    Serial.print("\t");
    Serial.print(temp);
    Serial.print("\t");
    Serial.print(temp_ito);
    Serial.print("\t");
    Serial.print(temp_cham);
    Serial.print("\t");
    Serial.print(t);
    Serial.print("\t");
    Serial.print(Output);
    Serial.print("\t");
    Serial.print(Output_ito);
    Serial.print("\t");
    Serial.print(h);
    Serial.print("\t");
    Serial.println(stateloop);
    ii++;
  }
}

```

```

oracle();
diff = Setpoint - temp;
diff_ito = Setpoint - temp_ito;
diffc = Setpoint - temp_cham;
float humLowTriggeroffset = humLowTrigger - 1.5;
if (abs(diffc) > 1 && ambient > Setpoint && temp_cham > Setpoint)
{
    if (abs(diffc) <= 2)
    {
        if (h < humLowTrigger)
        {
            if (++loopCnt2 == 9) {
                enablepump = !enablepump;
                enableatom = !enableatom;
                if (enablepump == true && h < humLowTrigger) {
                    digitalWrite(RelayPin, LOW);
                }
                else {
                    digitalWrite(RelayPin, HIGH);
                }
            }
            if (loopCnt2 == 11) {
                if (enableatom == true && h < humLowTriggeroffset)
                {
                    digitalWrite(RelayPin2, LOW);
                    loopCnt2 = 0;
                }
                else
                {
                    digitalWrite(RelayPin2, HIGH);
                }
            }
        }
    }
}

```

```

    }
    loopCnt2 = 0;
}
}
else
{
    digitalWrite(RelayPin, HIGH);
    digitalWrite(RelayPin2, HIGH);
    loopCnt2 = 0;
}
if (h > humLowTrigger) {
    digitalWrite(RelayPin, HIGH);
    digitalWrite(RelayPin2, HIGH);
    loopCnt2 = 0;
}
stateloop = 1;
double kkp = 0.0625 * 36 * 10;
double kki = 0.03125 / 2;
double kkd = 0.125 * 2;
unsigned long timz = 120000 / 8;
SetTunings(kkp, kki, kkd);
SetSampleTime(timz);
Setpoint_ito = Setpoint;
double kkp_ito = 0.0625 * 36 / 2;
double kki_ito = 0.03125 / 2;
double kkd_ito = 0.125 * 2;
unsigned long timz_ito = 120000 / 8;
SetTunings_ito(kkp_ito, kki_ito, kkd_ito);
SetSampleTime_ito(timz_ito);

```

```

Computel();
Computelto();
if (Output > 0)
{
    digitalWrite(pinDirfan, LOW);
    analogWrite(pinPwmfan, abs(Output));
}
else if ( Output < 0)
{
    digitalWrite(pinDirfan, HIGH);
    analogWrite(pinPwmfan, abs(Output));
}
analogWrite(pinPwmcham, abs(Output_ito));
    oracle();
}
if (((abs(diffc) < 0.25 || temp_cham < Setpoint) && ambient > Setpoint))
{
    if (abs(diffc) < 2)
    {
        if (h < humLowTrigger)
        {
            if (++loopCnt2 == 9) {
                enablepump = !enablepump;
                enableatom = !enableatom;
                if (enablepump == true && h < humLowTrigger) {
                    digitalWrite(RelayPin, LOW);
                }
            }
            else {
                digitalWrite(RelayPin, HIGH);
            }
        }
    }
}

```

```

}
if (loopCnt2 == 11) {
    if (enableatom == true && h < humLowTriggeroffset)
    {
        digitalWrite(RelayPin2, LOW);
        loopCnt2 = 0;
    }
    else
    {
        digitalWrite(RelayPin2, HIGH);
    }
    loopCnt2 = 0;
}
}
}
else
{
    digitalWrite(RelayPin, HIGH);
    digitalWrite(RelayPin2, HIGH);
    loopCnt2 = 0;
}
if (h > humLowTrigger) {
    digitalWrite(RelayPin, HIGH);
    digitalWrite(RelayPin2, HIGH);
    loopCnt2 = 0;
}
stateloop = 2;
double kkp = 0.0625 * 36 / 4;
double kki = 0.03125 / 2;
double kkd = 0.125 * 2;

```

```

unsigned long timz = 120000 / 8;
SetTunings(kkp, kki, kkd);
SetSampleTime(timz);
Setpoint_ito = Setpoint;
double kkp_ito = 0.0625 * 36 / 2;
double kki_ito = 0.03125 / 2;
double kkd_ito = 0.125 * 2;
unsigned long timz_ito = 120000 / 8;
SetTunings_ito(kkp_ito, kki_ito, kkd_ito);
SetSampleTime_ito(timz_ito);
ComputeC();
ComputeIto();
if (Output > 0)
{
    digitalWrite(pinDirfan, LOW);
    analogWrite(pinPwmfan, abs(Output));
}
else if ( Output < 0)
{
    digitalWrite(pinDirfan, HIGH);
    analogWrite(pinPwmfan, abs(Output));
}
analogWrite(pinPwmcham, abs(Output_ito));
oracle();
}
if (ambient < Setpoint && abs(diffc) > 20) //HEAT LARGE
{
    stateloop = 3;
    double kkp = 0.0625 * 36;
    double kki = 0.03125 / 2;

```

```

double kkd = 0.125 * 2;
unsigned long timz = 120000 / 8;
SetTunings(kkp, kki, kkd);
SetSampleTime(timz);
if (inside_fan == 0)
{
    Setpoint_ito = Setpoint + 15;
}
if (inside_fan == 1)
{
    Setpoint_ito = Setpoint;
}
double kkp_ito = 0.0625 * 36 / 2;
double kki_ito = 0.03125 / 2;
double kkd_ito = 0.125 * 2;
unsigned long timz_ito = 120000 / 8;
SetTunings_ito(kkp_ito, kki_ito, kkd_ito);
SetSampleTime_ito(timz_ito);
ComputeI();
ComputeIto();
if (Output > 0)
{
    digitalWrite(pinDirfan, LOW);
    analogWrite(pinPwmfan, abs(Output));
}
else if ( Output < 0)
{
    digitalWrite(pinDirfan, HIGH);
    analogWrite(pinPwmfan, abs(Output));
}

```

```

analogWrite(pinPwmcham, abs(Output_ito));
oracle();
}
if (abs(diffc) <= 20 && ambient < Setpoint && abs(diffc) > 7)
{
stateloop = 4;
double kkp = 0.0625 * 4; //0.0625 * 36/4
double kki = 0.03125 / 2;
double kkd = 200;//0.125
unsigned long timz = 120000 / 10;//120000 / 8
SetTunings(kkp, kki, kkd);
SetSampleTime(timz);
if (inside_fan == 0)
{
Setpoint_ito = Setpoint;
}
if (inside_fan == 1)
{
Setpoint_ito = Setpoint;
}
double kkp_ito = 0.0625 * 4; //0.0625 * 36/2 newer 0.0625 * 36/8
double kki_ito = 0.25;//0.03125 / 2 or 0.03125 / 8
double kkd_ito = 100;//0.125 * 2*4
unsigned long timz_ito = 120000 / 16;//120000 / 16*
SetTunings_ito(kkp_ito, kki_ito, kkd_ito);
SetSampleTime_ito(timz_ito);
ComputeI();
ComputeIto();
if (Output > 0)
{

```

```

digitalWrite(pinDirfan, LOW);
analogWrite(pinPwmfan, abs(Output));
}
else if ( Output < 0)
{
digitalWrite(pinDirfan, HIGH);
analogWrite(pinPwmfan, abs(Output));
}
analogWrite(pinPwmcham, abs(Output_ito));
oracle();
}
if (ambient < Setpoint && abs(diffc) < 7) //Setpoint < temp_cham) STATE 5*****
{
if (abs(diffc) < 2)
{
if (h < humLowTrigger)
{
if (++loopCnt2 == 9) {
enablepump = !enablepump;
enableatom = !enableatom;
if (enablepump == true && h < humLowTrigger) {
digitalWrite(RelayPin, LOW);
}
else {
digitalWrite(RelayPin, HIGH);
}
}
}
if (loopCnt2 == 11) {
if (enableatom == true && h < humLowTriggeroffset)
{

```

```

    digitalWrite(RelayPin2, LOW);
    loopCnt2 = 0;
}
else
{
    digitalWrite(RelayPin2, HIGH);
}
loopCnt2 = 0;
}
}
}
else
{
    digitalWrite(RelayPin, HIGH);
    digitalWrite(RelayPin2, HIGH);
    loopCnt2 = 0;
}
if (h > humLowTrigger) {
    digitalWrite(RelayPin, HIGH);
    digitalWrite(RelayPin2, HIGH);
    loopCnt2 = 0;
}
stateLoop = 5;

double kkp = 0.0625 * 36 / 4;
double kki = 0.03125 / 2;
double kkd = 0.125 * 2;
unsigned long timz = 120000 / 8;
SetTunings(kkp, kki, kkd);
SetSampleTime(timz);

```

```

if (inside_fan == 0)
{
    Setpoint_ito = Setpoint;
}
if (inside_fan == 1)
{
    Setpoint_ito = Setpoint;
}

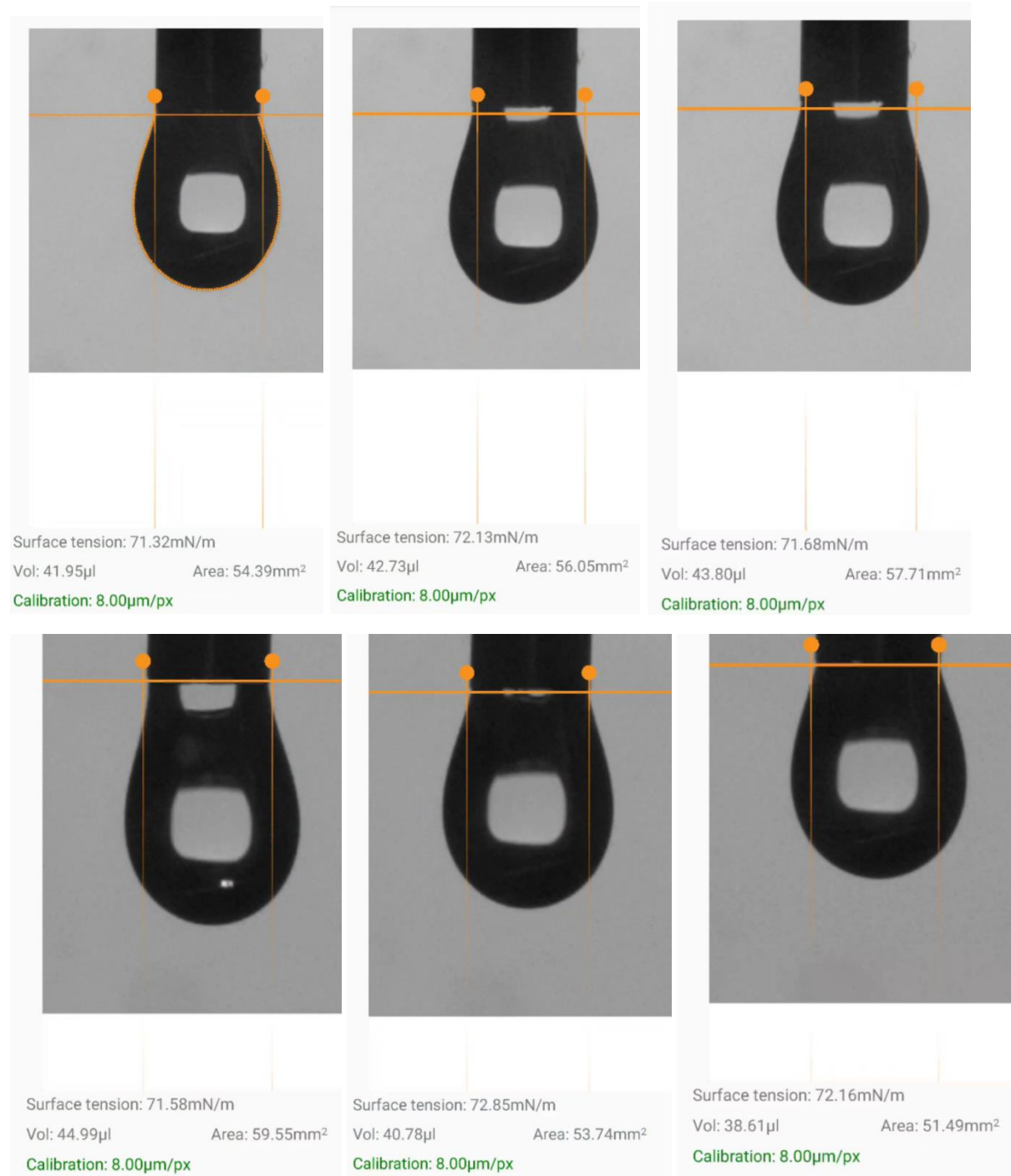
    double kkp_ito = 0.0625 * 36 / 2;
double kki_ito = 0.03125 / 2;
double kkd_ito = 0.125 * 2 * 4;
unsigned long timz_ito = 120000 / 8;
SetTunings_ito(kkp_ito, kki_ito, kkd_ito);
SetSampleTime_ito(timz_ito);
ComputeC();
ComputeIto_c();
if (Output > 0)
{
    digitalWrite(pinDirfan, LOW);
    analogWrite(pinPwmfan, abs(Output));
}
else if ( Output < 0)
{
    digitalWrite(pinDirfan, HIGH);
    analogWrite(pinPwmfan, abs(Output));
}
analogWrite(pinPwmcham, abs(Output_ito));
oracle();
}
}

```

Appendix D - Benchmark and literature tests raw data

D-1 Surface tension of water at various ambient environmental conditions

D-1-1 Surface tension at 15°C and 45 %RH



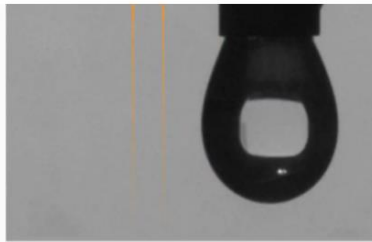


Surface tension 15°C and 78.9 %RH

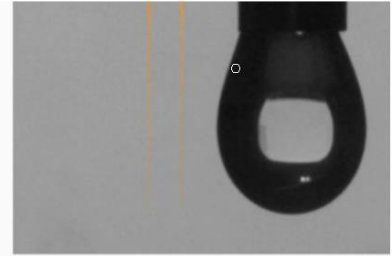




Surface tension: 72.67mN/m
 Vol: 40.66µl Area: 54.64mm²
 Calibration: 7.89µm/px

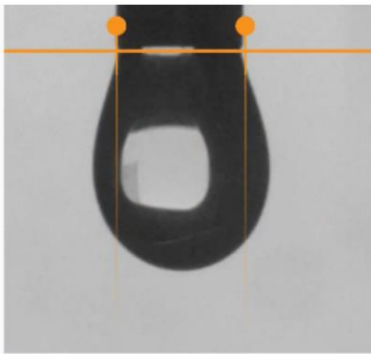


Surface tension: 72.60mN/m
 Vol: 34.12µl Area: 48.13mm²
 Calibration: 7.89µm/px

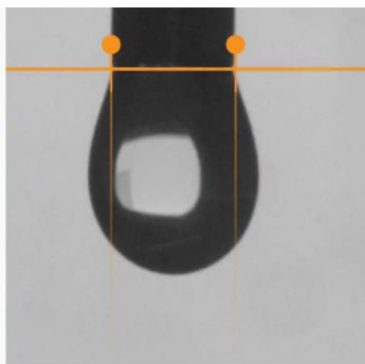


Surface tension: 72.84mN/m
 Vol: 36.08µl Area: 49.54mm²
 Calibration: 7.89µm/px

D-1-2 Surface tension 15°C and 79.4 %RH



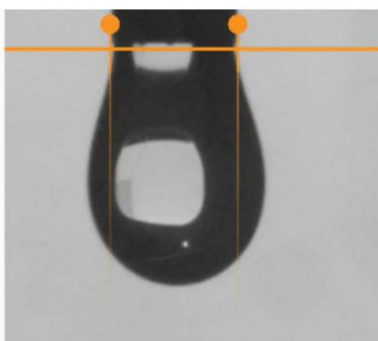
Surface tension: 71.16mN/m
 Vol: 39.48µl Area: 52.52mm²
 Calibration: 7.89µm/px



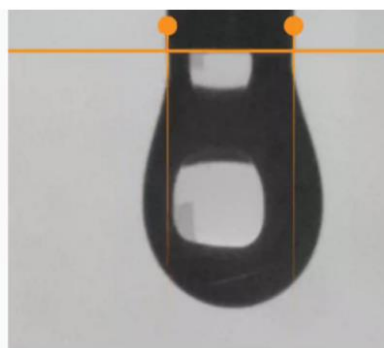
Surface tension: 71.11mN/m
 Vol: 37.13µl Area: 50.18mm²
 Calibration: 7.89µm/px



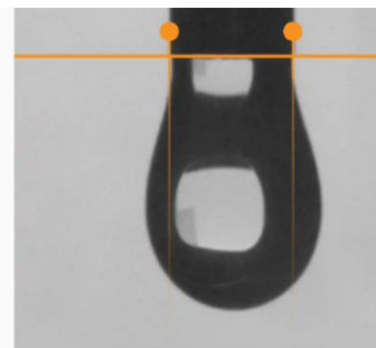
Surface tension: 72.95mN/m
 Vol: 41.82µl Area: 54.74mm²
 Calibration: 7.89µm/px



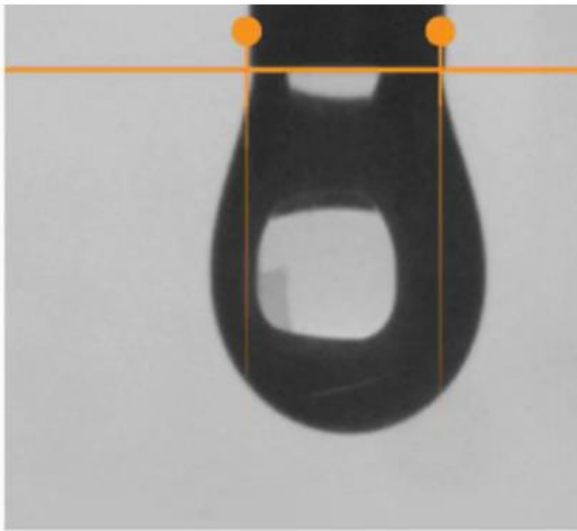
Surface tension: 72.27mN/m
 Vol: 44.08µl Area: 57.63mm²
 Calibration: 7.89µm/px



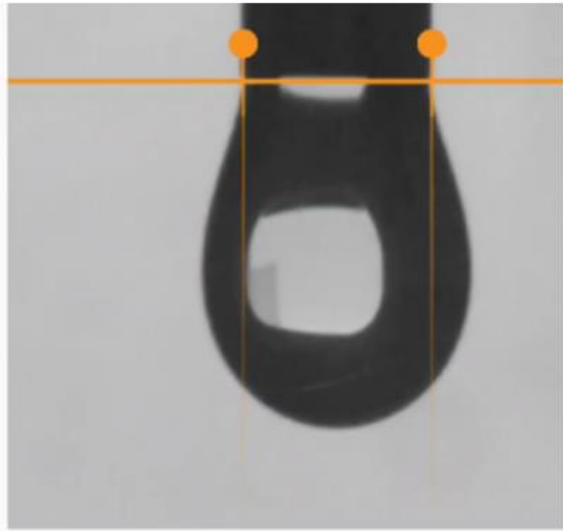
Surface tension: 71.16mN/m
 Vol: 44.61µl Area: 59.30mm²
 Calibration: 7.89µm/px



Surface tension: 71.04mN/m
 Vol: 44.81µl Area: 59.79mm²
 Calibration: 7.89µm/px

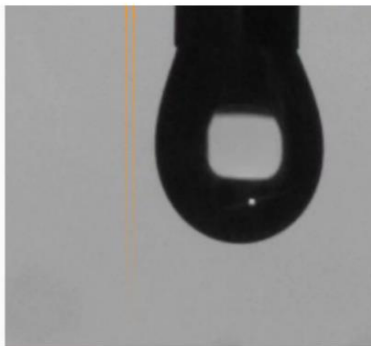


Surface tension: 71.12mN/m
Vol: 41.36 μ l Area: 55.06mm²
Calibration: 7.89 μ m/px

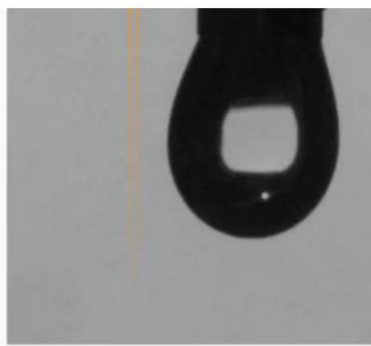


Surface tension: 71.66mN/m
Vol: 41.73 μ l Area: 55.67mm²
Calibration: 7.89 μ m/px

D-1-3 Surface tension 40 °C at 44%RH



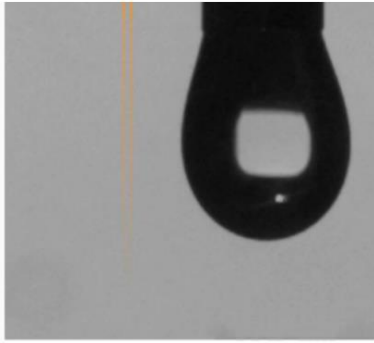
Surface tension: 69.88mN/m
Vol: 32.96 μ l Area: 45.77mm²
Calibration: 7.89 μ m/px



Surface tension: 71.04mN/m
Vol: 33.54 μ l Area: 45.90mm²
Calibration: 7.89 μ m/px



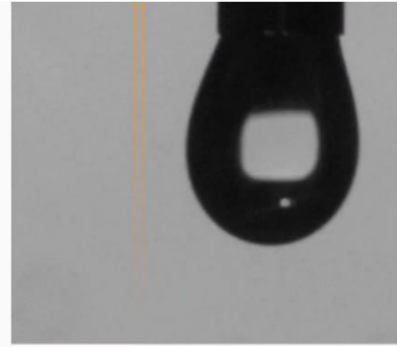
Surface tension: 72.25mN/m
Vol: 37.11 μ l Area: 50.30mm²
Calibration: 7.89 μ m/px



Surface tension: 70.36mN/m
Vol: 37.60 μ l Area: 48.91mm²
Calibration: 7.89 μ m/px

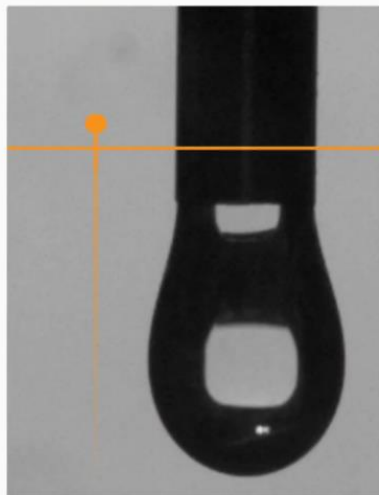


Surface tension: 69.48mN/m
Vol: 39.91 μ l Area: 54.11mm²
Calibration: 7.89 μ m/px

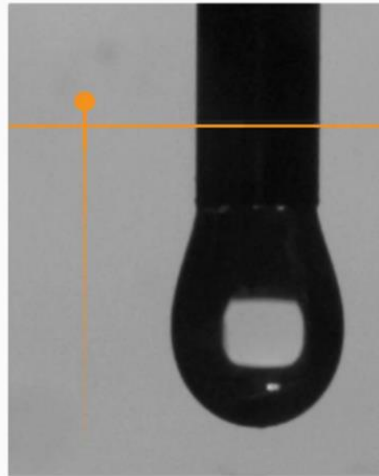


Surface tension: 70.71mN/m
Vol: 34.73 μ l Area: 47.90mm²
Calibration: 7.89 μ m/px

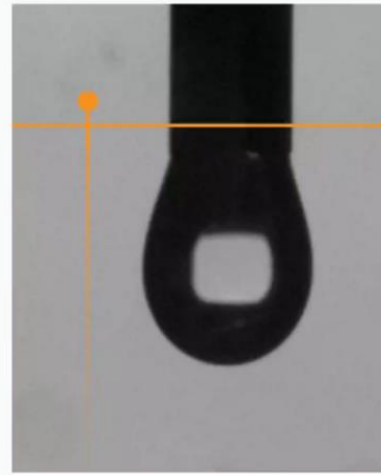
Surface tension 40 °C at 54%RH



Surface tension: 69.41mN/m
Vol: 43.93 μ l Area: 58.48mm²
Calibration: 7.89 μ m/px



Surface tension: 71.40mN/m
Vol: 39.74 μ l Area: 51.64mm²
Calibration: 7.89 μ m/px



Surface tension: 70.41mN/m
Vol: 37.07 μ l Area: 50.25mm²
Calibration: 7.89 μ m/px



Surface tension: 71.85mN/m
Vol: 37.09 μ l Area: 49.84mm²
Calibration: 7.89 μ m/px

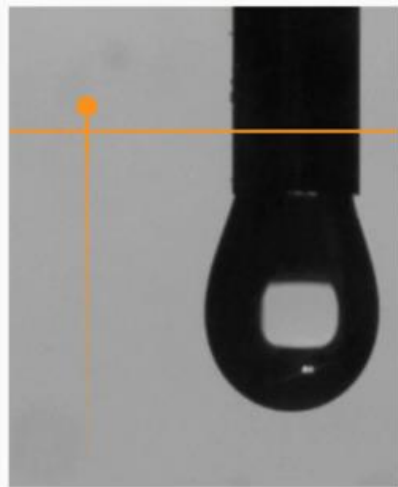
D-1-4 Surface tension 40 °C at 64%RH



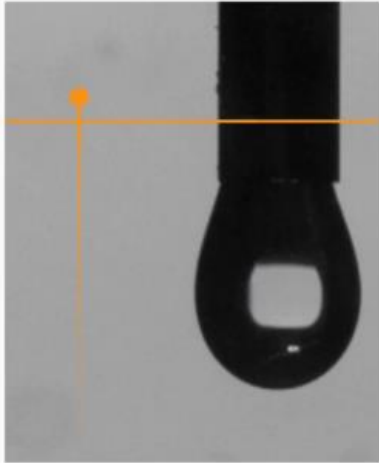
Surface tension: 71.40mN/m
Vol: 39.74 μ l Area: 51.64mm²
Calibration: 7.89 μ m/px



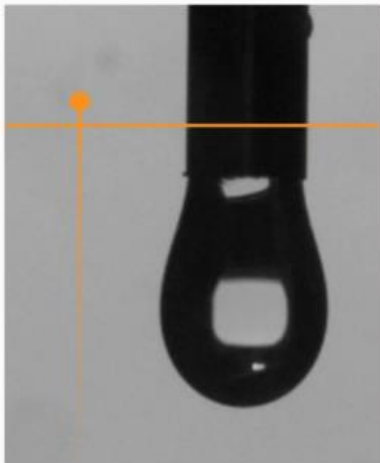
Surface tension: 68.65mN/m
Vol: 38.09 μ l Area: 51.49mm²
Calibration: 7.89 μ m/px



Surface tension: 71.08mN/m
Vol: 36.92 μ l Area: 50.77mm²
Calibration: 7.89 μ m/px



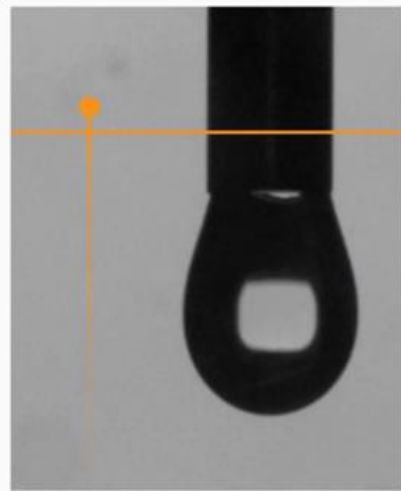
Surface tension: 69.92mN/m
Vol: 36.59 μ l Area: 50.18mm²
Calibration: 7.89 μ m/px



Surface tension: 68.82mN/m
Vol: 40.20 μ l Area: 53.93mm²
Calibration: 7.89 μ m/px

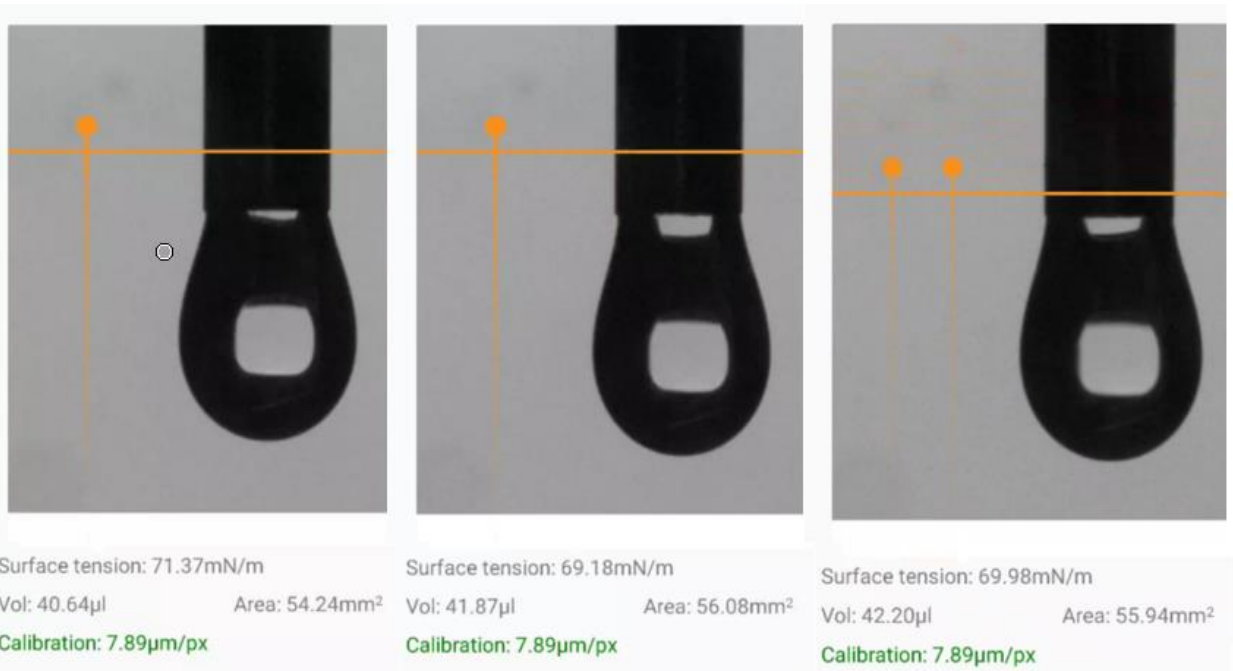


Surface tension: 69.55mN/m
Vol: 35.37 μ l Area: 48.42mm²
Calibration: 7.89 μ m/px

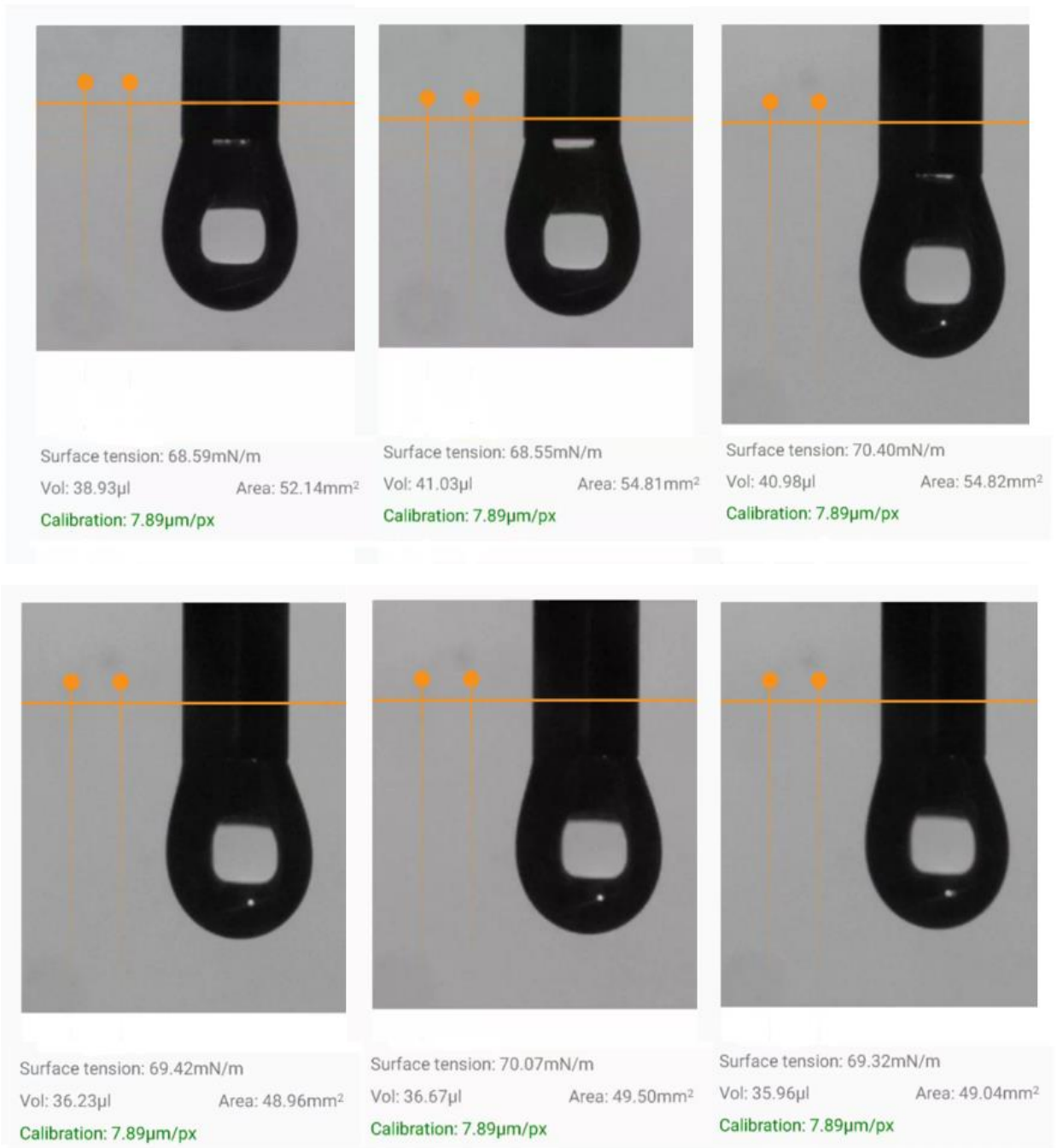


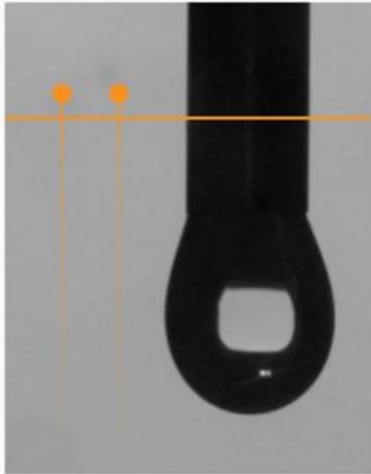
Surface tension: 70.09mN/m
Vol: 38.91 μ l Area: 52.40mm²
Calibration: 7.89 μ m/px

D-1-5 Surface tension 40 °C at 70%RH



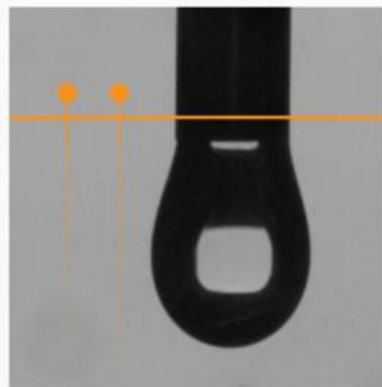
D-1-6 Surface tension 40 °C at 81.5%RH



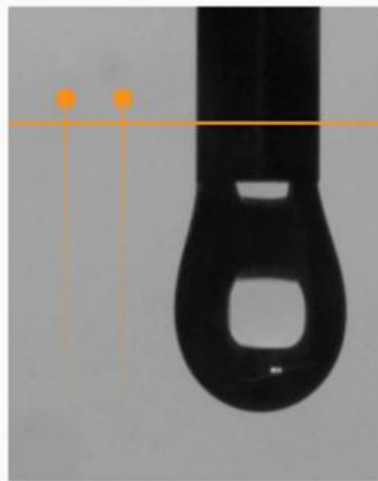


Surface tension: 71.15mN/m
 Vol: 37.06 μ l Area: 49.82mm²
 Calibration: 7.89 μ m/px

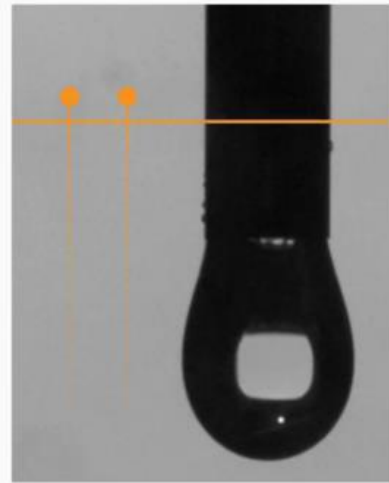
D-1-7 Surface tension 40 °C at 91%RH



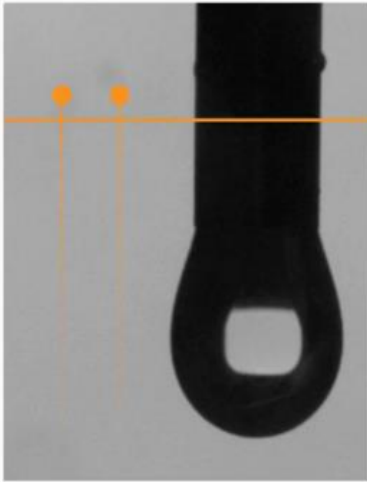
Surface tension: 68.87mN/m
 Vol: 40.67 μ l Area: 54.10mm²
 Calibration: 7.89 μ m/px



Surface tension: 68.52mN/m
 Vol: 42.62 μ l Area: 56.91mm²
 Calibration: 7.89 μ m/px



Surface tension: 68.04mN/m
 Vol: 38.65 μ l Area: 51.56mm²
 Calibration: 7.89 μ m/px



Surface tension: 69.85mN/m

Vol: 36.68 μ l

Area: 48.18mm²

Calibration: 7.89 μ m/px



Surface tension: 69.98mN/m

Vol: 29.74 μ l

Area: 42.08mm²

Calibration: 7.89 μ m/px

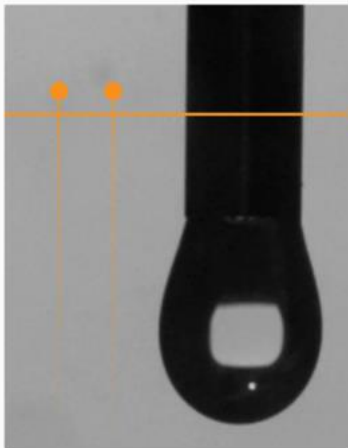


Surface tension: 69.63mN/m

Vol: 37.45 μ l

Area: 50.73mm²

Calibration: 7.89 μ m/px



Surface tension: 70.08mN/m

Vol: 39.83 μ l

Area: 53.35mm²

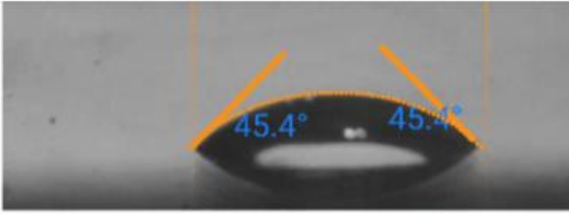
Calibration: 7.89 μ m/px

D-1-8 Surface tension 40 °C at 98%RH



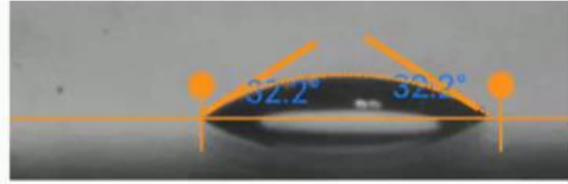
D-2 Receding contact angle measurements of an evaporating water droplet on a glass surface; ambient conditions 27.5 °C and 61% Relative humidity

D-2-1 Test 1



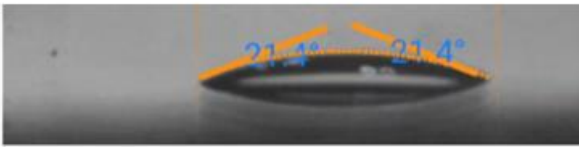
Left Angle: 45.37° Right Angle: 45.37°
Vol: 13.20μl Area: 26.88mm²

Calibration: 6.99μm/px
Young-Laplace Alg.



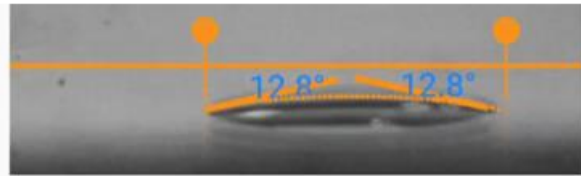
Left Angle: 32.24° Right Angle: 32.24°
Vol: 8.53μl Area: 22.93mm²

Calibration: 6.99μm/px
Young-Laplace Alg.



Left Angle: 21.40° Right Angle: 21.40°
Vol: 5.37μl Area: 21.24mm²

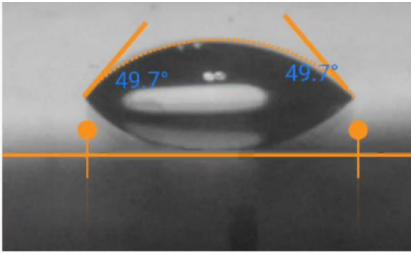
Calibration: 6.99μm/px
Young-Laplace Alg.



Left Angle: 12.77° Right Angle: 12.77°
Vol: 2.95μl Area: 21.64mm²

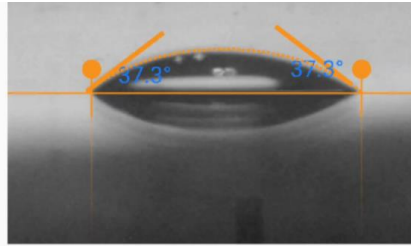
Calibration: 6.99μm/px
Young-Laplace Alg.

D-2-2 Test 2



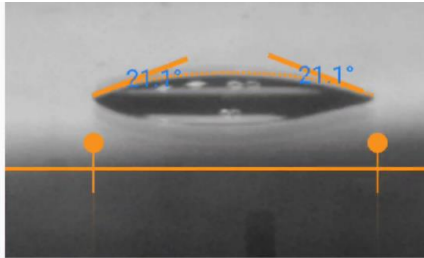
Left Angle: 49.70° Right Angle: 49.70°
Vol: 13.94μl Area: 26.36mm²

Calibration: 6.90μm/px
Young-Laplace Alg.



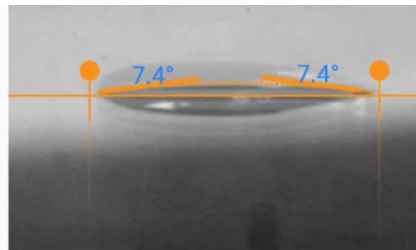
Left Angle: 37.34° Right Angle: 37.34°
Vol: 10.37μl Area: 25.14mm²

Calibration: 6.90μm/px
Young-Laplace Alg.



Left Angle: 21.09° Right Angle: 21.09°
Vol: 4.96μl Area: 21.37mm²

Calibration: 6.90μm/px
Young-Laplace Alg.



Left Angle: 7.42° Right Angle: 7.42°
Vol: 1.73μl Area: 19.42mm²

Calibration: 6.90μm/px
Young-Laplace Alg.



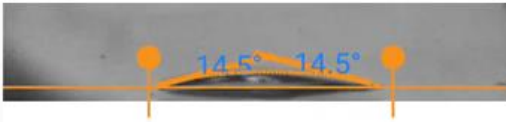
Left Angle: 40.49° Right Angle: 40.49°
Vol: 15.71µl Area: 36.82mm²

Calibration: 6.81µm/px
Young-Laplace Alg.



Left Angle: 32.72° Right Angle: 32.72°
Vol: 9.10µl Area: 28.82mm²

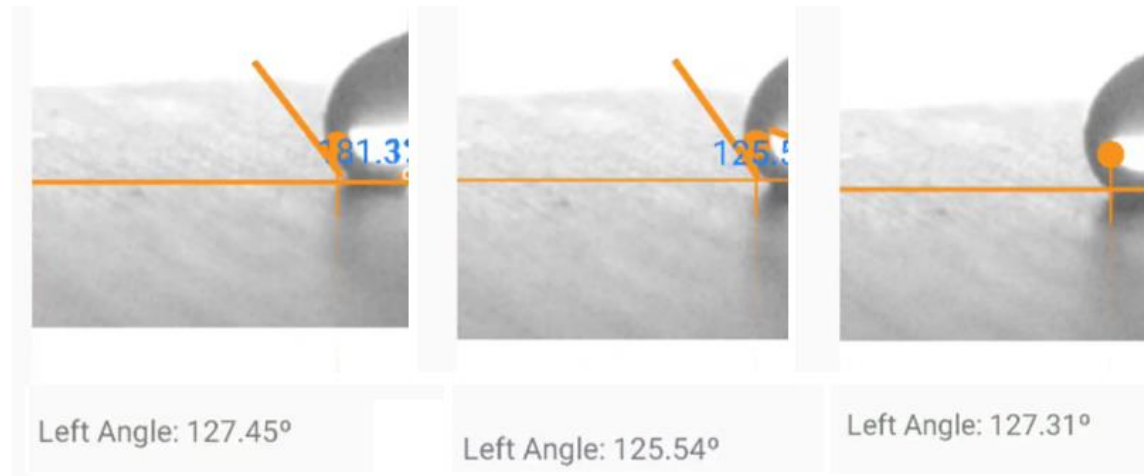
Calibration: 6.81µm/px
Young-Laplace Alg.



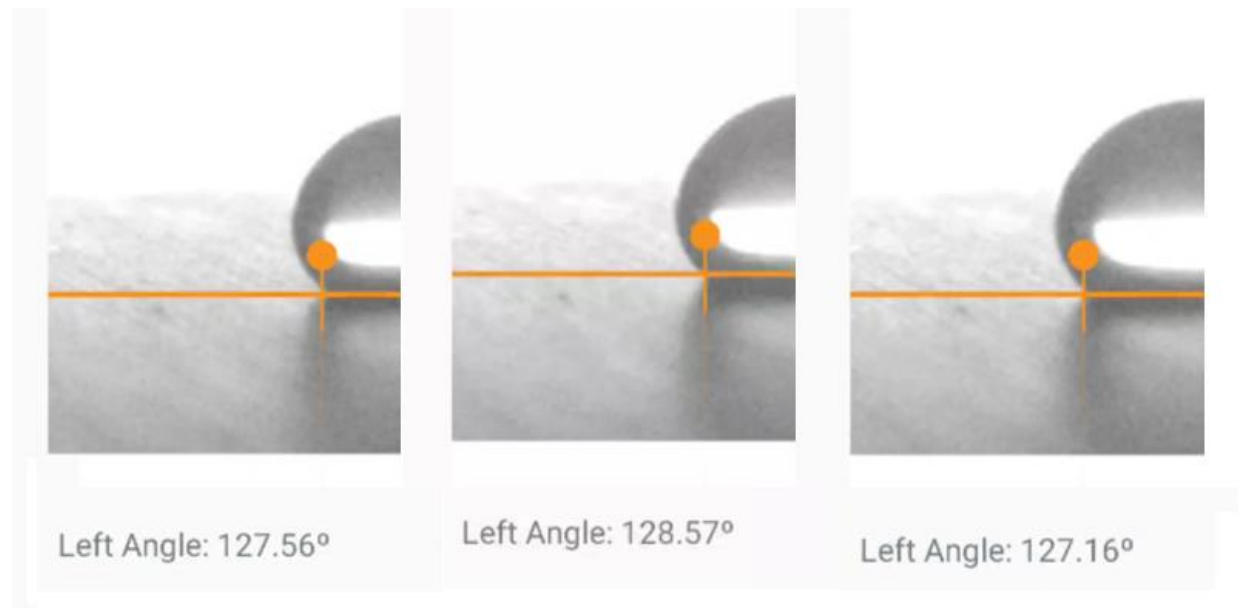
Left Angle: 14.51° Right Angle: 14.51°
Vol: 3.33µl Area: 19.26mm²

Calibration: 6.81µm/px
Young-Laplace Alg.

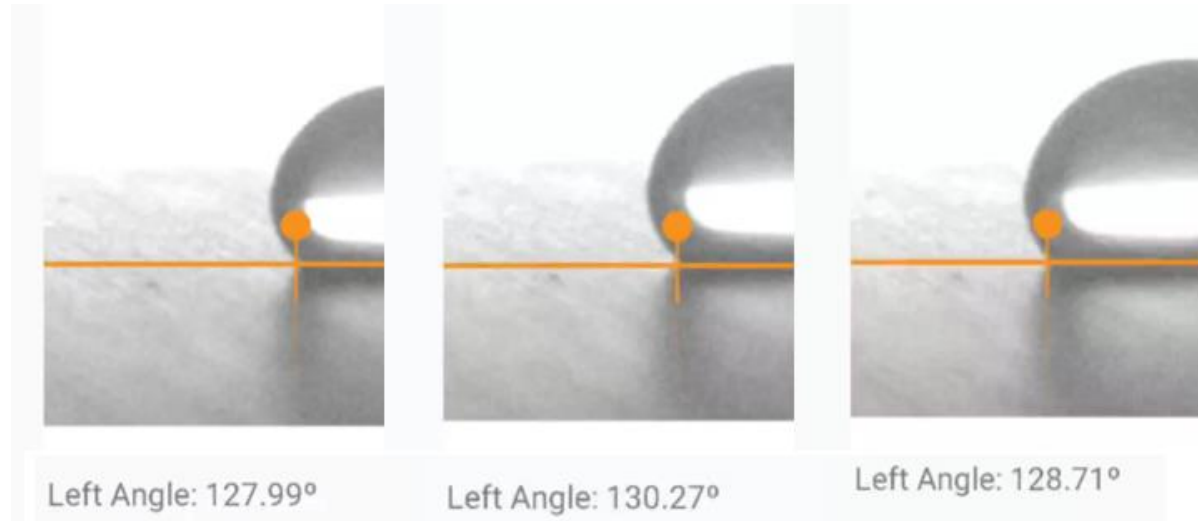
D-3 Advancing contact angle of a water droplet on a Teflon surface
D-3-1 humidity range 53-65 %RH; temperature 53 °C



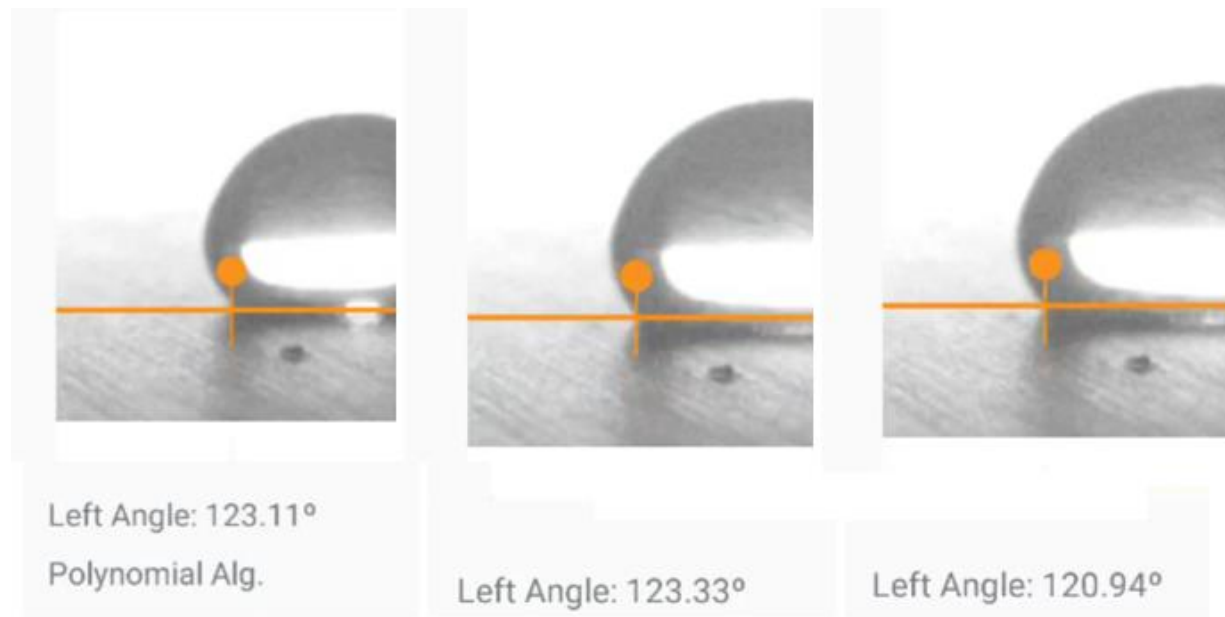
D-3-2 humidity range 53-65 %RH; temperature 60 °C



D-3-3 humidity range 53-65 %RH; temperature 69 °C



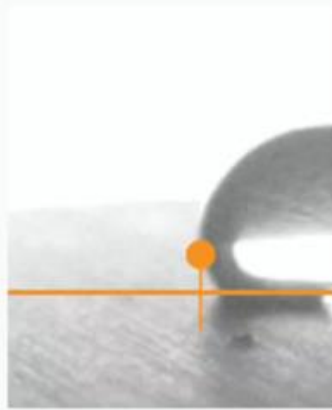
D-3-4 humidity range 94-100 %RH, temperature 50°C



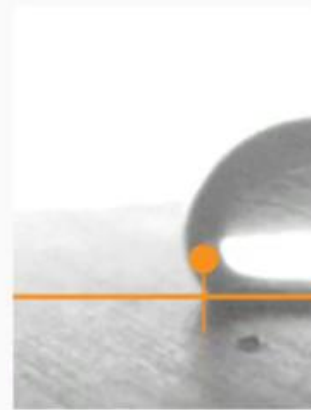
D-3-6 humidity range 94-100 %RH, temperature 61°C



Right Angle: 121.82°

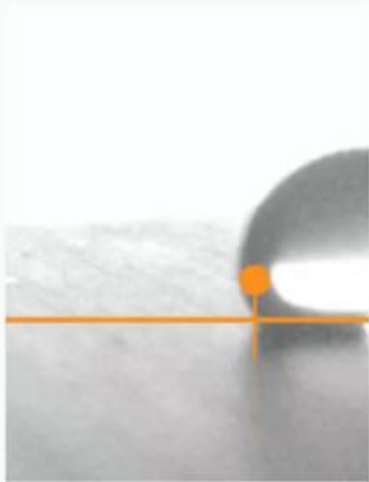


Left Angle: 124.65°

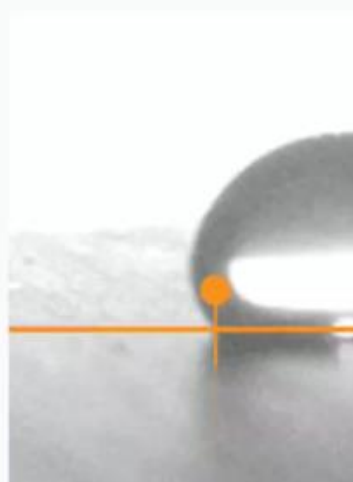


Left Angle: 123.22°

D-3-5 humidity range 94-100 %RH, temperature 70°C



Left Angle: 121.90°



Left Angle: 122.48°



Left Angle: 124.68°